A contribution of understanding the stability of commercial PLA films for food packaging and its surface modifications

Jeancarlo Renzo Rocca Smith

UNIVERSITA' DEGLI STUDI DI UDINE **UNIVERSITE DE BOURGOGNE FRANCHE-COMTE**

PhD dissertation

In Food Science

A CONTRIBUTION OF UNDERSTANDING THE STABILITY OF COMMERCIAL PLA FILMS FOR FOOD PACKAGING AND ITS SURFACE MODIFICATIONS

By

Jeancarlo Renzo Rocca Smith

March 2017

Reviewers

Pr. Luciano Piergiovanni — University of Milan
Pr. Laurent Lebrun — Université de Rouen

Examiners

Pr. Patrizia Fava — University of Modena
Pr. Frédéric Prochazka — Université de Saint Etienne
Dr. Francesca Piasente — Taghleef Industries

Advisors

Pr. Frédéric Debeaufort — Université de Bourgogne Franche-Comté
Dr. Thomas Karbowiak — Université de Bourgogne Franche-Comté
Pr. Alessandro Sensidoni — Università degli Studi di Udine

Università degli Studi di Udine
Dipartimento di Scienze degli Alimenti

UNIVERSITÀ
ITALO
FRANCESE

“Rugby is a beastly game played by gentlemen” (Rugby quote)

For those persons who live in my hearth everywhere and everytime,

to my mother, to my mamama, to my papapa,

and for those who will never hesitate to give everything for me,

to my father and to my mami.

Acknowledgments

It is pretty easy for me to start with this part, since without them I couldn't have reached any objective, so the first lines are for my family. We decided together some years ago to star my adventure as a student in Italy, well and now that adventure is getting at the end I cannot not say, muchas gracias viejo, mami, hermanos, los extraño y los quiero mucho. I am looking forward for new adventures with you!

Now things get more complicated because of the large number of people who helped me in this adventure… so I will continue with any logical thinking, I will just let that feelings flow.

Thanks to my both universities for giving me the opportunity to do this PhD, these three years were just fantastic. But since institutions are nothing without people, I have to thank those people that were of great of importance, grazie mille prof. Sensidoni for thinking on me for this project and for giving me such stimulating topic, without you this PhD wouldn't have been started. Grazie mille anche a te Eva for guiding me during my first steps as PhD student and for pushing me to continue my adventure in Dijon. Merci beaucoup Prof. Debeaufort for accepting being my co-advisor, and also merci beaucoup Thomas for being not only my supervisor, but also a friend. Working with both of you was amazing; you are a great example of the kind of researcher I would like to become one day, with such high qualities that are strange to find all together in one person, hard work, intelligence, creativity, competence, dynamicity and most important goodhearted. Muchas gracias de verdad, ha sido un gran honor trabajar con ustedes.

Thanks also to you Fabio and Francesca, for our friendship and for making my time in Italy even better. Grazie ragazzi anche se siamo lontani, vi porto sempre nel cuore. Merci Aurelie, I consider you not only as a friend but as my South West French sister. I don't think it is just a coincidence, I started my very first experiments in France with you, I finished my last experiments also with you…and very important, I will finish tomorrow to shape my thesis always with you… ce n'est pas normal!. You are key person for me, and I would like to be the same for you. Thanks also to my French bureau friends, Kevin, Aline and Ann, I will always remind our working time, but especially our not working time there, between Comte cheese, Thai accent and really bad music.

I cannot forget all the professors and researchers who spent their time with me, and from who I learnt. Thanks Dominique for pushing me to try to find the most appropriate way to explain all the phenomena occurring, and for teaching me that going deep in experiments for properly understand the results is never useless. Thanks also to Dr. Claire-Helene Brachais, prof. Jean Pierre Bellat, Dr. Jerome Rousseau, prof. Stephane Fontaine and prof. Bourillot for opening labs to this PhD and for being always available for me with an honest smile. Merci Bernadette for being the real boss of the lab, and for your help anytime.

I also want to thank to all the trainees that worked with me during this PhD. I was very nice for me to be in the lab with you guys, and I hope I could teach you something during your experience in the lab. Thanks Francesco, Jessica, Marco, Danielle, Nathan, Roberta and Orla.

Thanks as well to Taghleef industries and in particular to Dr. Piasente for this pleasant collaboration.

I would like as well to thank the Jury members of this PhD dissertation, for being available to review this thesis.

Even if this PhD began three years ago, I would like to thank as well my previous advisors and professors. If I could get the grant for this PhD, it was also for you. You formed me during my first steps as researcher, and pushed me to give always the best. So these lines are also for you, thanks prof. Anese, prof. Nicoli, prof. Manzocco, prof. Labuza and Dr. Rao.

The last lines are for those persons, who even not directly involved in this PhD are of great importance for me (most of them hate the university), I am talking about of my rugby team mates from la Leonorso in Udine, and from Rugby Club Dijonnais in Dijon. Training and playing every Sunday with you guys is not only joyful, but it is essentially an honour.

Thanks again to all of you for making of this PhD a great experience….. ¡Nos vemos pronto!

I think that there was a quite logical thinking when I wrote this part, even if didn't want…. side effects of being a PhD candidate.

Abstract

Poly(lactic acid) (PLA) is a biodegradable and renewable polyester, which is considered as the most promising eco-friendly substitute of conventional plastics. It is mainly used for food packaging applications, but some drawbacks still reduce its applications. On the one hand, its low barrier performance to gases (*e.g.* O_2 and CO_2) limits its use for applications requiring low gas transfer, such as modified atmosphere packaging (MAP) or for carbonate beverage packaging. On the other hand, its natural water sensitivity, which contributes to its biodegradation, limits its use for high moisture foods with long shelf life.

Other biopolymers such as wheat gluten (WG) can be considered as interesting materials able to increase the PLA performances. WG is much more water sensitive, but it displays better gas barrier properties in dry surroundings. This complementarity in barrier performances drove us to study the development of multilayer complexes PLA-WG-PLA and to open unexplored application scenarios for these biopolymers.

This project was thus intended to better understand how food components and use conditions could affect the performances of PLA films, and how these performances could be optimized by additional processing such as surface modifications (*e.g.* corona treatment and coatings).
To that aim, three objectives were targeted:

- To study the stability of industrially scale produced PLA films in contact with different molecules (CO_2 and water) and in contact with vapour or liquid phases, with different pH, in order to mimic a wide range of food packaging applications.
- To better understand the impact of some industrial processes such as corona or hot press treatments on PLA.
- To combine PLA with WG layer to produce high barrier and biodegradable complexes.

Different approaches coming from food engineering and material engineering were adopted. PLA films were produced at industrial scale by Taghleef Industries with specific surface treatments like corona. Wheat gluten films, coatings and layers were developed and optimized at lab scale as well as the 3-layers PLA-WG-PLA complexes. Different technologies able to mimic industrial processes were considered such as hot press, high pressure homogenization, ultrasounds, wet casting and spin coating. The physical and chemical properties of PLA films were then studied at the bulk and surface levels, from macroscopic to nanometer scale. The functional properties like permeability to gases (*e.g.* O_2 and CO_2) and water, gas and vapour sorption, mechanical and surface properties were also investigated.

Exposed to CO_2, PLA films exhibited a linear sorption behaviour with pressure, but the physical modifications induced by high pressure did not affect its use for food packaging. However, when exposed to moisture in both liquid and vapour state (*i.e.* environments from 50 to 100 % relative humidity (RH)), PLA was significantly degraded after two months at 50 °C (accelerated test) due to hydrolysis. This chemical

deterioration was evidenced by a significant decrease of the molecular weight, which consequently induced a loss of transparency and an increase of the crystallinity. The hydrolysis was accelerated when the chemical potential of water was increased, and it was surprisingly higher for vapour compared to liquid state. In addition, pH did not affect the rate of hydrolysis.

Knowing much better the limitation of PLA films, the challenge was to improve its functional properties by combining them with WG, as a high gas barrier bio-sourced and biodegradable polymer. The use of high pressure homogenization produced homogeneous WG coatings, with improved performances. This process was thus selected for making 3 layer complexes by assembly of a wheat gluten layer between two layers of PLA, together with corona treatment and hot press technologies.

Corona treatment applied to PLA physically and chemically modified its surface at the nanometer scale. It induced an enhancement of the PLA surface tension and of its polar contribution, as well as its barrier properties of around 20 %. A strong influence of the hot press technology on PLA was also observed. Hot press induced further crystallization in PLA, increasing its overall barrier properties to water and oxygen of approximately 60 %. Hot press was also found to be a suitable technology for producing the PLA-WG-PLA complexes. It induced a particular restructuration in WG coatings, which generated a reduced adhesion between layers, but unexpectedly improved the barrier properties to gases of the complexes. The barrier properties of PLA-WG-PLA complexes to water were improved from 10 to 20 times compared to WG, depending on the RH differential, while those to O_2 and CO_2 were also improved of same magnitude compared to PLA. This improvement can be considered satisfactory, considering that the transfer rates were determined in realistic conditions for food packaging application (50 % RH), and were comparable to high barrier conventional plastics such as poly(ethylenterephtalate) (PET), polyamide 6 (PA 6) or rigid poly(vinyl chloride) (PVC).

This project thus showed the real potential of biopolymer complexes such as PLA-WG-PLA as an eco-friendly and sustainable strategy for substituting conventional plastics for high barrier requirements for food products. These findings gave strong basis for going further on the processing aspects for industrial applications. Additionally the results of this project could motivate the investigations on multilayer complexes with PLA using other biopolymers/hydrocolloids with similar high barrier performances, coming from agro industrial waste or by products.

.

Riassunto

I materiali plastici convenzionali trovano impiego in tutti campi della nostra vita, specialmente nel settore del *packaging* alimentare, ed in seguito all'utilizzo contaminano e danneggiano il nostro ecosistema. Materiali plastici derivanti da risorse naturali e biodegradabili, come acido polilattico (PLA), sono attualmente disponibili sul mercato anche se caratterizzati da *performances* inferiori.

Questo progetto di dottorato è mirato 1) allo studio della stabilità di *film* di PLA a varie condizioni di stoccaggio come temperatura, umidità relativa, pH, o esposizione a vapori o gas; 2) a comprendere meglio le influenze di alcuni processi industriali come trattamento corona e *hot press* nelle proprietà dei *film* di PLA; 3) a sviluppare complessi multistrato tra *film* di PLA e di glutine che abbiano proprietà barriera più elevate rispetto ai singoli *film*.

Gli imballaggi a base di PLA sono stati prodotti da *Taghleef Industries*, produttore *leader* nel settore e dotato di infrastrutture atte ai trattamenti di modificazione di superfice come il trattamento corona. I film a base di glutine e i *coatings* sono stati sviluppati e ottimizzati su scala di laboratorio, così come i complessi trilaminari PLA-glutine-PLA.

Le proprietà fisiche e chimiche dei *film* di PLA sono state investigate a livello di superficie, così come a livello di *bulk*. Diverse tecniche analitiche, provenienti dal campo delle scienze dei materiali e delle scienze degli alimenti, sono state adottate in questo progetto di dottorato come calorimetria differenziale a scansione (DSC), termogravimetria (TGA), cromatografia di esclusione molecolare (SEC), microscopia a forza atomica (AFM), microscopia elettronica a scansione (SEM), spettrofotometria infrarossa a trasformata di Fourier in riflettanza totale attenuata (ATR-FTIR) e spettroscopia fotoelettronica a raggi X (XPS).

Le proprietà funzionali come le permeabilità al vapore acqueo (H_2O), all'ossigeno (O_2), al diossido di carbonio (CO_2) o all'elio (He) sono state investigate, cosi come l'assorbimento di gas e/o vapori, le proprietà meccaniche e le proprietà di superfice.

Nonostante i *film* di PLA assorbano linearmente CO_2 a pressioni crescenti, l'assorbimento di tale gas è ridotto a basse pressioni in modo da non modificare le sue proprietà fisiche – come contrariamente osservato quando il PLA è esposto a CO_2 ad alte pressioni – e da non influenzare negativamente il suo utilizzo come imballaggio alimentare. Ad ogni modo, quando i *film* di PLA sono esposti ad ambienti umidi, o quando sono immersi in acqua liquida, sono significativamente degradati per idrolisi dopo due mesi di stoccaggio a 50 °C (test accelerato). Questo deterioramento chimico è stato evidenziato da una significativa riduzione del peso molecolare del PLA che, conseguentemente, induce una sua perdita di trasparenza e ne incrementa la sua cristallinità. Inoltre, è stato evidenziato che il pH non influenza la velocità di idrolisi. Quest'informazione ha importanza pratica per possibili utilizzi di PLA come imballaggio di alimenti ad alta umidità.

Il glutine è stato scelto per le sue alte proprietà barriera, quando è protetto da ambienti ad alta umidità. Si è visto che l'incorporazione di lipidi non porta con sé grandi miglioramenti nelle *performances* dei *film* a base di glutine. Invece, l'utilizzo della tecnologia di omogeneizzazione ad alte pressioni permette una migliore dispersione del glutine, ottenendo *film* più omogenei e con migliori proprietà funzionali. Questa tecnologia è stata quindi scelta per produrre i complessi multistrato, intercalando i film di glutine tra due *film* di PLA, usando il trattamento *hot press* (10 MPa, 130 °C, 10 min). Si è osservato che il trattamento *hot press* modifica le proprietà dei *film* di PLA, di glutine e dei film multistrato *Hot press* induce cristallizzazione in PLA, e conseguentemente aumenta le sue proprietà barriera complessive, approssimativamente al 40 % all'acqua e al 60 % all'ossigeno.

Gli evidenti miglioramenti apportati dal trattamento *hot press* alle proprietà barriera dei film hanno mascherato quelli ottenuti in seguito al trattamento corona, quando le due tecniche sono state utilizzate contemporaneamente.

Hot press probabilmente induce una particolare re-strutturazione delle catene glutiniche in conseguenza ad un fenomeno di evaporazione d'acqua all'interfaccia glutine/PLA. Questo fenomeno di evaporazione inaspettatamente provoca un aumento delle proprietà barriera ai gas nei film multistrato ma, allo stesso tempo, riduce l'affinità tra gli strati, quindi l'adesione tra questi. Ulteriori azioni volte a ottimizzare la produzione dei *film* multistrato sono state pianificate con l'impiego di altre tecnologie a diposizione e utilizzando come parametri d'analisi l'umidità dell'acqua e lo spessore dei *coating*.

Résumé

Les plastiques sont aujourd'hui des matériaux ubiquitaires utilisés dans tous les aspects de notre vie quotidienne, en particulier pour l'emballage alimentaire. Cependant, après usage, les plastiques sont une source de pollution de notre environnement naturel. Certains plastiques biodégradables et biosourcés sont déjà disponibles sur le marché, comme l'acide polylactique (PLA), mais ils présentent des performances inférieures. Ce travail de thèse vise à: 1) étudier la stabilité des films de PLA dans diverses conditions de température, d'humidité relative, de pH, d'exposition à des liquides ou à des vapeurs... 2) mieux comprendre l'impact de certains procédés industriels tels que les traitements corona ou pressage à chaud sur le PLA 3) combiner le PLA à des couches de gluten de blé afin de produire des complexes ayant des propriétés barrière plus élevées.

Les films de PLA ont été produits par la société Taghleef Industries sur demande et avec des traitements de surface spécifiques, comme le traitement Corona. Des films et des enductions à basede gluten de blé ont été développés à l'échelle laboratoire ainsi que des complexes tricouches PLA- gluten-PLA. Les propriétés physiques et chimiques des films ont été étudiées par différentes techniques issues des sciences des matériaux et des aliments ont été utilisées, telles que l'analyse enthalpique différentielle (DSC), l'analyse thermogravimétrique (TGA), la chromatographie d'exclusion de taille (SEC), la microscopie de force atomique (AFM), la microscopie électronique (SEM), la spectroscopie infrarouge à transformée de Fourier (ATR-FTIR) et la spectroscopie de rayons X (XPS). Les propriétés fonctionnelles telles que la perméabilité à la vapeur d'eau, à l'oxygène (O_2), au dioxyde de carbone (CO_2) ou à l'hélium (He), la sorption de gaz et de vapeurs, les propriétés mécaniques et de surface ont également été étudiées.

Exposés au CO_2, les films de PLA présentent une isotherme de sorption linéaire avec l'augmentation de pression. Cependant les modifications physiques et chimiques induites à des pressions élevées n'affectent pas son utilisation dans le domaine d'application alimentaire. Au contraire, lorsque les films de PLA sont exposés à l'humidité à l'état liquide ou vapeur, leur dégradation survient après deux mois à 50 ° C (essai accéléré) suite à son hydrolyse. Cette détérioration chimique, mise en évidence par une diminution significative de la masse molaire, entraine une perte de transparence, mais également par une augmentation de la cristallinité. Par ailleurs, le pH n'affecte pas le taux d'hydrolyse, ce qui est d'un intérêt essentiel pour conditionner des aliments humides.

Les films à base gluten de blé ont été choisis pour leurs propriétés de barrière élevées lorsque l'humidité relative reste faible. L'incorporation de lipides n'a pas apporté d'amélioration de leurs performances barrières. Cependant, l'utilisation d'un procédé d'homogénéisation à haute pression a permis une meilleure dispersion du gluten, ce qui a conduit à des films plus homogènes ayant ainsi de meilleures propriétés fonctionnelles. Ces conditions ont donc été retenues pour réaliser des complexes à 3 couches par

assemblage d'une couche de gluten de blé entre deux couches de PLA en utilisant un pressage à chaud (10 MPa, 130 ° C, 10 min).

La technologie de pressage à chaud montre une forte influence sur les films de PLA, de gluten et sur les tricouches. Elle induit une cristallisation accrue du PLA, ce qui augmente ses propriétés de barrière d'environ 40% et 60%, respectivement pour l'eau et l'oxygène. Cela masque par contre l'effet du traitement corona. D'autre part, le pressage à chaud induit une restructuration du réseau de gluten qui améliore les propriétés de barrière aux gaz des complexes, mais provoque aussi une évaporation de l'eau à l'interface gluten / PLA défavorable à l'adhésion des couches. Une optimisation des procédés de fabrication des assemblages en 3 couches en contrôlant la teneur en eau de la couche de gluten de blé ainsi que son épaisseur sont donc envisagés.

Resumen

Los materiales plásticos tradicionales son utilizados en todos los campos de nuestra vida y en particular modo como embajales de productos alimenticios; los cuales después de ser utilizados contaminan y dañan nuesto medio ambiente. Materiales plásticos derivados de recursos naturales y biodegradables, como el ácido poliláctico (PLA) se encuentran actualmente disponibles en el mercado a pesar de sus menores *performances*. Este proyecto de doctorado está orientado 1) al estudio de la estabilidad de películas de PLA bajo diferentes condiciones como temperatura, humedad relativa, pH o exposición a vapores o gases, 2) comprender los efectos en las propiedades de las películas de PLA de algunos procesos industriales como el tratamiento corona y *hot press*, 3) desarrollar complejos multicapas de PLA y gluten que tengan propiedades barrera mejores que las de las películas individuales.

Los embalajes a base de PLA han sido producidos por *Taghleef Industries*, productor líder en el sector y dotado de las infraestructuras industriales adaptadas a los tratamientos superficiales como el tratamiento corona. Las películas de gluten y los *coatings* han sido desarrollados a escala de laboratorio, así como los complejos tricapa PLA-gluten-PLA.

Las propiedades físicas y químicas de las películas de PLA han sido investigadas a nivel de superficie así como a nivel de *bulk*. Diferentes técnicas de análisis, frecuentemente utilizadas en los campos de las ciencias de los materiales y de las ciencias de los alimentos, han sido empleadas en este proyecto como calorimetría diferencial de barrido (DSC), análisis termogravimétrico (TGA), cromotagrafía de exclusión por tamaño (SEC), microscopía de fuerza atómica (AFM), microscopía electrónica de barrido (SEM), espectroscopía de infrarrojos por transformada de Fourier con reflectancia total atenuada (ATR-FTIR) y espectroscopía fotoelectrónica de rayos X (XPS).

Las propiedades funcionales de los embalajes como las permeabilidades al vapor de agua, al oxígeno (O_2), al dióxido de carbono (CO_2) o al helio (He) han sido investigadas, asi como la absorción de gases/vapores, las propiedades mecánicas y las propiedades superficiales.

A pesar de que las películas de PLA absorven linealmente CO_2 a presiones mayores, la absorción del gas es reducida a bajas presiones y no modifica las propiedades físicas del PLA, como contrariamente sucede cuando el PLA es expuesto a altas presiones de CO_2. Por lo tanto, su influencia en las propiedades funcionales del PLA es mínima en las normales aplicaciones alimentarias. De todos modos cuando los embalajes de PLA son expuestos a ambientes húmedos o cuando son sumergidos en agua, procesos de hidrólisis los degradan significativamente después de dos meses de conservación a 50 °C (test acelerado). Este deterioramiento químico ha sido evidenciado por una significativa reducción del peso molecular del PLA, que en consecuencia induce una pérdida de transparencia y un aumento de su cristalinidad. Además,

se ha observado que el pH no influye en la velocidad de hidrólisis. Esta información tiene una importancia práctica para posibles usos del PLA como embalajes de alimentos a alta humedad.

El gluten ha sido elegido por sus altas propiedades barrera cuando es protegido de ambientes a alta humedad. La incorporación de lípidos en las películas de gluten no han mejorado sus *performances*. Pero la tecnología de la homogenización a altas presiones ha permitido mejorar la dispersión del gluten, obteniendo películas más homogéneas y con mejores propiedades funcionales. Esta tecnología ha sido, por lo tanto, elegida para producir los complejos multicapa, intercalando las películas de gluten entre dos de PLA, utilizando el tratamiendo *hot press* (10 MPa, 130 °C, 10 min). Se ha observado que el tratamiento *hot press* modifica fuertemente las propiedades de las películas de PLA, de gluten y los complejos multicapa. *Hot press* induce cristalinización en PLA, y en consecuencia aumenta sus propiedades barrera en general, aproximadamente del 40 % al agua y del 60 % al oxígeno.

Los evidentes mejoramientos dados a las propiedades barrera de las películas por el tratamiento *hot press* han cubierto los efectos del tratamiendo corona, cuando ambas técnicas han sido utlizadas contemporáneamente. *Hot press* probablemente provoca una particular restructuración de las cadenas poliméricas del gluten, como consecuencia de un fenómeno de evaporación de agua que se verifica al interfaz gluten/PLA. Este fenómeno de evaporación inesperadamente ha provocado un aumento de las propiedades barrera a los gases de los complejos multicapa, pero al mismo tiempo ha reducido la afinidad de las capas, produciendo poca adhesión entre ellos. Acciones adicionales con el objetivo de optimizar la producción de los complejos multicapa han sido planificados con el uso de otras tecnologías, controlando parámetros como humedad del agua y el espesor de los *coatings.*

Curriculum Vitae

Professional Experiences

2014-17 *(3 years)* **PhD student in Food Science**
Supervisors: Prof. Alessandro Sensidoni, Dr. Thomas Karbowiak, Prof. Frederic Debeaufort.

2013 *(10 months)* **Scholar,** Department of Food Science, University of Udine (Udine, Italy).
Supervisors: Prof. Alessandro Sensidoni and Dr. Eva Marcuzzo.
Projects: Study on wheat gluten edible films and Study of stability of commercial ready to eat foods.

2011 *(11 months)* **Visiting Scholar (M.S. thesis)**, Department of Food Science and Nutrition, University of Minnesota (Saint Paul, USA).
Supervisors: Prof. Theodore P. Labuza and Dr. Qinchun Rao.
Project: Egg protein aggregation.

2008-09 *(1 year)* **Logistician**, Transportes Chiavari (Lima, Peru).

2008 *(3 months)* **Quality assurance assistant and quality control technician,** Molinera del Centro S.A (Lima, Peru).

2007 *(6 months)* **Scholar (B.S. thesis)**, Department of Food Science, University of Udine (Udine, Italy).
Supervisor: Prof. Monica Anese.
Project: Acrylamide in cookies.

2006 *(2 months)* **Internship production of sugar from sugar cane**, Agroindustrias San Jacinto (Ancash, Peru), Azucarera del Norte (Lambayeque, Peru).

Educational Experiences

2014-17 **PhD student in Food Science**, University of Udine and University of Burgundy, dual supervision PhD, grade: *très honourable.*

2009-13 **M.S. in Food Science and Technology,** University of Udine, grade: 110/110 *cum laude.*

2003-08 **B.S. in Food Science and Technology,** University of Udine, grade: 110/110 *cum laude.*

2003 Equivalence of the Peruvian secondary school qualification with the scientific Italian secondary school qualification.

Theses

PhD	A contribution of understanding the stability of commercial PLA Films for food packaging and its surface modifications (wrote in English). *Advisors:* Prof. Alessandro Sensidoni, Dr. Thomas Karbowiak, Prof. Frederic Debeaufort. *Related scientific articles:* 5 papers were published and 1 is planned to be submitted.
M.S.	Stability of egg white protein and hydrolysates in model systems (wrote in English). *Advisors:* Prof. Theodore P. Labuza, Dr. Qinchun Rao and Dr. Lara Manzocco *Related scientific articles:* 3 papers were published.
B.S.	Effect of heat pre-treatments on acrylamide production in baked products (*Effetto di pretrattamenti termici sulla formazione di acrilammide*, wrote in Italian). *Advisor:* Prof. Monica Anese.

Languages

Spanish	Native speaker
Italian	C2
English	C1
French	Learning

List of publications and communications

Articles

Rocca-Smith, J. R.; Karbowiak, T.; Marcuzzo, E.; Sensidoni, A.; Piasente, F.; Champion, D.; Heinz, O.; Vitry, P.; Bourillot, E.; Lesniewska, E.; Debeaufort, F. Impact of corona treatment on PLA film properties. *Polymer Degradation and Stability* 2016, *132*, 109-116.

Rocca-Smith, J. R.; Marcuzzo, E.; Karbowiak, T.; Centa, J.; Giacometti, M.; Scapin, F.; Venir, E.; Sensidoni, A.; Debeaufort, F. Effect of lipid incorporation on functional properties of wheat gluten based edible films. *Journal of Cereal Science* 2016, *69*, 275-282.

Rocca-Smith, J.R.; Lagorce-Tachon, A.; Iaconelli, C.; Bellat, J.P; Marcuzzo, E.; Sensidoni, A.; Piasente, F.; Debeaufort, F.; Karbowiak, T. How high pressure CO_2 impacts PLA film properties. *Express Polymer Letters* 2017, *11*, 320-330.

Rocca-Smith, J.R.; Chau, N.; Champion, D.; Brachais C.-H.; Marcuzzo, E.; Sensidoni, A.; Piasente, F.; Karbowiak, T.; Debeaufort, F. Effect of the state of water and relative humidity on ageing of PLA film *Food Chemistry* 2017. Doi: 10.1016/j.foodchem.2017.02.113

Rocca-Smith, J.R.; Whyte, O.; Brachais, C.-H.; Champion, D.; Piasente, F.; Marcuzzo, E.; Sensidoni, A.; Debeaufort F. and Karbowiak T. Beyond biodegradability of PLA: physical and chemical stability in humid environments. *ACS Sustainable Chemistry & Engineering* 2017, *5*, 2751-2762

Rocca-Smith J.R; Pasquarelli R.; Lagorce-Tachon A.; Rousseau J.; Fontaine S.; Karbowiak T. and Debeaufort F *PLA/protein complex gluten films: multilayer process and properties* (to be submitted to ACS Applied Materials and Interfaces).

Oral communications

Rocca-Smith, J.R.; Karbowiak, T.; Marcuzzo, E.; Sensidoni, A.; Piasente, F.; Vitry P.; Bourillot, E.; Debeaufort F. Impact of corona treatment on PLA film properties. *MATBIM 2015, 3rd International Conference on Packaging Material/Bioproduct Interaction*, Zaragoza, Spain, 17-19 June 2015.

Rocca-Smith, J.R.; Chau, N.; Brachais, C-H; Marcuzzo, E.; Sensidoni, A.; Piasente F., Karbowiak T., Debeaufort F. Accelerated stability testing of PLA under wet conditions. *EuroFoodWater 2016, the 9th International Conference on Water in Food, 2016,* Leuven, Belgium, 22-24 May.

Rocca-Smith, J.R.; Chau, N.; Brachais, C-H; Marcuzzo, E.; Sensidoni, A.; Piasente, F.; Karbowiak, T.; Debeaufort F. Accelerated stability testing of PLA under wet conditions. *FJC 2016, 22e Forum des Jeunes Chercheurs*, Besanson, 16 – 17 June.

Rocca-Smith, J.R.; Karbowiak, T.; Champion, D.; Marcuzzo, E.; Sensidoni, A.; Piasente, F.; O Connell, D.; Debeaufort, F. Stability of PLA at temperatures far and close Tg in dry and wet environments. *ISOPOW XIII. International Symposium on the Properties of Water*, Lausanne, Swirzerland, 26 – 29 June 2016.

Rocca-Smith, J.R.; Pasquarelli, R.; Largorce-Tachon, A.; Rousseau, J.; Fontaine, S.; Karbowiak T.; Debeaufort F. PLA/protein complex films: multilayer process and properties. *MATBIM 2017, 4th International Conference on Packaging Material/Bioproduct Interaction*, Porto, Portugal, 26-28 April 2017 (Abstract submitted on 12/01/2017).

Poster communications

Rocca-Smith, J.R.; Sensidoni, A.; Debeaufort, F. Study of Coatings and Surface Modification and Characterizations of PLA Based Films for Food Packaging, *19th Workshop on the Developments in the Italian PhD Research on Food Science Technology and Biotechnology*, 24-26 September 2014, Bari, Italy.

Rocca-Smith, J.R.; Marcuzzo, E; Giacometti, M; Scapin F; Karbowiak, T; Debeaufort, F; Sensidoni, A. Effect of thickness of wheat gluten-based edible films on surface hydrophilicity and water vapour permeability. *18th Gums & Stabilisers for the Food Industry Conference - Hydrocolloid functionality for affordable and sustainable global food solutions*, June 23-26, 2015, Wrexham, UK.

Rocca-Smith, J.R.; Marcuzzo, E; Centa, J.; Karbowiak, T; Debeaufort, F; Sensidoni A. Effect of water activity on mechanical properties of wheat gluten-based edible films. *18th Gums & Stabilisers for the Food Industry Conference - Hydrocolloid functionality for affordable and sustainable global food solutions*, June 23-26, 2015, Wrexham, UK.

Rocca-Smith, J.R; Marcuzzo, E.; Centa, J.; Karbowiak, T.; Debeaufort, F. Sensidoni, A. Effect of water activity on mechanical properties of wheat gluten-based edible films. *MATBIM 2015, 3rd International Conference on Packaging Material/Bioproduct Interaction*, Zaragoza, Spain, 17-19 june 2015.

Rocca-Smith, J.R.; Karbowiak, T.; Marcuzzo, E.; Sensidoni, A.; Piasente, F.; Vitry, P. ; Bourillot, E.; Debeaufort F. Impact of corona treatment on PLA film properties. *21° Forum des Jeunes Chercheurs*, June 18 – 19, 2015, Dijon, France.

Rocca-Smith, J.R.; Sensidoni, A.; Debeaufort, F. Study of Coatings and Surface Modification and Characterizations of PLA Based Films for Food Packaging, *20th Workshop on the Developments in the Italian PhD Research on Food Science Technology and Biotechnology*, 23rd – 25th September, Perugia, Italy.

Rocca-Smith, J.R.; Karbowiak, T.; Lagorce-Tachon, A.; Bellat, J.P.; Marcuzzo, E.; Sensidoni, A.; Piasente, F.; Debeaufort, F. Effect of CO_2 sorption on PLA properties. *Biopol 2015*, *5th International Conference on Biobased and Biodegradable Polymers*, 6 – 9 October, 2015, Donostia – San Sebastian, Spain.

Rocca-Smith, J.R.; Karbowiak, T.; Champion, D.; Marcuzzo, E.; Sensidoni, A.; Piasente, F.; O Connell, D.; Debeaufort F. Changes in PLA structure and properties when ageing at various RH and temperatures far and close Tg. *Biopol 2015, 5th International Conference on Biobased and Biodegradable Polymers*, 6 – 9 October, 2015, Donostia – San Sebastian, Spain.

Rocca-Smith, J.R.; Karbowiak, T.; Champion, D.; Marcuzzo, E.; Sensidoni, A.; Piasente, F.; O Connell, D.; Debeaufort F. Influence of temperature and relative humidity on PLA ageing. *EuroFoodWater 2016, the 9th International Conference on Water in Food*, 2016, Leuven, Belgium, 22-24 May.

Rocca-Smith, J.R.; Chau, N.; Brachais, C-H; Karbowiak T.; Debeaufort F. PLA ageing kinetics as a function of the state of water in contact: impact on structure and functional properties. *MATBIM 2017, 4th International Conference on Packaging Material/Bioproduct Interaction*, Porto, Portugal, 26-28 April 2017 (Abstract submitted on 12/01/2017).

List of abbreviations

α	confidence level (5%)
ε_b	elongation at break (%)
ε_y	yield elongation (MPa)
θ	contact angle (°)
ϑ	lag time (s)
σ_b	tensile strength (MPa)
σ_y	yield strength (MPa)
γ_s	surface tension of film (mN·m^{-1})
γ_s^p	polar contribution to surface tension of film (mN·m^{-1})
γ_s^d	dispersive contribution to surface tension of film (mN·m^{-1})
γ_l	surface tension of liquid (mN·m^{-1})
γ_l^p	polar contribution to surface tension of liquid (mN·m^{-1})
γ_l^d	dispersive contribution to surface tension of liquid (mN·m^{-1})
Δm	weight loss (g)
ΔC_p	change of specific heat (J·g^{-1}·°C^{-1})
ΔC_{p1}	first change in specific heat (J·g^{-1}·°C^{-1})
ΔC_{p2}	second change in specific heat (J·g^{-1}·°C^{-1})
ΔC_p^0	variation of specific heat corresponding to a 100% amorphous PLA (J·g^{-1}·°C^{-1})
ΔH_{cc}	enthalpy of cold crystallization (J·g^{-1})
ΔH_m	enthalpy of melting (J·g^{-1})
ΔH_m^0	enthalpy of melting of pure component (J·g^{-1})
ΔH_{relax}	enthalpy of relaxation (J·g^{-1})
$A_b(t)$	base area of the water drop at time t (mm^2)
AFM	atomic force microscopy
ATR-FTIR	attenuated total reflectance Fourier transform infrared analysis
% RH	relative humidity
ANOVA	one–way analysis of variance
ASTM	American Society for Testing and Materials
a_w	water activity
BET model	Brunauer-Emmet-Teller model
Bio-PE	biobased polyethylene
Bio-PET30	30 % biobased poly(ethylenterephtalate)
C	surface heat constant of the GAB equation
CT	corona treated PLA films

CT-hot press	CT films submitted to hot press treatment
CT-treated	surface treated by corona of CT films
CT-untreated	untreated surface of CT films
CT/WG/CT	trilayer complex developed by hot press, from preformed single layers
CT+WG/CT	trilayer complex developed by hot press, from preformed bilayers (CT+WG) and additional CT layer
D	diffusion coefficient ($m^2 \cdot s^{-1}$)
D_{sorp}	diffusion coefficient calculated from sorption isotherm ($m^2 \cdot s^{-1}$)
D_{perm}	diffusion coefficient calculated from permeability measurements ($m^2 \cdot s^{-1}$)
$d_{4:3}$	mean volume diameter
d_{air}	gas density under atmospheric pressure ($g \cdot cm^{-3}$)
d_g	measured density of the gas ($g \cdot cm^{-3}$)
DSC	differential scanning calorimetry
E.B.	elongation at break (%)
EVOH	ethylene vinyl alcohol
EWG	emulsified wheat gluten film with lipid phase
EWG-air	surface of EWG films exposed to air during film drying
EWG-support	surface of EWG films in contact with the support during film drying
E_{Young}	Young's modulus (GPa)
FAOSTAT	Food and Agriculture Organization of the United Nations Statistics Division
GAB equation	Guggenheim-Anderson-de Boer equation
GTR	gas transfer rate ($mol \cdot m^{-2} \cdot s^{-1}$)
GTR_{CO_2}	carbon dioxide transfer rate ($mol \cdot m^{-2} \cdot s^{-1}$)
GTR_{O_2}	oxygen transfer rate ($mol \cdot m^{-2} \cdot s^{-1}$)
interface WG/PLA	interface WG/PLA formed by hot press
interface WG+PLA	interface WG+PLA formed by wet casting or spin coating
k	multilayer factor of the GAB equation
k_{app}	apparent rate constant
k_{gt}	adjustable parameter of the Gordon-Taylor equation
l	thickness of the membrane (m)
LWTR	liquid water transfer rate ($g \cdot m^{-2} \cdot s^{-1}$)
MAP	modified atmosphere packaging
m	moisture content (weight percentage in dry basis)
m_0	monolayer moisture content of the GAB equation (weight percentage in dry basis)
m_{app}	sum of apparent mass of the sample and the mass of the empty pan (g)

m_{Ar}	mass of the sample at equilibrium and after been corrected by the Archimedes buoyancy (g)
m_{exp}	experimental values of the total amount of sorbed (or desorbed) CO_2 (g)
m_{mod}	modeled values of the total amount of sorbed (or desorbed) CO_2 (g)
m_{∞}	total amount of sorbed CO_2 (or desorbed CO_2) at equilibrium (g)
m_p	mass of the empty pan (g)
m_t	total amount of sorbed CO_2 (or desorbed CO_2) at time t (g)
m_{wt}	wet mass of the sample at time t (g)
m_{dt}	dry mass of the sample at time t (g)
m_{di}	initial dry mass of the sample (g)
$\overline{M_n}$	number average molecular weight ($g \cdot mol^{-1}$)
$\overline{M_w}$	weight-average molecular weight ($g \cdot mol^{-1}$)
$\overline{M_{n0}}$	number average molecular weight of initial PLA ($g \cdot mol^{-1}$)
$\overline{M_{w0}}$	weight average molecular weight of initial PLA ($g \cdot mol^{-1}$)
NCT	non-corona treated films
NCT-A	surface A of the NCT film
NCT-B	surface B of the NCT film
NCT-hot press	NCT films submitted to hot press treatment
NCT/WG/NCT	trilayer complex developed by hot press, from preformed single layers
NCT+WG/NCT	trilayer complex developed by hot press, from preformed bilayers (NCT+WG) and additional NCT layer
P	permeability ($mol \cdot m^{-1} \cdot s^{-1} \cdot Pa^{-1}$)
P_{CO_2}	CO_2 permeance ($mol \cdot m^{-2} \cdot s^{-1} \cdot Pa^{-1}$)
P_{H_2O}	water vapour permeance ($g \cdot m^{-2} \cdot s^{-1} \cdot Pa^{-1}$)
P_{O_2}	O_2 permeance ($mol \cdot m^{-2} \cdot s^{-1} \cdot Pa^{-1}$)
PA	polyamide
PBAT	poly(butylene adipate-co-terephthalate)
PBS	poly(butylene succinate)
PCL	poly(caprolactone)
PDI	polydispersity index
PE	polyethylene
PEG	poly(ethylene glycol)
PET	poly(ethylene terephthalate)
PHA	poly(hydroxyalkanoates)
PLA	poly(lactic acid)
PLA/WG/PLA	trilayer complex formed by hot press, from preformed single layers

PLA+WG/PLA	trilayer complex formed by hot press, from preformed bilayers (PLA+WG) and additional PLA layer
PLA-WG-PLA	a general trilayer complex having a WG coating layer intercalated to two layers of PLA
PMMA	poly(methyl methacrylate)
PS	polystyrene
PTFE	poly(tetrafluoroethylene)
PTT	poly(trimethylene terephthalate)
PVA	poly(vinyl alcohol)
PVC	poly(vinyl chloride)
PVDC	poly(vinylidene chloride)
R^2	coefficient of determination
RH	relative humidity
R_{rms}	root mean squared roughness (nm)
S	solubility coefficient
S_{perm}	solubility coefficient calculated from manometric method ($mol \cdot m^{-3} \cdot Pa^{-1}$)
S.D.	standard deviation
SEC	size-exclusion chromatography
SEM	scanning electron microscopy
T.S.	tensile strength (MPa)
$t_{\alpha/2;n-2}$	is a value of *t* distribution
TD	transversal direction to process line
T_{cc}	temperature of cold crystallization (°C)
T_g	glass transition temperature (°C)
$T_{g\ onset}$	onset temperature of glass transition (°C)
T_{g1}	first glass transition temperature (°C)
T_{g2}	second glass transition temperature (°C)
T_{gm}	glass transition temperature of the mixture (°C)
T_m	temperature of melting (°C)
TGA	thermogravimetric analysis
V_p	the volume of the pan containing the sample (cm^3)
V_s	sample volume (cm^3)
W_a	work of adhesion ($mN \cdot m^{-1}$)
WAXS	wide-angle X-ray scattering
WG	wheat gluten films
WG- high pressure	WG films obtained with pressure homogenization treatment

WG- no high pressure	WG films obtained without pressure homogenization treatment
WG-air	surface of WG films exposed to air during film drying
WG-support	surface of WG films in contact with the support during film drying
wt%	weight percent (%)
WVTR	water vapour transfer rate ($g \cdot m^{-2} \cdot s^{-1}$)
X_c	crystallinity degree (%)
X_c^0	crystallinity percentage of initial PLA (%)
X_{MAP}	mobile amorphous phase (%)
X_{RAF}	rigid amorphous fraction (%)
Y.M.	Young's modulus (MPa)
XPS	X-ray photoelectron spectroscopy

TABLE OF CONTENTS

INTRODUCTION

Introduction

It is an undeniable fact that conventional plastics (*i.e.* oil based and non-biodegradable) have transformed our society since the beginning of their industrial production in the late 1940's.[1] Conventional plastics are nowadays ubiquitous materials, which are used in almost all aspects of our daily life such as in clothes, furniture, transportation, construction, heath care, electronics and packaging. The global production of conventional plastics has exponentially increased over the last half century (Figure 1). It reached 322 million tons in 2015 and it is estimated to double in the next 20 years.[2-3] They make our life more comfortable and also bring high economic benefits to our society. In Europe the conventional plastic industry employed more than 1.5 million people and generated a turnover above 340 billion euros in 2015.[2]

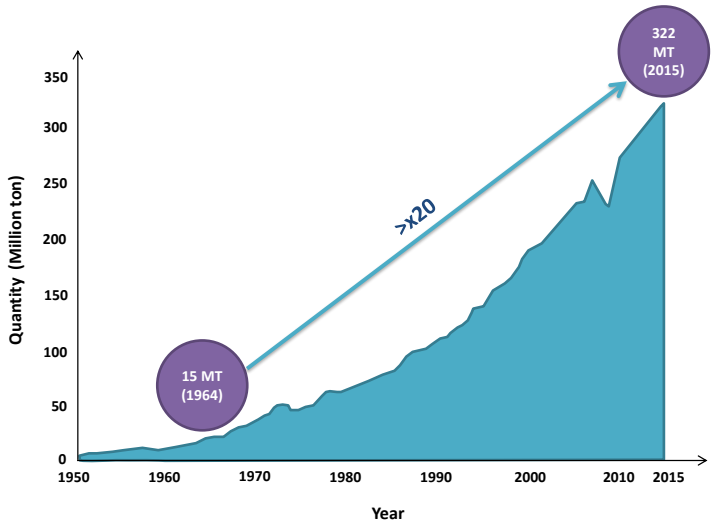

Figure 1. *Production of conventional plastics from virgin petroleum feedstock. It does not include bio-based, greenhouse gas-based or recycled feedstock (adapted from reference 3).*

Nevertheless, it is also unquestionable that after being used, conventional plastics pollute and negatively affect our natural environment. They contribute to the global warming when buried for energy recovery. They can last for a long time (several hundred years) as a waste product in landfills, contaminating lands that would be useful in the future. Additionally, if they do not extend to the waste management system, they are accumulated in natural environments, reaching the most remote areas of the planet as plastic debris.[4] It has been estimated that at least 8 million tons reach the ocean every year.[5] The quantity of conventional plastics in the ocean has recently valued to be higher than 150 million tons[6] and represents a serious risk for wildlife (*e.g.* marine species, birds, mammals).[4] Animals can ingest these contaminants or be entangled in them, causing lacerations, reduced fertility and death.[4, 7] Moreover, conventional plastic wastes are also vectors of harmful chemicals. They transport and release toxic molecules to the environment, such as bisphenols or phthalates, increasing the risk for the environment as well as for the human health.[1, 8] As a result of these negative externalities, the United Nations Environment Program

estimated in 2014 the total natural cost of conventional plastics over 75 billion dollars, of which more than 50 % was associated to plastic packaging. This amount exceeded the profit of plastic packaging industry.[3, 9]

A significant strategy to mitigate the environmental issues related to conventional polymers is to gradually replace them with more eco-friendly materials, called bioplastics. Bioplastics are a new generation of polymers that are either derived from natural resources, or are biodegradable, or have both properties. Bioplastics might thus be polymers derived from nature, and/or be able to return to nature (Figure 2). [10-11]

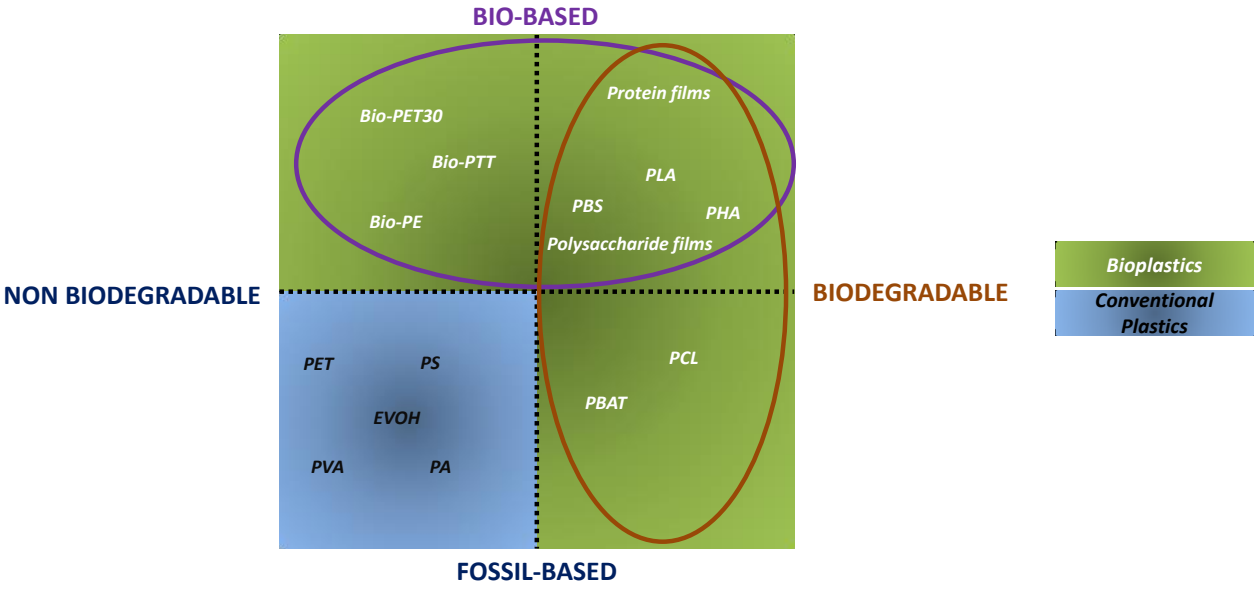

Figure 2. *Bioplastic material coordinate system (adapted from reference 10).*
EVOH = Ethylene vinyl alcohol, PA = Polyamide, PBAT = poly(butylene adipate-co-terephthalate), PBS = poly(butylene succinate), PCL = poly(caprolactone), PE = polyethylene, PET = Poly(ethylenterephtalate), PHA = poly(hydroxyalkanoates), PLA= poly(lactic acid), PS = polystyrene, PTT = poly(trimethylene terephthalate), PVA = poly(vinyl alcohol).

The world production of bioplastics reached around 1.7 million tons in 2014.[10] Although it represented less than 1 % of the world production of conventional plastics, the bioplastic market has been continuously growing over the last years, and it is estimated to quadruple in 2019.[10]

Different types of bioplastic materials are currently produced. 30 % biobased poly(ethylenterephtalate) (Bio-PET30), poly(lactic acid) (PLA) and biobased polyethylene (Bio-PE) are the most representative bioplastics in the market, sharing 35.4, 12.2 and 11.8 % of the bioplastic capacities in mass, respectively (Figure 3).[10] Between these three top ones, only PLA meets both the criteria of bio-sourcing and biodegradability, while the other two are partially bio-based and not biodegradable.

Although their industrial application is not extended as the over-mentioned materials, self-supported films based on proteins (*e.g*. wheat gluten, gelatine, zein) and polysaccharides (*e.g*. chitosan, carrageenan, pectin) can be also considered promising bioplastics, particularity when they are obtained from agro-food-industry waste or by-products. The polymer matrix of these materials is mainly constituted by bio-macromolecules directly extracted from biomass. They are hence intrinsically biodegradable, and according

to the processing conditions they can be used as well as edible packaging. However, their main drawback to overcome is their hydrophilicity.

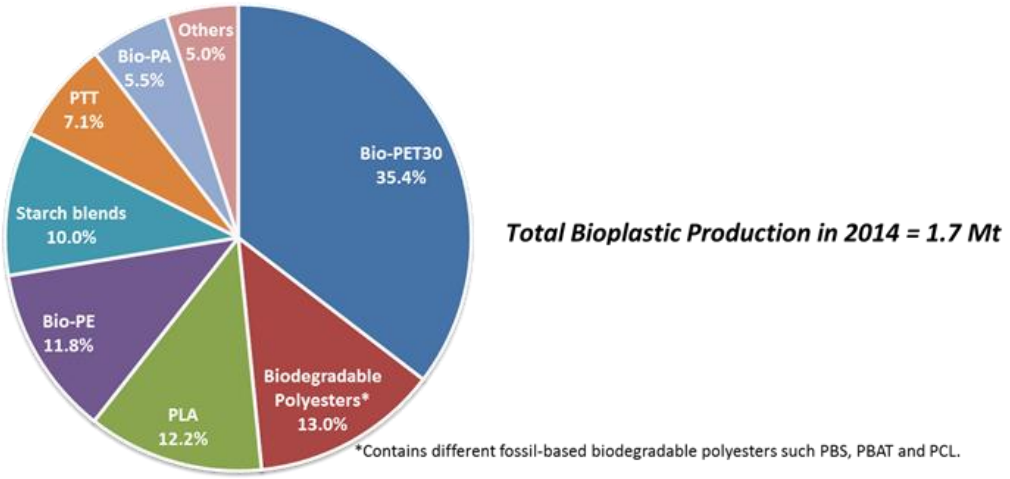

Figure 3. *Global production of bioplastics in 2014 (adapted from reference 10).*

PLA, an industrial polyester, is thus considered as the most promising substitute of conventional plastics.[12-13] It derives from natural carbohydrates sources such as corn starch, sugar cane, wheat straw and wood ships.[14] PLA can be produced and converted into biomass in similar time frames, helping to replenish the carbon cycle.[14-15]

The production of PLA goods involves several steps that could be summarized as lactic acid production, polymerization and industrial processing (Figure 4). More precisely, the biomass is converted into lactic acid molecules via enzymatic hydrolysis and microbial fermentation of carbohydrates. The lactic acid molecules are then polymerized to PLA. PLA producers mainly use three chemical processes for obtaining PLA at high molecular weight (>100 kDa): i) ring opening polymerization of lactides, ii) azeotropic dehydration condensation or iii) direct condensation polymerization.[13] The most frequently chemical method used is the ring opening polymerization of lactides, which consists in a controlled formation of the cyclic dimers of lactic acid (*L*- lactide, *D*-lactide and *meso*-lactide) followed by their polymerization with a catalyst. The obtained PLA polymer can then be processed using the conventional manufacturing techniques like extrusion, injection moulding, blow moulding, cast film extrusion and thermoforming, in order to achieve different PLA goods such as films, rigid containers, bottles and others. After been exposed to different environment conditions according to their application, the PLA goods can be fully biodegraded or recycled.[12-14]

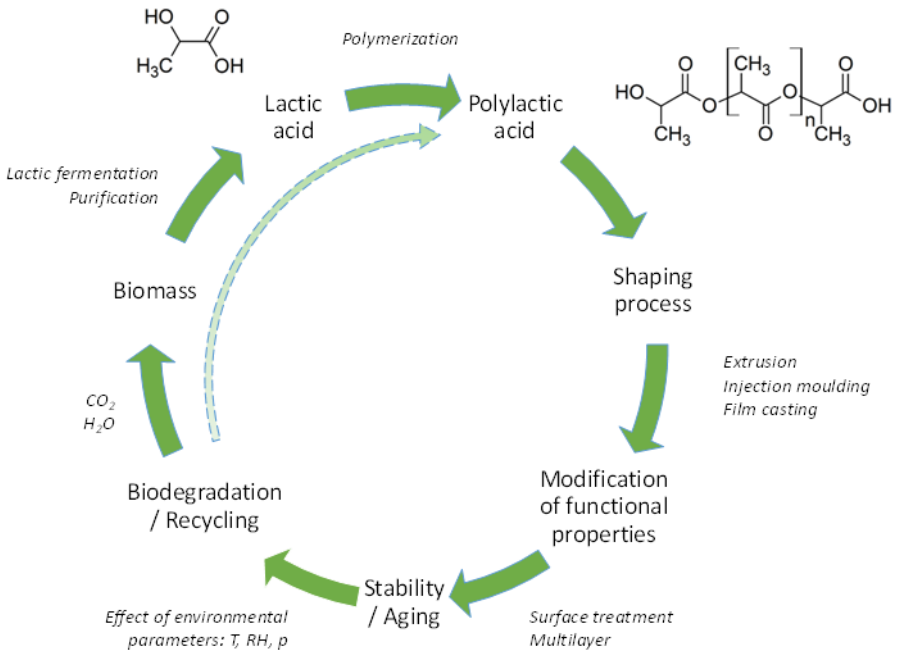

Figure 4. *Life cycle of PLA packaging*

PLA has been largely studied over the last two decades not only because of its eco-friendly nature, but also because of its high versatility (Figure 5). Compared to other biopolymers, PLA benefits of an interesting balance between cost, functional properties and processibility. Its overall properties can be tailored and improved with a relative easiness according to the final application (*e.g.* food packaging, 3D printing, bio-medical devises).

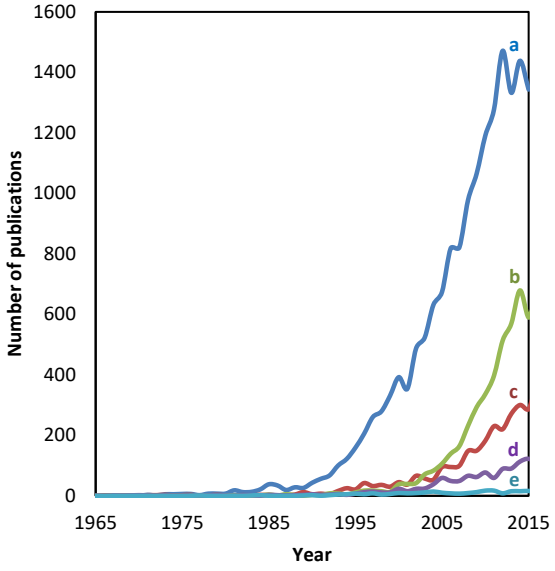

Figure 5. *Number of publications per year from 1965 to 2015 using as keywords: a) Poly (lactic acid); b) PLA composites, PLA biocomposites, PLA blends; c) edible films, edible coatings; d) PLA layers, PLA laminates, PLA multilayers, PLA bilayers; e) wheat gluten films. Research done in Scopus on November 2016.*

Different strategies aiming at modifying bulk and surface properties of PLA are studied and adopted by research and industry to increase the PLA applications.[16-17]

On the one hand, the bulk modification strategies mainly play with the physical structure (amorphous and crystalline phases) and the chemical composition of the PLA matrix, having a strong impact on the stability, through changes in the mechanical and thermal properties. Some technologies directly correlated to these strategies are processing manipulation (*e.g.* annealing, bi-orientation, super critical CO_2 sorption),[18-21] copolymerization, (*e.g.* PLA-PHA, PLA-PEG), sterochemical manipulation (*e.g.* lactide sterochemical composition, crystal sterocomplexation),[22-24] molecular architecture manipulation,[25] and blending with other substances like conventional polymers, bio-polymers,[26-30] natural antioxidants,[31] nanofillers,[32] plasticizers and chemical additives.

On the other hand, the surface modification technologies are principally used to tailor the roughness, surface chemistry and topography of PLA in order to enhance (or reduce) the interactions at the interface like adhesion/friction with other materials, wettability with liquids and sorption/release of specific molecules. Some technologies able to modify the PLA surface are biomolecules entrapment,[33] coatings,[34] plasma/corona treatments[35-36] and photografting.[37] A combination of these technologies makes possible to produce PLA-based goods for numerous applications.

The world production of PLA exceeded 207 thousand tons in 2014, and it is estimated to double in 2019.[10] The main application of this polyester is nowadays as packaging of foods, beverages and cosmetics, and they will probably last in the near future.[10] Nevertheless, PLA is also successfully used in others areas such as serviceware, bio-medical, fibres and textiles, plasticulture, electronics, automobile appliances and 3D printing, which are all expected to have a higher importance in the future.[10, 14]

Food corporations such as Danone (Germany), Del Monte (USA) and Noble Juice (USA), as well as leading food retailers such as Wal-Mart (USA), SPAR (Austria) and Auchan (France) are currently using PLA based packaging in some of their products.[14] Various types of food products are currently packed and commercialized with PLA based materials. They are characterized by different physical states, a wide range of water activity (a_w), pH and composition. Some examples are potato chips (amorphous solids, a_w = 0.1 – 0.3), fresh salads and vegetables (biological gels, a_w > 0.99), yogurts (gels, a_w > 0.99), citrus juices (acidic liquids, a_w = 0.97 – 0.99) and water (liquid, a_w > 0.99) (Figure 6).

* Withdrawn from the market because loud crinkling noise

Figure 6. *Examples of commercial applications of PLA as food packaging (images taken from Natureworks and brands website).*

Although there is a general interest to increase the trade of food products packed in PLA, several factors are currently limiting its application as a food packaging.

PLA displays lower barrier performances to water vapour, oxygen (O_2), carbon dioxide (CO_2) and nitrogen (N_2) compared to high barrier performance plastics, such as poly(ethylenterephtalate) (PET), polyamide (PA), poly(vinylidene chloride) (PVDC) or poly(vinyl alcohol) (PVA).[12-13] It limits the PLA applications in Modified Atmosphere Packaging (MAP) or (carbonated) beverages. Developing PLA based materials able to substitute these high performing plastics is thus an eco-friendly challenge for the near future. It could open new market scenarios for PLA, especially considering the high demand of individual (or reduced doses) of ready to eat and fresh products like meet, fish and cheese.

Another factor which reduces the use of PLA is its inherent water sensitivity. Even though PLA sorbs small quantities of water (< 1.1 wt% at T = 25 °C and close to saturation),[13, 38] it reacts with water molecules, and is hydrolysed during time, compromising the performance of the PLA material. As a consequence, industries generally guaranty six months of storage, which is low compared with long shelf-life food applications.

Another issue to face is the undesirable crinkling noise that PLA makes when it is handled. This problem was behind the withdrawn of chips bags from the market of a world leader company (Sunschips from Frito Lay) in 2014. The consumers did not well accepted the load crinkling noise from the packaging, even if the snack was commercialized as the world's first 100 % compostable chips package (Figure 7).[14]

Figure 7. *The Sunchips packaging (images taken from internet).*

Protein based and polysaccharide based films could help in reducing some of the limiting factors of PLA, without compromising the PLA biodegradability properties. These films are raising bioplastics, which have been principally studied by food scientist as edible films since the late 80's (Figure 5). Most of the advances in understanding their films properties have been reached in that research area.

These materials benefit of complementary properties than PLA. Indeed, they show much lower permeability to gases in dry conditions, sometimes similar than high barrier performance plastics. However, they display a higher permeability to water and higher water sensitivity.[39] It results hence evident that

complexes PLA + protein or PLA + polysaccharide could improve the overall properties of these materials and to overcome the drawbacks related to mass transfer.

The main approach currently adopted to produce complexes of PLA with another polymer is to create a blended or a composite morphology (Figure 5). This strategy consists in creating two or more distinct phases, where one phase (or more) is dispersed in another continuous phase. The discontinuous phase is constituted by another polymer, inorganic materials or fibres and according to the dimensions of the dispersive phase and to the source of the materials; it can be called blends, composites, nanocomposites or bio-composites. Although this strategy can be considered as effective enough to tailor the properties of PLA, it is not the most efficient approach to increase its barrier properties.

From a theoretical point of view, creating a laminate or multi-layered structure regarding the permeation path of molecules should be a more efficient structure, by taking maximum advantage of continuous phases (as layers or laminates) with complementary barrier performances.[34] Nevertheless, creating laminate complexes between bio-macromolecules, such as proteins, with polyesters, like PLA, is a real challenge. If these materials show complementary characteristics, their compatibility is a real challenge to overcome since they are thermodynamically immiscible (Figure 8). Protein based films are hydrophilic materials, while PLA can be considered as hydrophobic. Such difference might generate a non-appropriate adhesion of layers, which is of significant importance in food packaging applications. Adhesion failure could generate leakage, increase the rate of quality lost (physical changes, chemical reactions) and raise the risk of microbial contamination.

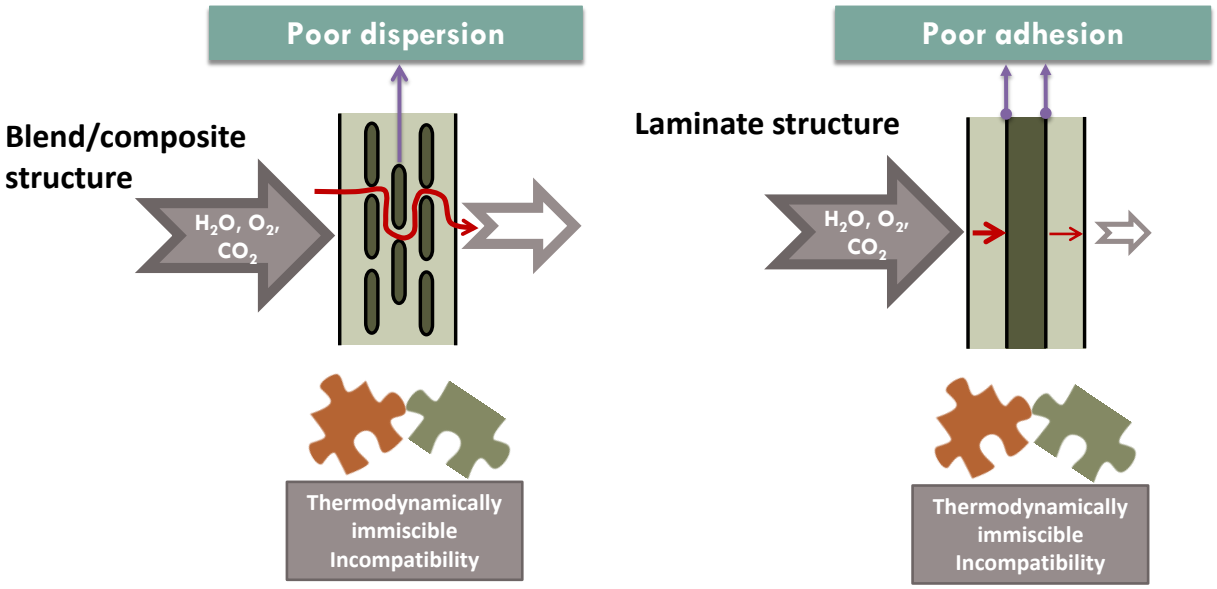

Figure 8. *Diagram showing a blend/composite and laminate structure of PLA complexes.*

Thanks to its particular functional properties, wheat gluten can be a good candidate for overcoming the drawbacks of PLA. As well-known, wheat gluten is a protein network composed of gliadins and glutenins,

which provides the essential viscoelastic properties for producing most of the wheat based food consumed by humans.[40] However, it has been shown that wheat gluten has good film forming properties,[41] which generates semipermeable membranes to water vapour, O_2 and CO_2 by casting and themoplasticization, having good mechanical properties and transparency.[42-44] It can be also used as an encapsulating agent for aroma compounds and for active/bioactive molecules.[45]

Although the water barrier properties of wheat gluten films (WG) are lower than conventional plastics and PLA, WG benefits of high gas barrier properties, especially at low relative humidity conditions. According to the literature, the O_2 permeability of wheat gluten films is close to Ethylene Vinyl Alcohol (EVOH) in dry conditions,[44] which means that complexes PLA + WG having a laminate structure could improve from 10 to 100 times (or more) the O_2 permeability of PLA.

The use of wheat gluten as laminates or coatings could be thus considered an eco-friendly strategy for enhancing the performances of PLA. It does not compromise the biodegradability of PLA and it is also innovative approach to valorise this protein (Figure 5), which is a co-product of wheat mill industry.

Based on these considerations, two main objectives were followed during this PhD project.

1) To better understand the interactions between PLA and two limiting molecules, which reduce the applications of PLA as a food packaging, as well as the induced modifications in the physical, chemical and functional properties of PLA. The limiting molecules considered in this PhD project were CO_2 and water. The selected conditions were chosen in order to simulate food packaging applications, and therefore to better study the stability of PLA (Figure 9).

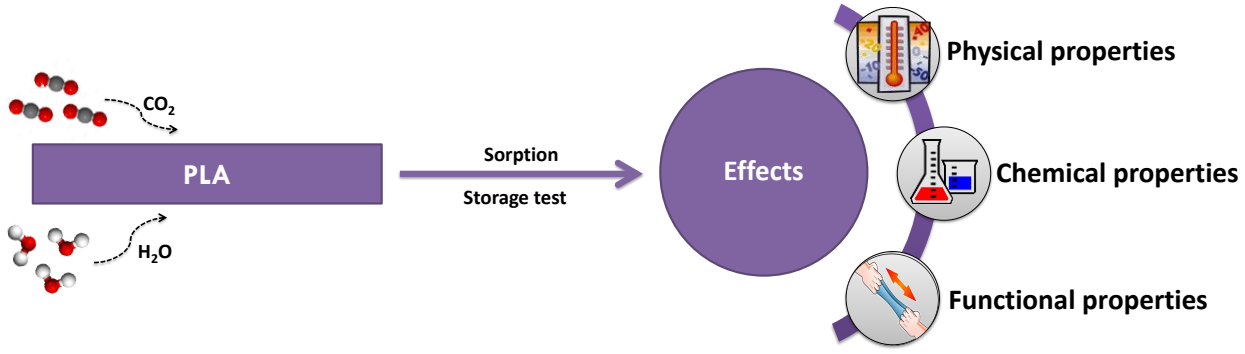

Figure 9. *Diagram showing the studies focusing on the interactions of CO_2 and H_2O molecules*

2) To propose a multilayer complex (PLA-wheat gluten-PLA) able to improve the barrier performances of PLA without compromising its biodegradability. To that target, PLA films were used as support layers, while wheat gluten films or coatings were used as a sandwiched layer. This superposition of layers would protect the wheat gluten film from water uptake to maintain its high gas barrier performances. Three main steps were carried out, characterization of supporting layers, development and characterization of coating layers and development of multilayer systems. Different technologies for producing these complexes were considered:

- For increasing the compatibility between layers, a surface modification technology such as corona treatment was studied.
- For casting solution preparation, ultrasound, high pressure homogenization and lipid incorporation technologies were considered.
- For multilayer shaping, processes such as wet casting, spin coating and hot press were adopted.

A particular attention on the surface properties (surface tension, surface chemistry, topography, adhesion) was paid to better understand the phenomena occurring at the film interfaces (Figure 10).

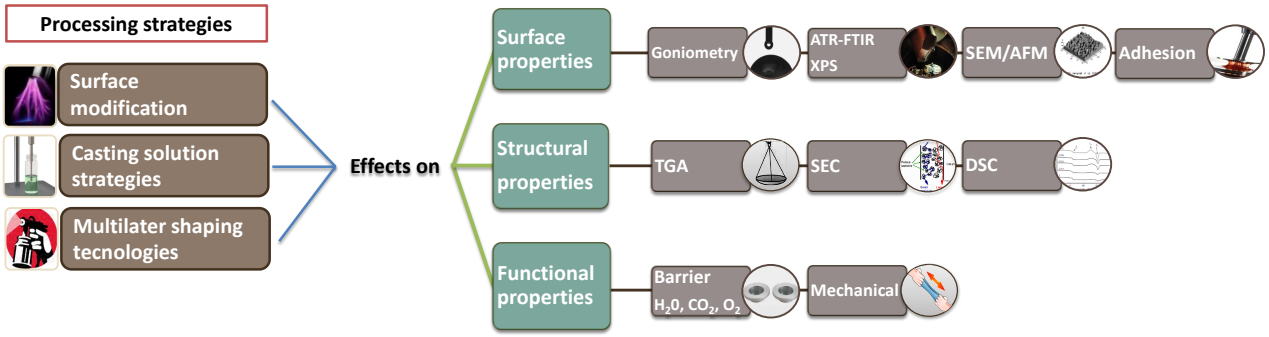

Figure 10. *Diagram showing the studies focusing on the multilayer PLA-Wheat gluten-PLA development.*

All PLA films used in this study were produced by a leading industry placed in San Giorgio di Nogaro (Udine, Italy). PLA films were thus produced with optimized and standardized processes that highly improve its overall performances, and are impossible to reproduce at the laboratory scale, such as for bi-orientation or corona treatment. Therefore, this industrial partnership allowed us to test the real feasibility of the project, using the latest advances reached by industries for food packaging productions and applications. This choice was of particular importance, because allowed us to work with films which are currently in the market for food packaging applications.

This PhD project was carried out through a dual supervision agreement (co-tutelle) between the University of Udine (Italy) and the University of Bourgogne Franche Comte (France), and in collaboration with Taghleef Industries (Italy). The development and characterization of the wheat gluten films and coatings was carried out principally at the University of Udine. The characterizations of the support layers (PLA), the studies related to the interactions CO_2-PLA, water-PLA, and the development of the multilayer complexes PLA-wheat gluten-PLA were mainly conducted in France. As previously mentioned the production of PLA films as well as the surface modification by corona treatment was carried out by the Taghleef Industries.

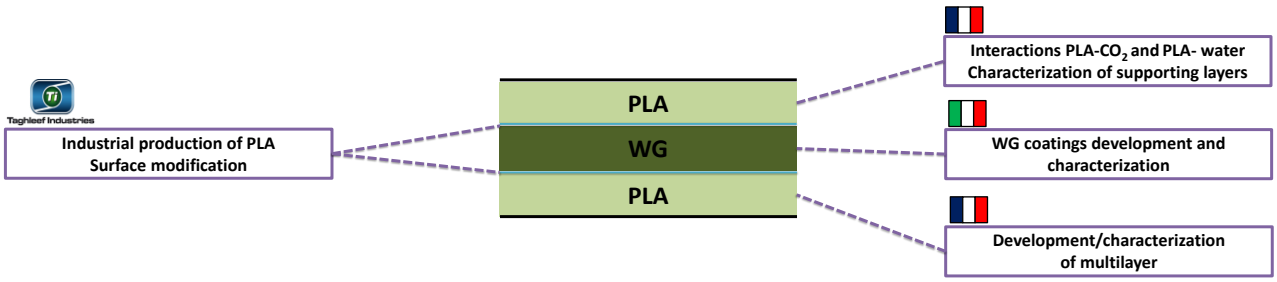

Figure 11. *Scheme showing the collaboration between the University of Udine (Italy), the University of Bourgogne Franche Comte (France) and Taghleef Industries*

This PhD project was awarded by the Doctor Europaeus Scholarship from the University of Udine, with the mobility grant Vinci 2015 (cap 2) from the Università Italo Francese, and with the mobility grant from the Doctoral School Environnement - Santé of the University of Bourgogne Franche Comte.

This PhD project involved the collaboration with different research teams specialized in food science, material science, polymer science and surface science in both universities.

This PhD thesis is written as compilation of scientific papers, and it is divided in three main sections followed by conclusions and perspectives.

Part I related to the first objective of this PhD thesis (interactions PLA-CO_2, PLA-water). It included three scientific papers.

- *Paper 1:* How high pressure CO_2 impacts PLA film properties (published paper, Express Polymer Letters).
- *Paper 2:* Effect of the state of water and relative humidity on ageing of PLA film (published paper, Food Chemistry).
- *Paper 3:* Beyond biodegradability of Poly(lactic acid): physical and chemical stability in humid environments (published paper, ACS Sustainable Chemistry & Engineering).

Part II related to the characterization of supporting layers, development and characterization of coating layers. It included two scientific papers

- *Paper 4:* Impact of corona treatment on PLA film properties (published paper, Polymer Degradation & Stability).
- *Paper 5:* Effect of lipid incorporation on functional properties of wheat gluten based edible films (published paper, Journal of Cereal Science).

Part III is the validation of the project by the development and characterization of the multilayer complexes PLA-Wheat gluten-PLA.

- *Paper 6:* Multilayer complexes from PLA and wheat gluten (to be submitted to ACS Applied Materials & Interfaces).

References

1. Halden, R. U. Plastics and Health Risks. *Annual Review of Public Health* **2010,** *31,* 179-194.

2. Plastics Europe Association. Plastics: The Facts 2016. http://www.plasticseurope.org/plastics-industry/market-and-economics.aspx. Retrieved on 25/12/2016

3. World Economic Forum. *The new plastics economy - Rethinking the future of plastics*, Geneva, 2016.

4. Cozar, A.; Echevarria, F.; Gonzalez-Gordillo, J. I.; Irigoien, X.; Ubeda, B.; Hernandez-Leon, S.; Palma, A. T.; Navarro, S.; Garcia-de-Lomas, J.; Ruiz, A.; Fernandez-de-Puelles, M. L.; Duarte, C. M. Plastic debris in the open ocean. *Proceedings of the National Academy of Sciences of the United States of America* **2014,** *111* (28), 10239-10244.

5. Jambeck, J. R.; Geyer, R.; Wilcox, C.; Siegler, T. R.; Perryman, M.; Andrady, A.; Narayan, R.; Law, K. L. Plastic waste inputs from land into the ocean. *Science* **2015,** *347* (6223), 768-771.

6. Ocean Conservancy and Mckinsey Center for Business and Enviroment. *Steamming the tide: land-based strategies for a plastic-free ocean*, Washington, DC, 2015.

7. Thompson, R. C.; Moore, C. J.; vom Saal, F. S.; Swan, S. H. Plastics, the environment and human health: current consensus and future trends. *Philosophical Transactions of the Royal Society B-Biological Sciences* **2009,** *364* (1526), 2153-2166.

8. Teuten, E. L.; Saquing, J. M.; Knappe, D. R. U.; Barlaz, M. A.; Jonsson, S.; Bjorn, A.; Rowland, S. J.; Thompson, R. C.; Galloway, T. S.; Yamashita, R.; Ochi, D.; Watanuki, Y.; Moore, C.; Pham Hung, V.; Tana, T. S.; Prudente, M.; Boonyatumanond, R.; Zakaria, M. P.; Akkhavong, K.; Ogata, Y.; Hirai, H.; Iwasa, S.; Mizukawa, K.; Hagino, Y.; Imamura, A.; Saha, M.; Takada, H. Transport and release of chemicals from plastics to the environment and to wildlife. *Philosophical Transactions of the Royal Society B-Biological Sciences* **2009,** *364* (1526), 2027-2045.

9. European Commission (DG Environment). Plastic waste in the environment – Revised final report, 2011. http://ec.europa.eu/environment/waste/studies/pdf/plastics.pdf. Retrieved on 07/01/2014.

10. European Bioplastics Association. Global production capacities of bioplastics 2014 (by material type) and applications. http://en.european-bioplastics.org/market. Retrieved on 25/01/2016.

11. Reddy, M. M.; Vivekanandhan, S.; Misra, M.; Bhatia, S. K.; Mohanty, A. K. Biobased plastics and bionanocomposites: current status and future opportunities. *Progress in Polymer Science* **2013,** *38* (10–11), 1653-1689.

12. Jamshidian, M.; Tehrany, E. A.; Imran, M.; Jacquot, M.; Desobry, S. Poly-lactic acid: production, applications, nanocomposites, and release studies. *Comprehensive Reviews in Food Science and Food Safety* **2010,** *9* (5), 552-571.

13. Auras, R.; Harte, B.; Selke, S. An overview of polylactides as packaging materials. *Macromolecular Bioscience* **2004,** *4* (9), 835-864.

14. Castro-Aguirre, E.; Iñiguez-Franco, F.; Samsudin, H.; Fang, X.; Auras, R. Poly(lactic acid)—Mass production, processing, industrial applications, and end of life. *Advanced Drug Delivery Reviews* **2016,** *107*, 333-366.

15. Kijchavengkul, T.; Auras, R. Perspective compostability of polymers. *Polymer International* **2008,** *57* (6), 793-804.

16. Rasal, R. M.; Janorkar, A. V.; Hirt, D. E. Poly(lactic acid) modifications. *Progress in Polymer Science* **2010,** *35* (3), 338-356.

17. Wang, S. G.; Cui, W. J.; Bei, J. Z. Bulk and surface modifications of polylactide. *Analytical and Bioanalytical Chemistry* **2005,** *381* (3), 547-556.

18. Nofar, M.; Park, C. B. Poly (lactic acid) foaming. *Progress in Polymer Science* **2014,** *39* (10), 1721-1741.

19. Jariyasakoolroj, P.; Tashiro, K.; Wang, H.; Yamamoto, H.; Chinsirikul, W.; Kerddonfag, N.; Chirachanchai, S. Isotropically small crystalline lamellae induced by high biaxial-stretching rate as a key microstructure for super-tough polylactide film. *Polymer* **2015,** *68*, 234-245.

20. Ouchiar, S.; Stoclet, G.; Cabaret, C.; Addad, A.; Gloaguen, V. Effect of biaxial stretching on thermomechanical properties of polylactide based nanocomposites. *Polymer* **2016,** *99*, 358-367.

21. Lim, L. T.; Auras, R.; Rubino, M. Processing technologies for poly(lactic acid). *Progress in Polymer Science* **2008,** *33* (8), 820-852.

22. Tsuji, H. Poly(lactic acid) stereocomplexes: A decade of progress. *Advanced Drug Delivery Reviews* **2016,** *107*, 97-135.

23. Tan, B. H.; Muiruri, J. K.; Li, Z.; He, C. Recent progress in using stereocomplexation for enhancement of thermal and mechanical property of polylactide. *ACS Sustainable Chemistry & Engineering* **2016,** *4* (10), 5370-5391.

24. Li, Z.; Tan, B. H.; Lin, T.; He, C. Recent advances in stereocomplexation of enantiomeric PLA-based copolymers and applications. *Progress in Polymer Science* **2016,** *62*, 22-72.

25. Corneillie, S.; Smet, M. PLA architectures: the role of branching. *Polymer Chemistry* **2015,** *6* (6), 850-867.

26. Yu, L.; Dean, K.; Li, L. Polymer blends and composites from renewable resources. *Progress in Polymer Science* **2006,** *31* (6), 576-602.

27. Armentano, I.; Bitinis, N.; Fortunati, E.; Mattioli, S.; Rescignano, N.; Verdejo, R.; Lopez-Manchado, M. A.; Kenny, J. M. Multifunctional nanostructured PLA materials for packaging and tissue engineering. *Progress in Polymer Science* **2013,** *38* (10-11), 1720-1747.

28. Johari, A. P.; Mohanty, S.; Kurmvanshi, S. K.; Nayak, S. K. Influence of different treated cellulose fibers on the mechanical and thermal properties of poly(lactic acid). *ACS Sustainable Chemistry & Engineering* ***2016,*** *4 (3), 1619-1629.*

29. Kai, D.; Ren, W.; Tian, L.; Chee, P. L.; Liu, Y.; Ramakrishna, S.; Loh, X. J. Engineering poly(lactide)–lignin nanofibers with antioxidant activity for biomedical application. *ACS Sustainable Chemistry & Engineering* **2016,** *4* (10), 5268-5276.

30. Lu, H.; Madbouly, S. A.; Schrader, J. A.; Srinivasan, G.; McCabe, K. G.; Grewell, D.; Kessler, M. R.; Graves, W. R. Biodegradation behavior of poly(lactic acid) (PLA)/distiller's dried grains with solubles (DDGS) composites. *ACS Sustainable Chemistry & Engineering* **2014,** *2* (12), 2699-2706.

31. Agustin-Salazar, S.; Gamez-Meza, N.; Medina-Juàrez, L. À.; Soto-Valdez, H.; Cerruti, P. From nutraceutics to materials: effect of resveratrol on the stability of polylactide. *ACS Sustainable Chemistry & Engineering* **2014,** *2* (6), 1534-1542.

32. Raquez, J.-M.; Habibi, Y.; Murariu, M.; Dubois, P. Polylactide (PLA)-based nanocomposites. *Progress in Polymer Science* **2013,** *38* (10–11), 1504-1542.

33. Zhu, H. G.; Ji, J.; Shen, J. C. Surface engineering of poly(DL-lactic acid) by entrapment of biomacromolecules. *Macromolecular Rapid Communications* **2002,** *23* (14), 819-823.

34. Fabra, M. J.; Busolo, M. A.; Lopez-Rubio, A.; Lagaron, J. M. Nanostructured biolayers in food packaging. *Trends in Food Science & Technology* **2013,** *31* (1), 79-87.

35. Morent, R.; De Geyter, N.; Desmet, T.; Dubruel, P.; Leys, C. Plasma surface modification of biodegradable polymers: a review. *Plasma Processes and Polymers* **2011,** *8* (3), 171-190.

36. Rocca-Smith, J. R.; Karbowiak, T.; Marcuzzo, E.; Sensidoni, A.; Piasente, F.; Champion, D.; Heinz, O.; Vitry, P.; Bourillot, E.; Lesniewska, E.; Debeaufort, F. Impact of corona treatment on PLA film properties. *Polymer Degradation and Stability* **2016,** *132*, 109-116.

37. Janorkar, A. V.; Metters, A. T.; Hirt, D. E. Modification of poly(lactic acid) films: enhanced wettability from surface-confined photografting and increased degradation rate due to an artifact of the photografting process. *Macromolecules* **2004,** *37* (24), 9151-9159.

38. Witzke, D. R. Introduction to properties, engineering, and prospects of polylactide polymers. Michigan State University East Lansing, MI, 1997. PhD thesis.

39. Emuscado, M. E.; Huber, K. C. *Edible Films and Coatings for Food Applications*;Springer: Dordrecht; London, 2009.

40. Lagrain, B.; Goderis, B.; Brijs, K.; Delcour, J. A. Molecular basis of processing wheat gluten toward biobased materials. *Biomacromolecules* **2010,** *11* (3), 533-541.

41. Gontard, N.; Guilbert, S.; Cuq, J.-L. Edible wheat gluten films: influence of the main process variables on film properties using response surface methodology. *Journal of Food Science* **1992,** *57* (1), 190-195.

42. Gontard, N.; Thibault, R.; Cuq, B.; Guilbert, S. Influence of relative humidity and film composition on oxygen and carbon dioxide permeabilities of edible films. *Journal of Agricultural and Food Chemistry* **1996,** *44* (4), 1064-1069.

43. Gontard, N.; Guilbert, S.; Cuq, J.-L. Water and glycerol as plasticizers affect mechanical and water vapor barrier properties of an edible wheat gluten film. *Journal of Food Science* **1993,** *58* (1), 206-211.

44. Guilbert, S.; Gontard, N.; Morel, M. H.; Chalier, P.; Micard, V.; Redl, A., Formation and properties of wheat gluten films and coatings. In *Protein-based films and coatings*; Gennadios, A., Ed. CRC Press: Boca Raton, 2002.

45. Marcuzzo, E.; Debeaufort, F.; Sensidoni, A.; Tat, L.; Beney, L.; Hambleton, A.; Peressini, D.; Voilley, A. Release behavior and stability of encapsulated D-limonene from emulsion-based edible films. *Journal of Agricultural and Food Chemistry* **2012,** *60* (49), 12177-12185.

PART I

INTERACTIONS OF PLA WITH CARBON DIOXIDE AND MOISTURE

How high pressure CO_2 impacts PLA film properties

Rocca-Smith, J.R.; Lagorce-Tachon, A.; Iaconelli, C.; Bellat, J.P; Marcuzzo, E.; Sensidoni, A.; Piasente, F.; Debeaufort, F.; Karbowiak, T. How high pressure CO_2 impacts PLA film properties. *Express Polymer Letters* 2017, 11, 320-330.

Abstract

This work investigated the sorption and the diffusion properties of CO_2 under high pressure and the further modifications induced in Poly(lactic acid) (PLA) thin layers. Poly(ethylene terephtalate) was also considered for comparative purposes. Firstly, from thermodynamic equilibrium, the CO_2 sorption isotherm (two sorption-desorption cycles, up to 25 bar, at 25 °C) gave strong evidence of a physisorption mechanism and of a hysteresis phenomenon. Infrared spectroscopy analysis confirmed that no chemical reaction occurred. Secondly, from the kinetics aspect, the CO_2 diffusion coefficient was found around 10^{-13} $m^2 \cdot s^{-1}$ and was slightly faster for sorption compared to desorption. Additionally, when CO_2 sorption occurred, the PLA structure and its functional properties were modified due to plasticization and swelling. CO_2 plasticization reduced the glass transition temperature of PLA and accelerated the physical ageing of the polymer. These results are therefore of significant importance in industrial processing and applications which involve close contact between CO_2 and PLA.

Keywords

Biodegradable polymers, PLA, carbon dioxide gas, polymer ageing, mass transfer

1 Introduction

Poly (lactic acid) or PLA is a renewable and biodegradable polyester, which holds a strategic place in the bioplastic market. It is considered as one of the most interesting candidates for substituting conventional (non-biodegradable and oil-based) plastics.[1-3] The European Bioplastic Association has reported that the worldwide production of PLA exceeded 207 thousand tons in 2014, and it is expected to double in 2019.[4] According to that association, the largest consumption of PLA is currently as packaging for foods, beverages and cosmetics, and almost certainly they would remain as the main application of PLA in the near future.[4] PLA is also a competitive material in other market segments, which are believed to have a higher importance in the next years, such as bio-medical devices, textiles, automobile appliances, electrical appliances and 3D printing, thanks to its biocompatibility nature and relative easiness to modify its functional properties.

Poly(ethylene terephtalate) or PET is one of the most frequently conventional plastic used in food packaging. The European production of this polyester exceeded 4 million tons in 2014 and it is largely used as bottles of soft drinks and water, containers for fruits and trays for pre-cooked meals.[5] PLA can be considered as a good candidate for a gradual replacement of PET in food packaging, since both polyesters are similar in appearance, thermal and in mechanical properties.[1] However, substituting PET with PLA is currently a suitable strategy for food packaging applications with only low barrier requirements. PLA indeed displays lower barrier performances to water vapour, oxygen (O_2), carbon dioxide (CO_2) and nitrogen (N_2).[1-2] This can compromise the quality and the safety of some products such as foods packed in Modified Atmosphere Packaging (MAP) or carbonated beverages. Developing PLA based materials able to compete with PET and with other high performing plastics – such as polyamide (PA), poly (vinylidene chloride) (PVDC) or poly (vinyl alcohol) (PVA) – is thus an ecofriendly challenge for the near future, which could open new application scenarios to PLA.

CO_2 plays a key role in food processing and food packaging. On one hand, food industries largely draw on this gas as ingredient of carbonated beverages (*e.g*. soft drinks, sparkling wines or carbonate water) and for extending the shelf life of fresh, dairy and meat products in MAP, by limiting oxidation reactions, colour changes and microbial growth.[6-8] On the other hand, due to its technological advantages there is an increasing interest in the use of CO_2 as a supercritical fluid (pressure > 73.8 bar and temperature > 31.1 °C).[9] Supercritical CO_2 is used for extracting nutraceuticals or functional ingredients (*e.g.* vitamins, essential oils, antioxidants) from biological materials,[10-11] fractionating and deodorizing lipids,[12] decaffeinating green coffee beans, defatting foods, removing ethanol from alcoholic beverages (*e.g.* beer and wine)[13] and inactivating microorganism and enzymes.[14-15]

Based on those considerations, there is a clear interest in studying the interactions between CO_2 and PLA, and the modifications that such molecule could induce in the PLA material, which is suitable as a substitute of PET. For now, most of the related literature is focused on the effects of supercritical CO_2 (or conditions

near to it) on the PLA properties, such as foaming properties,[16] thermal behavior,[17-19] hydrophobic drug encapsulation[20-21] or swelling.[22-23] Nevertheless, there is not enough available information related to the effects of CO_2 at conditions lower than its supercritical point, which are often the conditions encountered in food packaging and food processing.

The main objective of this research was thus to study the sorption properties of PLA regarding CO_2 and the modification induced by CO_2 in PLA thin layer films at high pressures conditions. The CO_2 sorption isotherm (two sorption-desorption cycles) of PLA at 25 °C up to 25 bar was first determined. The related effective diffusion coefficients were then calculated and the modifications on chemical and functional properties of the material were evaluated. PET films were also used in this study for comparative purpose.

2 Experimental

2.1 Samples

Semicrystalline PLA (Polylactic acid) commercially available for food packing applications was used in this study (thickness = 30 µm, $\overline{M_w}$ ≈ 200 000 g·mol^{-1}, PDI ≈ 2.2, D-level ≥ 4.25%). These PLA films were subjected to a biaxial orientation and annealing during production and were supplied by Taghleef Industries (commercial name: Nativia NTSS, Udine, Italy). Amorphous PET (Polyethylene terephthalate) films were also used for comparison purposes (thickness = 200 µm). PET films were not subjected to bi-orientation and were purchased from WIPAK Gryspeert SAS (commercial name: APET 200, Bousbecque, France).

2.2 CO_2 sorption properties

The sorption and diffusion properties of CO_2 in PLA and PET were determined by thermogravimetry at 25 ° C.

2.2.1 Sorption isotherm

The CO_2 sorption isotherms of PLA and PET films were determined at 25 °C for pressure ranging from 0 to 25 bar, using a magnetic suspension balance (Rubotherm GMbH, Bochum, Germany). Rectangular film samples (≈ 75 mg) were first outgassed under primary vacuum (nXDS Scroll Pumps, Edwards, Czech Republic) at a pressure of about 10^{-5} bar until mass equilibration before being exposed to CO_2 sorption. The CO_2 pressure was then increased step by step waiting for equilibrium before changing the pressure. Equilibrium was considered to be reached when the mass of sample remained constant for at least 12 hours. For each film, 2 cycles of sorption and desorption were performed. The quantity of sorbed CO_2 was calculated according to Equation 1.

$$m_{sorb} = \frac{m_{Ar} - m}{m} \times 100 \qquad (Eq. 1)$$

Where m_{sorb} is the quantity of sorbed CO_2 (wt% of outgassed weight sample) by the material, m_{Ar} is the mass of the sample at equilibrium and after been corrected by the Archimedes buoyancy (g) according to Equation 2, and m is the sample mass after been outgassed (g).

$$m_{Ar} = m_{app} + d_g(V_p - V_s) - m_p - d_{air}(V_p + V_s) \qquad (Eq.2)$$

Where m_{app} (g) is the sum of apparent mass of the sample and the mass of the empty pan, d_g is the measured density of the gas at the running pressure ($g \cdot cm^{-3}$), V_p is the volume of the pan containing the sample (cm^3), V_s is the sample volume (cm^3), m_p is the mass of the empty pan (g) and d_{air} is the gas density under atmospheric pressure ($g \cdot cm^{-3}$).

2.2.2 Diffusion coefficient

The effective diffusion coefficient of CO_2 in both films was calculated from the previous CO_2 sorption kinetics. The experimental data from each sorption step were modeled using an analytical solution to Fick's second law applied to membrane sorption, or desorption (Equation 3).[24] The system was characterized by a uniform gas concentration before the phenomenon took place. When it started, the gas concentration in both surfaces was kept constant while the sorption (or desorption) in both sides of the membrane occurred.

$$\frac{m_t}{m_\infty} = 1 - \sum_{j=0}^{\infty} \frac{8}{(2j+1)^2\pi^2} exp\left[\frac{-D_{sorp}(2n+1)^2\pi^2 t}{4l^2}\right] \qquad (Eq.3)$$

Where m_t and m_∞ are the total amount (g) of sorbed CO_2 (or desorbed CO_2) at time t (s) and at equilibrium, respectively; l is the half thickness of the membrane (m); D_{sorp} is the effective diffusion coefficient ($m^2 \cdot s^{-1}$).

The effective diffusion coefficient (D_{sorp}) was calculated using the reduction in the sum of squares scores between the model (Equation 3) and the experimental curve (*fminsearch* function in Matlab R2012a). A maximal value of 10 for *j* and a mean of the last 50 values for m_∞ were fixed. To determine the confidence interval of diffusion coefficient, the prevision interval of the amount of sorbed CO_2 was calculated based on the sum of squares between the model and experimental curve (Equation 4).

$$m_t = m_{mod} \pm t_{\alpha/2;n-2} \sqrt{\frac{\left(\sum_{i=1}^{n}(m_{mod} - m_{exp})^2\right)}{n-2}\left[1 + \frac{1}{n} + \frac{(\bar{t} - t)^2}{\sum_{i=1}^{n}(t_i - \bar{t})^2}\right]} \qquad (Eq.4)$$

Where $t_{\alpha/2;n-2}$ is a value of *t* distribution, α is the confidence level (5%), n is the number of points, m_{mod} and m_{exp} are the modeled and experimental values of the total amount of sorbed (or desorbed) CO_2, respectively.

Finally, the coefficient of determination (R^2) has been calculated with the total sum of squares (SS_{tot}) calculated according to Equation 5.

$$SS_{TOT} = \sum_{i}^{n} \left(m_{mod} - t \times \frac{m_n}{t_n} \right)^2 \qquad (Eq. 5)$$

For each curve, the diffusion coefficient has been calculated, along with the upper and lower bounds of the confidence interval as reported in the example given in Figure 1.

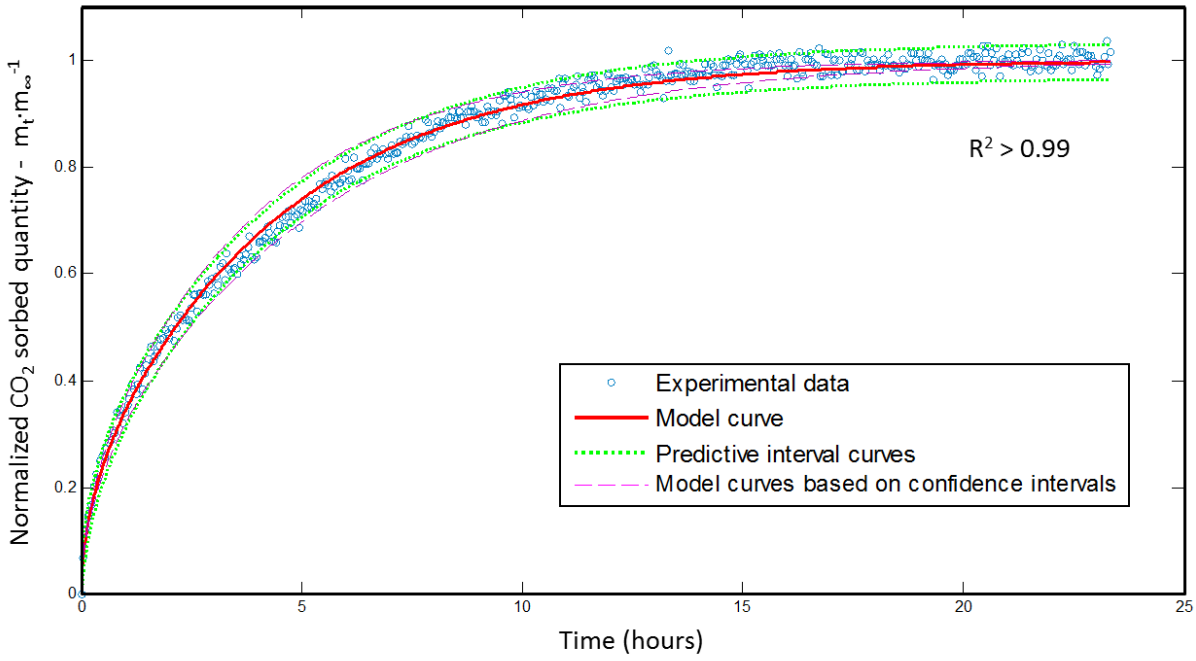

Figure 1. *Selected example of sorption kinetics of CO_2 on PET (between pressure 4.3 and 9.7 bar). Displayed are experimental data along with modeling according to Equation 3. Also indicated are the predictive interval curves and model curves base on confidence intervals at 95 %.*

2.3 Modifications induced by CO_2 sorption

Selected functional properties of PLA and PET films were compared prior to and after CO_2 sorption at 25 °C, under the same high pressure conditions as previously used.

2.3.1 Sorption conditions

PLA films were subjected to primary vacuum before and after gas sorption. In the case of PLA films, gas sorption took place in a chamber saturated with CO_2 at 25 bar for 5 days. PLA films stored in a chamber with N_2 under same conditions, and PLA films stored at 1 bar of CO_2 for 5 days were used as control samples, for non-reactive gas and non-pressurized sample, respectively. In the case of PET films, samples from CO_2 sorption isotherm were analysed. This sorption condition also involved high pressure treatments at 25 bar. Similarly, PET films stored for 5 months at room conditions, and PET films stored for 5 days under 1 bar of CO_2 were analysed as control samples for long time ageing and non-pressurized sample, respectively.

2.3.2 Surface chemistry

Changes in the surface chemistry were evaluated using Attenuated Total Reflectance Fourier Transform InfraRed analysis (ATR-FTIR) with a spectrometer (Spectrum 65, PerkinElmer, Waltham, MA, USA) equipped with ZnSe crystal. The wavenumber investigated ranged from 4000 to 650 cm^{-1}, with a resolution of 2 cm^{-1}. 128 scans were collected for each spectrum. Six samples for each films condition were analysed. Film spectra were normalized according to the height of the peak at 1452 cm^{-1}, corresponding to the bending vibration mode of $–CH_3$ and $–CH_2$ of PLA and PET, respectively.[25-26]

2.3.3 Phase transitions

The thermal events of PLA and PET films were determined by Differential Scanning Calorimetry (DSC), using a Q20 calorimeter (TA instruments, New Castle, DE, USA). Films were weighed (around 5 mg) and sealed into aluminium pans (TA instruments) before being subjected to a double heating-cooling cycle at 10 °C·min^{-1} under N_2 atmosphere (flow rate = 25 mL·min^{-1}). For PLA films the temperature range investigated was from -10 to 200 °C, while for PET films it was from -10 to 300 °C. The thermal events related to glass transition (inflection point of glass transition temperature T_g and variation of specific heat ΔC_p), associated endothermic event (enthalpy of relaxation ΔH_{relax}), cold crystallization (temperature of cold crystallization T_{cc} and enthalpy of cold crystallization ΔH_{cc}) and melting (temperature of melting T_m and enthalpy of melting ΔH_m) were calculated from the first heating cycle, using TA Universal Analysis 2000 software (version 4.5 A, TA instruments). The reversibility of thermal events was assessed from the second heating cycle.

The crystallinity degree (X_c) of films was also calculated, according to Equation 6.

$$X_c = \frac{\Delta H_m - \sum \Delta H_{cc}}{\Delta H_m^\circ} \times 100\% \qquad (Eq. 6)$$

Where $\sum \Delta H_{cc}$ (J·g^{-1}) is the sum of cold crystallization peaks and ΔH_m° is the enthalpy of melting of the pure polymer (PLA = 93 J·g^{-1}; PET = 140 J·g^{-1}).[27, 28]

2.3.4 Mechanical properties

The mechanical behaviour of PLA films was assessed by uniaxial tensile testing at room conditions (T ≈ 25 °C) using a texture analyser (TA HD plus, Texture Technologies, Hamilton, MA, USA) and according to NF EN ISO 527-1 standard.[29] The initial gauge length was 10 cm, a 100 kg load cell was used and tests were performed with a constant crosshead speed of 1 mm·min^{-1}. 7 to 12 rectangular specimens (dimensions of 15 x 2.5 cm) were prepared with a precision cutter (JDC, Thwing Albert Instrument Company, West Berlin, NJ, USA) and analysed for each condition. The transversal direction to process line (TD) of films was considered for this analysis. The Young's modulus (E_{Young}, GPa), yield strength (σ_y, MPa), yield elongation (ε_y, %) tensile strength (σ_b, MPa) and elongation at break (ε_b, %) were determined from the resulting stress – strain curves.

2.3.5 Barrier properties to CO_2

The permeability (*P*) of PLA films to CO_2 was determined using a manometric method on a GDP-C permeameter apparatus (Brugger Feinmechanik GmbH, Munich, Germany) in dry conditions (0 % Relative Humidity, RH) at 25 °C. The system was outgassed under primary vacuum before testing. At time zero one side of the film was flushed with the gas (flow ≈ 100 $cm^3 \cdot min^{-1}$) and the pressure increase on the other side was recorded over time. Permeability was determined from the steady state of transfer.

From the lag time, the effective diffusion coefficient (D_{perm}) (Equation 7) and the solubility coefficient (S_{perm}) were also calculated (Equation 8).

$$D_{perm} = \frac{l^2}{6\vartheta} \qquad (Eq.7)$$

$$P = D_{perm} \times S_{perm} \qquad (Eq.8)$$

Where, D_{perm} is the effective diffusion coefficient ($m^2 \cdot s^{-1}$), *l* is the thickness of the film (m), ϑ is the lag time (s), *P* is the measured permeability ($mol \cdot m^{-1} \cdot s^{-1} \cdot Pa^{-1}$) and S_{perm} is the solubility ($mol \cdot m^{-3} \cdot Pa^{-1}$). The subscript *perm* of *D* and *S* parameters denotes that they were determined from the manometric method, to differentiate them from their counterparts calculated from the CO_2 sorption isotherm (D_{sorp}).

2.4 Statistical analysis

Data were analysed with Student t-test and, when required (groups > 2), with one–way analysis of variance (ANOVA) and with Tukey-Kramer multiple comparison test, using GraphPad Prism software (version 5.01, GraphPad Software Inc., La Jolla, CA, USA). The significance level of all statistical tests was fixed at 0.05.

3 Results and discussion

The results and discussion section is firstly focused on the CO_2 sorption properties of PLA film compared to PET material. Secondly, the modifications induced by the CO_2 sorption on the functional and barrier properties of films are investigated with particular attention paid to PLA.

3.1 Sorption properties for CO_2

3.1.1 CO_2 sorption isotherm

Although several CO_2 sorption studies have been conducted on PLA,[19, 22, 30-34] no information concerning the solubility of CO_2 during consecutive sorption/desorption cycles are available in the literature. These steps are crucial because they provide information on the interactions between the sorbent and the polymer. For example, if hysteresis between sorption/desorption steps is detected, it indicates that these interactions modified the polymer. If an increase in the polymer weight is noticeable after outgassing following the first sorption/desorption cycle, it suggests that the polymer chemically fixed the sorbent via covalent bounds (chemisorption). On the contrary, if the polymer returns back to its initial weight, it indicates that only low energy interactions or physical modifications occurred during sorption. Thus, to better understand the type

of interactions between CO_2 and PLA, the CO_2 sorption isotherm was determined at 25 °C from 0 to 25 bar involving two sorption/desorption cycles (Figure 2).

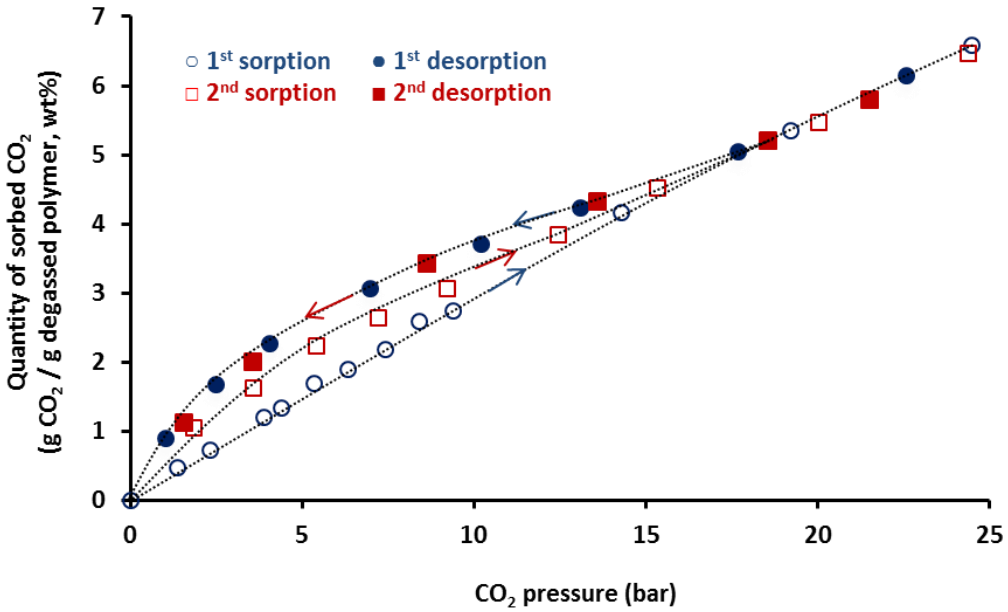

Figure 2. *Sorption isotherms (2 cycles of sorption and desorption) of CO_2 of PLA at 25 °C.*

During the first sorption, the quantity of CO_2 sorbed by PLA linearly increased with pressure, for the whole range of pressure investigated from 0 to 25 bar. Such Henry's type isotherm was already observed in other studies involving pre-supercritical conditions.[19, 30-32] A plateau (or pseudo plateau) was only reported when supercritical conditions (pressure > 73.8 bar and temperature > 31.1 °C) were exceeded.[22-23, 33] The quantity sorbed at CO_2 pressure close to 25 bar was rather high, around 7 wt% of the initial mass of the polymer, which represents a molar ratio of 0.11 mol of CO_2 per mol of PLA monomer unit. Similar quantities of CO_2 (≈ 7-10 %wt) were sorbed by PLA at ≈ 25 bar at 40 °C in previous studies.[19, 22] Thus, this suggested a great sorption capacity of PLA polymer for CO_2 molecules, possibly as a consequence of a high amount of sorption sites.

Now looking at the first desorption, the shape of the isotherm exhibited a nonlinear behaviour. Sorbed quantities of CO_2 were higher than those for the first sorption, unambiguously indicating hysteresis phenomenon in PLA. At the end of the desorption step, the PLA returned to its initial weight, showing the PLA capability to release all the sorbed CO_2 molecules when the sample is taken back under vacuum. It gave strong evidence that CO_2 molecules were only physically retained, without involving covalent bond formation (chemisorption), and thus suggesting that modifications revealed by the hysteresis concerned only the physical state of PLA like swelling or plasticization.

The second sorption did not follow the same way as the first sorption. In this case, a nonlinear increasing trend was observed, with sorbed CO_2 values lying between the first sorption and desorption cycle. The behaviour of second desorption was rigorously analogous to the first one. At the end of the second

desorption cycle, all CO_2 molecules were also fully desorbed from the PLA polymer when maintained under vacuum at 25 °C. Such hysteresis confirmed modifications in the physical state of the polymer, as a result of physical interactions like plasticization or swelling. PLA, as other polyesters, is known to establish low energy interactions (of Lewis acid-base nature) between CO_2 molecules (electron acceptor) and carbonyl groups of the polymer (electron donor), which leads to plasticization and swelling.[22, 34-36] As a result, PLA chains are becoming more spaced, PLA intermolecular interactions reduce, the system mobility increases and new sorption sites are exposed, favouring therefore CO_2 sorption.[22, 33, 37]

The CO_2 sorption isotherm of PET was also determined using the same gravimetric technique (Figure 3).

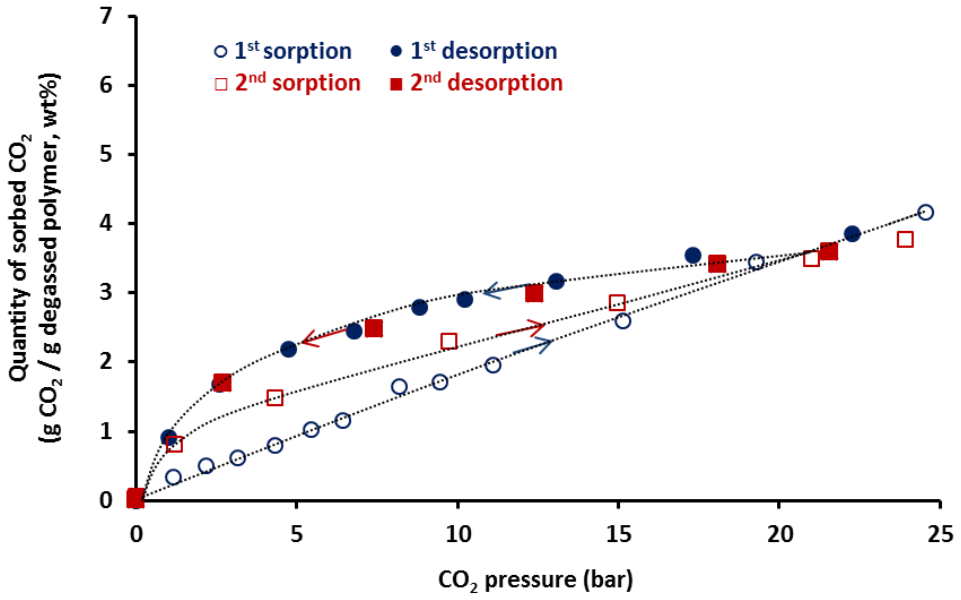

Figure 3. *Sorption isotherms (2 cycles of sorption and desorption) of CO_2 of PET at 25 °C.*

It is noteworthy that the sorption isotherm trends were analogous to those of PLA. The first CO_2 sorption also followed a linear behaviour according to Henry's law, while the successive steps highlighted once again a hysteresis phenomenon. Such similarity can be explained by the chemical nature of both polyesters. PET also has carbonyl groups able to interact with CO_2 molecules, leading to a plasticization effect. No chemisorption was detected, suggesting that modifications induced by CO_2 sorption only concerned the physical state of the polymer, in a similar way than for PLA. The main difference between PLA and PET was in the quantity of sorbed CO_2. Even if they lied in the same order of magnitude, PLA clearly sorbed more CO_2 than PET in the whole range of pressure studied (≈ 7 vs. 4 wt% at ≈ 25 bar). Lower CO_2 solubility in PET compared to PLA was also observed by Champeau *et al.*[22] in a sorption study involving supercritical CO_2. This difference is firstly surprising when considering that PET was mainly amorphous contrarily to PLA which was semicrystalline (X_c = 3.0 vs. 24.8 %, respectively, Table 1). Crystals are known to have a lower free volume and thus reduce the regions swelled due to sorption.[30] Therefore, such a lower CO_2 solubility in PET may come from the lower density of carbonyl groups compared to PLA (approximately one carbonyl

group each 96.08 and 72.06 g·mol^{-1}, respectively) and from the presence of phenyl groups, which are less susceptible to interact with CO_2. It is possible thus to infer that the chemical structure of the polymer had a major influence in the sorption properties rather than its physical and morphological structure (*e.g.* crystallinity degree and orientation of chains).

3.1.2 Diffusion properties

The time for equilibration for each sorption and desorption steps during thermogravimetric analysis ranged from 1 to 3 days. To go deeper in this analysis and to better understand if these differences were due to CO_2 sorption, and to consider the different thickness of both materials, the effective CO_2 diffusion coefficient (D_{sorp}) of PLA and PET was calculated from each of the sorption and desorption steps (Figure 4).

a)

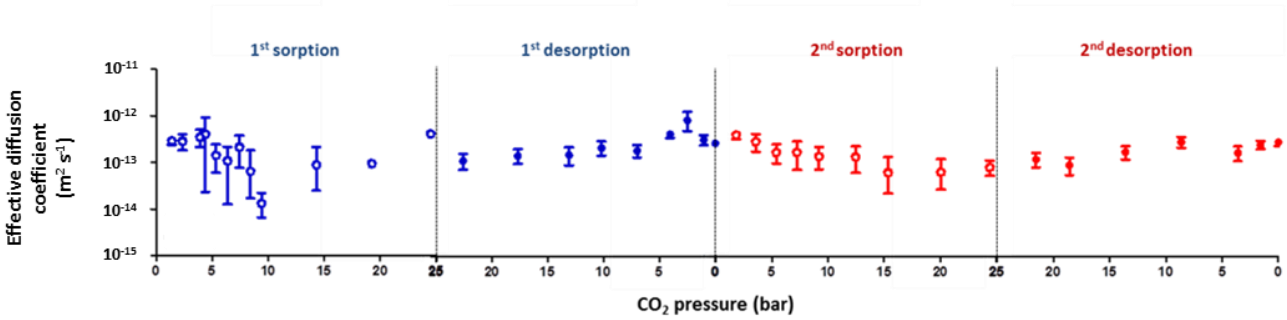

b)

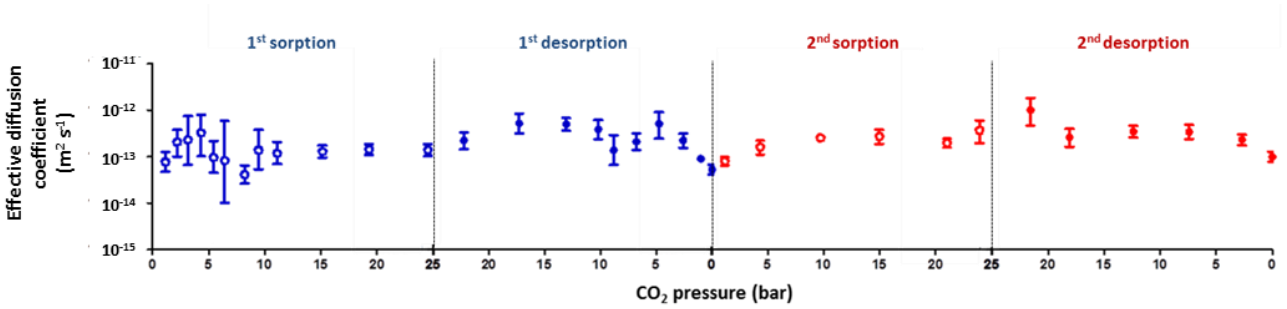

Figure 4. *Effective diffusion coefficients calculated from sorption isotherms kinetics of PLA (a) and PET (b). Error bars are the predictive intervals.*

As displayed in Figure 4, there was no significant effect of the pressure of CO_2 on D_{sorp} in PLA. They oscillated around 10^{-13} $m^2 \cdot s^{-1}$ for all sorption experiments. The same order of magnitude for D_{sorp} values were also observed in other studies.[38-39] However, when successive sorption cycles were considered significant differences were noticeable. Firstly, the first sorption cycle was characterized by a high variability, while the variability of other cycles was smaller and rather constant. This was possibly because the initial structure of PLA was highly modified during the first sorption. Secondly, if the mean of all D_{sorp} values for each sorption and desorption cycles are considered, a slight but significant (p-value = 0.03) increase in D_{sorp} values during desorption steps is observed. This could be due to formation of CO_2 clusters in the polymer structure or to CO_2-CO_2 interactions that appeared to be easily removed.

The D_{sorp} values of PET followed a similar trend to PLA and same considerations thus applied in this case. More precisely, no significant difference was noticed between PLA and PET. Both D_{sorp} values were around 10^{-13} $m^2 \cdot s^{-1}$. For PET Similar D_{sorp} values were also observed in other studies.[40-42] The variability of first sorption was higher than the others cycles, and for desorption steps, the equilibrium was reached faster than for sorption.

3.2 Modifications of polymer film induced by CO_2 sorption

The modifications induced by CO_2 sorption at high pressure on the chemical properties, thermal events and functional properties (*i.e.* mechanical and barrier) of films were assessed.

3.2.1 Chemical modifications

Findings of ATR-FTIR analyses were in line with previous sorption isotherm observations, and gave strong evidence that modification in films functional properties was a consequence of physical reorganization, occurring in the polymer structure.

The ATR-FTIR spectra of PLA and PET films displayed the typical vibrations bands of these materials in accordance with other studies (Figure 5 and 6).[25-26, 43-44] For PLA, -C=O stretching (1720 cm^{-1}), $-CH_3$ bending (1452 cm^{-1}), -C=O bending (1270 cm^{-1}), -C-O-C stretching (1185 cm^{-1}), -C-O- stretching (1130 and 1088 cm^{-1}), -OH bending (1046 cm^{-1}) and -C-C- stretching attributed to amorphous and crystalline phases (863 and 758 cm^{-1}, respectively).[25, 44] For PET, -C=O stretching (1752 cm^{-1}), $-CH_2$ bending (1452 cm^{-1}), -C=O bending (1260 and 1246 cm^{-1}), O-C stretching (1118 and 1098 cm^{-1}) and the vibration modes associated to the aromatic ring (1578, 1506, 1018, 874 and 726 cm^{-1}).[26, 43]

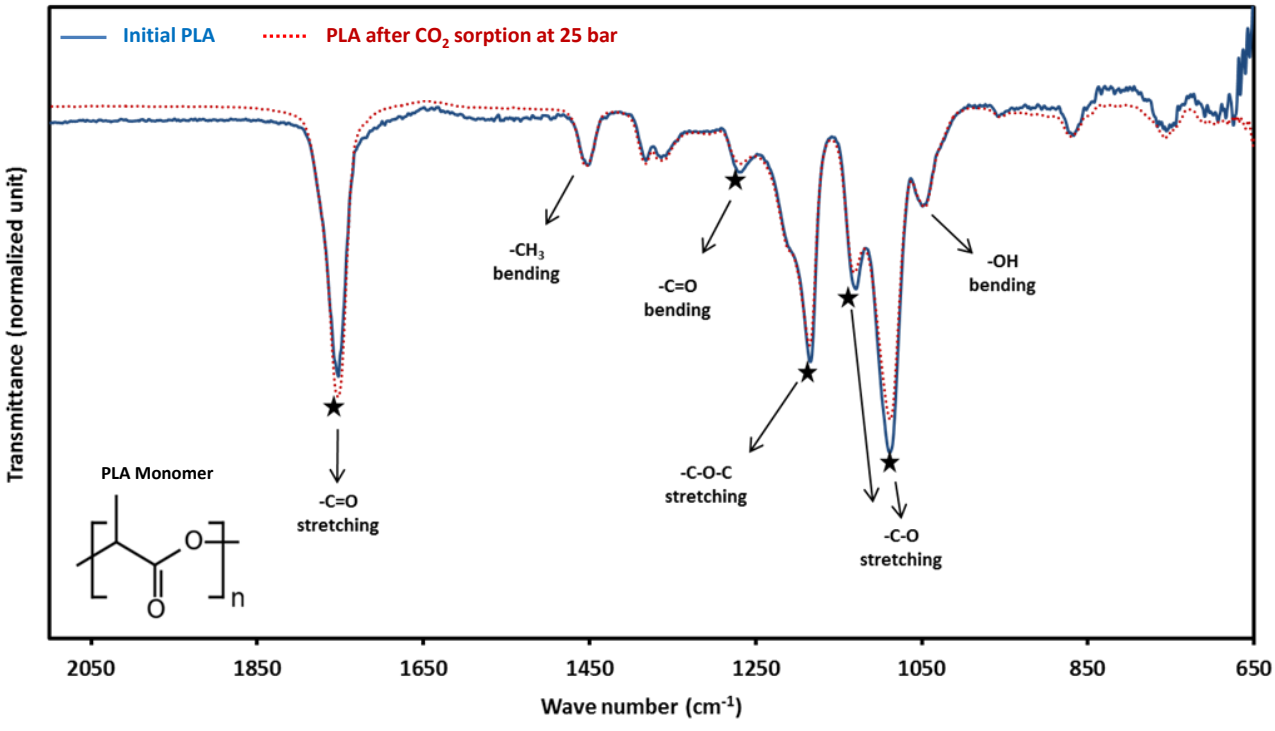

Figure 5. *ATR-FTIR spectra of PLA before and after been subjected to CO_2 sorption isotherm analysis. Significant differences are evidenced with stars.*

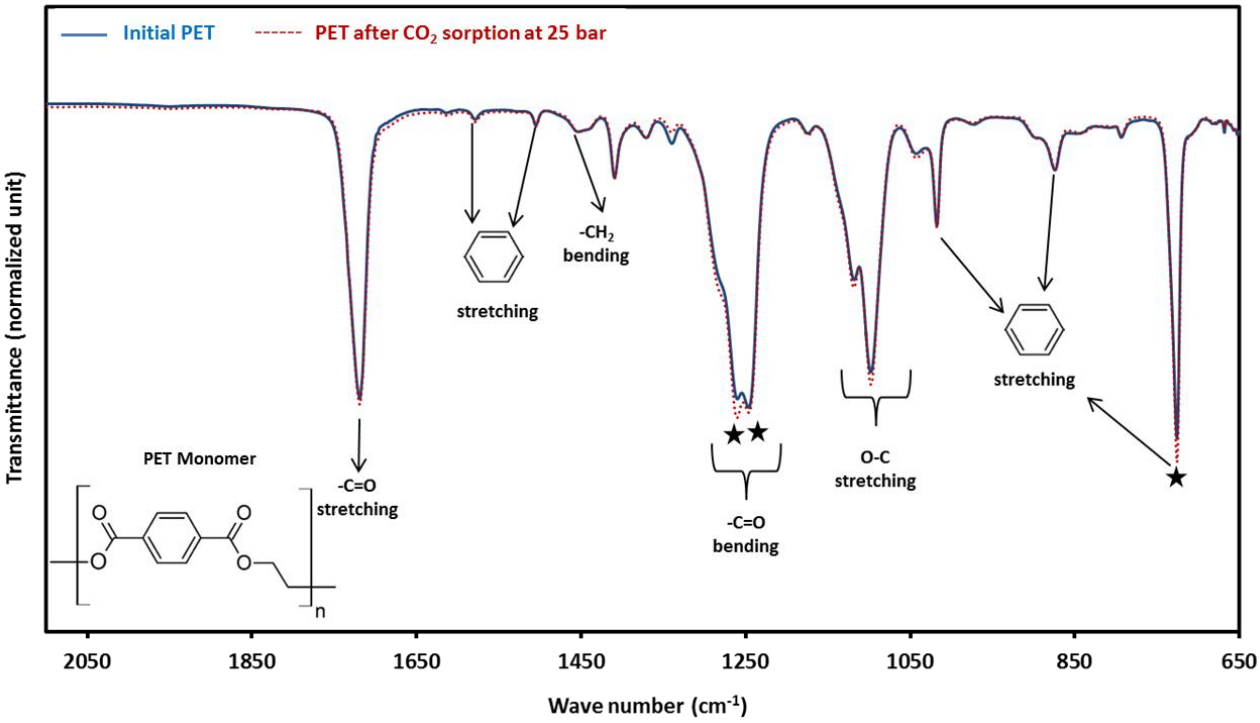

Figure 6. *ATR-FTIR spectra of PET before and after been subjected to CO_2 sorption isotherm determination. Significant differences are evidenced with stars.*

When the properties of polymer materials are modified by chemical reactions such as degradation, polymerization or chemical bonds creation, formation of new bands or chemical shifts are expected in the ATR-spectra. Neither PLA nor PET displayed shifts or new bands after the two cycles of CO_2 sorption and desorption, indicating that no chemical reaction occurred during this CO_2 sorption in isothermal conditions. However, significant changes in the relative intensity of peaks related to vibration of carbonyl groups (PLA) as well as groups associated to carbonyls (PLA and PET) and aromatic cycle (PET) were observed. These modifications can be attributed to structural rearrangements induced by plasticization and swelling of polymer chains during CO_2 sorption. The sorption sites (carbonyls) and the chemical groups near to them were the most affected in both materials. Furthermore, it appeared that the impact of such modifications were more pronounced in PLA, probably as a consequence of the higher CO_2 sorbed quantity and interactions with carbonyls groups as previously displayed by sorption isotherms.

3.2.2 Physical modifications

The thermal events of PLA and PET films stored under various sorption conditions were determined using DSC analysis, after pressure release from the samples. Only the first heating scan was considered in order to take into account the physical modifications induced by interactions with the CO_2. The related DSC curves for PLA and thermal parameters are reported in Figure 7 and Table 1, respectively.

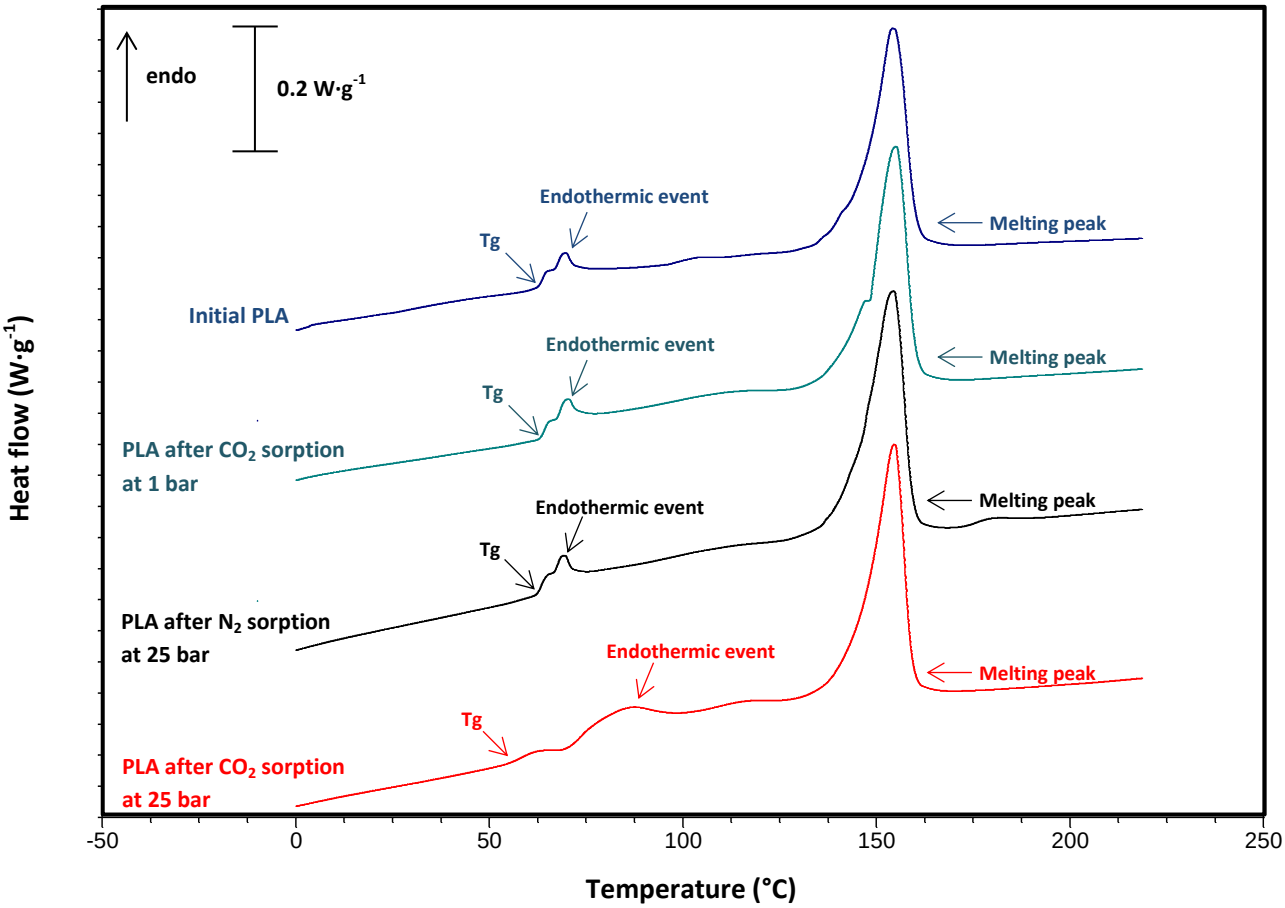

Figure 7. *DSC curves (First heating) of PLA films: starting material and following different treatments (previously equilibrated at 25 °C with CO_2 at 1 bar and 25 bar, or with N_2 at 25 bar).*

All PLA film samples displayed the typical thermal events of semicrystalline materials, namely glass transition, endothermic event associated to glass transition and melting of crystals, which are characteristic of the coexistence of amorphous and crystalline phases in the PLA structure. As previously reported, the multi peak around glass transition was most likely due to bi-orientation process, which induced an organized structure of the PLA chains and crystals.[45]

The initial PLA material was compared with a sample subjected to CO_2 sorption at 25 bar, which corresponds to the higher pressure step of the previous sorption isotherm (Figure 2). For the latter, the T_g decreased of ≈ 6 °C when compared to the initial material, and the enthalpy of the associated endothermic event increased of around 5 times. However, when PLA was placed in contact with N_2 at the same pressure of 25 bar, no change was noticeable. This clearly meant that those modifications could not be attributed only to high pressure treatments, but were unambiguously related to CO_2 sorption at this pressure. Similarly, when CO_2 pressure was only 1 bar, no modification appeared. Therefore, this suggested that two conditions were required to induce changes in the amorphous phase of PLA: sorption of CO_2 molecules and at high pressure conditions. When relatively high quantity of CO_2 were sorbed under high pressure (≈ 7 % at 25 bar, Figure 2), it induced structural changes in the PLA polymer which were not totally recovered even

when the pressure was released, and notwithstanding the fact that the CO_2 only interacted by low energy interactions.

Nofar and coworkers[46-47] have observed a clear T_g depletion in PLA as a consequence of solubilizing CO_2 in the polymer matrix. They reported a T_g decrease from ≈ 55 to 35 °C for different types of PLA *(e.g.* branched, linear, amorphous, and semicrystalline) under CO_2 at 25 bar using high pressure differential scanning calorimetry. Based on these considerations, it can be hypothesized that the increase of the endothermic event associated to glass transition was a consequence of an accelerated physical ageing favoured by T_g depletion, which came close to operative temperature (25 °C) for the highest pressure steps of the sorption isotherm. Physical ageing could be defined as the slow molecular rearrangements occurring in amorphous polymers, when stored at lower temperatures than T_g, which tend to reduce its free-energy and free volume.[48-49] As consequence of these molecular rearrangements, the polymer structure get continuously denser and becomes more glass-like and less rubber-like.[48]

A relevant finding from the present work is the T_g reduction observed for the PLA film sample placed in CO_2 environment at 25 °C and 25 bar, but for which all CO_2 molecules were desorbed at the time of analysis. Such result indicated that structural modifications were induced by CO_2 physisorption. There was no complete return of PLA to its initial physical state when removing CO_2. It probably led to a less compact network with increased free volume. This result is of particular interest, because it revealed that bulk properties of PLA films can be modified by CO_2 sorption/desorption cycles at conditions lower than the supercritical point and have to be considered for development of PLA-based materials.

The CO_2 sorption at high pressure did not influence the crystallinity degree of PLA films (Table 1), probably because the T_g depletion during sorption conditions still remained higher than operative conditions (25 °C). Indeed, lower T_g temperatures could induce transitions from glassy to rubbery state, favouring crystallization. However, a small but statistical significant increase in crystallinity degree was observed in PLA after N_2 sorption at high pressures (28.1 vs. 24.8 %). This increase was unexpected, since no modifications in the amorphous phase were observed and only very low interactions (and therefore no-plasticization) between PLA and N_2 were suggested in the corresponding literature.[39, 50-51] Indeed, N_2 solubility in PLA was reported to be around 1 – 2 magnitude lower than the corresponding CO_2 values.[39, 50-51]

In the case of PET, the effects of CO_2 sorption at high pressure were evaluated by analysing outgassed samples from CO_2 sorption isotherm (Figure 3). Since determining CO_2 sorption isotherm involved ≈ 2.5 months, samples stored at room conditions (close to 25 °C) for 5 months were used as control specimens to evaluate if physical ageing occurred. Films subjected to CO_2 sorption at 1 bar were also considered to evaluate the modifications induced by sorption of CO_2 at low pressure. The related DSC curves and thermal parameters are reported in Figure 8 and Table 1.

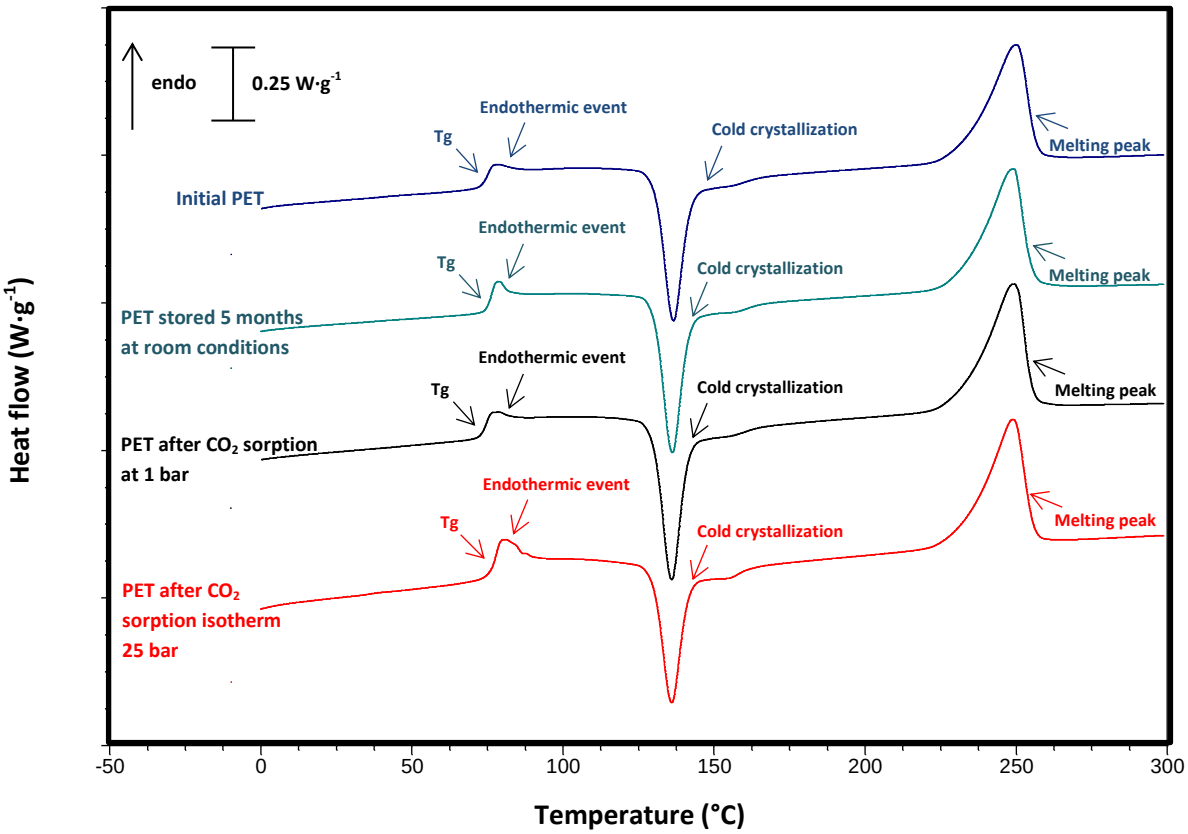

Figure 8. *DSC curves (First heating) of PET films: starting material and PET following different treatments and storage conditions (storage for 5 months at room conditions, previously equilibrated with CO_2 at 1 bar and previously submitted to CO_2 sorption isotherm determination up to 25 bar).*

PET films displayed the typical thermal events of purely amorphous materials: glass transition, endothermic event associated to glass transition, and equivalent exothermic and endothermic transitions related to cold crystallization and melting of PET crystals, respectively. When the melting enthalpy was subtracted to the cold crystallization enthalpy, a small percentage of crystals (3 %) were found in PET.

A significant increase (p-value < 0.001) of the endothermic event related to glass transition was noteworthy for PET sample placed under high CO_2 pressure (up to 25 bar) during the sorption isotherm experiment. No significance increase (p-value > 0.05) in such thermal event was observed in control samples neither consecutively to long time storage (5 months) nor following sorption of CO_2 at low pressure (1 bar), suggesting an acceleration of physical ageing when in contact with high pressure of CO_2, in an analogous way to PLA. Several studies have already reported a decrease of T_g in PET films when CO_2 molecules are solubilized in the polymer,[52-55] with values ranging between 40 and 60 °C at ≈ 20-25 bar using high pressure differential scanning calorimetry.[52-53]

Although a T_g decrease is observed in the over-mentioned studies, a small increase in T_g of PET samples after CO_2 sorption at high pressure was observed in this study. Such an increase can be considered in line with the effects of physical ageing, since no CO_2 molecules remained in the polymer matrix during the DSC analysis. In fact, the molecular rearrangements in physical ageing involve a densification of the polymer

structure, which can decrease the free volume.[48-49] In contrast to PLA, it seems that swelling induced by CO_2 sorption was less pronounced in PET, probably due to the lower CO_2 sorption level.

Lastly, a small increase in the crystallinity degree (from 3 to ≈ 4.5 %) was observed in samples used for CO_2 sorption determination and on samples stored for 5 months at room conditions, which could result from relaxation phenomena during ageing, which led to the formation of crystallites.

3.2.3 Impact on the functional properties

In order to investigate if the modifications induced in the physical state of PLA also influenced its main functional properties, the mechanical behaviour under tensile stress and the barrier properties to CO_2 of PLA prior to and after CO_2 sorption at 25 bar were measured.

Mechanical properties

Table 2 reports the Young's modulus (E_{Young}), yield strength (σ_y), yield elongation (ε_y), tensile strength (σ_b) and elongation at break (ε_b) of PLA.

The mechanical behaviour of films was influenced by the previous sorption of CO_2 at high pressure. However, a not clear effect of CO_2 plasticization was observed, since a significant decrease (p-value = < 0.0001) of strength at the yield point (σ_y), followed by a significant increase (p-value = 0.014) of strength at the break point (σ_b) and no change in elongation at break (ε_b) were noticed in PLA samples after CO_2 sorption. This ambiguous result could be explained by the two phenomena occurring consecutively to CO_2 sorption. The plasticization effect of CO_2, which tended to swell PLA chains, could generate the decrease of σ_y, while the acceleration of physical ageing could induce the increase of σ_b, due to a densification of the PLA structure. If p-values related to the significativity of difference for both parameters are compared, a much lower value is found in σ_y compared to σ_b, suggesting a weak domination of CO_2 plasticization over PLA structure densification.

Barrier properties

The permeability (P), the diffusion coefficient (D_{perm}) and the solubility coefficient (S_{perm}) of PLA films to CO_2, determined by manometric method are reported in Table 2.

The permeability of PLA films to CO_2 increased of ≈ 11 % consecutively to CO_2 sorption at high pressure, in agreement with the T_g decrease detected by DSC. The solubility coefficient increased of around 50 %, which was in line with CO_2 sorption isotherm, which displayed a similar increase during the second sorption step (Figure 2). These results confirmed that CO_2 acted as plasticizer and physically intercalated between polymer chains, which in turn expose new sorption sites. These sites would be still available for the next sorption step once the CO_2 molecules were desorbed.

In contrast, a small decrease in the effective diffusion coefficient D_{perm} was noticeable for films after CO_2 sorption. Some studies showed a decrease in water and oxygen permeability for different types of PLA (*e.g.* totally amorphous, semicrystalline, with/without plasticizers) as a result of PLA structure densification

during physical ageing.[56-58] Based on these considerations, it could be hypothesized that such decrease in the diffusion properties originated from the acceleration of physical ageing during CO_2 sorption.

Lastly, the diffusion coefficient obtained by the permeability measurement were slightly different from the values obtained during the sorption isotherm experiment (D_{perm} $\approx 10 \cdot 10^{-13} \cdot m^2 \cdot s^{-1}$ vs. D_{sorp} $\approx 2 \cdot 10^{-13} \cdot m^2 \cdot s^{-1}$), possibly because the experimental conditions for calculating such values were not the same. In particular, the former determination (D_{perm}) involves a dynamic system with continuous gas flow; while the latter (D_{sorp}) involves a static system and establishes a boundary layer, which acts as an additional resistance to mass transfer. Nevertheless, the values could be considered very similar between them, since they remained in the same order of magnitude.

4 Conclusions

The CO_2 sorption isotherm (two sorption/desorption cycles) gave evidence of physisorption and hysteresis phenomena in PLA. These results were in line with ATR-FTIR analysis, which did not reveal any chemical differences in the samples before and after been subjected to CO_2 sorption. The effective CO_2 diffusion coefficients of PLA (D_{sorp}) oscillated around 10^{-13} $m^2 \cdot s^{-1}$ and no effect of CO_2 pressure was found, however the D_{sorp} associated to desorption steps were faster than the sorption steps, probably due to formation of CO_2 clusters or CO_2-CO_2 interactions in the polymer matrix.

The thermal properties revealed physical modifications in the amorphous structure of PLA after CO_2 sorption at high pressure of 25 bar. CO_2 solubilization in PLA induced a T_g depletion, which accelerated the physical ageing of PLA. Two phenomena with opposite effects occurred. On one hand, CO_2 plasticization tended to swell PLA chains, increasing its free volume. On the other hand, the physical ageing tended to get denser the PLA structure. As a result of these bulk modifications, the functional properties of PLA changed. The results of this study are of particular interest because they provide evidence to the capacity of CO_2 to physically modify the bulk properties of PLA even at lower conditions than its supercritical point, which could be considered when materials based on PLA are developed.

Lastly, the behaviour of PET after CO_2 sorption was very similar to PLA. All the analyses displayed (sorption isotherm, diffusion coefficient, ATR-FTIR and thermal event) that the PET structure was physically modified by CO_2 sorption in a similar way to PLA. But as a consequence of its lower CO_2 solubility, the impact of such modifications was of minor intensity. Therefore, the results of this study contribute in giving new evidences of the PLA feasibility as starting material able to substitute PET in packaging applications involving CO_2.

Acknowledgements

The authors acknowledge the European Social Fund – Friuli Venezia Giulia Region – Operational Program 2007/2013 for supporting this project (Regional code: FP1340303009).

Table 1. *Thermal events of PLA and PET prior to and after gas sorption under various conditions.*

Film	Condition	Glass transition		Endothermic event	Cold crystallization		Melting		Crystallinity
		T_g (°C)	ΔC_p ($J \cdot g^{-1} \cdot °C^{-1}$)	ΔH_{relax} ($J \cdot g^{-1}$)	T_{cc} (°C)	ΔH_{cc} ($J \cdot g^{-1}$)	T_m (°C)	ΔH_m ($J \cdot g^{-1}$)	X_c (%)
PLA	Initial	64.4 ± 0.9^{a}	0.13 ± 0.03^{a}	0.47 ± 0.14^{a}	§	§	155.1 ± 0.9^{a}	23.0 ± 2.0^{a}	24.8 ± 2.1^{a}
	N_2 (25 bar)	63.7 ± 0.4^{a}	0.18 ± 0.01^{b}	0.60 ± 0.06^{a}	§	§	154.7 ± 0.4^{a}	26.2 ± 0.1^{b}	28.1 ± 0.2^{b}
	CO_2 (1 bar)	64.1 ± 0.7^{a}	0.15 ± 0.01^{ab}	0.75 ± 0.11^{a}	§	§	154.0 ± 0.5^{a}	25.1 ± 0.8^{ab}	27.0 ± 0.9^{ab}
	CO_2 (25 bar)	58.9 ± 0.8^{b}	0.13 ± 0.01^{a}	3.24 ± 0.14^{b}	§	§	154.5 ± 0.2^{a}	25.0 ± 0.4^{ab}	26.9 ± 0.4^{ab}
PET	Initial	74.2 ± 0.4^{x}	0.44 ± 0.03^{xy}	0.40 ± 0.03^{x}	136.4 ± 0.1^{x}	32.0 ± 0.6^{x}	250.1 ± 0.2^{x}	36.2 ± 1.0^{x}	3.0 ± 0.4^{x}
	5 months	75.4 ± 0.1^{y}	0.43 ± 0.02^{xy}	0.73 ± 0.21^{x}	135.9 ± 0.3^{x}	31.5 ± 1.0^{x}	248.8 ± 0.4^{x}	37.3 ± 1.0^{xy}	4.1 ± 0.1^{y}
	CO_2 (1 bar)	74.0 ± 0.2^{x}	0.49 ± 0.02^{y}	0.42 ± 0.13^{x}	135.9 ± 0.2^{x}	33.2 ± 0.6^{x}	249.1 ± 0.5^{x}	39.0 ± 0.8^{y}	4.2 ± 0.3^{y}
	CO_2 (isotherm)	76.4 ± 0.2^{z}	0.48 ± 0.02^{xy}	2.55 ± 0.15^{y}	136.1 ± 0.3^{x}	31.9 ± 0.3^{x}	249.0 ± 0.8^{x}	38.4 ± 0.4^{y}	4.7 ± 0.5^{y}

§Transition not detectable.

Values are reported as mean ± S.D. Significant differences (p. value < 0.05) are indicated with different letters in the same column. For each parameter, two independent ANOVA tests were carried out, one for PLA (subscripts a,b) and one fore PET (subscripts x,y,z). T_g = glass transition temperature, ΔC_p = specific heat variation, ΔH_{relax} = enthalpy of endothermic event associated to glass transition, T_{cc} = cold crystallization temperature, ΔH_{cc} = cold crystallization enthalpy, T_m = melting temperature, ΔH_m = melting enthalpy and X_c = crystallinity degree.

Table 2. *Mechanical and barrier properties to CO_2 of PLA prior to and after CO_2 sorption at 25 bar for 5 days at 25 °C.*

Film	Mechanical properties					Barrier properties to CO_2		
		Yield point		Break point				
	E_{Young} (GPa)	σ_y (MPa)	ε_y (%)	σ_b (MPa)	ε_b (%)	P ($10^{-16} \cdot mol \cdot m^{-1} \cdot s^{-1} \cdot Pa^{-1}$)	D_{perm} ($10^{-13} \cdot m^2 \cdot s^{-1}$)	S_{perm} ($10^{-4} \cdot mol \cdot m^{-3} \cdot Pa^{-1}$)
Initial PLA	4.0 ± 0.1^{a}	78.8 ± 1.0^{a}	2.7 ± 0.2^{a}	98.8 ± 5.4^{a}	66.9 ± 10.9^{a}	2.83 ± 0.03^{a}	10.3 ± 0.9^{a}	2.8 ± 0.2^{a}
PLA after CO_2 sorption at 25 bar	4.1 ± 0.2^{a}	70.3 ± 1.3^{b}	2.5 ± 0.2^{a}	105.8 ± 3.4^{b}	67.7 ± 4.3^{a}	3.13 ± 0.04^{b}	7.8 ± 0.7^{b}	4.0 ± 0.3^{b}

Values are reported as mean ± S.D. Significant differences (p. value < 0.05) are indicated with different letters in the same column (subscripts a,b). E_{Young} = Young's modulus, σ_y = yield strength, $\varepsilon_{y\ =}$ yield elongation, σ_b = tensile strength, ε_b = elongation at break, P = permeability, D_{perm} = diffusion coefficient from manometric method, S_{perm} = solubility coefficient from manometric method.

References

1. Auras, R.; Harte, B.; Selke, S. An overview of polylactides as packaging materials. *Macromolecular Bioscience* **2004,** *4* (9), 835-864.

2. Jamshidian, M.; Tehrany, E. A.; Imran, M.; Jacquot, M.; Desobry, S. Poly-lactic acid: production, applications, nanocomposites, and release studies. *Comprehensive Reviews in Food Science and Food Safety* **2010,** *9* (5), 552-571.

3. Rasal, R. M.; Janorkar, A. V.; Hirt, D. E. Poly(lactic acid) modifications. *Progress in Polymer Science* **2010,** *35* (3), 338-356.

4. European Bioplastics Association. Global production capacities of bioplastics 2014 (by material type) and applications. http://en.european-bioplastics.org/market. Retrieved on 25/01/2016.

5. Plastics Europe Association. Plastics: The Facts 2015. http://www.plasticseurope.org/plastics-industry/market-and-economics.aspx. Retrieved on 25/01/2016.

6. McMillin, K. W. Where is MAP Going? A review and future potential of modified atmosphere packaging for meat. *Meat Science* **2008,** *80* (1), 43-65.

7. Singh, P.; Wani, A. A.; Karim, A. A.; Langowski, H.-C. The use of carbon dioxide in the processing and packaging of milk and dairy products: a review. *International Journal of Dairy Technology* **2012,** *65* (2), 161-177.

8. Sandhya Modified atmosphere packaging of fresh produce: current status and future needs. *Lwt-Food Science and Technology* **2010,** *43* (3), 381-392.

9. Cooper, A. I. Polymer synthesis and processing using supercritical carbon dioxide. *Journal of Materials Chemistry* **2000,** *10* (2), 207-234.

10. Knez, Z.; Markocic, E.; Leitgeb, M.; Primozic, M.; Hrncic, M. K.; Skerget, M. Industrial applications of supercritical fluids: a review. *Energy* **2014,** *77*, 235-243.

11. Herrero, M.; Cifuentes, A.; Ibanez, E. Sub- and supercritical fluid extraction of functional ingredients from different natural sources: Plants, food-by-products, algae and microalgae - a review. *Food Chemistry* **2006,** *98* (1), 136-148.

12. Sahena, F.; Zaidul, I. S. M.; Jinap, S.; Karim, A. A.; Abbas, K. A.; Norulaini, N. A. N.; Omar, A. K. M. Application of supercritical CO_2 in lipid extraction - A review. *Journal of Food Engineering* **2009,** *95* (2), 240-253.

13. Brunner, G. Supercritical fluids: technology and application to food processing. *Journal of Food Engineering* **2005,** *67* (1-2), 21-33.

14. Damar, S.; Balaban, M. O. Review of dense phase CO_2 technology: microbial and enzyme inactivation, and effects on food quality. *Journal of Food Science* **2006,** *71* (1), R1-R11.

15. Kamihira, M.; Taniguchi, M.; Kobayashi, T. Sterilization of microorganisms with supercritical carbon-dioxide. *Agricultural and Biological Chemistry* **1987,** *51* (2), 407-412.

16. Nofar, M.; Park, C. B. Poly (lactic acid) foaming. *Progress in Polymer Science* **2014,** *39* (10), 1721-1741.

17. Marubayashi, H.; Akaishi, S.; Akasaka, S.; Asai, S.; Sumita, M. Crystalline structure and morphology of poly(l-lactide) formed under high-pressure CO_2. *Macromolecules* **2008,** *41* (23), 9192-9203.

18. Lan, Q.; Yu, J.; He, J.; Maurer, F. H. J.; Zhang, J. Thermal behavior of poly(L-lactide) having low L-isomer content of 94% after compressed CO_2 treatment. *Macromolecules* **2010,** *43* (20), 8602-8609.

19. Kasturirangan, A.; Koh, C. A.; Teja, A. S. Glass-transition temperatures in CO_2 + polymer systems: modeling and experiment. *Industrial & Engineering Chemistry Research* **2011,** *50* (1), 158-162.

20. Wischke, C.; Schwendeman, S. P. Principles of encapsulating hydrophobic drugs in PLA/PLGA microparticles. *International Journal of Pharmaceutics* **2008,** *364* (2), 298-327.

21. Kim, J. H.; Paxton, T. E.; Tomasko, D. L. Microencapsulation of naproxen using rapid expansion of supercritical solutions. *Biotechnology Progress* **1996,** *12* (5), 650-661.

22. Champeau, M.; Thomassin, J. M.; Jerome, C.; Tassaing, T. In situ FTIR micro-spectroscopy to investigate polymeric fibers under supercritical carbon dioxide: CO_2 sorption and swelling measurements. *Journal of Supercritical Fluids* **2014,** *90*, 44-52.

23. Pini, R.; Storti, G.; Mazzotti, M.; Tai, H.; Shakesheff, K. M.; Howdle, S. M. Sorption and swelling of poly(DL-lactic acid) and poly(lactic-co-glycolic acid) in supercritical CO_2: An experimental and modeling study. *Journal of Polymer Science Part B-Polymer Physics* **2008,** *46* (5), 483-496.

24. Crank, J. *The mathematics of diffusion*; Clarendon Press: Oxford, Eng, 1975.

25. Garlotta, D. A literature review of poly(lactic acid). *Journal of Polymers and the Environment* **2001,** *9* (2), 63-84.

26. Liang, C. Y.; Krimm, S. Infrared spectra of high polymers: Part IX. Polyethylene terephthalate. *Journal of Molecular Spectroscopy* **1959,** *3* (1–6), 554-574.

27. Fischer, E. W.; Sterzel, H. J.; Wegner, G. Investigation of the structure of solution grown crystals of lactide copolymers by means of chemical reactions. *Kolloid-Zeitschrift and Zeitschrift fur polymere* **1973,** *251*, 980-990.

28. Ajji, A.; Guèvremont, J.; Cole, K. C.; Dumoulin, M. M. Orientation and structure of drawn poly(ethylene terephthalate). *Polymer* **1996,** *37* (16), 3707-3714.

29. International Organization for Standardization (ISO). Plastiques 2012. Détermination des propriétés en traction. Partie 1: Principes généraux NF EN ISO 527-1.

30. Oliveira, N. S.; Dorgan, J.; Coutinho, J. A. P.; Ferreira, A.; Daridon, J. L.; Marrucho, I. M. Gas solubility of carbon dioxide in poly(lactic acid) at high pressures. *Journal of Polymer Science Part B-Polymer Physics* **2006,** *44* (6), 1010-1019.

31. Oliveira, N. S.; Dorgan, J.; Coutinho, J. A. P.; Ferreira, A.; Daridon, J. L.; Marrucho, I. M. Gas solubility of carbon dioxide in poly(lactic acid) at high pressures: Thermal treatment effect. *Journal of Polymer Science Part B-Polymer Physics* **2007,** *45* (5), 616-625.

32. Kasturirangan, A.; Grant, C.; Teja, A. S. Compressible lattice model for phase equilibria in CO_2+polymer systems. *Industrial & Engineering Chemistry Research* **2008,** *47* (3), 645-649.

33. Aionicesei, E.; Skerget, M.; Knez, Z. Measurement of CO_2 solubility and diffusivity in poly(L-lactide) and poly(D,L-lactide-co-glycolide) by magnetic suspension balance. *Journal of Supercritical Fluids* **2008,** *47* (2), 296-301.

34. Kazarian, S. G.; Vincent, M. F.; Bright, F. V.; Liotta, C. L.; Eckert, C. A. Specific intermolecular interaction of carbon dioxide with polymers. *Journal of the American Chemical Society* **1996,** *118* (7), 1729-1736.

35. Nalawade, S. P.; Picchioni, F.; Marsman, J. H.; Grijpma, D. W.; Feijen, J.; Janssen, L. Intermolecular interactions between carbon dioxide and the carbonyl groups of polylactides and poly(epsilon-caprolactone). *Journal of Controlled Release* **2006,** *116* (2), E38-E40.

36. Nalawade, S. P.; Picchioni, F.; Marsman, J. H.; Janssen, L. The FT-IR studies of the interactions of CO_2 and polymers having different chain groups. *Journal of Supercritical Fluids* **2006,** *36* (3), 236-244.

37. Kazarian, S. G.; Brantley, N. H.; West, B. L.; Vincent, M. F.; Eckert, C. A. In situ spectroscopy of polymers subjected to supercritical CO_2: Plasticization and dye impregnation. *Applied Spectroscopy* **1997,** *51* (4), 491-494.

38. Kanehashi, S.; Kusakabe, A.; Sato, S.; Nagai, K. Analysis of permeability; solubility and diffusivity of carbon dioxide; oxygen; and nitrogen in crystalline and liquid crystalline polymers. *Journal of Membrane Science* **2010,** *365* (1–2), 40-51.

39. Bao, L.; Dorgan, J. R.; Knauss, D.; Hait, S.; Oliveira, N. S.; Maruccho, I. M. Gas permeation properties of poly(lactic acid) revisited. *Journal of Membrane Science* **2006,** *285* (1–2), 166-172.

40. McGonigle, E. A.; Liggat, J. J.; Pethrick, R. A.; Jenkins, S. D.; Daly, J. H.; Hayward, D. Permeability of N_2, Ar, He, O_2 and CO_2 through biaxially oriented polyester films - dependence on free volume. *Polymer* **2001,** *42* (6), 2413-2426.

41. Burgess, S. K.; Kriegel, R. M.; Koros, W. J. Carbon dioxide sorption and transport in amorphous poly(ethylene furanoate). *Macromolecules* **2015,** *48* (7), 2184-2193.

42. Brolly, J. B.; Bower, D. I.; Ward, I. M. Diffusion and sorption of CO_2 in poly(ethylene terephthalate) and poly(ethylene naphthalate). *Journal of Polymer Science Part B-Polymer Physics* **1996,** *34* (4), 769-780.

43. Krimm, S., Infrared spectra of high polymers. In *Fortschritte Der Hochpolymeren-Forschung / Advances in polymer science*; Ferry, J. D.; Overberger, C. G.; Schulz, G. V.; Staverman, A. J.; Stuart, H. A., Eds.; Springer – Verlag: Berlin, 1960.

44. Molinaro, S.; Romero, M. C.; Boaro, M.; Sensidoni, A.; Lagazio, C.; Morris, M.; Kerry, J. Effect of nanoclay-type and PLA optical purity on the characteristics of PLA-based nanocomposite films. *Journal of Food Engineering* **2013,** *117* (1), 113-123.

45. Rocca-Smith, J. R.; Karbowiak, T.; Marcuzzo, E.; Sensidoni, A.; Piasente, F.; Champion, D.; Heinz, O.; Vitry, P.; Bourillot, E.; Lesniewska, E.; Debeaufort, F. Impact of corona treatment on PLA film properties. *Polymer Degradation and Stability* **2016,** *132*, 109-116.

46. Nofar, M.; Zhu, W.; Park, C. B. Effect of dissolved CO_2 on the crystallization behavior of linear and branched PLA. *Polymer* **2012,** *53* (15), 3341-3353.

47. Nofar, M.; Ameli, A.; Park, C. B. The thermal behavior of polylactide with different D-lactide content in the presence of dissolved CO_2. *Macromolecular Materials and Engineering* **2014,** *299* (10), 1232-1239.

48. Struik, L. C. E. Physical aging in plastics and other glassy materials. *Polymer Engineering & Science* **1977,** *17* (3), 165-173.

49. Hutchinson, J. M. Physical aging of polymers. *Progress in Polymer Science* **1995,** *20* (4), 703-760.

50. Lehermeier, H. J.; Dorgan, J. R.; Way, J. D. Gas permeation properties of poly(lactic acid). *Journal of Membrane Science* **2001,** *190* (2), 243-251.

51. Oliveira, N. S.; Oliveira, J.; Gomes, T.; Ferreira, A.; Dorgan, J.; Marrucho, I. M. Gas sorption in poly(lactic acid) and packaging materials. *Fluid Phase Equilibria* **2004,** *222*, 317-324.

52. Chiou, J. S.; Barlow, J. W.; Paul, D. R. Plasticization of glassy-polymers by CO_2. *Journal of Applied Polymer Science* **1985,** *30* (6), 2633-2642.

53. Zhong, Z. K.; Zheng, S. X.; Mi, Y. L. High-pressure DSC study of thermal transitions of a poly(ethylene terephthalate) carbon dioxide system. *Polymer* **1999,** *40* (13), 3829-3834.

54. Shieh, Y.-T.; Li, Y.-H.; Huang, C.-C.; Wang, T.-L. Effects of CO_2 treatments on the dual glassy relaxations and dual melting peaks in poly(ethylene terephthalate). *The Journal of Supercritical Fluids* **2010,** *55* (1), 373-380.

55. Zhang, Z. Y.; Handa, Y. P. CO_2-assisted melting of semicrystalline polymers. *Macromolecules* **1997,** *30* (26), 8505-8507.

56. Kwon, M.; Lee, S. C.; Jeong, Y. G. Influences of physical aging on enthalpy relaxation behavior, gas permeability, and dynamic mechanical property of polylactide films with various D-isomer contents. *Macromolecular Research* **2010,** *18* (4), 346-351.

57. Burgos, N.; Martino, V. P.; Jimenez, A. Characterization and ageing study of poly(lactic acid) films plasticized with oligomeric lactic acid. *Polymer Degradation and Stability* **2013,** *98* (2), 651-658.

58. Martino, V. P.; Ruseckaite, R. A.; Jimenez, A. Ageing of poly(lactic acid) films plasticized with commercial polyadipates. *Polymer International* **2009,** *58* (4), 437-444.

Effect of the state of water and relative humidity on ageing of PLA film

Rocca-Smith, J.R.; Chau, N.; Champion, D.; Brachais C.-H.; Marcuzzo, E.; Sensidoni, A.; Piasente, F.; Karbowiak, T.; Debeaufort, F. Effect of the state of water and relative humidity on ageing of PLA film. *Food Chemistry 2017. Doi: 10.1016/j.foodchem.2017.02.113.*

Abstract

Various types of food are now commercialized in packaging materials based on poly (lactic acid) (PLA) due to its eco-friendly nature. However, one of the main limitations related to PLA is its reactivity with water. For food applications, it is of critical importance to better understand the hydrolysis of PLA driven by water molecules either in liquid or in vapour state. This work focuses on the modifications of PLA induced by water when simulating contact with semi-dry foods ($a_w \approx 0.5$), high moisture foods ($a_w \approx 1$) and liquid foods ($a_w \approx 1$). This study undoubtedly shows that both the chemical potential of water and its physical state influence the hydrolytic degradation of PLA films. From a practical point of view, PLA packaging is very well suited for semi-dry foods, but is highly sensitive to high moisture and liquid foods.

Keywords

PLA, hydrolysis, food packaging, water, storage test, thermal properties, molecular weight distribution

1 Introduction

Food industry is always interested in using the most suitable and performing packaging for preserving the quality of the food products over their shelf life. The increase in the environmental concern over the past decades is pushing towards the development of new packaging systems with eco-friendly characteristics, such as renewability, biodegradability and compostability.[1] The main challenge is to develop a packaging material, having a good balance between its durability and biodegradability, to guarantee the quality of various food products and to ensure an easy treatment of wastes with low environmental impact.[2] This means that a new challenge is to find good adequacy between the food shelf life and the packaging shelf life.

A biopolymer with the potential to satisfy most of the overall requirements is poly (lactic acid), or PLA. PLA is a renewable and biodegradable polyester, which derives from carbohydrates sources such as starch corn, sugar cane and biomass waste like wood ships, bagasse and wheat straw.[3] Thanks to enzymatic and microbial fermentations, these renewable resources are converted to lactic acid, the building block of PLA. The monomer is polymerized for obtaining PLA at high molecular weight (> 100 kDa) via different chemical processes, such ring opening polymerization of lactides (*i.e.* cyclic dimers of lactic acid), direct condensation polymerization or azeotropic dehydration condensation.[4] Compared to other biopolymers, PLA shows interesting functional properties, reduced cost and easier facility to be industrially processed. It is considered as the most promising candidate for replacing conventional plastics and it is currently used as food packaging and food serviceware.[4-5]

Academia and industry are largely studying this polymer since a decade for tailoring its overall properties and increasing its applications.[6-7] Although more efforts are still needed, the reached advances brought to PLA to play an important role in the current bioplastic market. The European Bioplastic Association [8] recently reported that the world production of this polymer exceeded 207 thousand tons in 2014, representing the 12 % of the bioplastic market. The main application of PLA is food packaging and it will probably remain the main use of PLA in the near future. PLA is also used in other areas such as medical, agriculture, textiles, 3D printing, electronics and automobile applications, which are all expected to have a higher importance in the following years.[8]

Food corporations such as Danone (Germany), Del Monte (USA) and Noble Juice (USA), as well as leading food retailers such as Wal-Mart (USA), SPAR (Austria) and Auchan (France) are currently using PLA based packaging in some of their products.[3] Various types of food products are currently packed and commercialized with PLA based materials. They are characterized by different physical states, a wide range of water activity (a_w), pH and composition. Some examples are potato chips (amorphous solids, a_w = 0.1 – 0.3), fresh salads and vegetables

(biological gels, a_w > 0.99), yogurts (gels, a_w > 0.99), citrus juices (acid liquids, a_w = 0.97 – 0.99) and water (liquid, a_w > 0.99).

Although a general interest is noticeable to increase the trade food products packed in PLA, there is not enough information related to the interactions between food products and PLA based packaging available in the scientific literature. Such information is of relevant importance considering that one of the main limitations, related to the PLA packaged food, is the inherent water sensitivity of PLA that can compromise its stability. Even if PLA absorbs very small quantities of water (< 1.5 wt%),[4, 9] PLA can interact with water molecules from the packed food, and can be hydrolysed during the time of storage. As a result of these chemical reactions, its performance for food packaging may be reduced during packed food storage, compromising therefore the quality and the safety of food.

The hydrolysis mechanism of PLA has been principally studied for applications of biomedical devices, such as implants and carriers of drug for controlled release.[10-12] Due to the importance in understanding the interactions between the polymer and the biological fluids, most of the available literature is focused on the hydrolysis of different types of PLA (*e.g.* amorphous, semi-crystalline, copolymerized)[13-14] having different shapes (*e.g.* microspheres, plates, cylinders)[15-17] in aqueous or liquid buffer solutions, which simulate biological fluids (*e.g.* Ringer's solution, phosphate buffer solutions).[18-20] Nevertheless, only few studies have been focused on the PLA hydrolysis carried out by water in the vapour phase [21-23] and they generally do not consider PLA produced at large scale. This lack of information is of significant importance, since the interactions between packaging and water molecules of non-liquid foods are in the vapour phase.

Based on these considerations, the objective of this study was to better understand the modifications induced by water on the properties of PLA films during storage time, focusing on semi-dry foods (a_w ≈ 0.5), high moisture foods (a_w ≈ 1) and liquid foods in contact (a_w ≈ 1) with PLA. In order to simulate these conditions, accelerated ageing tests were carried out for these three different wet environments. PLA films produced at industrial scale were placed at 50 °C in environments at 50 or 100 % relative humidity (RH) or immersed in liquid water. The storage temperature chosen was able to accelerate the chemical reaction rates, without inducing significant modifications in the physical state of PLA. Indeed, transitions from the glassy to the rubbery states occurred at 5-10 °C higher than 50 °C. The first two conditions provided information related to the interactions between PLA and water in the vapour state, while the third one gave information regarding interactions with liquid water. The functional properties, the molecular weight distribution, the surface properties and the thermal events of PLA films were assessed over a 2 months storage period.

2 Materials and methods

2.1 PLA films

Semi-crystalline PLA films (D-level ≥ 4.25 %) available in the market for food packing applications were used in this study. They were produced and supplied by Taghleef Industries (thickness = 17 µm, commercial name: Nativia NTSS, Udine, Italy). During production, films were subjected to a biaxial orientation and annealing to induce crystallization and to improve their mechanical properties. The number-average molecular weight ($\overline{M_n}$), the weight-average molecular weight ($\overline{M_w}$) and the polydispersity index (*PDI*) of initial PLA films was approximately 70 000 g·mol^{-1}, 160 000 g·mol^{-1} and 2.3, respectively.

2.2 Storage conditions of accelerated ageing test

Rectangular PLA films (21 x 15 cm) were stored up to 69 days (≈ 2 months) in different humidity conditions at 50 °C using microclimate chambers. The PLA samples were immersed in water or placed in environments at ≈ 50 or 100 % relative humidity (RH) environments. These different storage conditions were maintained using NaBr (50.9 % RH at 50 °C, Sigma Aldrich, St. Louis, MO, USA)[24] saturated solution and distilled water, respectively. Samples from each storage condition were collected at different time for analysis: every day during the first week, 3 times a week during the second week, and then 2 times a week. To reduce the impact of the time between sampling and experiments, the film samples were stored at -30 °C before analyses.

2.3 Physical and chemical characterizations

Selected physical and chemical properties were followed for PLA samples stored under the three different ageing conditions.

2.3.1 Film appearance

The modifications in the appearance and opacity were assessed during sampling. Images of films at different storage conditions and times were acquired using the camera (12 MPixels) of an iPhone SE (Apple, Cupertino, CA, USA).

2.3.2 Microstructure analysis

The microstructure of both surface and cross-section of PLA was assessed by Scanning Electron Microscopy (SEM) analysis. Images were collected using a JSM-7600F scanning electron microscope (JEOL USA Inc., Peabody, MA, USA) with 1 kV as accelerated voltage of observation, 9x10^{-6} Pa for the vacuum and lower detector (LEI) as secondary electron detector.

2.3.3 Surface hydrophobicity

The surface hydrophobicity was determined using water contact angle measurements by goniometry. A water drop (≈ 1 µL) was deposited on the film surface and the contact angle was measured using a goniometer (Drop

Shape Analyser 30, Krüss GmbH, Hamburg, Germany) equipped with an image analysis software (ADVANCE – Drop Shape, version 1.4.2, KRÜSS GmbH). Five replicates were performed for each tested sample.

2.3.4 Molecular weight distribution

The molecular weight distribution of PLA samples was analysed over time by Size-Exclusion Chromatography (SEC), using a 1260 Infinity liquid chromatography system (Agilent Technologies, Santa Clara, CA, USA). It was composed of 2 Polypore Size Exclusion columns (Agilent Technologies, Santa Clara, CA, USA) connected in series. PLA samples (≈ 50 mg) were placed in 10 mL vials, 1 mL of TetraHydroFuran (THF, Carlo Erba reagents, Val de Reuil, France) was added and the mix was shaken for 20 min at room temperature (PL-SP 260VS, Agilent technologies, Santa Clara, CA, USA) until total dissolution of PLA. The dissolved samples were then filtrated using Whatman Syringe filter with a polytetrafluoroethylene (PTFE) membrane (pore diameter 0.2 µm, GE Healthcare Bio-Sciences, Pittsburgh, PA, USA) and transferred in 1.5 mL vials. Volumes of 10 µL were automatically injected in the instrument. Filtered THF with a constant flow rate of 1 mL·min^{-1} was used as the mobile phase and a Varian 390-LC refractive index detector was used in this analysis. The chromatographic separation was carried out at a controlled temperature of 45 °C. A calibration curve performed with polystyrene standards (ranging from 1.28 to 1820 kDa, Advancing Polymer Solutions, Agilent Technologies, Santa Clara, CA, USA) was used. $\overline{M_n}$, $\overline{M_w}$ and *PDI* were calculated from the resulted molecular weight distribution curve using Agilent GPC/SEC software (version 1.2, Agilent Technologies, Santa Clara, CA, USA), according to Equations 1, 2 and 3, respectively. The analysis was carried out in duplicates.

$$\overline{M_n} = \frac{\sum n_i M_i}{\sum n_i} \qquad (Eq.1)$$

$$\overline{M_w} = \frac{\sum n_i {M_i}^2}{\sum n_i M_i} \qquad (Eq.2)$$

$$PDI = \frac{\overline{M_w}}{\overline{M_n}} \qquad (Eq.3)$$

Where M_i is the molecular weight (g·mol^{-1}) of a molecule and n_i is the number of molecules having that molecular weight.

2.3.5 Thermal analysis

The evolution of the thermal events of PLA films was studied by Differential Scanning Calorimetry (DSC) using a Q20 calorimeter (TA instruments, New Castle, DE, USA). Film samples were weighed (3- 5 mg) and sealed into aluminium pans (T-zero, T.A. Instruments, New Castle, DE, USA) before being subjected to a double heating-cooling cycle at 10 °C·min^{-1} under N_2 atmosphere (flow rate = 25 mL·min^{-1}).

Two different heating programs were used. The first temperature program consisted in a double heating cycle in a narrow temperature range (from -10 to 100 °C) in order to only focus on the thermal events related to the amorphous phase of PLA. The first cycle of this heating program allowed to remove the excess of enthalpy associated to the glass transition, while the second one allowed to better estimate the variation of specific heat (ΔC_p) and the temperature of glass transition (T_g inflection point). The second temperature program investigated a broader temperature range (double heating from – 10 to 190 °C) in order to also study the transition related to the crystalline phase of PLA, such as melting temperature (T_m) and associated melting enthalpy (ΔH_m). In this case, the thermal parameters were estimated from the first heating, while the reversibility of the overall events was assessed from the second heating. At least two samples were run for each heating program, and the thermal parameters were determined using TA Universal Analysis 2000 software (version 4.5 A, TA instruments, New Castle, DE, USA).

The crystallinity percentage (X_c) of films was further calculated according to Equation 4.

$$X_c = \frac{\Delta H_m - \Delta H_{cc}}{\Delta H_m^\circ} \times 100 \qquad (Eq. 4)$$

Where ΔH_m (J·g^{-1}) is the enthalpy corresponding to the area under the melting peak, ΔH_m° (= 93 J·g^{-1})[25] is the enthalpy of melting of pure crystalline PLA and ΔH_{cc} (J·g^{-1}) is the enthalpy corresponding to the area associated to cold crystallization. Since no cold crystallization was observed in the first heating of the program related to the crystalline phase, its value is null (ΔH_{cc}= 0 J·g^{-1}).

2.4 Kinetics analysis

The experimental values of $\overline{M_n}$ and $\overline{M_w}$ over time were modeled using the first apparent order kinetics (Equations 5 and 6). The rate constants (k_{app}) were estimated using the static software GraphPad Prims 5 (version 5.04, GraphPad Software, Inc., La Jolla, CA, USA). Rate constants were considered significantly different when no intersection in their 95% confidence interval was found.

$$\ln \overline{M_n} = \ln \overline{M_{n0}} \pm k_{app(\overline{M_n})} t \ (Eq. 5)$$

$$\ln \overline{M_w} = \ln \overline{M_{w0}} \pm k_{app(\overline{M_w})} t \ (Eq. 6)$$

Where $\overline{M_{n0}}$ and $\overline{M_{w0}}$ are the number average molecular weight and the weight average molecular weight of initial PLA, respectively. t is the time (day). $k_{app(\overline{M_n})}$, $k_{app(\overline{M_w})}$ are the corresponding apparent rate constants (day^{-1}).

3 Results and Discussion

3.1 Macroscopic modifications of PLA films during ageing

As evidenced in Figure 1, the appearance of the samples stored at 50 °C and 50 % RH was very similar to the initial film for the whole duration of the ageing test. On the contrary, the visual aspect of the samples at 100 % RH and of those immersed in liquid water was strongly modified during the test. They were characterized by a loss of transparency as a function of time. This macroscopic observation unambiguously highlighted that water interacted with PLA, leading to physical plasticization, especially when PLA was in direct contact with water molecules in the liquid state or in the vapour state under saturation conditions. These interactions most likely lead modifications in the PLA chains such as physical plasticization, swelling, chemical reactions, and/or crystal grow. A similar behaviour was observed in PLA films stored at high relative humidity (specific RH values non-mentioned) at 25 °C, and in PLA films immersed in phosphate buffer at 37 °C or in liquid water at 58 °C by Holm *et al.*[22], Paul *et al.*[26] and Pantani *et al.*[27], respectively.

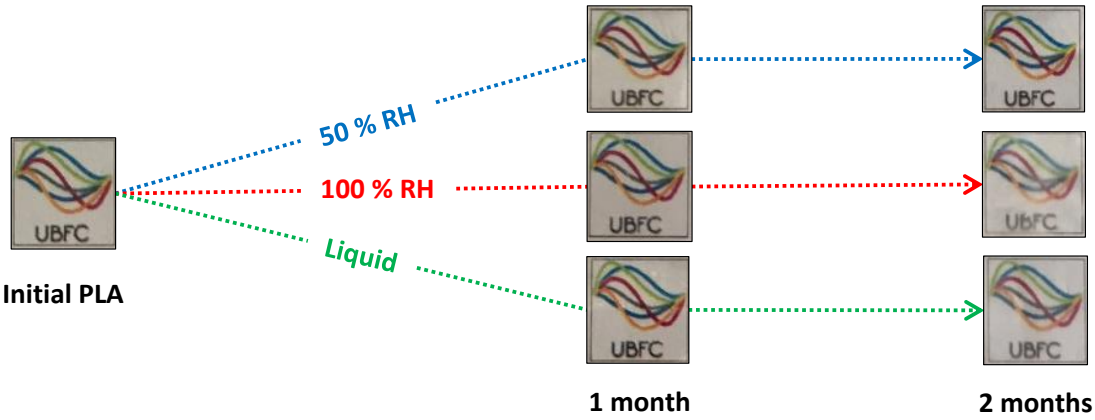

Figure 1. *Appearance of PLA films stored at 50 % RH, 100 % RH or immersed in liquid water at 50 °C during the storage test. Transparency estimated by covering the logo of the University of Burgundy Franche-Comté with PLA films.*

3.2 Modifications in the molecular weight distribution induced by ageing

In order to assess if the previously observed modifications were due (totally or partly) to a hydrolysis phenomenon, the $\overline{M_n}$, $\overline{M_w}$ and *PDI* values of PLA samples stored in the three conditions were measured over time. The corresponding results are reported in Figure 2.

It is worthy to note an unambiguous effect of the chemical potential of water on the molecular weight distribution of PLA (Figure 2a and 2b). $\overline{M_n}$ and $\overline{M_w}$values of the samples stored at ≈ 50 % RH did not change during the storage, indicating that no hydrolysis occurred in that condition. This was strengthen by modeling the data with the first apparent order kinetic equation, which displayed reduced rates and no significant different than zero (Table 1, supplementary material). On the contrary, when the relative humidity increased to

100 % RH or when PLA was in direct contact with liquid water, a fast and significant decrease of $\overline{M_n}$ and $\overline{M_w}$ values was observed, confirming the hydrolysis of PLA (Table 1, supplementary material). Indeed, the weight-average molecular weight of PLA was reduced by 6.5 times after two months, from ≈160 to ≈25 kDa. These observations were in concordance with Ho *et al.*[21], Copinet *et al.*[23] and Holm *et al.*[22], who reported that an increase in relative humidity induced a faster degradation. Nevertheless, they observed a more aggressive hydrolysis in their PLA samples, since a decrease of $\overline{M_w}$ and $\overline{M_n}$ parameters were clearly evident at milder storage conditions. Copinet *et al*.[23] found a significant decrease of $\overline{M_w}$ from ≈ 200 to ≈ 160 KDa after 60 days of storage at 30 °C and 50 % RH. In a similar way, Holm *et al.*[22] detected a decrease of $\overline{M_n}$ from ≈ 80 to ≈ 60 KDa at 58 % RH and 25 °C after 60 days of storage. A possible explanation of the higher stability of the PLA films used in this study could be found in the process used at industrial scale. In fact, industries generally use optimized strategies, which are difficult to reproduce at laboratory scale, such as bi-orientation, annealing, crystallization and inclusion of compounds able to limit the hydrolytic degradation and water sensitivity of PLA films.

When hydrolysis occurred, it is also noticeable that it did not strongly influence the *PDI* values of films (*PDI*, Figure 2c). When the polymer chain is cut in a preferential way, increasing or decreasing trends in *PDI* are expected. In this study, the *PDI* values were similar to the initial one (≈ 2.3) and no big changes were observed, suggesting that the degradation mechanism did not favour the formation of small or big oligomers in a preferential way, but randomly and/or end chain degraded the polymer. This behaviour can be also deduced by the similar decreasing trends of the parameters $\overline{M_n}$ and $\overline{M_w}$, and by the monomodal molecular weight distribution curve, which only moved to lower values at increasing storage time, without changing its width, nor forming new peaks (Figure 7, supplementary material). Similar results were also observed in others studies involving degradation of PLA films in aqueous media at 37 and 58 °C for one and two months, respectively,[28-29] as well as in degradation studies involving PLA fibres exposed to 100 % RH at 40 °C for 3 months.[30]

An interesting influence of the state of water (*i.e*. liquid *vs.* vapour) in the hydrolysis of PLA was also noticed in this study. Although the hydrolysis of the samples at 100 % RH and immersed in liquid water apparently proceeded at the same rate during the first month of storage, the hydrolysis appeared to be slightly faster during the second month of storage in the 100 % RH condition. The $\overline{M_n}$ and $\overline{M_w}$ values become lower in the saturated vapour condition than in the liquid water conditions (Figure 2a and 2b). This particular behaviour was confirmed by the kinetic analysis, which displayed a significant difference of the apparent rates of $\overline{M_n}$ and $\overline{M_w}$ between the two storage conditions (Table 1, supplementary material). This finding of the present study is of relevant interest, since such an effect of the state of water in the hydrolysis of PLA films has not been previously reported.

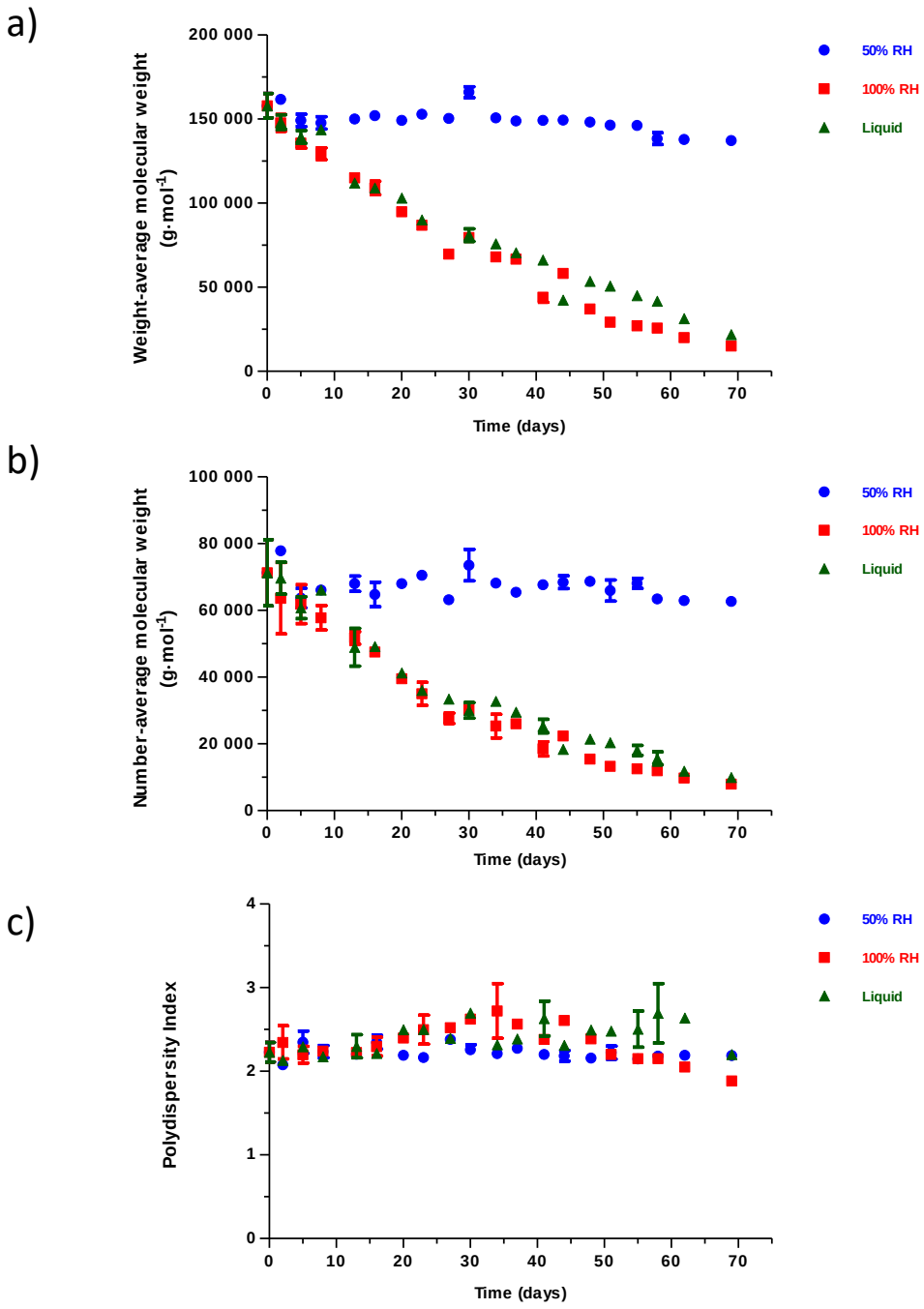

Figure 2. *Modifications in the molecular weight distribution of PLA films stored at 50 % RH (●), 100 % RH (■) or immersed in liquid water (▲) at 50 °C during time. a) Number average molecular weight ($\overline{M_n}$). b) Weight average molecular weight ($\overline{M_w}$). c) Polydispersity index (PDI). Error bars are standard deviation.*

Hydrolysis of PLA films was thus evidenced at high a_w with both liquid and vapour contact. It is also important to better know their impacts for PLA applications. Therefore, the changes in functional properties of PLA according to these ageing conditions were deeply investigated.

3.3 Modifications in the surface properties

3.3.1 Surface hydrophobicity

Water contact angle can be used as an indicator of the surface hydrophobicity of packaging materials.[31] As shown in Figure 3, no modifications in the surface hydrophobicity were noticed during the first 23 days of storage, whatever the condition. Water contact angle values oscillated around 85 °. After that storage period of 23 days of storage, water contact angle of the samples stored at 50 % RH and of those immersed in liquid water still remained approximatively the same as the initial value. On the contrary, the surfaces of films stored at 100 % RH became hydrophilic, with contact angle values decreasing down to a 60° - 40° range.

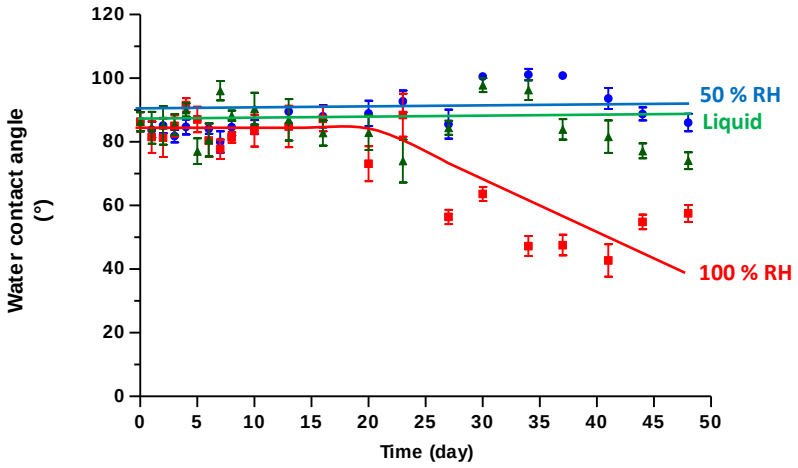

Figure 3. *Modifications in the surface hydrophobicity of PLA films stored at 50 % RH (●), 100 % RH (■) or immersed in liquid water (▲) at 50 °C during time. Error bars are standard deviation. Lines are guide for the eyes.*

Such a decrease of the surface hydrophobicity in PLA samples in which hydrolysis occurred was an expected phenomenon, since the degradation products of PLA (lactic acid and its oligomers) have a higher density of hydroxyl and carboxyl groups than the initial polymer, and therefore a higher affinity for water. The increase in the surface hydrophilicity indicated a chemical change of the surface of the samples stored at 100 % RH. Such a change was not observed in the samples stored in liquid water, although these samples were also exposed to a strong hydrolysis as previously evidenced by SEC. A possible explanation of this contradictory behaviour comes from the state of water. On the one hand, when films were directly placed in contact with liquid water, the degradation products could be transferred and dissolved into the liquid phase as suggested by the pH change in the liquid. Indeed, a decrease of the pH from 5.7 to 3.9 was measured. On the other hand, when films were stored in saturated water vapour atmosphere, such dissolution or mass transfer of small molecules from the PLA film to the liquid water was no longer possible. Thus, a progressive accumulation of degradation products, lactic acid and its oligomers, may occur on the film surface, leading to the observed phenomenon.

The different behaviour of the degradation products according to the state of water can also explain the different rates of hydrolysis observed in liquid and 100 % RH conditions (Table 1, supplementary material). It is well known that the degradation products of PLA are catalysts of the hydrolysis reactions.[10, 12] Thus, an accumulation of lactic acid and oligomers in the films not only can increase their surface hydrophilicity, but also can catalyse the hydrolysis, increasing its rate, as it occurs when PLA is exposed to 100 % RH (and not when PLA is immersed in liquid water).

In order to strengthen this hypothesis an additional experiment was performed. The surface hydrophobicity of PLA films subjected to ageing at 100 % RH and 50 °C for 48 days was measured before and after being rinsed in distilled water for 2 hours. The water contact angle of such films highly increased from 58 up to 76 ° after being rinsed. This last value was also equivalent to the values of the samples stored in liquid conditions. Therefore, this confirms the key role of the state of water in the hydrolysis mechanism. Liquid water also acts as a dissolution medium for the mass transfer of the degradation products from PLA polymer, limiting their influence as catalysts of the hydrolysis reaction.

It is also worthy to note that the decrease of the surface hydrophobicity was evidenced after 20 days in the samples stored at 100 % RH, while the decrease of the molecular weight occurred since the 7th day of storage. This lack of correlation suggested that the degradation products produced during the first days of ageing were big enough in average to keep their hydrophobic properties and/or need longer time to migrate to the film surface.

3.3.2 Microstructure observation

The surface and cross-section of PLA films submitted to the three testing conditions after one and two months were observed by Scanning Electron Microscopy (SEM) (Figure 4).

The microstructure of the surface of the films stored at 50 % RH was very similar to the initial films for the whole duration of the storage test, as a result of the low interactions with water molecules and the absence of hydrolysis in such films. On the contrary, when the interactions with water were favoured and hydrolysis occurred, remarkable modifications were observed. The impact of the hydrolysis in the surface microstructure was clearly evident after 1 month of storage when the samples were stored in saturated water vapour conditions. Their surface were characterized by the presence of shadows of ≈ 50 µm of diameter, which also favours the hypothesis of the accumulation of degradation products on the PLA surface, as previously discussed, with an increase of water affinity for these samples. Nevertheless, the surface microstructure of the samples immersed in liquid water for 1 month was comparable to the initial conditions, even if high hydrolysis of PLA also occurred in this storage condition. The most probable explanation comes again from the different state of water. In the last condition, the degradation products can be dissolved or transferred in the liquid, as

previously indicated by pH and water hydrophobicity measurements, and therefore not accumulated in the film. Mass transfer to the liquid media of degradation products such as lactic acid has been also observed by Iñiguez-Franco et *al.*[32] in a degradation study of PLA films conducted in liquid water and hydro-ethanol solutions at 40 °C. Increasing concentrations of lactic acid were detected in all the liquid media at increasing degradation time, using a liquid chromatographer coupled to mass spectrometer (LC/MS/MS system).

The modifications of the surfaces became more intense during the second month of storage. The surface of the samples stored at saturated water vapour condition or immersed in liquid water appeared highly degraded and with an increased roughness, particularly in the 100 % RH condition. Both surfaces were characterized by the presence of regular and parallel lines, possibly indicating the existence of zones where the hydrolysis was favoured (*e.g.* amorphous phases), and zones where it was restricted (*e.g.* crystalline phases). A possible explanation of such phenomenon could come from the bi-orientation step during the industrial production of PLA. This process aimed to improve the mechanical properties of PLA films and consists in a biaxial stretching of films (from 2 to 6 times of the initial length) at temperatures between T_g and T_m.[33] These conditions favours the development of a highly organized structure of PLA, where the PLA amorphous chains and PLA crystallites are regularly orientated in both directions of the film.[34-36]

The microstructure of the cross-section of PLA films was clearly consistent with the previous considerations, suggesting similar degradation mechanism than in the surface. On the one hand, no big modifications were observed during the entire ageing test in the cross-section of the samples stored at 50 % RH, since no hydrolysis occurred in this condition. On the other hand, big changes were observed in the samples stored in the other two conditions. The analysis of the cross-section also confirmed the influence of the state of water. The hydrolysis has more impact in the samples stored in water vapour saturated condition than in the samples stored in liquid water. Furthermore, the cross-section of the samples stored at 100 % RH for one month were characterized by the presence of numerous aggregates, which were most probably degradation products of PLA. On the contrary, the cross-section of the samples immersed in water for the same time did not show any aggregates and appeared as clear as the initial film, as a consequence of a mass transfer to the liquid medium.

These results thus indicate that the degradation occurred with the same intensity in both surface and bulk of the PLA films, in contrast of PLA materials with thickness between 0.5 – 2 mm and 7.4 mm stored in aqueous media, which are known to degrade faster in the core than in the surface, due to an autocatalytic reaction driven by the monomers and degradation products accumulated in the core.[10, 12, 17-18]

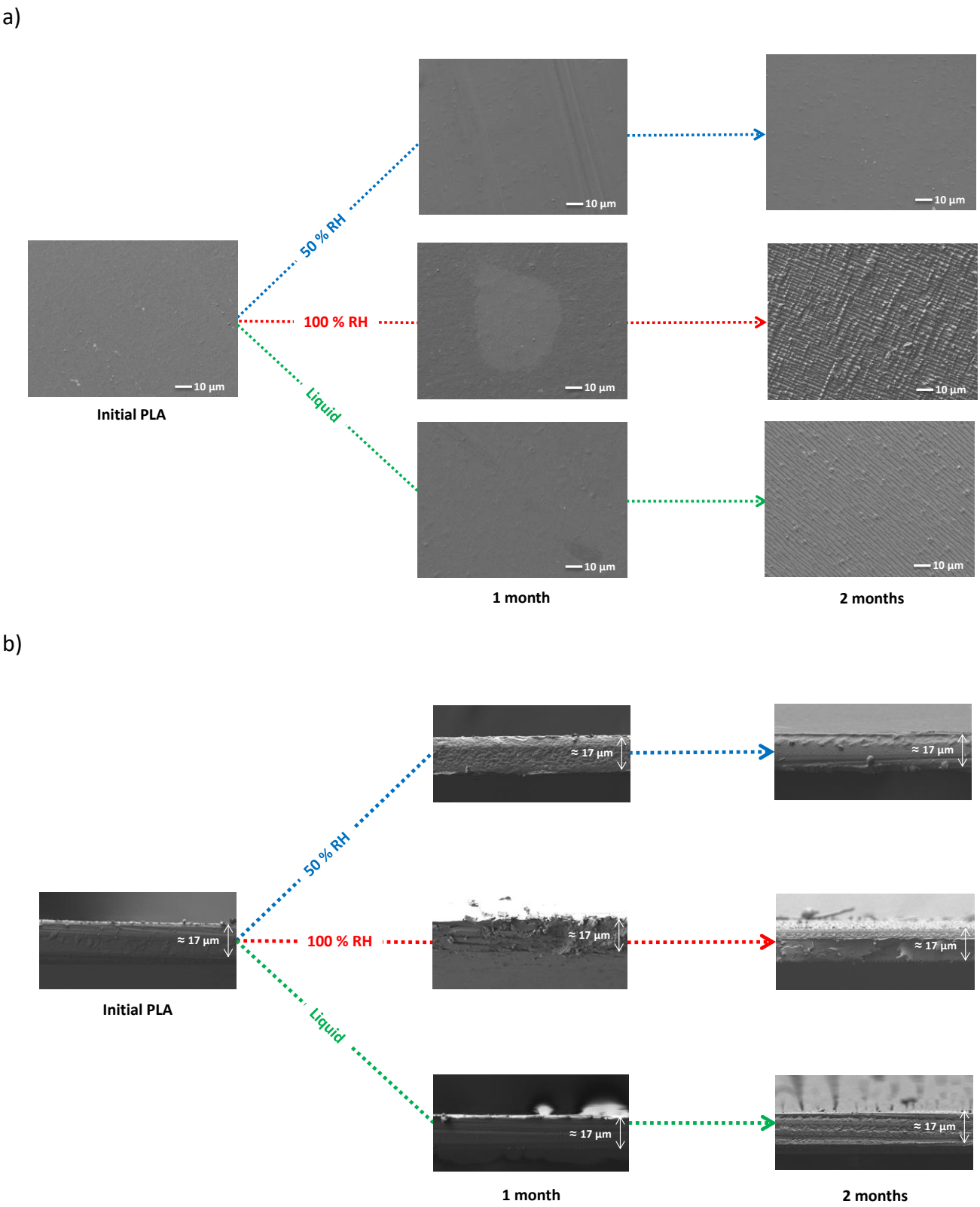

Figure 4. *Modifications in the microstructure of PLA films stored at 50 % RH, 100 % RH or immersed in liquid water at 50 °C during time a) Surface microstructure b) Cross-section microstructure.*

a)

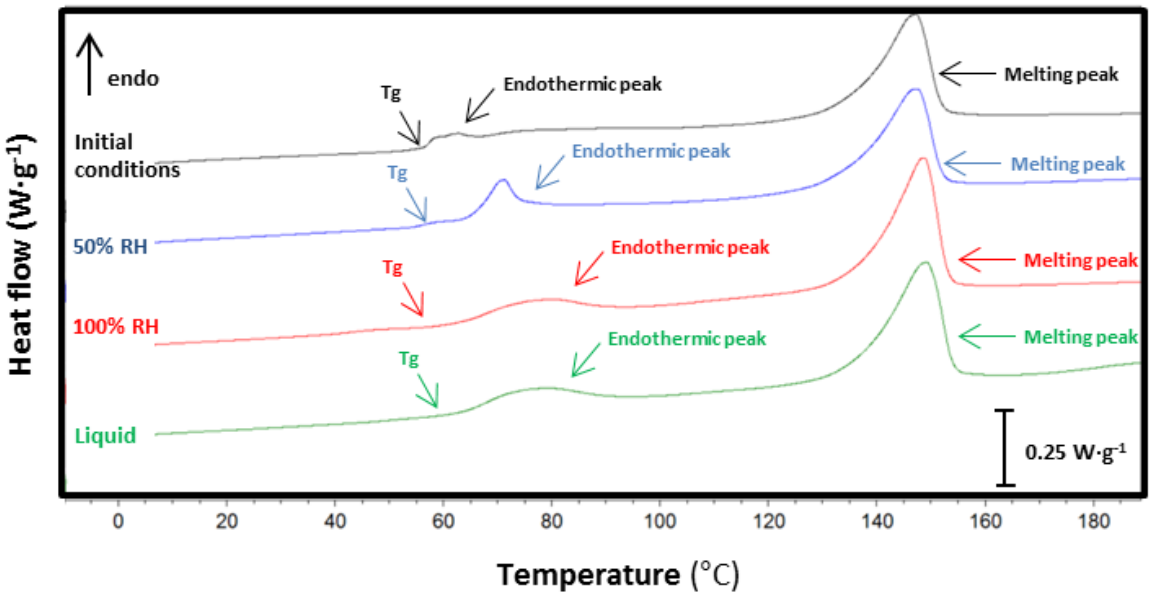

b)

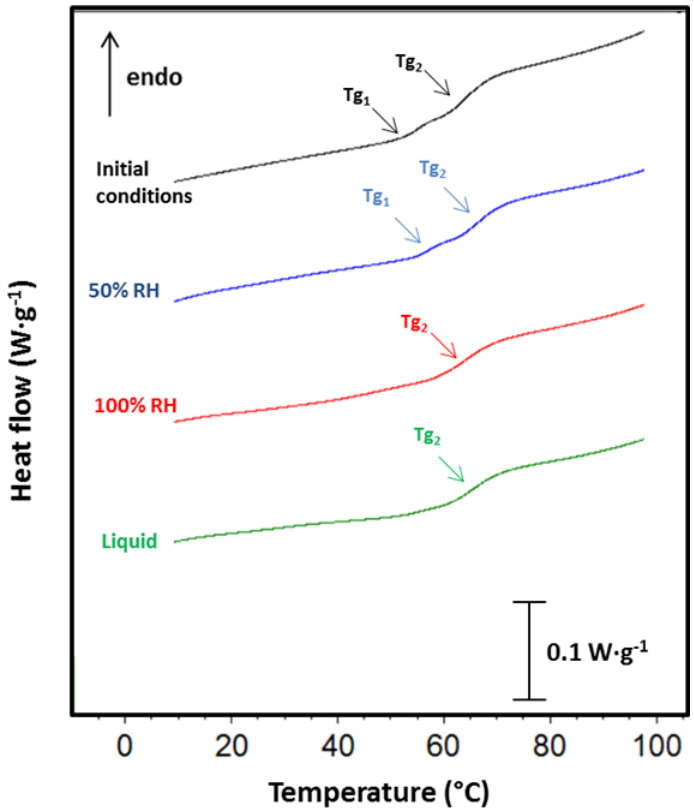

Figure 5. *DSC curves of PLA films stored at 50 % RH, 100 % RH or immersed in liquid water at 50 °C after 27 days. a) First heating thermograms of samples subjected to heat program at higher temperatures (from -10 to 190 °C). b) Second heating thermograms of samples obtained after a first heating of the heat program at lower temperatures before melting (from -10 to 100 °C).*

3.4 Modifications in the thermal transitions induced by ageing

The thermal events of the PLA films were also followed during storage test. The PLA films used in this study were semi-crystalline materials as shown in Figure 5. Thermograms displayed the characteristic thermal events of such materials. Glass transition, relaxation peak associated to glass transition and melting of crystals indicated the co-existence of an amorphous phase and a crystalline phase in the PLA physical structure.

Considering the effect of ageing conditions, Figure 5 unambiguously demonstrated that the thermal events related to both the amorphous and the crystalline phases were modified during the first month of storage and for all three different storage conditions. As described in material and method section, the PLA samples were subjected to two different heating programs in order to better study the transitions related to the crystalline and amorphous phases.

3.4.1 Changes related to the crystalline phase

The evolution of the melting temperature of crystals as well as the calculated crystallinity percentage of the PLA samples stored in the three conditions are reported in Figure 6a and 6b. No significant change was observed in the T_m and X_c values of the samples stored at 50 % RH, indicating that no modification occurred in the crystalline phase induced in that condition. In contrast, the crystalline phase of the samples stored in vapour saturated conditions or immersed in liquid water was clearly modified. The X_c values linearly increased from ≈ 28 to ≈ 40 % in both conditions. The corresponding T_m values slightly increased during the first month and then decreased during the second month, for both conditions. The decrease was faster and reached a lower value in the samples stored in saturated water vapour condition due to the previously described effect of the state of water.

The increase of crystallinity degree in PLA materials is a well-known phenomenon which occurs even when amorphous PLA is hydrolytically degraded. This particular behaviour of PLA has been confirmed by different authors using different analyses such FTIR (Fourier Transform InfraRed spectroscopy), WAXS (Wide-Angle X-ray Scattering) and DSC.[10, 12, 17-19, 29, 37] A possible explanation of this phenomenon could be an increase in the local mobility of the PLA amorphous chains as induced by hydrolysis, which favours their crystallization.

Tsuji *et al.*[20] and Tsuji and Ikada[19] have reported similar increasing and the decreasing T_m values in semi-crystalline poly (L-lactic acid) (PLLA or optically pure PLA obtained from L-lactide stereoisomers) samples stored in phosphate buffer solutions at 37 °C for 36 months. These authors suggested that an increase of the size of PLLA crystallites might be behind the increase in T_m, as a consequence of a higher chain mobility induced by the smaller chains and plasticization by water, favouring the formation of more thermostable crystals. The decrease of T_m could be due to a decrease their size during the late stage of ageing, which reduce their thermostability.

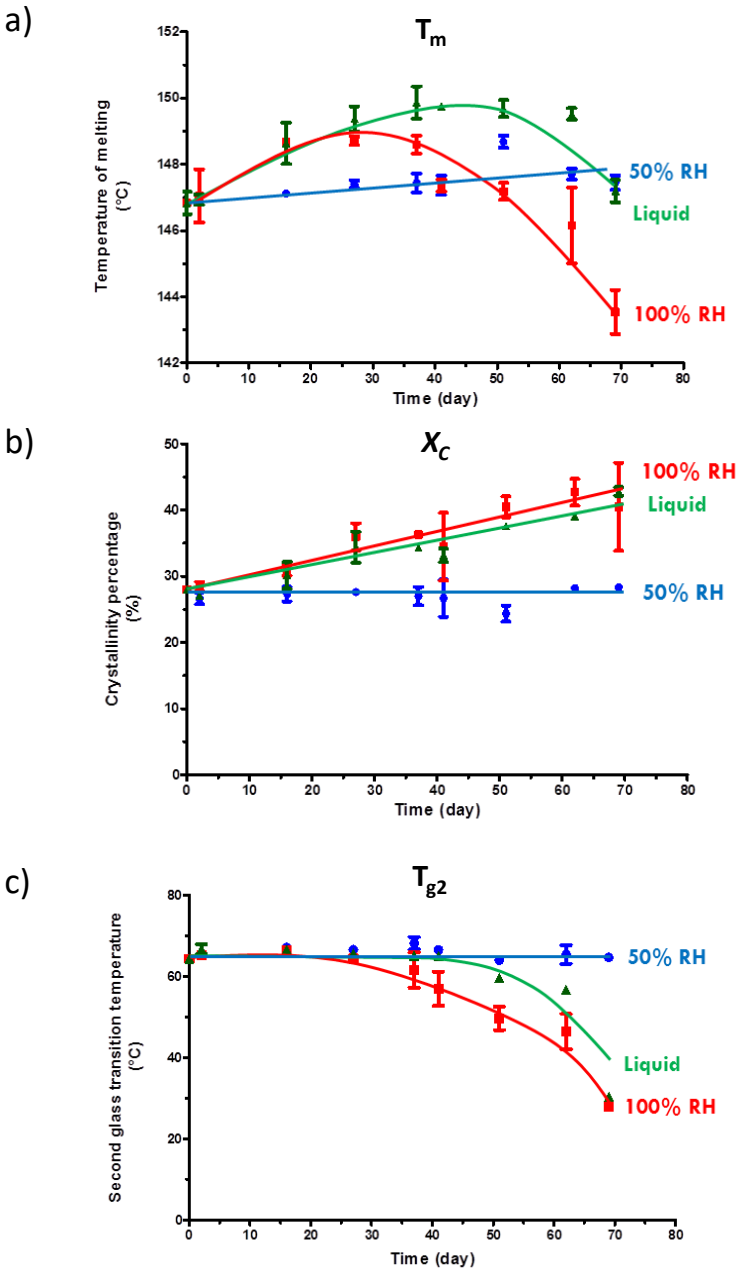

Figure 6. *Modifications of the thermal events of PLA films stored at 50 % RH (●), 100 % RH (■) or immersed in liquid water (▲) at 50 °C during time. a) Temperature of melting (T_m). b) Crystallinity percentage (X_c). c) Second glass transition (T_{g2}). Error bars are standard deviation. Lines are guide for the eyes.*

3.4.2 Changes related to the amorphous phase

The amorphous phase was also subjected to modifications (Figure 5). For all three storage conditions, PLA samples were characterized by an increase of the endothermic peak associated to the glass transition. This is related to the so-called physical ageing phenomena as described by Hutchinson[38] and Struik[39]. This corresponds to slow molecular rearrangements occurring in amorphous polymers when stored at temperatures lower than T_g, which tend to reduce their free-energy and free volume. As a consequence of these molecular

rearrangements, the polymer structure gets continuously denser and becomes more glass-like and less rubber-like. These molecular rearrangements are accelerated when the storage temperature is close to T_g.
In addition, it is worthy to note that a clear effect of the water chemical potential on the shape of the endothermic peak. The peak was narrower at 50 % RH, while at 100 % RH it was largely spread. This difference cannot only be attributed to the different molecular weight distribution of PLA induced by hydrolysis. Such different shapes were already noticed during the second day of storage, when hydrolysis was very limited. Moreover, when the hydrolysis was more intense no important changes were observed. Other interactions between water and PLA seem to occur behind that phenomenon, which needs to be better understood.

DSC curves of PLA samples stored at the three conditions, deriving from the second heating at lower temperatures, are shown in Figure 5. They clearly displayed that the glass transition of the samples at initial conditions occurred in two steps from ≈ 55 to ≈ 64 °C. This double step in the glass transition was previously hindered by the endothermic events (Figure 5a) related to physical ageing, and it could be a consequence of the presence of two different amorphous regions in the PLA matrix as induced by the bi-orientation step during processing. It is well known that this process modifies the whole physical structure of the polymer by promoting the formation of oriented PLA crystals and PLA amorphous chains as suggested by Delpouve et *al.*[35] and Jariyasakoolroj *et al.* [34] For data analysis, both steps were considered as two thermal transitions and they were referred to as glass transition 1 (T_{g1}) and glass transition 2 (T_{g2}) for the event at low and high temperature, respectively.

The first glass transition was no longer detectable after the 16th day of storage for the samples at 100 % RH and after the 41st day for those in liquid conditions. The second glass transition remained always detectable (Figure 6c). This observation suggested that the first thermal event was more sensitive to hydrolysis. This was most likely because that glass transition was more related to a PLA phase associated to higher amount of amorphous PLA. The first glass transition of films at 50 % RH was always detectable and could be considered constant. Its corresponding T_g and C_p values oscillated around their initial values during storage time (≈ 56 °C and ≈ 0.07 $J \cdot g^{-1} \cdot °C^{-1}$). Also, the parameters related to the second glass transition of such condition could be considered as stable during storage time (≈ 66 °C and ≈ 0.18 $J \cdot g^{-1} \cdot °C^{-1}$), which was in agreement with the absence of hydrolysis in such condition, as already evidenced by previous experiments (Figure 6).

The T_g value of the second transition of the PLA samples stored at 100 % RH or immersed in liquid water decreased, which is related to the effect of hydrolysis (Figure 6).[10, 12] This decrease was significant higher (t-student test, p level < 0.05) when films were aged in the saturated water vapour condition. T_g decreased from an initial value of ≈ 66 °C to ≈ 56 °C in the PLA films stored after 62 days in direct contact with liquid water, and

to ≈ 46 °C when stored in 100 % RH. Similar decreasing trends in T_g have also been reported in other studies involving hydrolytic degradation of PLA materials.[15, 18-20, 23]

The effect of the physical state of water on the hydrolysis mechanism was more evident in the thermal events analysis. The modifications in both the crystalline and the amorphous phase were unambiguously faster when the PLA was stored in saturated water vapour conditions even compared to samples in contact with liquid water. Such acceleration is almost certainly linked to the degradation products. As previously shown, there was an accumulation of such products in the film bulk and surface when PLA was stored in saturated water vapour conditions. It is well known that acid molecules such as the degradation compounds from PLA act as auto-catalysts of hydrolysis.[10, 12] In addition, since they are also hydrophilic molecules and have smaller size than the polymer, they can increase the interaction with water and act themselves as plasticizers, increasing therefore the mobility of the system and reactivity.

4 Conclusions

This study undoubtedly evidenced that the chemical potential of water and its physical state (liquid or vapour) influenced the chemical stability of PLA films and its hydrolysis mechanism. The results of this study were consistent between them and agreed with most of the literature related to this topic.

The samples stored in the conditions at the lowest chemical potential of water (50 % RH) were chemically stable for the whole accelerated study at 50 °C, and were only subjected to physical ageing. No hydrolysis was detected in this condition and no modification was observed, neither in the appearance, surface hydrophobicity, and microstructure, nor in the main thermal events related to the amorphous (T_g) and crystalline phases (T_m, X_c). Only a fast increase in the relaxation peak associated to glass transition was noticeable, as consequence of the storage at a temperature close to T_g, which accelerated the physical ageing phenomenon. On the contrary, when PLA films were stored in environments at the highest chemical potential of water (100 % RH or immersed in liquid water) chemical degradation by hydrolysis occurred and important modifications were observed. The PLA films were characterized by a loss of transparency, microstructure degradation and changes in the amorphous and crystalline phases.

The influence of the physical state of water was clearly evidenced when the kinetics of the physical and chemical properties of the PLA films stored in liquid and saturated vapour conditions were compared. Although the chemical potential of water is the same in these two conditions, the reduction of the main parameters ($\overline{M_n}$, $\overline{M_w}$, T_{g1}, T_{g2}, T_m) during the second month of storage were always faster in the PLA samples stored in saturated vapour conditions. The surface hydrophobicity analysis and the microstructure observations highlighted the key role of the degradation products in the hydrolysis, which are autocatalysts of hydrolysis. In liquid

environment the degradation products (*e.g.* lactic acid and oligomers) were released from PLA, but when PLA is stored in saturated vapour conditions, they remained and were accumulated in the films, catalysing the hydrolysis reaction. In addition, they can further favour the hydrolysis reaction by increasing the interactions with water and by acting as plasticizer.

From a practical point of view, the results of this study indicated that PLA films is a very suitable packaging for semi-dried or dried foods, which are characterized by $a_w \leq 0.5$, since in this conditions PLA was chemically stable, no hydrolysis occurred and no modification was observed. However, when PLA is used to pack high moisture foods or beverages having $a_w \approx 1$, a particular attention should be paid. In this case not only a shelf life testing of the food product is required, but also a shelf life testing of the packaging, since the PLA can highly interact with the water molecules coming from the food and be altered. As a consequence, the functional properties of the packaging can be modified and the protection of the food quality can be lost during time. Additionally, this study also put in evidence the necessity of migration studies, especially when liquid products are packed in PLA. PLA is an industrial product, which is very attractive for food packaging companies. It comes evident that this combination can increase the risk of over utilization of additives, which could be transferred by the water molecules directly (solubilization) or indirectly (by PLA hydrolysis) to the food.

5 Supplementary material

5.1 Kinetic analysis of hydrolysis

Table 1. *Kinetic parameters of number average molecular weight loss ($\overline{M_n}$), weight average molecular weight loss ($\overline{M_w}$) of PLA films stored in different wet environments at 50 °C for 69 days.*

Parameter	Constant rate	Storage conditions		
		50 % RH	**100 % RH**	**Liquid**
$\overline{M_n}$	k_{app} ($day^{-1} \cdot 10^{-3}$)	1.1[a]	31.8[b]	27.4[c]
	95 % CI	0 – 2.3	29.9 – 33.6	25.3 – 29.7
	R^2	0.20	0.99	0.98
$\overline{M_w}$	k_{app} ($day^{-1} \cdot 10^{-3}$)	1.5[a]	33.0[b]	25.6[c]
	95 % CI	0 -2.3	29.8 – 36.2	22.9 – 28.3
	R^2	0.49	0.96	0.96

k_{app} is the apparent rate constant
95 % CI are the 95 % confidence intervals
R^2 is the coefficient of determination
Values having the same superscript letter in a same row are not significantly different at p-level 0.05.

5.2 Molecular weight distribution curves of PLA films during storage test

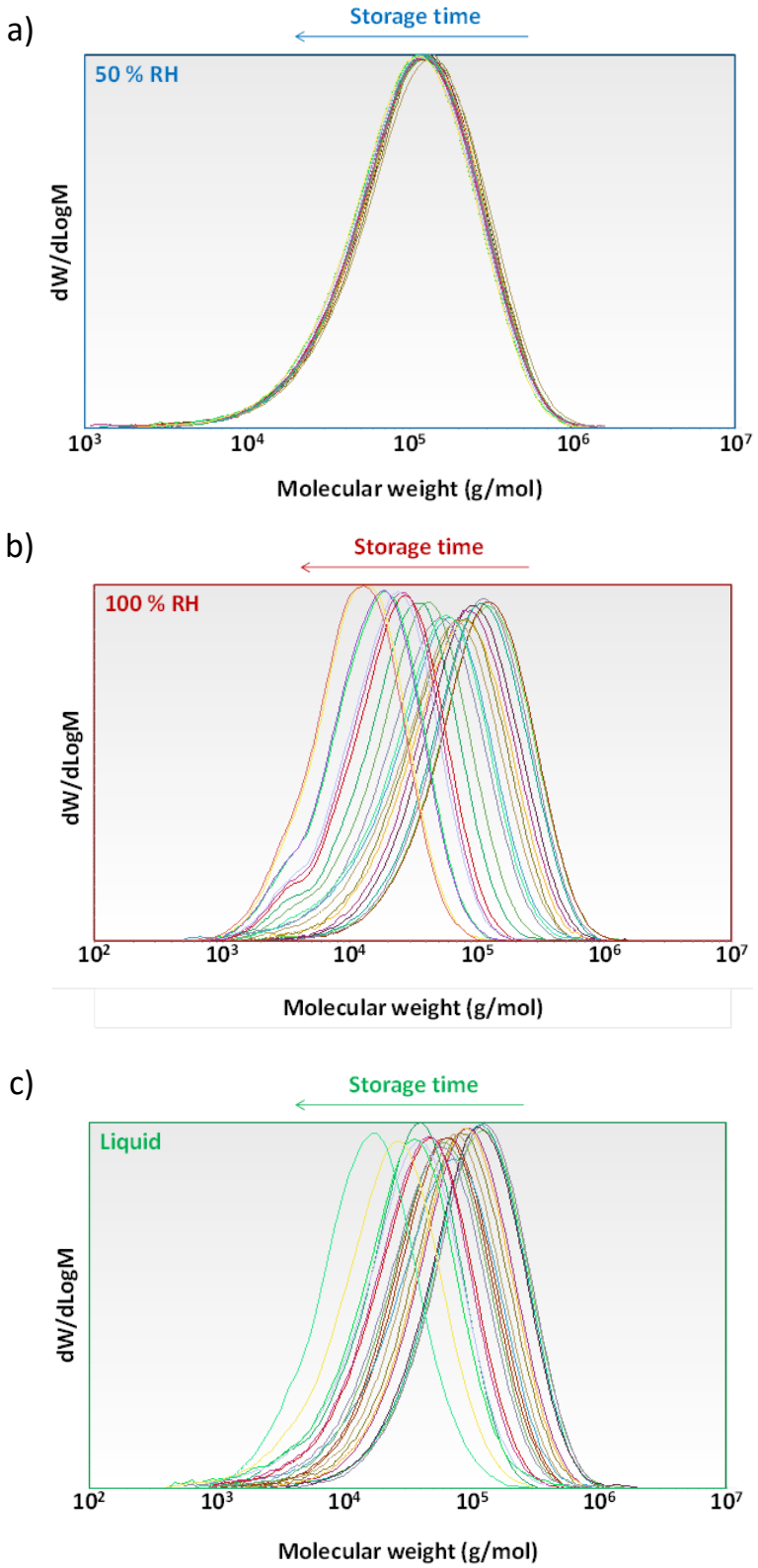

Figure 7. *Molecular weight distribution curves of PLA films stored at 50 % RH (a), 100 % RH (b) or immersed in liquid water (c) at 50 °C during time (69 days).*

Acknowledgements

The authors acknowledge the European Social Fund – Friuli Venezia Giulia Region – Operational Program 2007/2013 for supporting this project (Regional code: FP1340303009), the Università Italo-Francese for mobility grant (Bando Vinci 2015 Cap II, project code C2-64), the RMB plateau of UMR PAM for thermal and goniometry analyses, the ICMUB research unit for SEC analyses, and Frederic Herbst from the University of Burgundy-Franche-Comté for SEM analyses.

References

1. Cozar, A.; Echevarria, F.; Gonzalez-Gordillo, J. I.; Irigoien, X.; Ubeda, B.; Hernandez-Leon, S.; Palma, A. T.; Navarro, S.; Garcia-de-Lomas, J.; Ruiz, A.; Fernandez-de-Puelles, M. L.; Duarte, C. M. Plastic debris in the open ocean. *Proceedings of the National Academy of Sciences of the United States of America* **2014,** *111* (28), 10239-10244.

2. Kale, G.; Kijchavengkul, T.; Auras, R.; Rubino, M.; Selke, S. E.; Singh, S. P. Compostability of bioplastic packaging materials: An overview. *Macromolecular Bioscience* **2007,** *7* (3), 255-277.

3. Castro-Aguirre, E.; Iñiguez-Franco, F.; Samsudin, H.; Fang, X.; Auras, R. Poly(lactic acid)-Mass production, processing, industrial applications, and end of life. *Advanced Drug Delivery Reviews* **2016**.

4. Auras, R.; Harte, B.; Selke, S. An overview of polylactides as packaging materials. *Macromolecular Bioscience* **2004,** *4* (9), 835-864.

5. Jamshidian, M.; Tehrany, E. A.; Imran, M.; Jacquot, M.; Desobry, S. Poly-lactic acid: production, applications, nanocomposites, and release studies. *Comprehensive Reviews in Food Science and Food Safety* **2010,** *9* (5), 552-571.

6. Rasal, R. M.; Janorkar, A. V.; Hirt, D. E. Poly(lactic acid) modifications. *Progress in Polymer Science* **2010,** *35* (3), 338-356.

7. Wang, S. G.; Cui, W. J.; Bei, J. Z. Bulk and surface modifications of polylactide. *Analytical and Bioanalytical Chemistry* **2005,** *381* (3), 547-556.

8. European Bioplastics Association. Global production capacities of bioplastics 2014 (by material type) and applications. http://en.european-bioplastics.org/market. Retrieved on 25/01/2016.

9. Witzke, D. R. Introduction to properties, engineering, and prospects of polylactide polymer. Michigan State University 1997. PhD thesis.

10. Tsuji, H., Hydrolytic degradation. In *Poly(lactic acid): synthesis, structures, properties, processing, and applications*; Auras, R.; Lim, L.-T.; Selke, S. E. M.; Tsuji, H., Eds.; Wiley: Hoboken, N.J., 2010.

11. Göpferich, A. Mechanisms of polymer degradation and erosion. *Biomaterials* **1996,** *17* (2), 103-114.

12. Li, S. M. Hydrolytic degradation characteristics of aliphatic polyesters derived from lactic and glycolic acids. *Journal of Biomedical Materials Research* **1999,** *48* (3), 342-353.

13. Ramchandani, M.; Pankaskie, M.; Robinson, D. The influence of manufacturing procedure on the degradation of poly(lactide-co-glycolide) 85:15 and 50:50 implants. *Journal of Controlled Release* **1997,** *43* (2–3), 161-173.

14. Tsuji, H.; Ikarashi, K.; Fukuda, N. poly(L-lactide): XII. Formation, growth, and morphology of crystalline residues as extended-chain crystallites through hydrolysis of poly(L-lactide) films in phosphate-buffered solution. *Polymer Degradation and Stability* **2004,** *84* (3), 515-523.

15. Gonzalez, M. F.; Ruseckaite, R. A.; Cuadrado, T. R. Structural changes of polylactic-acid (PLA) microspheres under hydrolytic degradation. *Journal of Applied Polymer Science* **1999,** *71* (8), 1223-1230.

16. Grizzi, I.; Garreau, H.; Li, S.; Vert, M. Hydrolytic degradation of devices based on poly(dl-lactic acid) size-dependence. *Biomaterials* **1995,** *16* (4), 305-311.

17. Kucharczyk, P.; Hnatkova, E.; ZdenekDvorak; Sedlarik, V. Novel aspects of the degradation process of PLA based bulky samples under conditions of high partial pressure of water vapour. *Polymer Degradation and Stability* **2013,** *98* (1), 150-157.

18. Migliaresi, C.; Fambri, L.; Cohn, D. A study on the in-vitro degradation of poly(lactic acid). *Journal of Biomaterials Science-Polymer Edition* **1994,** *5* (6), 591-606.

19. Tsuji, H.; Ikada, Y. Properties and morphology of poly(L-lactide) 4. Effects of structural parameters on long-term hydrolysis of poly(L-lactide) in phosphate-buffered solution. *Polymer Degradation and Stability* **2000,** *67* (1), 179-189.

20. Tsuji, H.; Mizuno, A.; Ikada, Y. Properties and morphology of poly(L-lactide). III. Effects of initial crystallinity on long-term in vitro hydrolysis of high molecular weight poly(L-lactide) film in phosphate-buffered solution. *Journal of Applied Polymer Science* **2000,** *77* (7), 1452-1464.

21. Ho, K. L. G.; Pometto, A. L.; Hinz, P. N. Effects of temperature and relative humidity on polylactic acid plastic degradation. *Journal of Environmental Polymer Degradation* **1999,** *7* (2), 83-92.

22. Holm, V. K.; Ndoni, S.; Risbo, J. The stability of poly(lactic acid) packaging films as influenced by humidity and temperature. *Journal of Food Science* **2006,** *71* (2), E40-E44.

23. Copinet, A.; Bertrand, C.; Govindin, S.; Coma, V.; Couturier, Y. Effects of ultraviolet light (315 nm), temperature and relative humidity on the degradation of polylactic acid plastic films. *Chemosphere* **2004,** *55* (5), 763-773.

24. Greenspan, L. Humidity fixed points of binary saturated aqueous solutions. *Journal of Research of the National Bureau of Standards Section a-Physics and Chemistry* **1977,** *81* (1), 89-96.

25. Fischer, E. W.; Sterzel, H. J.; Wegner, G. Investigation of the structure of solution grown crystals of lactide copolymers by means of chemical reactions. *Kolloid-Zeitschrift and Zeitschrift fur polymere* **1973,** *251*, 980-990.

26. Paul, M. A.; Delcourt, C.; Alexandre, M.; Degée, P.; Monteverde, F.; Dubois, P. Polylactide/montmorillonite nanocomposites: study of the hydrolytic degradation. *Polymer Degradation and Stability* **2005,** *87* (3), 535-542.

27. Pantani, R.; De Santis, F.; Auriemma, F.; De Rosa, C.; Di Girolamo, R. Effects of water sorption on poly(lactic acid). *Polymer* **2016,** *99*, 130-139.

28. Hakkarainen, M.; Karlsson, S.; Albertsson, A. C. Rapid (bio)degradation of polylactide by mixed culture of compost microorganisms - low molecular weight products and matrix changes. *Polymer* **2000,** *41* (7), 2331-2338.

29. Gorrasi, G.; Pantani, R. Effect of PLA grades and morphologies on hydrolytic degradation at composting temperature: Assessment of structural modification and kinetic parameters. *Polymer Degradation and Stability* **2013,** *98* (5), 1006-1014.

30. Mitchell, M. K.; Hirt, D. E. Degradation of PLA fibers at elevated temperature and humidity. *Polymer Engineering and Science* **2015,** *55* (7), 1652-1660.

31. Karbowiak, T.; Debeaufort, F.; Voilley, A. Importance of surface tension characterization for food, pharmaceutical and packaging products: a review. *Critical Reviews in Food Science and Nutrition* **2006,** *46* (5), 391-407.

32. Iñiguez-Franco, F.; Auras, R.; Burgess, G.; Holmes, D.; Fang, X.; Rubino, M.; Soto-Valdez, H. Concurrent solvent induced crystallization and hydrolytic degradation of PLA by water-ethanol solutions. *Polymer* **2016,** *99*, 315-323.

33. Perego, G.; Cella, G. D., Mechanical properties. In *Poly(lactic acid): synthesis, structures, properties, processing, and applications*; Auras, R.; Lim, L.-T.; Selke, S. E. M.; Tsuji, H., Eds.; Wiley: Hoboken, N.J., 2010.

34. Jariyasakoolroj, P.; Tashiro, K.; Wang, H.; Yamamoto, H.; Chinsirikul, W.; Kerddonfag, N.; Chirachanchai, S. Isotropically small crystalline lamellae induced by high biaxial-stretching rate as a key microstructure for super-tough polylactide film. *Polymer* **2015,** *68*, 234-245.

35. Delpouve, N.; Stoclet, G.; Saiter, A.; Dargent, E.; Marais, S. Water barrier properties in biaxially drawn poly(lactic acid) films. *Journal of Physical Chemistry B* **2012,** *116* (15), 4615-4625.

36. Stoclet, G.; Seguela, R.; Lefebvre, J. M.; Rochas, C. New insights on the strain-induced mesophase of poly(D,L-lactide): in situ WAXS and DSC study of the thermo-mechanical stability. *Macromolecules* **2010,** *43* (17), 7228-7237.

37. Harris, A. M.; Lee, E. C. Heat and humidity performance of injection molded PLA for durable applications. *Journal of Applied Polymer Science* **2010,** *115* (3), 1380-1389.

38. Hutchinson, J. M. Physical aging of polymers. *Progress in Polymer Science* **1995,** *20* (4), 703-760.

39. Struik, L. C. E. Physical aging in plastics and other glassy materials. *Polymer Engineering & Science* **1977,** *17* (3), 165-173.

Beyond biodegradability of Poly(lactic acid): physical and chemical stability in humid environments

Rocca-Smith, J.R.; Whyte, O.; Brachais, C.-H.; Champion, D.; Piasente, F.; Marcuzzo, E.; Sensidoni, A.; Debeaufort F. and Karbowiak T. Beyond biodegradability of PLA: physical and chemical stability in humid environments. *ACS Sustainable Chemistry & Engineering* 2017, *5*, 2751-2762.

Abstract

Poly (lactic acid) (PLA) is the most traded biodegradable and biobased material. It is largely used as eco-friendly substitute of conventional plastics. Nevertheless, one of the main limiting factors is its water sensitivity. PLA reacts with water and it is hydrolysed during time, compromising its performances. Limited information related to the hydrolysis mechanism driven by water in vapour state is available in scientific literature. Literature is mainly focused on the effects of water in liquid state. This lack of information is of significant importance, since PLA interacts with water in both phases. This work was aimed to give a full depiction of the chemical and physical changes of PLA in a large range of relative humidity environments (from 50 to 100 % RH) and in contact with liquid water. This research clearly showed that the stability of PLA was influenced not only by the chemical potential of water molecules, but also by their physical state due to a different behaviour of degradation products. From a practical point of view, the findings of this study can be used as strong scientific basis for giving recommendations about the use of this material in its applications as packaging or mulch films.

Keywords

Bioplastic, ageing, hydrolysis, amorphous phase, state of water

1 Introduction

It is an undeniable fact that plastics have transformed our society since the beginning of their industrial production in the late 1940's.[1] Plastics materials are nowadays ubiquitous and are used in almost all aspects of our daily life, such as in clothes, furniture, transport, buildings, electronic devices and packaging.[1-2] They make our life more comfortable and also bring economic benefits to our society. Nevertheless, it is also unquestionable that conventional plastic waste (*i.e.* oil-derived and non-biodegradable) pollutes and negatively affects our natural environment. They also contribute to the global warming and they can last for a long time (several hundred years) as a waste in landfills. In addition, plastic wastes are vectors of harmful chemicals. They can transport and release toxic molecules to the environment such as bisphenols or phthalates, increasing the risk as well for the environment as well as human health.[1, 3]

Bioplastics can be defined as plastics which are derived from natural resources, or are biodegradable, or have both properties.[4-5] They can substitute (partially or completely) conventional plastics in packaging applications and contribute to reduce the negative effects of conventional plastics.[6] 30 % biobased Poly(EthylenTerephtalate) (Bio-PET30), Poly(Lactic Acid) (PLA) and Biobased PolyEthylene (Bio-PE) are the three most representative bioplastics in the market, but only PLA meets both the criteria of bio-sourcing and biodegradability.[4]

PLA derives from natural carbohydrate sources such as corn starch, sugar cane, wheat straw and wood ships.[7] The production of PLA goods (*e.g.* films, rigid containers, bottles and others) involves several steps that could be summarized as lactic acid production, polymerization and industrial processing like extrusion, injection moulding, blow moulding, cast film extrusion and thermoforming.[7-9]

PLA has largely been studied over the last two decades not only because of its eco-friendly nature, but also because of its high versatility. Compared to other biopolymers, PLA benefits of an interesting balance between cost, functional properties and processibility. Different strategies aiming at modifying bulk[10-14] and surface[15-18] properties of PLA are studied and adopted by research and industry to increase the PLA applications, particularly for food industry.[19-20] However, one of the main limitations related to PLA polymer, especially for durable goods applications, is its inherent water sensitivity and biodegradability. Although PLA sorbs small quantities of water molecules (< 1.1 wt% at T = 25 °C and close to saturation),[8, 21] it reacts with water molecules, and is hydrolysed during time, compromising the performance of the PLA material.

Hydrolysis reduces the molecular weight of PLA and is considered as the preceding step of biodegradation, since it generates the metabolites for microbial degradation.[22] The hydrolysis mechanism of PLA has been principally studied for bio-medical applications and most of the related studies have been carried out in specific liquid media, which simulate biological systems.[23-26] For example, Makino *et al*. (1985)[27] reported activation

energy values around 83.5 kJ·mol^{-1} in PLA capsules stored in physiological saline solutions at temperatures between 21 and 45 °C, which means that the reaction is around 3 times accelerated for 10 °C of temperature increase. Nevertheless, the main application of PLA is currently as industrial films, and according to its final use (*e.g.* packaging or mulch films) they can be exposed to numerous environments having various pH, relative humidity and temperature. In addition, the interactions with water are not only limited to the liquid state, but also occur in the vapour state. Although all these different conditions are known to influence chemical reactions, only scarce information related to their influence on the stability of PLA is reported in literature.

Based on these considerations, the objective of the present work was to study the modifications induced on PLA films when they are exposed to water environments in the vapour or in the liquid state. To that aim, an accelerated ageing study was carried out under seven wet condition environments to cover a wide range of situations. The PLA films were placed at 50, 65, 75, 85, 95, 100 % RH or immersed in liquid water at 50 °C. Macroscopic, chemical and physical modifications were assessed over a long time period of 70 days.

2 Experimental

2.1 PLA films

Semicrystalline PLA films (D-level ≥ 4.25 %), industrially processed and commercially available for food packaging applications, were used in this study (Nativia NTSS, Taghleef Industries, Udine, Italy). During industrial processing, PLA films were subjected to biaxial stretching and annealing to induce crystallization and to improve their mechanical properties. The technical characteristics of the films used are: thickness = 20 µm, water vapour transmission rate = 440 g·m^{-2}·d^{-1}(38 °C, 90% RH) and oxygen transmission rate = 1100 cm^3·m^{-2}·d^{-1}(23 °C, 0% RH). The thickness of films was measured in at least 5 different positions using a micrometer (Coolant Proof micrometer IP 65, Mitutoyo, Aurora, IL, USA).

2.2 Sample preparation and controlled storage conditions

The commercial PLA films were first submitted to primary vacuum (EKF56CX-4, ABM Greiffenberfer, Marktredwitz, Germany) for three days at room temperature (23 ± 2 °C), to remove any water and volatile molecules entrapped in the polymer matrix. Rectangular samples of 20 cm^2 (5 x 4 cm) or 10 cm^2 (5 x 2 cm) were initially weighed. Samples mass was approximately 50.0 mg (± 0.2) or 25.0 mg (± 0.5), respectively. PLA samples were then placed in 10 mL vials and stored in different microclimate chambers at 50 °C for 70 days. The storage temperature chosen was able to accelerate the chemical reactions, without inducing strong modifications in the physical state of PLA, such as transitions from glassy to rubbery state, since it was 5-10 °C lower than the glass transition temperature (T_g) Seven storage conditions were considered in this study. For studying the impact of the water molecules in the vapour state, 20 cm^2 surface area PLA samples were exposed to

environments at ≈ 50, 65, 75, 85, 95 and 100 % Relative Humidity (RH), using saturated salt solutions of NaBr (Sigma Aldrich, St. Louis, MO, USA), KI (Sigma Aldrich), NaCl (Sigma Aldrich), KNO_3 (Riedel-de Haën, Morristown, NJ, USA), K_2SO_4 (Sigma Aldrich) and distilled water, respectively.[28] Concerning the impact of water molecules in the liquid state, 10 cm^2 surface area PLA samples were immersed in 10 mL distilled water. Three to four samples were collected every week of each storage condition. These aged samples were then equilibrated at room temperature at least for two hours. They were weighed before and after been dried up to equilibrium, under primary vacuum from three to seven days at room temperature. In the case of immersed samples in liquid water, samples were removed from the liquid, rinsed with distilled water. The excess of water was removed using tissue paper before submission to primary vacuum in same conditions. The dried samples were then stored at – 30 °C up to analyses.

2.3 Physical and chemical characterizations

2.3.1 Water content and dry matter variation

The water content and the dry matter variation of PLA samples were measured gravimetrically and calculated according to the Equations 1 and 2, respectively. The analyses were complete in triplicates.

$$Water\ content\ (\%) = \frac{m_{wt} - m_{dt}}{m_{dt}} * 100 \quad (Eq. 1)$$

$$Dry\ matter\ variation\ (\%) = \frac{m_{dt} - m_{di}}{m_{di}} * 100 \quad (Eq. 2)$$

Where m_{wt} is the wet mass (g) of the sample at time t, m_{dt} is the dry mass (g) of the sample at time t and m_{di} is the initial dry mass of the sample (g), before starting the storage test.

2.3.2 pH

The pH of the liquid water in contact with the samples was analysed during time using a pH meter (C561, Consort, Turnhout, Belgium) equipped with a pH electrode (VWR, Radnor, PA, USA). The calibration of the device was conducted using standard solutions at 4 and 7 pH (High resolution pH buffer, Fischer Scientific, Pittsburgh, PA, USA). The initial pH of the liquid water was 5.7. Samples were equilibrated at room temperature before being analysed. The analysis was done in triplicate.

2.3.3 Molecular weight distribution

The molecular weight distribution of the PLA samples was analysed during time by Size-Exclusion Chromatography (SEC), using a 1260 Infinity liquid chromatography system (Agilent Technologies, Santa Clara, CA, USA). The device was composed of 2 Polypore Size Exclusion columns (Agilent Technologies) connected in series. PLA samples (approx. 50 or 25 mg) were completely dissolved in 1 mL of tetrahydrofuran (THF, Carlo Erba reagents, Val de Reuil, France) using a shaker (PL-SP 260VS, Agilent technologies) for 20 min at room

temperature. The dissolved samples were then filtrated using a syringe filter with a PTFE (polytetrafluoroethylene) membrane (pore diameter 0.2 µm, Dominique Dutscher SAS, Brumath, France) and transferred in 1.5 mL vials. 10 µL was automatically injected in the instrument. Filtered THF with a constant flow rate of 1 mL·min^{-1} was used as the mobile phase and a refractive index detector was used in this analysis. The separation was carried out at a controlled temperature of 45 °C. Polystyrene standards ranging from 1.28 to 1820 kDa (Advancing Polymer Solutions, Agilent Technologies) were used for calibration curve. The number average molecular weight ($\overline{M_n}$), the weight average molecular weight ($\overline{M_w}$) and the polydispersity index (*PDI*) were calculated from the experimental molecular weight distribution curve using Agilent GPC/SEC software (version 1.2, Agilent Technologies). The analysis was complete in duplicates.

2.3.4 Thermal transitions

The thermal transitions of PLA films were studied by Differential Scanning Calorimetry (DSC) using a Q20 calorimeter (TA instruments, New Castle, DE, USA). Samples were weighed (3-5 mg) and sealed into airtight aluminium pans (Tzero, T.A. Instruments) before being subjected to a double heating-cooling cycle at 10 °C·min^{-1} under N_2 atmosphere (flow rate of 25 mL·min^{-1}).

Two different heating programs were used. The first program consisted in a double heating cycle in a narrow temperature range (from -10 to 100 °C) to only focus on the thermal events related to the mobile amorphous phase of PLA. The first cycle of this heating program allowed to remove the excess of enthalpy associated to the glass transition, while the second one allowed to better estimate the variation of specific heat (ΔC_p) and the temperature of glass transition (T_g inflection point). The second program was performed on a broader temperature range (double heating from – 10 to 190 °C) to study the transitions related to the crystalline phase of PLA, such as melting temperature (T_m) and melting enthalpy (ΔH_m). In this case, the thermal parameters were estimated from the first heating, while the reversibility of the overall transitions was assessed from the second heating. At least two samples were run for each heating program, and the thermal parameters were determined using TA Universal Analysis 2000 software (version 4.5 A, TA instruments).

The crystallinity percentage (X_c) was calculated according to Equation 3.

$$X_c = \frac{\Delta H_m - \Delta H_{cc}}{\Delta H_m^0} \times 100\ \%\ (Eq.3)$$

Where ΔH_m (J·g^{-1}) is the enthalpy corresponding to the area under the melting peak, ΔH_m^0 (= 93 J·g^{-1})[29] is the enthalpy of melting of pure crystalline PLA and ΔH_{cc} (J·g^{-1}) is the enthalpy corresponding to the area associated to cold crystallization. Since no cold crystallization was observed in the first heating of the program related to the crystalline phase study, its value is null (ΔH_{cc}= 0 J·g^{-1}).

The percentage of Mobile Amorphous Phase (X_{MAP}) and the percentage of the Rigid Amorphous Fraction (X_{RAF}) in the PLA films were also calculated during time, according to Arnoult *et al.*[30] (Equations 4 and 5, respectively).

$$X_{MAP} = \frac{\Delta C_p}{\Delta C_p^0} \times 100\ \% \qquad (Eq.4)$$

$$X_c + X_{MAP} + X_{RAF} = 100\ \% \quad (Eq.5)$$

Where ΔC_p is the measured variation of specific heat for the glass transition associated to the mobile amorphous phase, and ΔC_p^0 is that one corresponding to a 100 % amorphous PLA sample ($\Delta C_p^0 = 0.48$ J·g^{-1}·K^{-1}).[30-31] Since two glass transitions were observed in the mobile amorphous phase, the ΔC_p used in the formula was the sum the both transitions ($\Delta C_p = \Delta C_{p1} + \Delta C_{p2}$).

2.3.5 Kinetics analysis

The experimental values of crystallinity percentage (X_c), the number average molecular weight ($\overline{M_n}$) and the weight average molecular weight ($\overline{M_w}$) over time were modeled using a zero and first apparent order kinetics (Equations 6, 7, and 8). The corresponding apparent rate constants (k_{app}) were estimated using the statistic software GraphPad Prims 5 (version 5.04, GraphPad Software, Inc., La Jolla, CA, USA). Rate constants were considered significantly different when no intersection in their 95% confidence interval was found.

$$X_c = X_{c0} \pm k_{app(X_c)} t \ (Eq.6)$$

$$\ln \overline{M_n} = \ln \overline{M_{n0}} \pm k_{app(\overline{M_n})} t \ (Eq.7)$$

$$\ln \overline{M_w} = \ln \overline{M_{w0}} \pm k_{app(\overline{M_w})} t \ (Eq.8)$$

Where X_{c0}, $\overline{M_{n0}}$ and $\overline{M_{w0}}$ are the crystallinity percentage, the number average molecular weight and the weight average molecular weight of initial PLA, respectively. t is the time (day). $k_{app(X_c)}$, $k_{app(\overline{M_n})}$, $k_{app(\overline{M_w})}$ are the corresponding apparent rate constants (in %·day^{-1}, day^{-1} and day^{-1} respectively).

3 Results and discussion

3.1 Macroscopic modifications of PLA films during ageing

Some simple measurements such as water content, dry matter variation and pH already provided a useful depiction of the stability of PLA submitted to accelerated ageing.

3.1.1 Water content

When PLA was stored in contact with water molecules from the vapour phase (50, 65, 75, 85, 95 and 100 % RH), the PLA capacity to sorb water clearly increased with time and with RH (Figure 1a). Whatever RH, the water content remained constant and close to 0 % during the first month of storage. After that time, the water content increased and reached a pseudo-plateau of ≈ 1 and 2.5 % for the samples stored at 95 and 100 % RH, respectively. A similar but slighter behaviour was also observed in the samples stored at the lower RH conditions (50, 65, 75 and 85 % RH), which reached a lower water content value (≈ 0.5 %) by the end of the test. Such increased capacity of PLA to sorb water molecules, after a relative long induction time, can be considered in line with the effects of PLA hydrolysis. It is well known that even if PLA sorbs small quantities of water molecules (<1.1 % wt at T = 25 °C and close to saturation),[8, 21] it can react and be hydrolysed by them, generating degradation products. [23-24] The degradation products of PLA (*e.g.* lactic acid and its oligomers) have an increased density of polar groups (*e.g.* hydroxyl and carboxyl) than the initial polymer, and are continuously produced over time. Therefore, an enhanced water affinity is expected to occur in the PLA samples under hydrolysis, as a consequence of the exposition of new water sorption sites. Several studies have also reported that hydrolysis of PLA, driven by water molecules from the vapour phase, induces a significant rise in the water sorption capacity.[32-34] As an example, Cairncross *et al.*[34] reported an increase of two and ten times of the water quantity sorbed by PLA films after storage for two and three days at 85 % RH and 80 °C, respectively. Accordingly, we can suggest that the PLA samples from the present study were hydrolytically degraded, when they were stored in contact with water vapour molecules. This even started at 50 % RH and the degradation was probably faster in the samples stored at the highest RH, as suggested by the increase in water uptake.

When PLA was immersed in liquid water, a totally different behaviour was observed (Figure 1a). The water content did not highly increase as in vapour contact, but oscillated around a rather low value (≈ 0.25 %) during the entire storage test. Lyu *et al.*[35] already reported a similar behaviour in PLA discs stored in liquid media (pH 7.4) for ≈ 400 days at 37 °C. They detected a very low and constant water content (≈ 0.01 wt%), even if such samples were highly hydrolytically degraded over time, with tremendous decrease of the $\overline{M_n}$ value from 290 kDa to ≈ 20 kDa. An increase in the water content was only observed when the PLA disks were degraded to lower $\overline{M_n}$ values. These results of Lyu *et al.*[35] suggested that a simple water content analysis cannot be only itself a good indicator of the hydrolysis reaction, especially when high molecular weight PLA is hydrolysed in liquid media. In these conditions, a mass transfer of degradation products from the polymer into the liquid media is possible, due to their high polarity and small size. Such molecules, offering additional sorption sites for water, thus do not accumulate in the polymer matrix, as it occurs when the hydrolysis is driven by water molecules in vapour phase. Therefore, hydrolysis cannot be simply discarded on the basis of low water uptake for PLA samples immersed in liquid water.

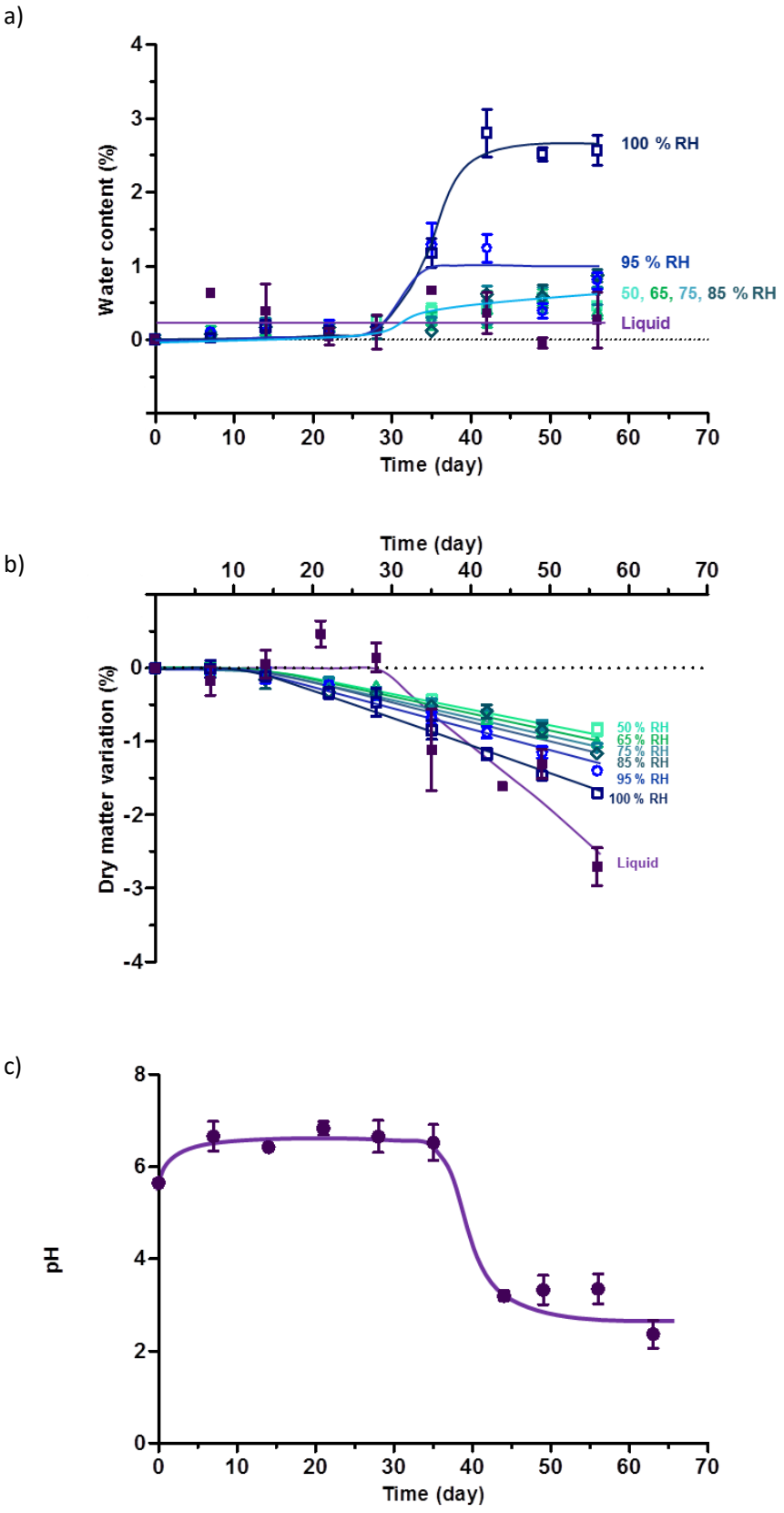

Figure 1. *Water content (a), dry matter variation (b) and pH (c) kinetics of PLA films stored at 50 % RH (□), 65 % RH (△), 75 % RH (▽), 85 % RH (◇), 95 % RH (○), 100 % RH (□) or immersed in liquid water (■), at 50 °C. Error bars are standard deviations. Lines are guide for the eyes.*

3.1.2 Dry matter variation

Now considering the change in the dry matter, all PLA samples progressively lost dry mass after a lag time, whatever the state of water in contact with (Figure 1b).

PLA samples immersed in liquid water were characterized by the longest lag time (approx. 30 days) and by the highest dry matter loss (≈ 3 % after ≈ 2 months of storage). Similar decreasing trends were also observed in degradation studies of semi-crystalline PLA films produced by annealing[26, 36] or by stereo-complexation[37] and immersed in buffer solutions (pH 7.4) at 37 °C, as well as in degradation studies of PLA plates[38] and PLA discs[35] exposed to similar aqueous media. As an example, Tsuji and Ikada[26] reported an induction time of 12 months, and a decrease in the dry mass of around 10 to 38 % in semicrystalline PLA films (X_c > 40 %) after 36 months storage in a phosphate buffer solution at 37 °C.

The decrease in the dry mass unambiguously confirmed the generation of compounds able to be solubilized and transferred to the liquid media, as previously hypothesized. The time needed to detect such decrease perfectly matched the time corresponding to a high increase of the water content in PLA samples stored in saturated vapour conditions (≈ 30 days, Figure 1a). This strongly suggested that the hydrophilic compounds able to induce a higher sorption capacity in the samples exposed to 100 % RH were, at the same time, highly water soluble, possible because of their small size and high polarity.

Considering PLA samples stored in contact with water vapour molecules (50, 65, 75, 85, 95 and 100 % RH) the lag time was around 10 days. The loss of dry matter progressively increased at higher RH conditions (≈ 0.8, 1.0, 1.1, 1.2, 1.4 and 1.7 %, respectively). These results thus indicated an increasing capacity of PLA to release volatile molecules, when PLA was stored in environments at increasing relative humidity. This phenomenon was unexpected, since degradation products such as lactic acid and its oligomers are low volatility compounds. Only few studies have reported a dry matter loss in PLA when it is stored in humid atmospheres.[33, 39] And not enough explanation of such phenomenon has been provided, since a large quantity of hydrolytic degradation studies has been carried out in liquid environments. There are several reasons that could explain such behaviour, like hydrolysis-induced release of impurities or solvent residuals entrapped in the polymer matrix, or most likely volatiles formation from oxidation reactions. In fact, it could be possible that molecular oxygen (O_2) reacts with compounds already included in the matrix (*e.g.* impurities, solvents residuals, additives, *etc.*) or continuously formed during hydrolysis, generating free radicals and volatiles (*e.g.* ketones, aldehydes, *etc.*). This hypothesis could explain the shorter induction time of the dry mater variation of these samples in contact with water vapour compared to the PLA immersed in liquid water. In that case, oxidation reactions should be limited by the presence of liquid water molecules, which surround the sample and act as a barrier to O_2. In contrast, when PLA is exposed to water molecules in the vapour state, it is also directly exposed to O_2, thus favouring oxidation reactions.

3.1.3 pH

The variation in the pH of the liquid water in contact with PLA was also followed during ageing (Figure 1c). A significant increase from an initial value ≈ 5.5 to ≈ 6.5 was observed during the first week of ageing. After that time, the pH remained constant until the fifth week of storage (approx. 35 days) and then rapidly decreased to ≈ 3.0.

The initial increase in pH was probably a consequence of alkaline compounds release, which may be incorporated during industrial production for enhancing the PLA performance. It is known that including alkaline compounds (*e.g.* magnesium oxide, tricalcium phosphate, caffeine and coral) is a suitable strategy to limit the hydrolysis reaction in PLA. Such compounds are able to neutralize the carboxyl groups of the degradation products, which are at the same time catalyst of the reaction.[23-24] Then, the fast decrease of the pH indicated that soluble and acidic compounds were generated after 35 days, confirming therefore that the mass loss was due to a mass transfer into the liquid medium in the form of soluble and acidic degradation products.

Similar pH trends were also noticed in other hydrolytic studies done on PLA films immersed in liquid water at 58 °C, [22] and PLA-based composites immersed in buffer solutions (pH 7.4) at 60 °C, [40] as well as in PLA plates placed in buffer solutions at 7.4 and 3.7 at 60 and 37 °C,[38] respectively.

3.2 Modifications in the molecular weight distribution induced by ageing

In order to better understand the effects of the RH and the effect of the physical state of the water molecules on PLA films, the molecular weight distribution in average number ($\overline{M_n}$), the molecular weight distribution in average weight ($\overline{M_w}$) and the polydispersity index (*PDI*) of PLA samples stored in all the conditions were assessed over time (Figure 2abc).

As suggested by the macroscopic analyses, a significant decrease in $\overline{M_n}$ and $\overline{M_w}$ was observed in all of the conditions. Thereby, it confirmed that all PLA films were subjected to hydrolysis (Figure 2ab). $\overline{M_n}$ decreased from an initial value of around 93 kDa to 66, 51, 40, 20, 5, 5 or 12 kDa after being stored at 50, 65, 75, 85, 95, 100 % RH or in liquid conditions for 70 days at 50 °C, respectively. Similarly, the corresponding $\overline{M_w}$ values decreased from around 190 kDa to 140, 110, 86, 51, 10, 10 or 25 kDa. This decreasing trend for both parameters followed a first apparent order, in agreement with several degradation studies carried out in liquid water or in water vapour conditions.[22, 38-39, 41-44]

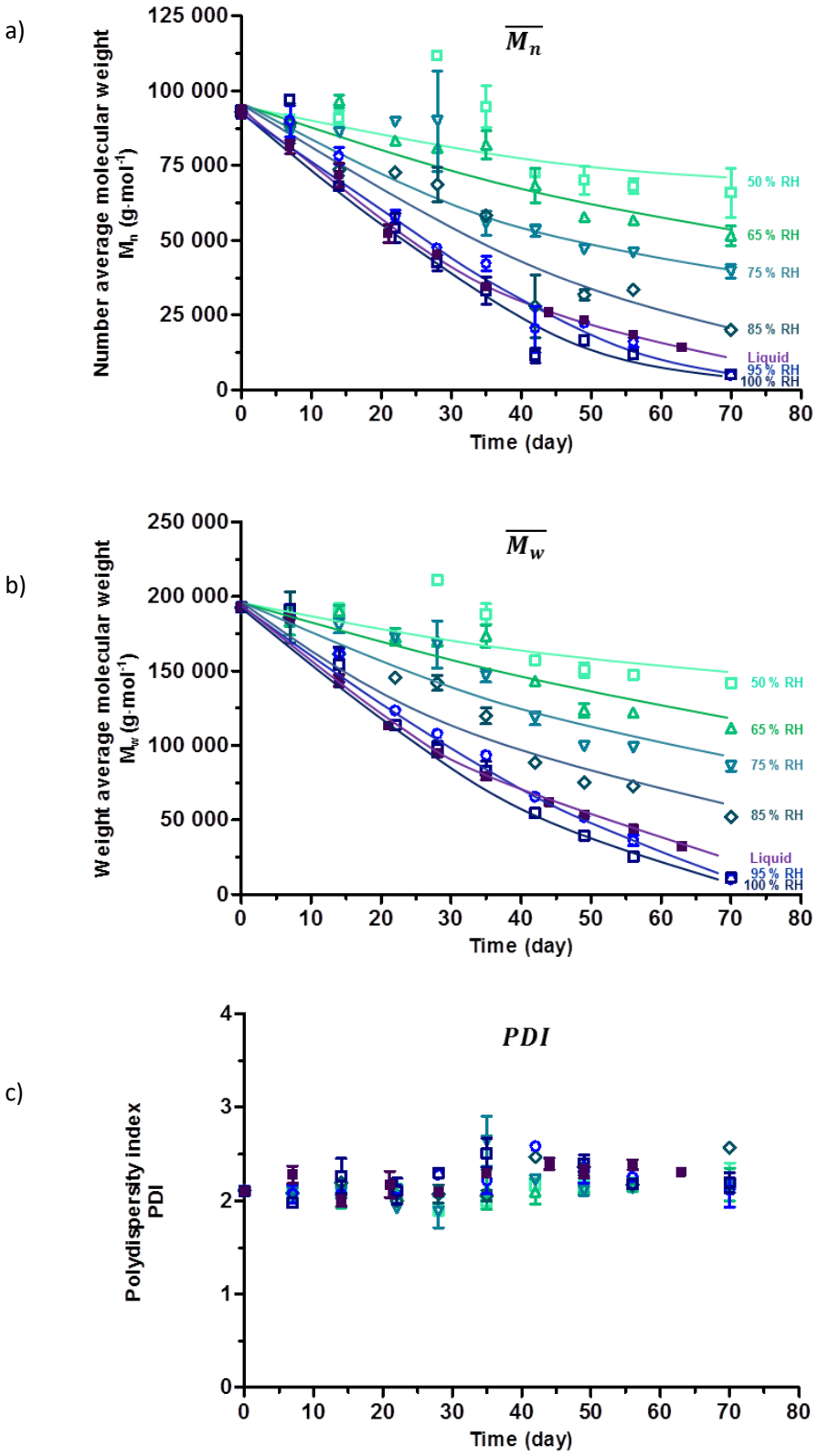

Figure 2. *Kinetics of the molecular weight distribution of PLA films stored at 50 % RH (□), 65 % RH (△), 75 % RH (▽), 85 % RH (◇), 95 % RH (○), 100 % RH (□) or immersed in liquid water (■), at 50 °C. a) Number average molecular weight ($\overline{M_n}$). b) Weight average molecular weight ($\overline{M_w}$). c) Polydispersity index (PDI). Error bars are standard deviations. Lines are guide for the eyes.*

The kinetic analysis of $\overline{M_n}$ and $\overline{M_w}$ pointed out some differences in the hydrolysis mechanism of PLA, associated to the RH and physical state of water molecules (Table 1). On the one hand, when PLA was stored in wet atmospheres, a progressive and significant acceleration in the apparent reaction rate occurred when RH increased, with respect to the chemical potential of water. On the other hand, when PLA was immersed in liquid water, the apparent reaction rate was higher than conditions below 85 % RH, but lower for 95 and 100 % RH. In this case, the chemical potential of water molecules cannot fully account for the reaction rate. The chemical potential of the liquid water molecules can be considered equivalent to the chemical potential of the water vapour molecules in saturated conditions (100 % RH). This means, from a theoretical point of view, that both environments should induce similar hydrolysis rates. Nevertheless, kinetics of $\overline{M_n}$ and $\overline{M_w}$ clearly indicated that the hydrolysis was significantly slower when PLA was immersed in liquid water.

Such deviation could result from the solubilization of the degradation products of small size, which act at the same time as catalysts of the reaction.[23-24] As evidenced by previous macroscopic analysis, these acidic molecules were transferred to the liquid media when PLA was immersed in liquid water, which therefore limit or annihilate their action as catalysts. On the contrary, when PLA was exposed to water vapour, the degradation products were accumulated in the polymer matrix, accelerating therefore the reaction. This hypothesis was further strengthened by the decrease in $\overline{M_w}$ and $\overline{M_n}$ for both conditions (Figure 2ab). The deviation in this decreasing trend was evident after 40 days storage in liquid water. This time was close to the time from which the soluble acidic molecules released in the liquid media modified the pH (≈ 30 days). The key role of the degradation products has also been reported in hydrolytic studies of PLA goods of big size (thickness between 0.5 – 2 mm and 7.4 mm) carried out in aqueous media.[23-25, 33] Such hydrolytic conditions favour an accumulation of the degradation products in the core of the PLA material. In a similar way to the present study, it allows a faster degradation in the bulk than in the surface, where the degradation products can be easily dissolved in the liquid media.[23-25, 33]

The hydrolysis did not highly influence the polydispersity index (*PDI*) (Figure 2c). The *PDI* oscillated around its initial value ≈ 2.1 and no particular trend was observed at any storage condition. When the hydrolysis mechanism favours the formation of small or big oligomers in a preferential way, an increase or decrease of *PDI* is expected, respectively. These results thus suggested that the PLA chains were randomly hydrolysed or end chain degraded in all the storage conditions. This behaviour was also confirmed by the monomodal molecular weight distribution curve, which moved to low molecular weights when time increased, but without any change in the curve width, and no apparition of new peaks. Similar findings were also reported in others studies, involving the degradation of PLA films in aqueous media for one and two months at 37 and 58 °C, respectively,[22, 45] as well as in degradation studies of PLA fibres exposed to environments at 100 % RH, for 3

months at 40 °C.[39] The results of this study also agreed with the considerations made by Gleadall *et al.* [46] in a study involving data modelling of 31 scientific papers. These authors concluded that the hydrolysis of PLA is carried out by a combination of random and end chain scission mechanism.[46] According to these authors, one mechanism cannot fully explain the behaviour of PLA during degradation, since the random scission mechanism is behind the fast decrease in molecular weight of PLA, while the end chain scission mechanism is behind the mass reduction of the polymer, as it produces soluble monomers.[46]

3.3 Modifications in the thermal transitions induced by ageing

The effect of hydrolysis in the physical structure of PLA was further investigated by Differential Scanning Calorimetry (DSC) analysis. PLA films used in this study were semi-crystalline materials. They were characterized by the presence of glass transition, endothermic peak associated to it and melting of crystals, clearly indicating the co-existence of amorphous and crystalline phases in the PLA physical structure (Figure 3ab).

The physical structure of semi-crystalline polymers, such as PLA and other polyesters, is generally described by the three-phase model.[30, 47-48] This model assumes that the semi-crystalline physical structure cannot be explained as a simple co-existence of an undisturbed amorphous phase and a crystalline phase without including a second and more rigid amorphous phase. The two amorphous regions are commonly named the "Mobile Amorphous Phase" (MAP) and the "Rigid Amorphous Fraction" (RAF). On the one hand, the MAP is the amorphous phase which behaves in a similar way than the fully amorphous polymer, having a similar glass transition temperature. On the other hand, the RAF is a fraction of the amorphous phase, which is closely associated to the crystalline phase. It is placed at the boundary between crystals and MAP. The mobility of the RAF polymer chains is highly restricted by the crystalline lamella, and it consequently behaves differently than MAP. RAF does not relax at the main glass transition temperature as MAP, but vitrificates at higher temperatures, between the MAP glass transition and melting of crystals, and depending on the polymer and processing sometimes at temperatures even higher than the melting temperature. [30, 47-52] Although this transition is difficult to be observed by conventional DSC analysis, its percentage in the polymer can easily be estimated from the measured variation of specific heat (ΔC_p) associated to the MAP glass transition and crystallinity percentage , as detailed in the experimental section.[30]

Thermograms (Figure 3ab) clearly showed that the amorphous phases and the crystalline phase of the PLA films were modified according to the time and to the storage conditions.

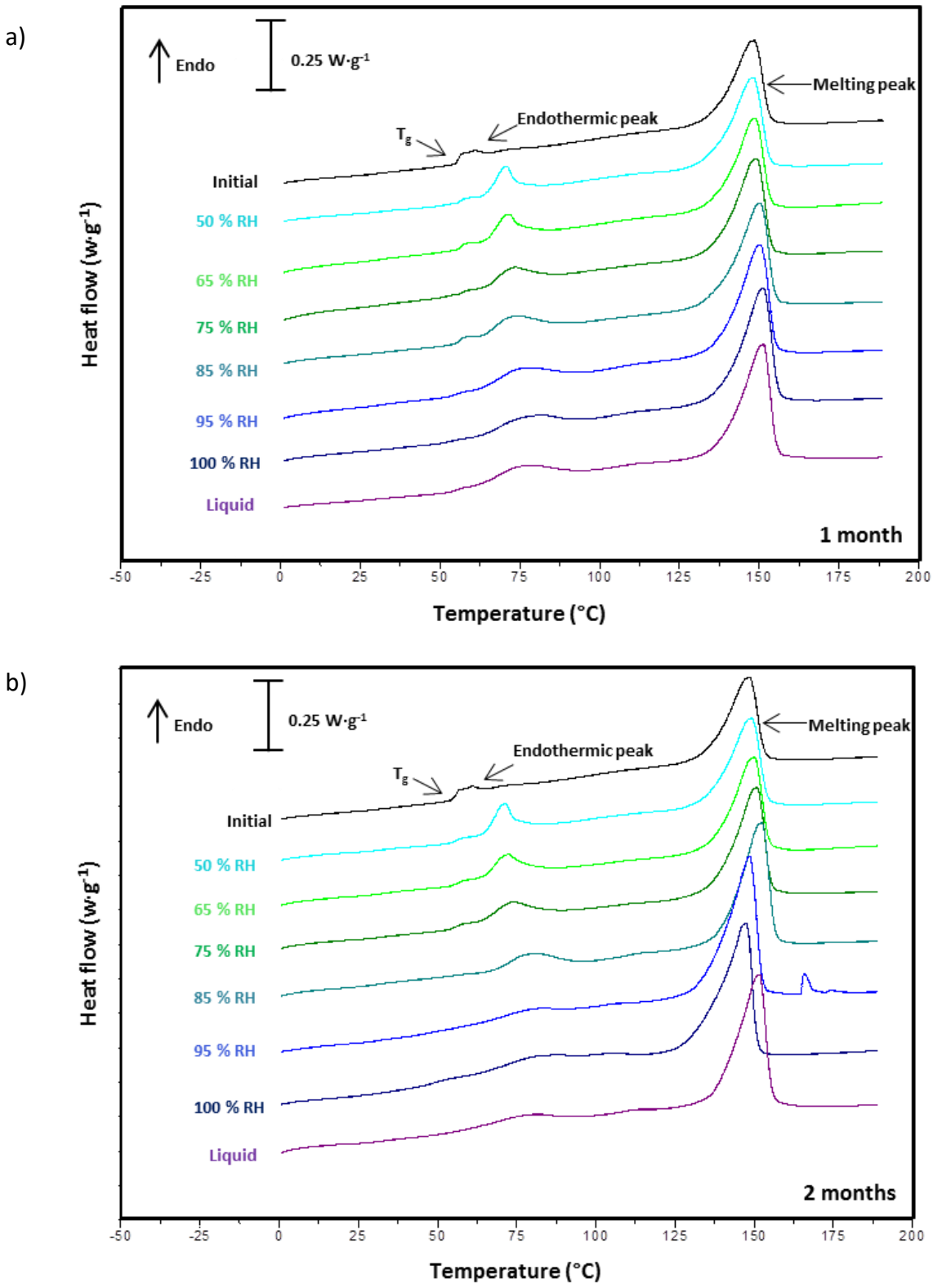

Figure 3. *First heating DSC curves of PLA films from -10 to 190 °C to achieve complete melting. PLA films were aged at 50 % RH, 65 % RH, 75 % RH, 85 % RH, 95 % RH, 100 % RH or immersed in liquid water at 50 °C. a) One month ageing (28 days). b) Two months ageing (56 days).*

3.3.1 Modifications in the Mobile Amorphous Phase (MAP)

Endothermic peak associated to glass transition

An endothermic peak associated to the glass transition was clearly noticeable in the PLA samples as revealed by the first heating in DSC (Figure 3ab). Its area increased and it was shifted to higher temperatures during time. A preliminary test indicated that these modifications fast occurred, and were already displayed after only two days of storage. These thermal events were in agreement with the so-called physical ageing of amorphous and semi-crystalline polymers. [53-54] When a polymer is stored at temperatures lower than its T_g, slow molecular rearrangements occur, which densify the polymer structure. These rearrangements tend to decrease the excess of free energy and free volume of the polymer. And they are accelerated when the storage temperature is close to T_g. As a consequence, when the polymer is stored at $T < T_g$, it becomes more glass-like and less rubber-like during time, and an endothermic peak appears after the glass transition. [53-54]

An interesting effect of the water molecules in the shape of the endothermic peak associated to glass transition was also detected. It became progressively broader with increasing relative humidity or when PLA is immersed in liquid water (Figure 3a). Such effect cannot be only attributed to the hydrolysis of PLA, since it was previously shown that during the first days of storage, the hydrolysis was very limited. In addition, no strong modification was observed in the endothermic peak shape – especially for samples stored at 85 % RH – during the second month of storage (Figure 3b), when the impact of hydrolysis was undoubtful (Figure 2ab). These findings thus indicated that water molecules played a key role in the physical interactions behind physical ageing. Vyavahare *et al.*[55] has recently reported that water molecules increase the segmental mobility of PLA chains and accelerate the kinetics of physical ageing, as a consequence of the formation of water-water interactions (clusters) promoted by PLA carbonyl groups. Based on these considerations, it could be possible that the samples of the present study were characterized by increased water-water interactions at higher RH, which favoured more heterogeneous molecular rearrangements.

Double step glass transition (T_{g1} and T_{g2})

The second heating in DSC, using lower temperatures program (from -10 °C to 100 °C), showed that the glass transition of MAP was actually constituted by a double step change, which was previously hindered by the endothermic peak related to physical ageing, during the first heating (Figure 4ab). For the starting material, the inflection point of the first and second step was ≈ 55 and 65 °C, and the change in specific heat was ≈ 0.09 and 0.17 $J \cdot g^{-1} \cdot C^{-1}$, respectively. It is attributed to a consequence of the bi-orientation during processing. It is well-know that this process modifies the PLA physical structure, and promotes the formation of orientated PLA crystals within PLA amorphous chains.[56-57] Different studies have observed the existence of two (and close)

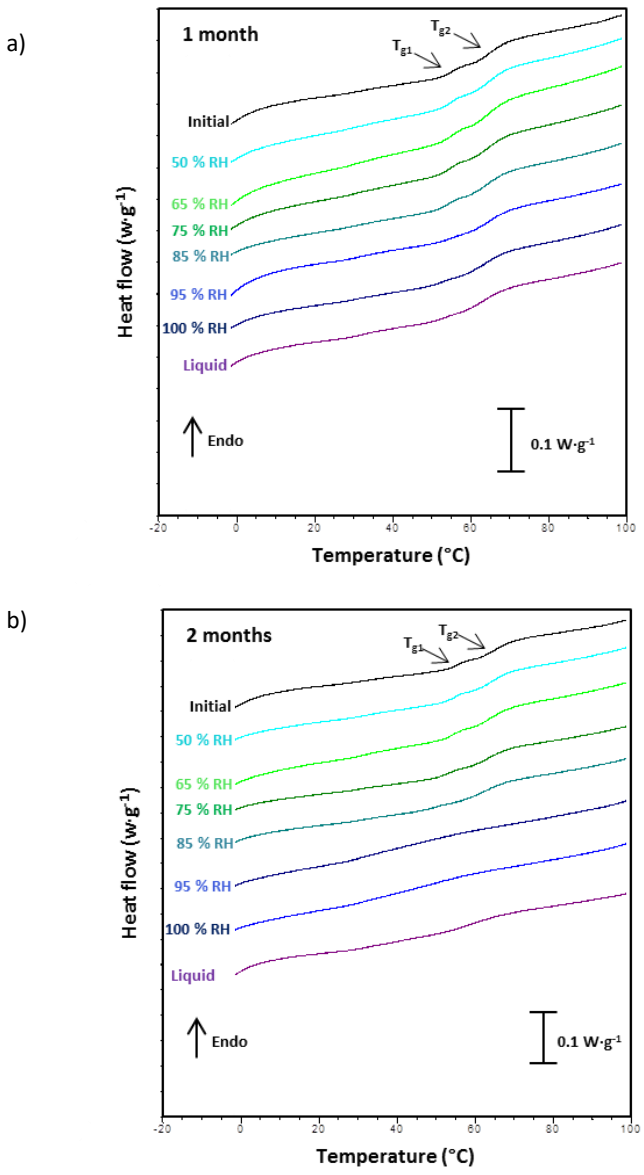

Figure 4. *Second heating DSC curves of PLA films from -10 to 100 °C (final temperature stopped before melting). PLA films were aged at 50 % RH, 65 % RH, 75 % RH, 85 % RH, 95 % RH, 100 % RH or immersed in liquid water at 50 °C. a) One month ageing (28 days). b) Two months ageing (56 days).*

glass transitions in semi-crystalline PLA as a consequence of different crystallization processes.[31, 58-60] According to the literature, these two different glass transitions confirm the presence of two amorphous mobile phases, one more mobile and the other more restricted. The more restricted phase is thought to be more associated to crystals, but differs from RAF since it is able to relax at temperatures higher but rather close to that of the characteristic T_g of the material. Based on these considerations, both T_g steps were considered as individual transitions. The step at lower temperature was referred to as T_{g1}, and the other one at higher temperature T_{g2}.

Figures 4ab and 5ab clearly show that T_{g1} and T_{g2} decreased during ageing. The decrease trends were similar between them and are in accordance with the kinetics of hydrolysis (Figure 2ab and Table 1): the decrease was as much pronounced as PLA was stored in environments at high RH or immersed in liquid water.

No strong modification was observed in the T_g of PLA samples stored at 50 and 65 % RH, probably as a consequence of the reduced hydrolysis in such conditions, which apparently do not highly increase the mobility of PLA chains. On the contrary, the modifications were progressively stronger at RH > 65 %, as expected from hydrolysis kinetics. Since the samples were dried before analyses, the decrease in both T_{g1} and T_{g2} cannot be attributed to a plasticizing effect of water, but to the lower molecular weight of PLA and to the plasticization effect of the small degradation products. Also in this case, the modifications of the PLA sample immersed in liquid water were slighter than for the samples stored at 100 % RH, in agreement with the conclusions achieved from the previous section. Decreasing trends in T_g were also reported in other degradation studies of PLA involving water molecules in liquid and vapour phase.[25-26, 36, 44, 61]

DSC analysis also indicated that both mobile amorphous phases had different water sensitivity, suggesting that the hydrolysis was faster in the mobile amorphous phase with the lower T_g. Such glass transition was no more detectable after 28, 42, 56 or 56 days when the PLA films were stored at 100 % RH, 95 % RH, 85 % RH or immersed in liquid water, respectively. On the contrary, the transition related to the more constrained MAP was always detectable (Figures 4ab and 5ab). The modifications of T_{g2} occurred mainly during the second month, while the modifications of T_{g1} were evidenced since the very first weeks of storage. In a similar way, ΔC_{p1} decreased much faster during the first month of storage than ΔC_{p2} (Figure 5cd). A possible explanation of this different water sensitivity in both MAP could be the different reduced mobility of the constrained MAP phase induced by crystals. It could be possible that the diffusion of water molecules is more difficult in that phase, reducing its reactivity.

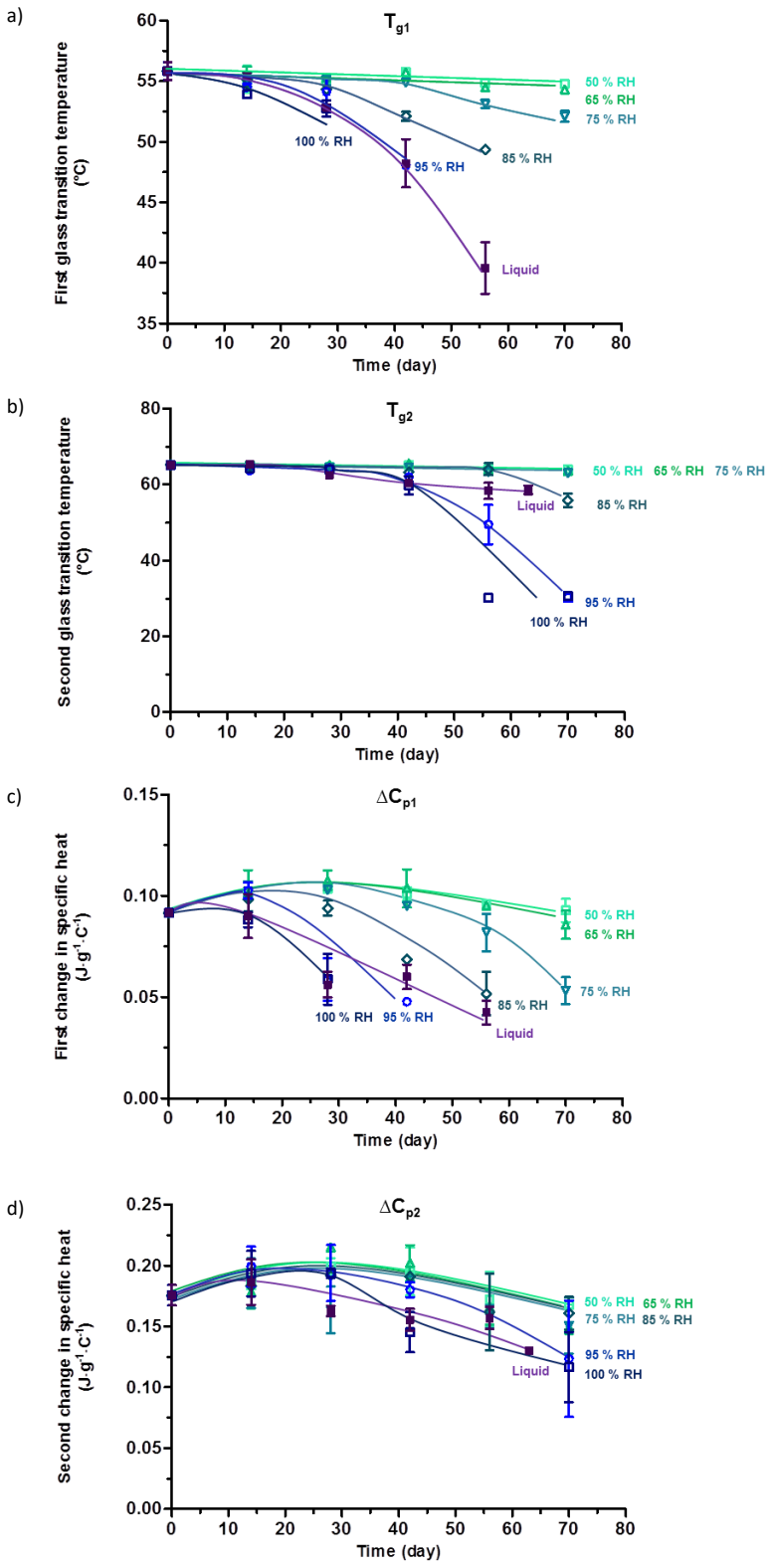

Figure 5. *Modification in the thermal transitions related to mobile amorphous phase as a function of time for PLA films stored at 50 % RH (□), 65 % RH (△), 75 % RH (▽), 85 % RH (◇), 95 % RH (○), 100 % RH (□) or immersed in liquid water (■), at 50 °C. a) First glass transition temperature (T_{g1}). b) Second glass transition temperature (T_{g2}). c) First change in specific heat (ΔC_{p1}). d) Second change in specific heat (ΔC_{p2}). Error bars are standard deviations. Lines are guide for the eyes.*

3.3.2 Modifications in the crystalline phase

The crystalline phase of PLA was clearly modified during time, and in agreement with all of the analysis discussed, the modifications were progressively higher at increased RH (Figure 6ab).

The temperature of melting (T_m) was constant (approx. 149 °C) for the samples stored at 50 % RH, but when the humidity increased, T_m slightly but significantly increased to approx. 151 °C. The samples stored at the conditions ≥ 85 % RH were characterized by a further decrease in that value. After 70 days of storage the T_m of the samples stored at 85, 95 and 100 % RH reached around 147, 135 and 133 °C, respectively. Similar increasing and then decreasing trend was also noticed by Tsuji and Ikada[26] and by Tsuji *et al.*[36] in PLA samples stored in phosphate buffer solutions at 37 °C for 3 years. According to these authors, the increase in T_m could be due to an increase in the thickness of PLA crystallites, which is promoted by the higher chain mobility induced by hydrolysis, favouring the thermostability of the crystals. On the contrary, the decrease of T_m indicates a reduction of the lamella thickness, which generates less thermostable crystals at increased ageing times.

The crystallinity percentage (X_c) of PLA films was highly influenced by the storage conditions. When the samples were stored at 50 % RH, no significant change in initial X_c (≈ 23 %) was observed, but when the RH increased or when the PLA samples were immersed in liquid water, the X_c linearly increased during time. As revealed by the kinetic analysis, such modifications followed an apparent zero order and had higher rates at increased RH (Table 1). X_c of the films kept at 65, 75, 85, 95 and 100 % RH was ≈ 26, 29, 34, 36 and 37 % by the end of the storage test. When the PLA films were immersed in liquid water, X_c was between the values at 95 and 85 % RH, confirming once again the deviation from the samples stored at 100 % RH.

The increase of X_c is a well-known phenomenon in PLA under hydrolytic degradation, which occurs even in totally amorphous PLA. Hydrolysis-induced crystallization has been confirmed by different authors, using different techniques such as DSC, WAXS (Wide-Angle X–ray Scattering) and FTIR (Fourier Transform Infrared spectroscopy). The increased chain mobility induced by the small degradation products and water molecules, which may favour plasticization and also the crystallization of PLA chains.[22, 24-26, 33, 41]

3.3.3 Modifications in the Rigid Amorphous Fraction (RAF)

Initial PLA films contained a high quantity of rigid amorphous phase (X_{RAF} ≈ 21 %), which was around half quantity of the total mobile amorphous phase (X_{MAP} ≈ 56 %) and almost the same quantity of crystals (X_c ≈ 23 %). This indicated that the three-model phase suited very well, and would better describe the PLA physical structure than the two-phase model.

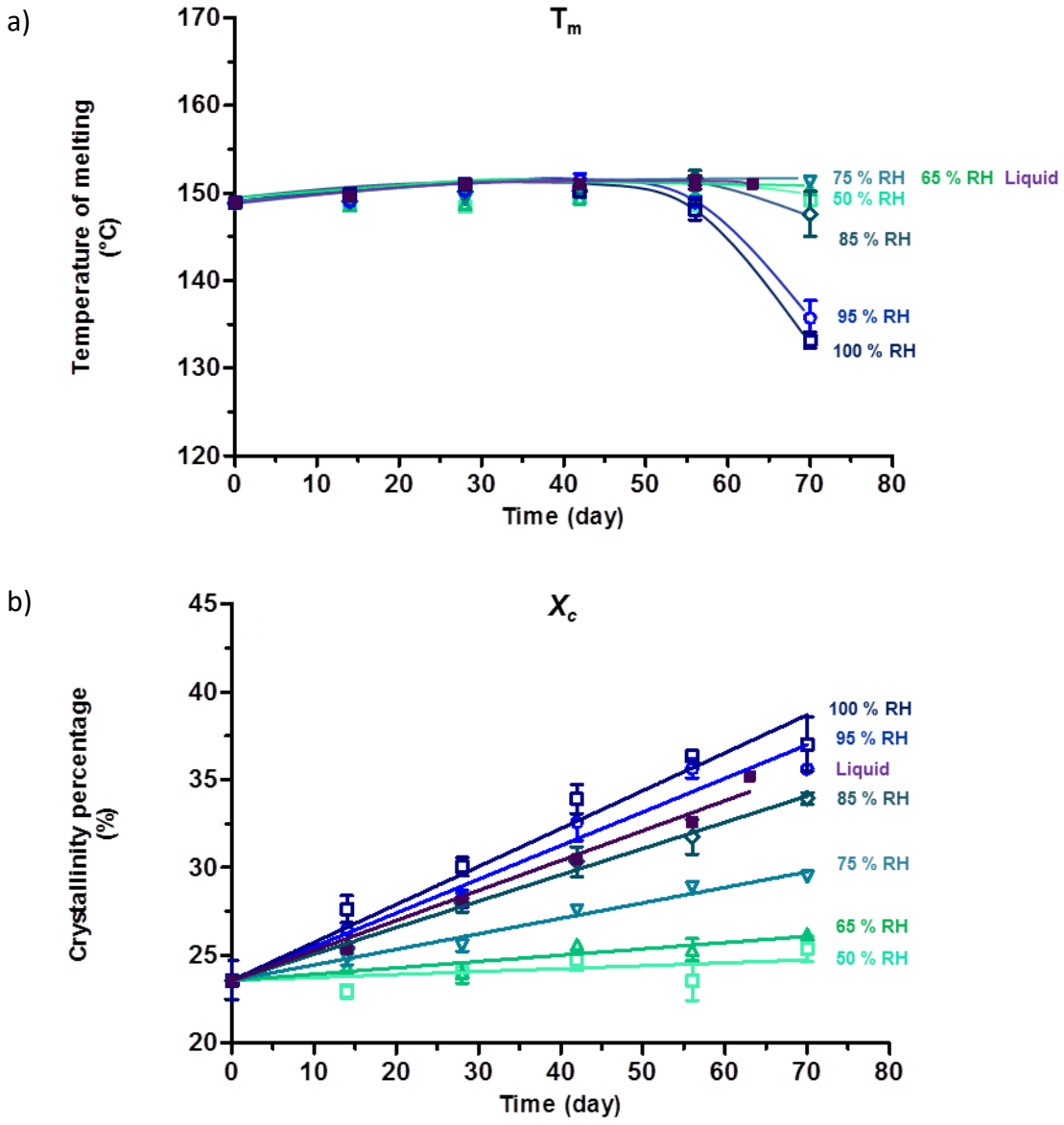

Figure 6. *Modification in the thermal transitions related to the crystalline phase as a function of time for PLA films stored at 50 % RH (□), 65 % RH (△), 75 % RH (▽), 85 % RH (◇), 95 % RH (○), 100 % RH (□) or immersed in liquid water (■), at 50 °C. a) Temperature of melting (T_m). b) Crystallinity percentage (X_c). Error bars are standard deviations. Lines are guide for the eyes.*

The changes in X_{RAF} and X_{MAP} during PLA ageing are reported in Figure 7ab. From the trends of these graphs, it is worthy to note that both phases have almost an opposite behaviour. When the hydrolysis is limited, X_{RAF} tends to decrease, while X_{MAP} tends to be constant or to slightly increase. When the hydrolysis is getting higher, X_{RAF} tends to increase, while X_{MAP} tends to decrease. A possible explanation of this behaviour could be that when the hydrolysis is limited, part of the RAF becomes more mobile due to the plasticization induced by degradation products. When the hydrolysis is extended, part of MAP becomes more constrained due to the

hydrolysis-induced crystallization of PLA, which most likely reduces the mobility of PLA chains and takes place more in MAP rather than in RAF.

These considerations can be considered in agreement with Tsuji and Miyauchi (2001)[62] and Tsuji *et al.* (2005)[63], who reported that the amorphous chains associated to RAF are much more hydrolysis-resistant in comparison to the amorphous chains related to MAP, from enzymatic degradation studies of PLA films conducted in alkaline environments (pH 8.6) at 37 °C.

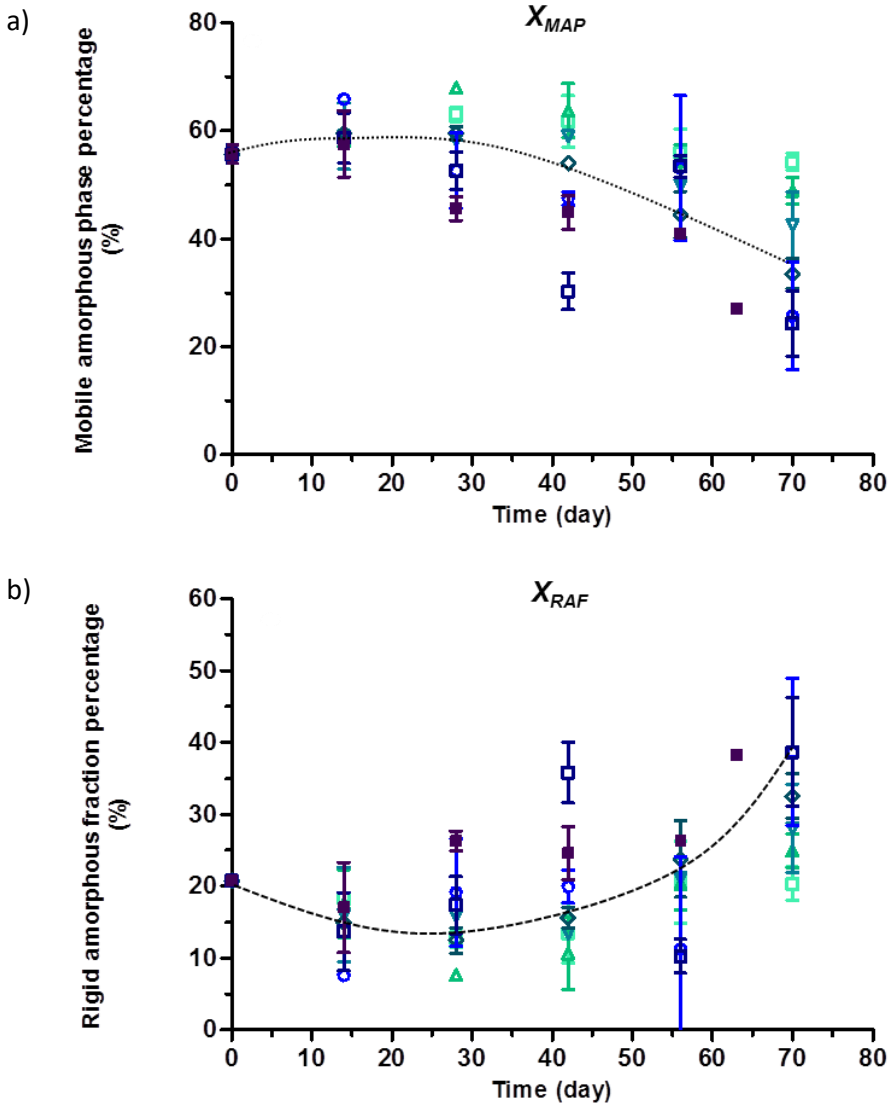

Figure 7. *a) Percentage of the mobile amorphous phase (X_{MAP}) and b) Percentage of the rigid amorphous fraction (X_{RAF}) of PLA films stored at 50 % RH (□), 65 % RH (△), 75 % RH (▽), 85 % RH (◇), 95 % RH (○), 100 % RH (▭) or immersed in liquid water (■) at 50 °C as a function of time. Error bars are standard deviations. Lines are guide for the eyes.*

4 Conclusion

This study gave a full depiction of the physical and chemical stability of PLA as thin films in a large range of RH environments, and in contact with liquid water. Findings unambiguously showed that the PLA stability was influenced by the chemical potential and by the physical state of water molecules.

The macroscopic analyses pointed out an increased production of hydrophilic and acidic degradation products when the chemical potential of water increased. The behaviour was different as a function of the physical state of water. When PLA was exposed to water vapour in a range from 50 to 100 % RH, the degradation products were accumulated in the matrix, increasing water sorption and reactivity. When PLA was immersed in liquid water, they were solubilised, transferred to the aqueous medium and no water sorption further occurred in the polymer.

The change in the molecular weight distribution ($\overline{M_n}$ and $\overline{M_w}$) confirmed that PLA was subjected to hydrolysis reaction for all of the storage conditions. The kinetic analysis revealed that the reaction was accelerated when the chemical potential of water increased. Nevertheless, the reaction was significantly slower when PLA was immersed in liquid water conditions compared to the 100 % RH condition, even if water molecules had an equivalent chemical potential. Such deviation was a consequence of the accumulation of degradation products in PLA films at 100 % RH, which also act as auto-catalyst.

The physical structure of PLA suited very well with the three-model phase (X_{RAF} + X_{MAP} + X_c = 100 %). All the three phases were modified during hydrolysis. The rates of these modifications (T_{g1}, T_{g2}, $\Delta C_{p1,}$ ΔC_{p2}, T_m, X_c, $X_{RAF,}$ X_{MAP}) matched in almost all the cases the trend determined by the kinetics of hydrolysis determined from SEC analysis: 50 % RH < 65 % RH < 75 % RH < 85 % RH < liquid < 95 % RH < 100 % RH. When the hydrolysis was favoured X_{RAF} increased, X_{MAP} decreased and X_c increased. Thus this indicated that hydrolysis induced crystallization of MAP polymer chains, which in turn constrained additional MAP chains, transforming them into RAF.

From a practical point of view the findings of this research can be used as strong scientific basis for giving recommendations about the use of this material, and for estimating its shelf life in its applications as packaging or mulch films.

Acknowledgments

The authors acknowledge the European Social Fund – Friuli Venezia Giulia Region – Operational Program 2007/2013 for supporting this project (Regional code: FP1340303009), the Università Italo-Francese for mobility grant (Bando Vinci 2015 Cap II, project code C2-64), the RMB plateau of UMR PAM for thermal analyses and the ICMUB research unit for SEC analyses.

Table 1. *Kinetic parameters of number average molecular weight loss ($\overline{M_n}$), weight average molecular weight loss ($\overline{M_w}$) and crystallinity percentage increase (X_c) of PLA films stored in different wet environments at 50 °C for 70 days. k_{app} is the apparent rate constant, 95 % CI are the 95 % confidence intervals and R^2 is the coefficient of determination. Different letters in the same raw mean significant difference. The rate constants were considered significantly different when no intersection was found in their 95% confidence interval.*

Parameter	**Constant rate**	**Storage conditions**						
		50 % RH	**65 % RH**	**75 % RH**	**85 % RH**	**95 % RH**	**100 % RH**	**Liquid**
$\overline{M_n}$	k_{app} ($day^{-1}\cdot10^{-3}$)§	5.9^{a}	9.6^{a}	14.0^{ab}	23.0^{bc}	40.5^{de}	43.7^{e}	30.5^{cd}
	95 % CI	1.3 – 10.6	7.0 – 12.2	9.5 – 18.5	16.3 – 29.7	31.4 – 49.5	35.1 – 52.3	28.7 – 32.3
	R^2	0.56	0.90	0.87	0.89	0.93	0.94	0.99
$\overline{M_w}$	k_{app} ($day^{-1}\cdot10^{-3}$)§	5.1^{a}	8.6^{ab}	13.0^{b}	19.7^{c}	38.5^{de}	40.7^{e}	28.4^{d}
	95 % CI	2.0 – 8.2	6.2 – 11.0	10.0 – 16.0	16.8 – 22.6	28.4 – 48.6	33.8 – 47.6	26.5 – 30.3
	R^2	0.68	0.90	0.93	0.97	0.91	0.96	0.99
X_c	k_{app} (%·$day^{-1}\cdot10^{-2}$)¥	2.3^{a}	3.6^{a}	8.9^{b}	14.9^{c}	18.8^{c}	19.8^{c}	17.9^{c}
	95 % CI	0– 5.7	1.6 – 5.6	7.2 – 10.6	13.4 – 16.4	13.5 – 24.1	14.8 – 24.9	15.0 – 20.7
	R^2	0.48	0.86	0.98	0.99	0.96	0.97	0.99

§ First apparent order
¥ Zero apparent order
CI Confidence Interval
Values having the same superscript letter in a same row are not significantly different at p-level 0.05.

References

1. Halden, R. U. Plastics and Health Risks. *Annual Review of Public Health* **2010,** *31,* 179-194.

2. Thompson, R. C.; Moore, C. J.; vom Saal, F. S.; Swan, S. H. Plastics, the environment and human health:

3. Teuten, E. L.; Saquing, J. M.; Knappe, D. R. U.; Barlaz, M. A.; Jonsson, S.; Bjorn, A.; Rowland, S. J.; Thompson, R. C.; Galloway, T. S.; Yamashita, R.; Ochi, D.; Watanuki, Y.; Moore, C.; Pham Hung, V.; Tana, T. S.; Prudente, M.; Boonyatumanond, R.; Zakaria, M. P.; Akkhavong, K.; Ogata, Y.; Hirai, H.; Iwasa, S.; Mizukawa, K.; Hagino, Y.; Imamura, A.; Saha, M.; Takada, H. Transport and release of chemicals from plastics to the environment and to wildlife. *Philosophical Transactions of the Royal Society B-Biological Sciences* **2009,** *364* (1526), 2027-2045.

4. European Bioplastics Association. Global production capacities of bioplastics 2014 (by material type) and applications. http://en.european-bioplastics.org/market. Retrieved on 25/01/2016.

5. Reddy, M. M.; Vivekanandhan, S.; Misra, M.; Bhatia, S. K.; Mohanty, A. K. Biobased plastics and bionanocomposites: Current status and future opportunities. *Progress in Polymer Science* **2013,** *38* (10–11), 1653-1689.

6. Mekonnen, T.; Mussone, P.; Khalil, H.; Bressler, D. Progress in bio-based plastics and plasticizing modifications. *Journal of Materials Chemistry A* **2013,** *1* (43), 13379-13398.

7. Castro-Aguirre, E.; Iñiguez-Franco, F.; Samsudin, H.; Fang, X.; Auras, R. Poly(lactic acid)—Mass production, processing, industrial applications, and end of life. *Advanced Drug Delivery Reviews* **2016,** *107*, 333-366.

8. Auras, R.; Harte, B.; Selke, S. An overview of polylactides as packaging materials. *Macromolecular Bioscience* **2004,** *4* (9), 835-864.

9. Jamshidian, M.; Tehrany, E. A.; Imran, M.; Jacquot, M.; Desobry, S. Poly-lactic acid: production, applications, nanocomposites, and release studies. *Comprehensive Reviews in Food Science and Food Safety* **2010,** *9* (5), 552-571.

10. Tan, B. H.; Muiruri, J. K.; Li, Z.; He, C. Recent progress in using stereocomplexation for enhancement of thermal and mechanical property of polylactide. *ACS Sustainable Chemistry & Engineering* **2016,** *4* (10), 5370-5391.

11. Corneillie, S.; Smet, M. PLA architectures: the role of branching. *Polymer Chemistry* **2015,** *6* (6), 850-867.

12. Kai, D.; Ren, W.; Tian, L.; Chee, P. L.; Liu, Y.; Ramakrishna, S.; Loh, X. J. Engineering Poly(lactide)–Lignin Nanofibers with Antioxidant Activity for Biomedical Application. *ACS Sustainable Chemistry & Engineering* **2016,** *4* (10), 5268-5276.

13. Agustin-Salazar, S.; Gamez-Meza, N.; Medina-Juàrez, L. À.; Soto-Valdez, H.; Cerruti, P. From nutraceutics to materials: effect of resveratrol on the stability of polylactide. *ACS Sustainable Chemistry & Engineering* **2014,** *2* (6), 1534-1542.

14. Arrnentano, I.; Bitinis, N.; Fortunati, E.; Mattioli, S.; Rescignano, N.; Verdejo, R.; Lopez-Manchado, M. A.; Kenny, J. M. Multifunctional nanostructured PLA materials for packaging and tissue engineering. *Progress in Polymer Science* **2013,** *38* (10-11), 1720-1747.

15. Zhu, H. G.; Ji, J.; Shen, J. C. Surface engineering of poly(DL-lactic acid) by entrapment of biomacromolecules. *Macromolecular Rapid Communications* **2002,** *23* (14), 819-823.

16. Fabra, M. J.; Busolo, M. A.; Lopez-Rubio, A.; Lagaron, J. M. Nanostructured biolayers in food packaging. *Trends in Food Science & Technology* **2013,** *31* (1), 79-87.

17. Rocca-Smith, J. R.; Karbowiak, T.; Marcuzzo, E.; Sensidoni, A.; Piasente, F.; Champion, D.; Heinz, O.; Vitry, P.; Bourillot, E.; Lesniewska, E.; Debeaufort, F. Impact of corona treatment on PLA film properties. *Polymer Degradation and Stability* **2016,** *132*, 109-116.

18. Janorkar, A. V.; Metters, A. T.; Hirt, D. E. Modification of poly(lactic acid) films: enhanced wettability from surface-confined photografting and increased degradation rate due to an artifact of the photografting process. *Macromolecules* **2004,** *37* (24), 9151-9159.

19. Rasal, R. M.; Janorkar, A. V.; Hirt, D. E. Poly(lactic acid) modifications. *Progress in Polymer Science* **2010,** *35* (3), 338-356.

20. Wang, S. G.; Cui, W. J.; Bei, J. Z. Bulk and surface modifications of polylactide. *Analytical and Bioanalytical Chemistry* **2005,** *381* (3), 547-556.

21. Witzke, D. R. Introduction to properties, engineering, and prospects of polylactide polymers. Michigan State University East Lansing, MI, 1997. PhD thesis.

22. Gorrasi, G.; Pantani, R. Effect of PLA grades and morphologies on hydrolytic degradation at composting temperature: Assessment of structural modification and kinetic parameters. *Polymer Degradation and Stability* **2013,** *98* (5), 1006-1014.

23. Li, S. M. Hydrolytic degradation characteristics of aliphatic polyesters derived from lactic and glycolic acids. *Journal of Biomedical Materials Research* **1999,** *48* (3), 342-353.

24. Tsuji, H., Hydrolytic degradation. In *Poly(lactic acid): synthesis, structures, properties, processing, and applications*; Auras, R.; Lim, L.-T.; Selke, S. E. M.; Tsuji, H., Eds.; Wiley: Hoboken, N.J., 2010.

25. Migliaresi, C.; Fambri, L.; Cohn, D. A study on the in-vitro degradation of poly(lactic acid). *Journal of Biomaterials Science-Polymer Edition* **1994,** *5* (6), 591-606.

26. Tsuji, H.; Ikada, Y. Properties and morphology of poly(L-lactide) 4. Effects of structural parameters on long-term hydrolysis of poly(L-lactide) in phosphate-buffered solution. *Polymer Degradation and Stability* **2000,** *67* (1), 179-189.

27. Makino, K.; Arakawa, M.; Kondo, T. Preparation and invitro degradation properties of polylactide microcapsules. *Chemical & Pharmaceutical Bulletin* **1985,** *33* (3), 1195-1201.

28. Greenspan, L. Humidity fixed points of binary saturated aqueous solutions. *Journal of Research of the National Bureau of Standards Section a-Physics and Chemistry* **1977,** *81* (1), 89-96.

29. Fischer, E. W.; Sterzel, H. J.; Wegner, G. Investigation of the structure of solution grown crystals of lactide copolymers by means of chemical reactions. *Kolloid-Zeitschrift and Zeitschrift fur polymere* **1973,** *251*, 980-990.

30. Arnoult, M.; Dargent, E.; Mano, J. F. Mobile amorphous phase fragility in semi-crystalline polymers: Comparison of PET and PLLA. *Polymer* **2007,** *48* (4), 1012-1019.

31. Delpouve, N.; Arnoult, M.; Saiter, A.; Dargent, E.; Saiter, J. M. Evidence of two mobile amorphous phases in semicrystalline polylactide observed from calorimetric investigations. *Polymer Engineering and Science* **2014,** *54* (5), 1144-1150.

32. Holm, V. K.; Ndoni, S.; Risbo, J. The stability of poly(lactic acid) packaging films as influenced by humidity and temperature. *Journal of Food Science* **2006,** *71* (2), E40-E44.

33. Kucharczyk, P.; Hnatkova, E.; ZdenekDvorak; Sedlarik, V. Novel aspects of the degradation process of PLA based bulky samples under conditions of high partial pressure of water vapour. *Polymer Degradation and Stability* **2013,** *98* (1), 150-157.

34. Cairncross, R. A.; Becker, J. G.; Ramaswamy, S.; O'Connor, R. Moisture sorption, transport, and hydrolytic degradation in polylactide. *Applied Biochemistry and Biotechnology* **2006,** *131* (1-3), 774-785.

35. Lyu, S. P.; Schley, J.; Loy, B.; Lind, D.; Hobot, C.; Sparer, R.; Untereker, D. Kinetics and time-temperature equivalence of polymer degradation. *Biomacromolecules* **2007,** *8* (7), 2301-2310.

36. Tsuji, H.; Mizuno, A.; Ikada, Y. Properties and morphology of poly(L-lactide). III. Effects of initial crystallinity on long-term in vitro hydrolysis of high molecular weight poly(L-lactide) film in phosphate-buffered solution. *Journal of Applied Polymer Science* **2000,** *77* (7), 1452-1464.

37. Tsuji, H. Poly(lactide) stereocomplexes: Formation, structure, properties, degradation, and applications. *Macromolecular Bioscience* **2005,** *5* (7), 569-597.

38. Li, S. M.; McCarthy, S. Further investigations on the hydrolytic degradation of poly(DL-lactide). *Biomaterials* **1999,** *20* (1), 35-44.

39. Mitchell, M. K.; Hirt, D. E. Degradation of PLA fibers at elevated temperature and humidity. *Polymer Engineering and Science* **2015,** *55* (7), 1652-1660.

40. Olewnik-Kruszkowska, E. Influence of the type of buffer solution on thermal and structural properties of polylactide-based composites. *Polymer Degradation and Stability* **2016,** *129*, 87-95.

41. Harris, A. M.; Lee, E. C. Heat and humidity performance of injection molded PLA for durable applications. *Journal of Applied Polymer Science* **2010,** *115* (3), 1380-1389.

42. Ho, K. L. G.; Pometto, A. L.; Hinz, P. N. Effects of temperature and relative humidity on polylactic acid plastic degradation. *Journal of Environmental Polymer Degradation* **1999,** *7* (2), 83-92.

43. Mohd-Adnan, A.-F.; Nishida, H.; Shirai, Y. Evaluation of kinetics parameters for poly(l-lactic acid) hydrolysis under high-pressure steam. *Polymer Degradation and Stability* **2008,** *93* (6), 1053-1058.

44. Copinet, A.; Bertrand, C.; Govindin, S.; Coma, V.; Couturier, Y. Effects of ultraviolet light (315 nm), temperature and relative humidity on the degradation of polylactic acid plastic films. *Chemosphere* **2004,** *55* (5), 763-773.

45. Hakkarainen, M.; Karlsson, S.; Albertsson, A. C. Rapid (bio)degradation of polylactide by mixed culture of compost microorganisms - low molecular weight products and matrix changes. *Polymer* **2000,** *41* (7), 2331-2338.

46. Gleadall, A.; Pan, J.; Kruft, M.-A.; Kellomaki, M. Degradation mechanisms of bioresorbable polyesters. Part 1. Effects of random scission, end scission and autocatalysis. *Acta Biomaterialia* **2014,** *10* (5), 2223-2232.

47. Wunderlich, B. Reversible crystallization and the rigid–amorphous phase in semicrystalline macromolecules. *Progress in Polymer Science* **2003,** *28* (3), 383-450.

48. Kattan, M.; Dargent, E.; Grenet, J. Three phase model in drawn thermoplastic polyesters: comparison of differential scanning calorimetry and thermally stimulated depolarisation current experiments. *Polymer* **2002,** *43* (4), 1399-1405.

49. Magoń, A.; Pyda, M. Study of crystalline and amorphous phases of biodegradable poly(lactic acid) by advanced thermal analysis. *Polymer* **2009,** *50* (16), 3967-3973.

50. Bai, H.; Huang, C.; Xiu, H.; Zhang, Q.; Fu, Q. Enhancing mechanical performance of polylactide by tailoring crystal morphology and lamellae orientation with the aid of nucleating agent. *Polymer* **2014,** *55* (26), 6924-6934.

51. Delpouve, N.; Delbreilh, L.; Stoclet, G.; Saiter, A.; Dargent, E. Structural dependence of the molecular mobility in the amorphous fractions of polylactide. *Macromolecules* **2014,** *47* (15), 5186-5197.

52. Righetti, M. C.; Tombari, E. Crystalline, mobile amorphous and rigid amorphous fractions in poly(L-lactic acid) by TMDSC. *Thermochimica Acta* **2011,** *522* (1–2), 118-127.

53. Hutchinson, J. M. Physical aging of polymers. *Progress in Polymer Science* **1995,** *20* (4), 703-760.

54. Struik, L. C. E. Physical aging in plastics and other glassy materials. *Polymer Engineering & Science* **1977,** *17* (3), 165-173.

55. Vyavahare, O.; Ng, D.; Hsu, S. L. Analysis of structural rearrangements of poly(lactic acid) in the presence of water. *Journal of Physical Chemistry B* **2014,** *118* (15), 4185-4193.

56. Delpouve, N.; Stoclet, G.; Saiter, A.; Dargent, E.; Marais, S. Water barrier properties in biaxially drawn poly(lactic acid) films. *Journal of Physical Chemistry B* **2012,** *116* (15), 4615-4625.

57. Jariyasakoolroj, P.; Tashiro, K.; Wang, H.; Yamamoto, H.; Chinsirikul, W.; Kerddonfag, N.; Chirachanchai, S. Isotropically small crystalline lamellae induced by high biaxial-stretching rate as a key microstructure for super-tough polylactide film. *Polymer* **2015,** *68*, 234-245.

58 Righetti, M. C.; Prevosto, D.; Tombari, E. Time and temperature evolution of the rigid amorphous fraction and differently constrained amorphous fractions in PLLA. *Macromolecular Chemistry and Physics* **2016,** *217* (18), 2013-2026.

59. Dionisio, M.; Viciosa, M. T.; Wang, Y. M.; Mano, J. F. Glass transition dynamics of poly(L-lactic acid) during isothermal crystallisation monitored by real-time dielectric relaxation spectroscopy measurements. *Macromolecular Rapid Communications* **2005,** *26* (17), 1423-1427.

60. Wang, Y.; Ribelles, J. L. G.; Sanchez, M. S.; Mano, J. F. Morphological contributions to glass transition in poly(L-lactic acid). *Macromolecules* **2005,** *38* (11), 4712-4718.

61. Gonzalez, M. F.; Ruseckaite, R. A.; Cuadrado, T. R. Structural changes of polylactic-acid (PLA) microspheres under hydrolytic degradation. *Journal of Applied Polymer Science* **1999,** *71* (8), 1223-1230.

62. Tsuji, H.; Miyauchi, S. Poly(l-lactide): 7. Enzymatic hydrolysis of free and restricted amorphous regions in poly(l-lactide) films with different crystallinities and a fixed crystalline thickness. *Polymer* **2001,** *42* (9), 4463-4467.

63. Tsuji, H.; Tezuka, Y.; Yamada, K. Alkaline and enzymatic degradation of L-lactide copolymers. II. Crystallized films of poly(L-lactide-co-D-lactide) and poly(L-lactide) with similar crystallinities. *Journal of Polymer Science Part B: Polymer Physics* **2005,** *43* (9), 1064-1075.

PART II

INFLUENCE OF INDUSTRIAL PROCESSES ON PLA SUPPORT LAYER AND FORMULATION ON WHEAT GLUTEN COATING LAYER

Impact of corona treatment on PLA film properties

Rocca-Smith, J. R.; Karbowiak, T.; Marcuzzo, E.; Sensidoni, A.; Piasente, F.; Champion, D.; Heinz, O.; Vitry, P.; Bourillot, E.; Lesniewska, E.; Debeaufort, F. Impact of corona treatment on PLA film properties. *Polymer Degradation and Stability* 2016, *132*, 109-116.

Abstract

Different types of PLA films treated by corona are currently available in the market for coating or printing applications. However, data relative to its impact on PLA film properties are scarce and do not generally consider industrial scale production. The objective of this study was to assess the impact of corona treatment on the surface, structure and barrier properties of bi-oriented PLA films produced at industrial scale. Thus, a comparative study between corona treated (CT) and non-corona treated (NCT) PLA films was conducted.

The surface of films was studied using Attenuated Total Reflectance Fourier Infrared Spectroscopy (ATR-FTIR), X-ray Photoelectron Spectroscopy (XPS), Atomic Force Microscopy (AFM) and goniometry measurements. The structure of films was analysed with thermogravimetric analysis (TGA), differential scanning calorimetry (DSC) and uniaxial tensile analysis. The barrier properties of films to three gases (He, O_2, CO_2) were also determined.

This study unambiguously revealed that corona treatment led to modifications in both surface and bulk of PLA films. In particular, surface analysis displayed the well-known capability of corona treatment to chemically and physically modify the surface of PLA films at the nanometer scale by increasing polarity and roughness. The structural analysis displayed a slight increase in the crystallinity degree and slight modifications in mechanical properties of films. This probably originated from temperature increase associated to corona treatment, which favoured physical changes (*e.g.* relaxation, crystallization) of a part of the bi-orientated PLA chains, and therefore highlights the importance of such an industrial step on the film properties for packaging applications. As a result of these modifications, the barrier properties of films to three gases (He, O_2, CO_2) are also slightly improved.

Keywords

Poly (lactic acid) - PLA; corona treatment; surface modification; food packaging; biodegradable polymer

1 Introduction

Poly (lactic acid) or PLA is a biodegradable and renewable polymer, which is currently considered as one of the most promising candidates for replacing conventional plastics. The European Bioplastics Association recently reported that PLA global production exceeded 184 thousand tons in 2013. PLA was ranked the most produced biodegradable polymer followed by biodegradable starch blends, even if PLA production is still low compared to the production of conventional plastics (299 million tons in 2013). They also predicted that PLA production will double in 2018.[1,2] Behind this apparent success not only the ecofriendly and the biocompatibility nature of PLA play an important role, but also the interesting balance between functional properties, easy processability and reduced cost of the raw material compared to other biopolymers.[3-5]

The industrial production of PLA goods involves several steps that could be summarized as follows: lactic acid production, lactide formation, PLA polymerization and industrial processing. Lactic acid is generally produced through enzymatic hydrolysis and microbial fermentation of carbohydrates (*e.g.* starch, sucrose and glucose) derived from biomass (*e.g.* wheat, sugar beet, sugar cane or corn). Then, it is converted into its cyclic dimers L-lactide, D-lactide and meso-lactide. Specific stereocomposition of lactides are polymerized via ring opening polymerization reaction, which is the most commonly used method to produce high molecular weight PLA (> 100 MDa). The polymer is then processed with the conventional manufacturing techniques such as injection moulding, blow moulding, extrusion and thermoforming to obtain films, sheets, packaging and other goods made of PLA.[3,4,6]

A key driver of the ongoing increased interest on PLA is the relative easiness to tailor and to improve the properties of PLA according to the final application. Different strategies can be used during PLA production to modify its bulk and surface properties. On the one hand, the bulk modification strategies principally deal with mechanical, stability, crystallinity and thermal properties of PLA. Some technologies which are frequently used to modify the PLA bulk are stereochemical manipulation (*e.g.* lactide sterochemical composition), processing manipulation (*e.g.* orientation and annealing), copolymerization (*e.g.* PLA-PHA, PLA-PEG) and blending with other polymers or plasticizers. On the other hand, surface modification technologies are principally used to enhance (or to reduce) surface interactions with other materials by modifying roughness, surface chemistry and/or topography. Some technologies able to modify PLA surfaces are coatings, biomolecules entrapment, photografting, plasma treatment and corona treatment.[4,7] A combination of these technologies make possible to find different types of PLA on the market for packaging, bio medical devises textiles or 3D printing applications.

Corona treatment is a surface modification technology frequently used by the packaging industry for increasing surface tension and polarity of films in order to improve printability, wettability and adhesion properties. The

treatment consists in generating a visible electrical discharge from a linear array of electrodes over the polymer surface when applying low voltage (10 to 40 kV) at high frequency (1 to 4 kHz). The corona discharge causes partial ionization of the surrounding atmosphere and produces excited species (*e.g.* free radicals, ions or electrons). These chemical species are able to react and to oxidize the molecules exposed to the polymer surface, forming new polar functionalities such as hydroxyl, carboxyl, carbonyl and amide groups onto the surface. The resulting new functionalities have strong compatibility to hydrophilic materials and increase the adhesion with thin layers such coatings, varnishes, adhesives, membranes.[8,9] Another well-known effect of this partial ionization of the atmosphere is a physical surface nano-modification of the polymer, as consequence of an abrasion phenomenon called etching. Corona treatment could be thus considered as a simultaneous deposition/removing process of chemical species over surfaces driven by ions and radicals.[10]

To obtain polymer having good adhesion properties several factors need to be controlled such as voltage and frequency of the electromagnetic field, treatment duration time, composition of surrounding atmosphere, sample and electrode geometry. Undertreated polymer leads to insufficient generation of polar groups, resulting in poor adhesion and printability. On the contrary, overtreatment decreases the sealing properties, increases brittleness and produces pinholes or powdering of the surface. Besides these drawbacks, corona treatment technology is safe and economical. It is also suitable for treatment of blow and infection moulded materials. Moreover, it does not strongly influence the line speed and it modifies the film surface without changing its initial appearance.[8, 9]

Different types of PLA films treated by corona are currently available in the market for coatings or printing applications. However, the data relative to the impact of corona treatment on PLA film are scarce and do not generally consider industrial scale production. The objective of this research was to better understand the impact of corona treatment on the surface, structural and barrier properties of PLA films produced at industrial scale. Therefore, a comparative study between corona treated (CT) and non-corona treated (NCT) PLA films was conducted.

2 Material and methods

2.1 Samples

Corona Treated (CT) and Non-Corona Treated (NCT) PLA films, having a thickness from 17 to 20 µm, were produced in Taghleef Industries (Nativia NTSS, San Giorgio di Nogaro, Udine, Italy). During production, both films were subjected to bi-orientation and annealing to induce crystallization and to improve the film mechanical properties. Only one face of films was submitted to corona treatment (30 $W \cdot m^{-2} \cdot min^{-1}$) and that face will be called hereafter CT- treated side.

To minimize the effect of ageing on PLA film properties, samples were frozen at -30 °C and were analysed between 20 and 45 days after been produced.

2.2 Surface properties

The surface chemistry, surface topography/roughness and surface tension were evaluated using Attenuated Total Reflectance Fourier Infrared Spectroscopy (ATR-FTIR), X-ray Photoelectron Spectroscopy (XPS), Atomic Force Microscopy (AFM) and goniometry measurements respectively. These experiments focusing on surface characterization were always performed considering both sides of CT and NCT films. In case of CT films the surfaces were named CT-treated and CT-untreated; in case of NCT films the surfaces were named NCT-A and NCT-B.

2.2.1 Surface chemistry

The nature of chemical groups was first assessed by ATR-FTIR analysis (Spectrum 65, PerkinElmer, Waltham, MA, USA) using a ZnSe crystal, from 4000 to 650 cm^{-1}, with a resolution of 2 cm^{-1} and 128 scans. Analyses were done in triplicate.

The elemental composition of film surfaces was evaluated with XPS analysis. The XPS spectra were recorded with a PHI Versaprobe 5000 apparatus using monochromatic Al Kα X-ray (1486.6 eV). The average circular spot size was 200 µm of diameter. High-resolution (Pass energy = 58 eV.) 45 degrees emission angle integrated scans were acquired. Measurements were carried out at room temperature inside an ultra-high vacuum compartment (base pressure of 2.10^{-7} Pa). The use of low-energy (<10 eV) electron flood and ion gun allow to neutralize the surface charging induced by the photoelectron emission. The XPS data were calibrated according to adventitious carbon 1s line (284.8 eV).

2.2.2 Surface tension

The surface tension of films (γ_s) and its polar (γ_s^p) and dispersive (γ_s^d) components were determined using the Owens-Wendt method (Eq. 1).[11]

$$\gamma_l \cdot (1 + \cos\theta) = 2\left(\gamma_s^d \cdot \gamma_l^d\right)^{0.5} + 2\left(\gamma_s^p \cdot \gamma_l^p\right)^{0.5} \qquad (Eq.\,1)$$

Where, θ, γ_l, γ_l^d, γ_l^p are respectively the contact angle, the surface tension, the dispersive component and the polar component of the liquid tested; γ_s^p and γ_s^d are the polar and dispersive components of the surface tested. The contact angle is expressed in degrees and all the surface tension parameters are expressed in $mN{\cdot}m^{-1}$.

Five liquids (water, ethylene glycol, glycerol, formamide and diiodomethane) were used. According to Ström *et al.*[12] and Fowkes[13], their liquid polar contributions (γ_l^p) were 51.0, 16.8, 26.4, 18.7 and 0 mN·m^{-1}, while their corresponding dispersive contributions (γ_l^d) were 21.8, 30.9, 37.0, 39.5 and 50.8 mN·m^{-1}, respectively.

The contact angle measurements were carried out using the sessile drop method on a goniometer (Digidrop, GBX, Bourg de Peage, France) equipped with image analysis software (Visiodrop, version 1, GBX). Seven drops having a volume ≈ 1 µL were deposited on film surfaces for each liquid.

2.2.3 Surface topography and roughness

The surface topography and the root mean squared roughness (R_{rms}) (Eq. 2) of films were determined with Atomic Force Microscopy (Multimode 8, Bruker, Billerica, MA, USA) in tapping mode (resonance frequency of 70 kHz) from 10 µm x 10 µm images. Silicon nitride cantilevers were used (Scanasyst-Air, Bruker) with a nominal spring constant of 0.4 mN·m^{-1}. At least 3 different images were analysed for each film surface.

$$R_{rms} = \sqrt{\frac{1}{n}\sum_{i=1}^{n} Y^2(x_i)} \qquad (Eq.\,2)$$

Where, $Y(x_i)$ is the height of surface profile at position x_i and n is the number of data points.

2.3 Structural properties

The thermal and mechanical properties were analysed with thermogravimetric analysis (TGA), differential scanning calorimetry (DSC) and uniaxial tensile analysis.

2.3.1 Thermal stability

The thermal degradation of films was tested with TGA. Samples (7-9 mg) were heated from room temperature to 500 °C at 20 °C·min^{-1} using a thermogravimetric analyser (Discovery TGA, TA instruments, New Castle, DE, USA) under dry N_2 flow (40 mL·min^{-1}).

2.3.2 Thermal transitions

The thermal events related to glass transition (T_g inflection and variation of specific heat ΔC_p) and melting (T_m and enthalpy ΔH_m) of films were determined using DSC analysis. Around 5 mg of PLA films was weighed, and sealed into Tzero aluminium pans (TA instruments) before been subjected to a double heating-cooling cycle from -10 to 220 °C at 10 °C·min^{-1} under N_2 atmosphere (flow rate = 25 mL·min^{-1}), using a Q20 calorimeter (TA Instruments). The thermal properties were calculated from the first heating cycle using TA Universal Analysis 2000 software (version 4.5 A, TA instruments). The reversibility of thermal events was assessed from second cycle.

The crystallinity percentage (X_c) of films was calculated according to Eq. 3

$$X_c = \frac{\Delta H_m - \Delta H_{cc}}{\Delta H_m^\circ} \times 100 \qquad (Eq. 3)$$

Where ΔH_m (J·g^{-1}) is the enthalpy corresponding to the area under the melting peak, ΔH_m° (= 93 J·g^{-1}) [14] is the enthalpy of melting of pure crystalline PLA and ΔH_{cc} (J·g^{-1}) is the enthalpy corresponding to the area associated to cold crystallization. Since no cold crystallization was observed in the first DSC run, its value is null (ΔH_{cc}= 0 J·g^{-1}).

2.3.3 Mechanical properties

The mechanical behaviour of films was assessed by uniaxial tensile testing at room conditions (T ≈ 25 °C, RH ≈ 50 %) using a texture analyser (TA HD plus, Texture Technologies, Hamilton, MA, USA) calibrated with 2 kg mass and according to NF EN ISO 527-1 standard. [15] The initial gauge length was 10 cm, the load cell was 100 kg and the crosshead speed was 1 mm·min^{-1}. The Young modulus (E_{Young}, GPa), yield strength (σ_y, MPa), yield elongation (ε_y, %) tensile strength (σ_b, MPa) and elongation at break (ε_b, %) were determined from stress – strain curves. 7 to 12 rectangular specimens (dimensions of 15 x 2.5 cm) were tested for each condition. Samples were prepared using a precision cutter (JDC, Thwing Albert Instrument Company, West Berlin, NJ, USA). The machine and the transversal directions (MD and TD) of films were considered during analyses.

2.4 Barrier properties to gases

The permeability (P), diffusion coefficient (D) and solubility coefficient (S) of films for molecular oxygen (O_2) carbon dioxide (CO_2) and helium (He) were determined using a manometric method on a permeability testing apparatus (GDP-C permeameter, Brugger Feinmechanik GmbH, Munich, Germany) in dry conditions (0 % relative humidity, RH) at 25 °C. The permeability to the same gases was also determined in humid conditions (84 % RH) at 25 °C. The system was previously out gassed under primary vacuum. At time zero one side of the film was flushed with the gas (flow of ≈ 100 cm^3·min^{-1}) and the pressure increase was recorder over time on the other side. Permeability was determined from the steady state. The diffusion coefficient was calculated from lag time (Eq. 4) and the solubility coefficient was calculated from Eq. 5. Analyses were carried out in triplicate.

$$D = \frac{l^2}{6\vartheta} \qquad (Eq. 4)$$

$$P = D \times S \qquad (Eq. 5)$$

Where, D is the diffusion coefficient (m^2·s^{-1}), l is the thickness of the films (m), ϑ is the lag time (s), P is the measured permeability (mol·m^{-1}·s^{-1}·Pa^{-1}) and S is the solubility (mol·m^{-3}·Pa^{-1}).

2.5 Statistical analysis

Data were analysed using a student comparison test, and when required (groups >2), one–way analysis of variance (ANOVA) and Tukey-Kramer multiple comparison tests were performed. In all cases, the significance level was set to 0.05. Statistical tests were performed using GraphPad Prism software (version 5.01, GraphPad Software Inc., La Jolla, CA, USA).

3 Results and discussion

3.1 Surface properties

Findings in this section evidenced the capability of corona treatment to chemically and physically change the surface of PLA at the nanometer scale. All data related to surface properties are given in Table 1.

Table 1. *Surface properties of both sides of non-corona treated (NCT-A, NCT-B) and corona treated films (CT-untreated, CT-treated). Values are expressed as average ± S.D. Significant differences (p. value < 0.05) are indicated with different letters in the same column. C = carbon, O = oxygen, Rrms = root mean squared roughness, Θ = contact angle, γ_s = surface tension of the film tested, γ_s^p = polar contribution, and γ_s^d = dispersive contribution.*

Film surface	Elemental composition[1] (atomic %)			Roughness[2] (nm)	Water contact angle[3] (°)	Surface tension[4] (mN·m^{-1})		
	C	O	O/C	R_{rms}	Θ	γ_s^p	γ_s^d	γ_s
NCT-A	-	-	-	3.8 ± 0.4[a]	79.7 ± 1.8[a]	4.8	27.7	32.5
NCT-B	-	-	-	3.6 ± 1.1[a]	81.2 ± 1.6[a]	4.1	28.3	32.4
CT-untreated	73	27	0.37	2.3 ± 0.9[a]	75.2 ± 2.1[b]	6.0	28.6	34.6
CT-treated	68	32	0.47	7.4 ± 1.7[b]	70.8 ± 0.5[c]	7.0	32.2	39.2

[1]Determined by XPS analysis
[2] Determined by AFM analysis
[3]Determined by goniometry analysis
[4]Determined using the Owens-Wendt method

3.1.1 Surface chemistry

The ATR-FTIR spectra of NTC and CT film surfaces allowed us to detect the typical vibration bands of PLA, as already observed in different studies.[16-20] In particular, -C=O stretching (≈1752 cm^{-1}), -CH_3 bending (≈ 1453 cm^{-1}), -C=O bending (≈ 1270 cm^{-1}), -C-O-C stretching (≈ 1185 cm^{-1}), -C-O- stretching (≈ 1130 and ≈ 1088 cm^{-1}), -OH bending (≈ 1046 cm^{-1}), -C-C- stretching attributed to amorphous and crystalline phases (≈ 863 and ≈ 758 cm^{-1}, respectively). From these peaks, we did not observed shifts, or change of relative intensities (reference peak was the vibration C=O at 1752 cm^{-1}) between the 4 surfaces tested (Figure 1). This is most likely due to the penetration depth of the infra-red electromagnetic radiation for several micrometres into film bulk, which may therefore give a global response and not a local analysis at the scale of the first chemical groups on the surface.

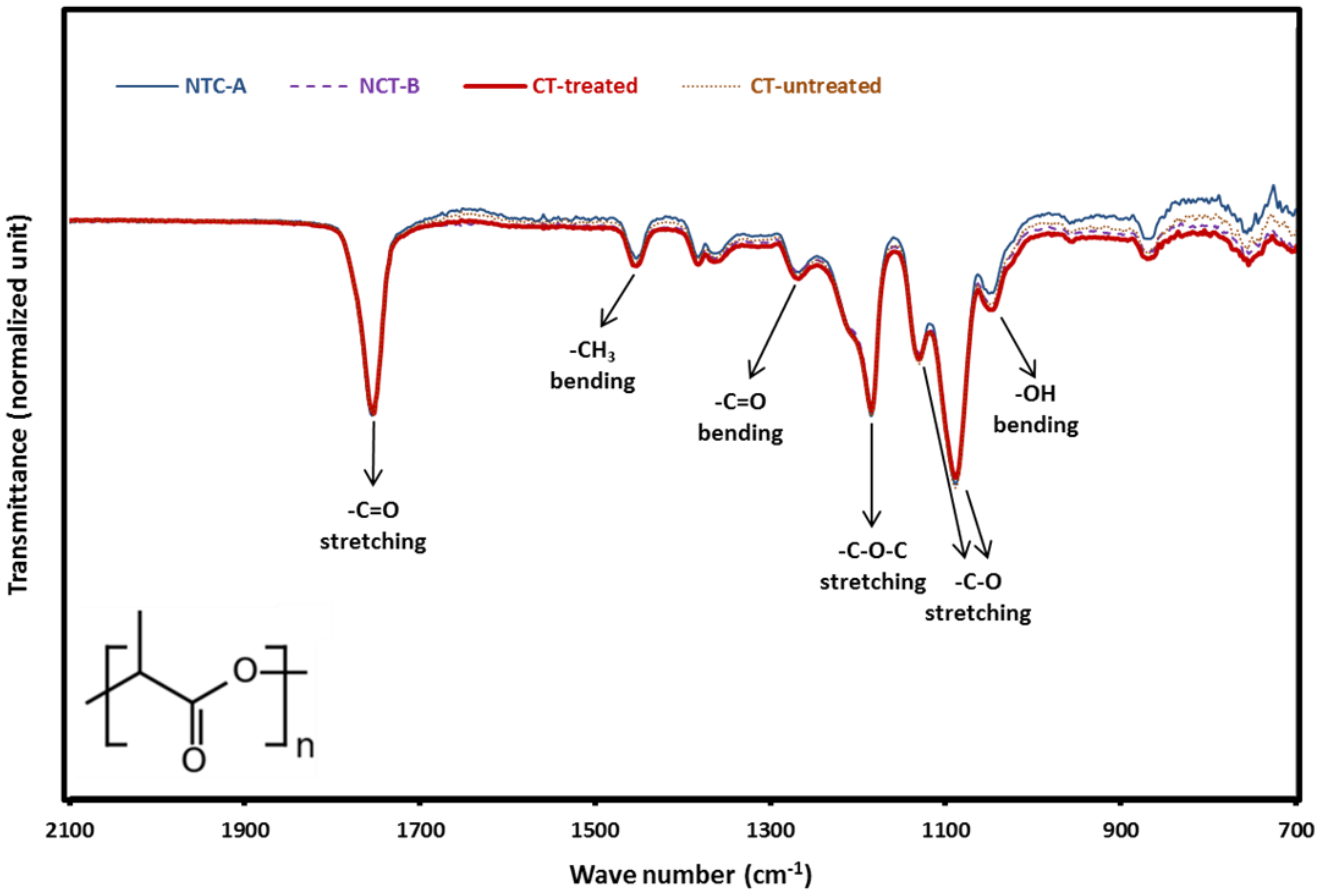

Figure 1. *ATR-FTIR spectra of both sides of non-corona treated (NCT-A, NCT-B) and corona treated films (CT-untreated, CT-treated).*

On the contrary, XPS analysis is a sensitive technique able to identify the elemental composition of the very top nanolayers (< 10 nm). It revealed slight differences on film surfaces (Table 1). In particular, there was an increase in the O/C ratio of about 10 % when the PLA surface was treated with corona. Similar increase was also observed in previous studies, which involved air or atmospheric plasma treatments in PLA.[21-24] Both findings and literature hence give evidence that new oxygen-contained groups were created onto the surface during the corona treatment.

3.1.2 Surface topography and roughness

AFM analysis revealed that the corona treatment also modified the topography of PLA films (Figure 2).

In particular, the roughness of the treated surface significantly increased of about 100 % (Table 1). This clearly shows the ability of corona treatment to physically change the surface of PLA films. Similar findings were also observed in studies involving plasma treatments with different gases such as air,[18,22,25-27] O_2,[28] N_2,[22] Ar,[22] Ar-N_2-O_2 mixtures,[29] SF_6,[17] and CF_4[30]. The main mechanism behind the physical nano-modification is a surface

abrasion phenomena called etching, which impact depends on the treatment conditions such as gas used, treatment time, power, electrode distance and number of cycles.[17,18,22,25,27-30] A real challenge for researches and industries is therefore to better understand and to better control this physical phenomena for increasing in a controlled way the interfacial structure of PLA, which could favour or reduce the adhesion of hydrophilic coatings as well as the interactions with the surrounding area (*e.g.* interfacial diffusion of biomolecules). This is of particular interest in active/intelligent food packaging development.

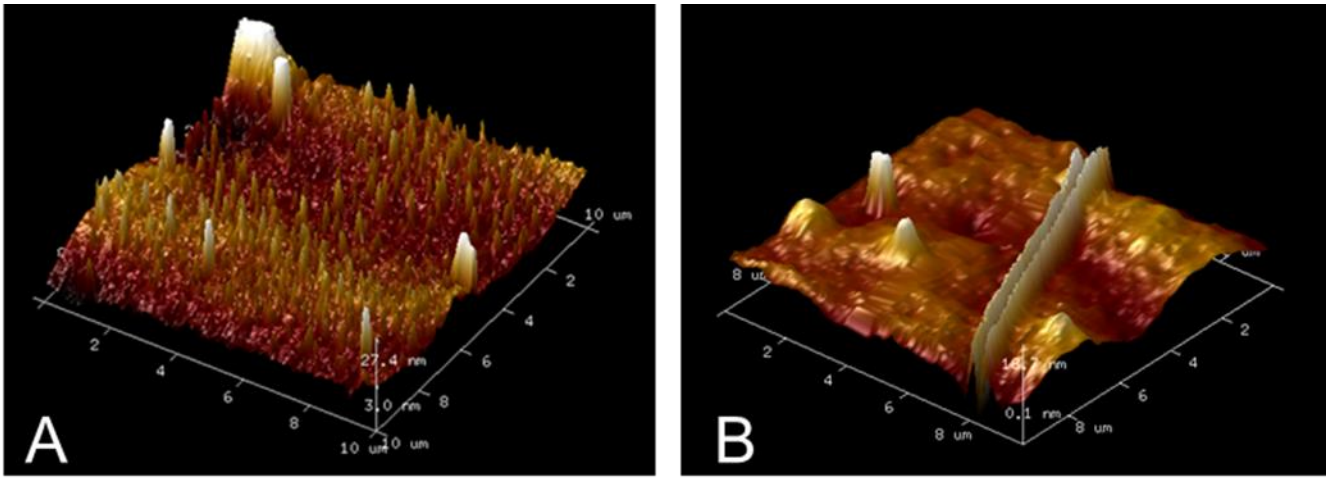

Figure 2. *Surface topography of treated (A) and untreated surface (B) of corona treated PLA films analysed by atomic force microscopy.*

3.1.3 Surface tension

CT-treated surface displayed the lowest contact angle for all the liquid tested compared to the other surfaces. NCT surfaces showed higher values. When surface tension was calculated, this trend was also followed. As a result, the corona treatment was found to increase the polar contribution as well as the dispersive component by ≈ 59 % and ≈ 15 % respectively, with an overall surface tension increase of ≈ 21 % (Table 1). These results are in line with previous XPS findings and are also in accordance with other studies,[18,29,31] showing an increase in the polar contribution as a main consequence of polar groups formation induced by plasma/corona treatments. However, contact angle measurement is known to be affected not only by surface chemistry but also by surface topography and roughness.[32] In this study, topography/roughness could favoured spreading of nonpolar liquids (as diiodomethane) on the treated surface, even if more polar groups were present compared to the other surfaces.

An intermediate behaviour of CT-untreated surface compared to the other surfaces was also noticed. In particular, water contact angle and surface tension revealed a higher affinity to polar compounds than NCT surfaces but lower than CT-treated surface in such surface. A possible explanation of this behaviour can be

found in the rolling step after PLA production, which could induce a partial polarization of the CT-untreated surface as a result of the physical contact with the CT-treated surface.

3.2 Structural properties

Corona treatments as other plasma technologies are believed not to impact the bulk properties of the treated material.[9,18,33] In this study, however, the structural findings indicated that corona treatment lead to physical modifications in PLA bulk properties.

3.2.1 Thermal stability

Both NCT and CT films displayed a one-step mass loss from 300 to 410 °C and no differences in the thermal degradation was detected in that range. Indeed, neither loss mass curves nor derivative loss mass curves displayed any significant shift between the CT and NCT films. When polymer degradation or crosslinking occurs, the thermal stability is usually modified because of polymer chain length changes. This suggests that corona treatment did not induce chemical reactions such as polymerization, crosslinking or chain degradation, in accordance with ATR-FTIR analyses.

3.2.2 Thermal transitions

The thermal events were evaluated in the temperature range from -10 to 220 °C by DSC analysis. The first heat scan analysis was considered in order to take into account the corona treatment effect, and to evaluate the effective conditions of PLA films after their production stage. Figure 3 shows the characteristic DSC curves of NCT and CT films and Table 2 reports the corresponding values of related thermal events.

Films showed some similarities and some differences during DSC analysis. In particular, both films displayed the characteristic thermal transitions of semi-crystalline materials, such as glass transition and melting of crystals (not associated to cold crystallization), which indicated the existence of amorphous and crystalline phases in both polymer structures. Additionally, the behaviour of both films could be considered analogous up to the onset of glass transition (≈ 60 °C), since no thermal events were detected at lower temperatures, and no significant differences were found between their corresponding T_g (inflection point) and ΔCp. These findings were in line with other studies and evidenced that corona treatment did not highly influence the glass transition of PLA.[26, 29, 30]

On the other hand, differences in thermal events were noticeable after glass transition. NCT films were characterized by a broad endothermic event, similar to a relaxation peak, which could be ascribed to the melting of an organized area of PLA. Literature proposes that such organized area is a result of PLA chains ordering induced by biaxial orientation during film processing. It has been found that the stretching conditions, such as temperature, time, draw ratio, stretching rate and stretching mode (*e.g.* sequential or simultaneous, uniaxial or biaxial) influence the shape and the position of such endothermic event.[34-38] CT films did not display such broad event, but they were characterized by an amplified pre-melting peak compared to NCT, which

significant increased their crystallinity degree from 24.0 to 27.4 %. A reasonable explanation of this effect could originate in the rapid temperature increase induced by the corona discharge, which could allow the PLA bi-orientated chains to relax and for a part of them to fast crystallize with a non-perfect crystal configuration. As displayed by Jorda-Vilaplana,[39] a temperature increase up to 70 – 130 °C of the PLA film surface near to the electrodes was measured on line by a thermal imaging camera, during air atmospheric corona treatment. This recent work tends to confirm our hypothesis.

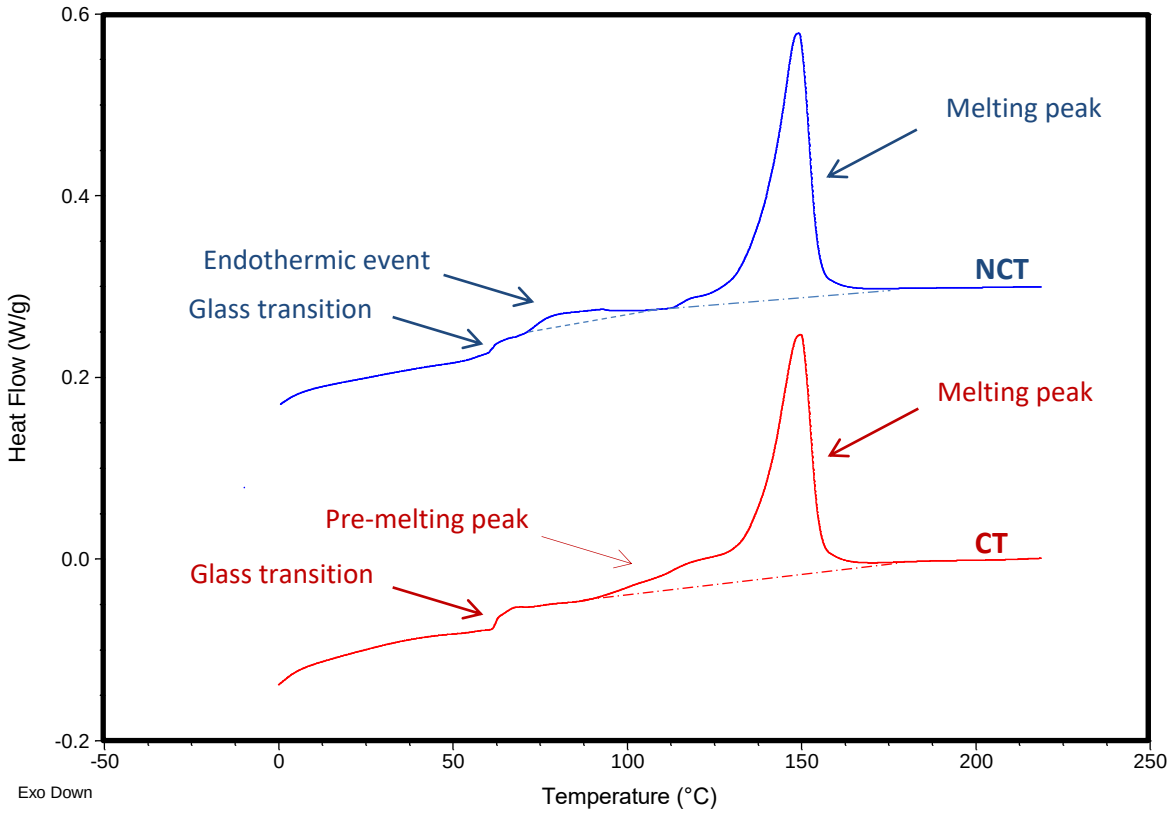

Figure 3. *DSC curves (first heating) of non-corona treated (NCT) and corona treated (CT) films.*

Table 2. *Crystallinity and thermal parameters related to glass transition and melting of non-corona treated (NCT) and corona treated (CT) films. Values are expressed as average ± S.D. Significant differences (p. value < 0.05) are indicated with different letters in the same column. T_g onset = onset temperature of glass transition, T_g inflection = inflection temperature of glass transition, ΔC_p = variation of specific heat, T_m = melting temperature, ΔH_m = enthalpy of melting peak, and X_c = crystallinity percentage.*

Film	Glass transition			Melting		Crystallinity
	T_g onset (°C)	T_g inflection (°C)	ΔC_p [§] ($J \cdot g^{-1} \cdot °C^{-1}$)	T_m (°C)	ΔH_m ($J \cdot g^{-1}$)	X_c (%)
NCT	59.2 ± 0.8[a]	61.1 ± 0.5[a]	0.14 ± 0.01[a]	149.3 ± 0.2[a]	22.3 ± 0.6[a]	24.0 ± 0.7[a]
CT	61.0 ± 0.3[b]	61.9 ± 0.3[a]	0.16 ± 0.03[a]	149.6 ± 0.1[a]	25.5 ± 0.4[b]	27.4 ± 0.4[b]

[§] corrected according to the amorphous phase.

3.2.3 Mechanical properties

Table 3 reports the Young modulus (E_{Young}), yield strength (σ_y), yield elongation (ε_y), tensile strength (σ_b) and elongation at break (ε_b) of NCT and CT films in both directions (Machine Direction, MD and Transversal Direction, TD).

Table 3. *Mechanical properties of non-corona treated (NCT) and corona treated (CT) films in the machine direction (MD) and transversal direction (TD).Values are expressed as average ± S.D. Significant differences (p. value < 0.05) at the same orientation condition are indicated with different letters in the same column. Young modulus (E_{Young}), yield strength (σ_y), yield elongation (ε_y) tensile strength (σ_b) and elongation at break (ε_b).*

Orientation	Film	E_{Young}	Yield point		Break point	
			σ_y	ε_y	σ_b	ε_b
		(GPa)	(MPa)	(%)	(MPa)	(%)
MD	NCT	3.0 ± 0.2^{a}	69.1 ± 0.1^{a}	3.2 ± 0.3^{a}	65.9 ± 0.5^{a}	126.3 ± 14.6^{a}
	CT	2.9 ± 0.1^{a}	66.0 ± 0.3^{b}	2.9 ± 0.3^{b}	57.1 ± 0.4^{b}	113.4 ± 46.5^{a}
TD	NCT	4.1 ± 0.2^{x}	73.2 ± 0.2^{x}	2.5 ± 0.2^{x}	92.9 ± 0.8^{x}	49.6 ± 7.7^{y}
	CT	4.0 ± 0.1^{x}	72.9 ± 0.2^{x}	2.3 ± 0.1^{y}	92.2 ± 0.7^{x}	71.8 ± 8.0^{x}

When mechanical properties were compared considering the direction tested, findings showed a clear anisotropy behaviour of films, indicating that the orientation of PLA chains and crystals was not equal in both directions. The MD of films showed lower Young modulus, lower stress values and higher elongation values at yield and break points compared to TD.

Bi-orientation of PLA films is an effective strategy used by industries to increase the tensile stress, elongation at break and elastic modulus of PLA films. It has been reported an increase of tensile strength from 50-60 to 100-200 MPa, elongation at break from 10 to 50 – 150 % and Young modulus from 2.5 to 3.3 GPa of semi-crystalline PLLA films after been biaxially orientated.[40] A recent study has suggested that such mechanical improvement is principally due to a formation of orientated nano-crystallinities (≈ 10 nm) in the polymer matrix, induced by high stretching rate and high draw ratio.[41] The bi-orientation step involves a biaxial stretching of films from 2 to 6 times in the machine direction (MD) and transverse direction (TD) at temperatures between T_g and T_m.[40] These conditions favour the development of an organized structure of PLA chains having enough mobility to crystallize, which drastically improve the PLA crystallization capability in terms of crystal content and kinetics.[42] Slight but significant differences were found in the mechanical parameters of NCT and CT films. Usually, the increase of polymer crystallinity induces a decrease of elongation at break, and an increase of Young modulus, yield strength and tensile strength. However, we observed an opposite effect in CT films even if DSC analysis revealed an increase of crystallinity. When the MD orientation was considered, an evident decrease in σ_y and σ_b was shown in such films. In a similar way when the TD orientation was considered, a significant increase in ε_b was evidenced after corona treatment. Based on these considerations, it appeared that the temperature

increase associated to corona treatment hindered the effects of bi-orientation, probably as a result of modifications on the organized structure of PLA and/or on the nano-crystallinities developed during bio-orientation. These changes in the bi-oriented structure are predominant on mechanical properties compared to the effect of crystallinity change.

3.3 Barrier properties to gases

The permeability of NCT and CT films to He, O_2 and CO_2 at two relative humidity conditions are reported in Figure 4 and in Table 4. Barrier properties of PLA films were slightly but statistically improved after corona treatment. No matter which gas or which relative condition was tested, all permeability values for CT films were significant lower than NCT films.

The reduction of He, O_2 and CO_2 permeability in dry conditions was around 6, 12 and 18 %, and it appeared to be higher in wet condition, around 15, 20 and 24 %, respectively. As previously evidenced, the increase in the crystallinity degree and the increase in surface polarity of bi-orientated PLA films as a consequence of corona treatment may affect the transport properties of the material.

The gas permeability order was as follows: He > CO_2 > O_2. He permeability was greater of one order of magnitude compared to the other two gases, while CO_2 permeability was around 3 times higher than O_2, even if the molecular weight of the former is higher than the latter. When diffusion (*D*) and solubility (*S*) coefficients were calculated (Tab. 5), only *D* followed the molecular weight trend (He > O_2 > CO_2), highlighting the importance of the solubility parameter and therefore of the compatibility between permeant and polymer, in particular considering the permeation of CO_2, which had the higher value.

The importance of affinity between permeant and polymer was also noticed when *D* and *S* of NCT and CT were compared. A decrease in solubility values associated to an unexpected increase of *D* values in corona treated films was observed although the crystallinity degree was higher. It seems therefore that the affinity of gases with PLA (all of them having a null net dipole) decreased as a consequence of the higher polarity.

Table 4. *Permeability (P) in dry and wet conditions (0 and 84 % RH) and diffusion (D) and solubility (S) coefficients of non-corona treated (NCT) and corona treated (CT) films of He, CO_2 and O_2 at 25 °C. Values are expressed as average ± S.D. Significant differences (p. value < 0.05) are indicated with different letters in the same column.*

Film	RH (%)	*P* (10^{-17} mol·m^{-1}·s^{-1}·Pa^{-1})			*D* (10^{-13} m^2·s^{-1})			*S* (10^{-5} mol·m^{-3}·Pa^{-1})		
		He	O_2	CO_2	He	O_2	CO_2	He	O_2	CO_2
NCT	0	358.3 ± 7.5^{a}	11.2 ± 0.2^{a}	34.8 ± 0.4^{a}	147.0 ± 12.8^{a}	22.4 ± 2.1^{a}	6.1 ± 0.1^{a}	24.6 ± 1.9^{a}	5.1 ± 0.5^{a}	57.3 ± 0.8^{a}
	84	364.3 ± 7.5^{a}	11.3 ± 0.3^{a}	39.3 ± 0.5^{b}	-	-	-	-	-	-
CT	0	338.7 ± 6.0^{ab}	9.8 ± 0.2^{b}	28.6 ± 0.4^{c}	183.7 ± 18.8^{b}	29.2 ± 3.0^{b}	5.4 ± 0.1^{b}	18.6 ± 1.8^{b}	3.4 ± 0.4^{b}	52.5 ± 1.6^{b}
	84	310.0 ± 19.1^{b}	9.1 ± 0.3^{c}	29.8 ± 0.9^{c}	-	-	-	-	-	-

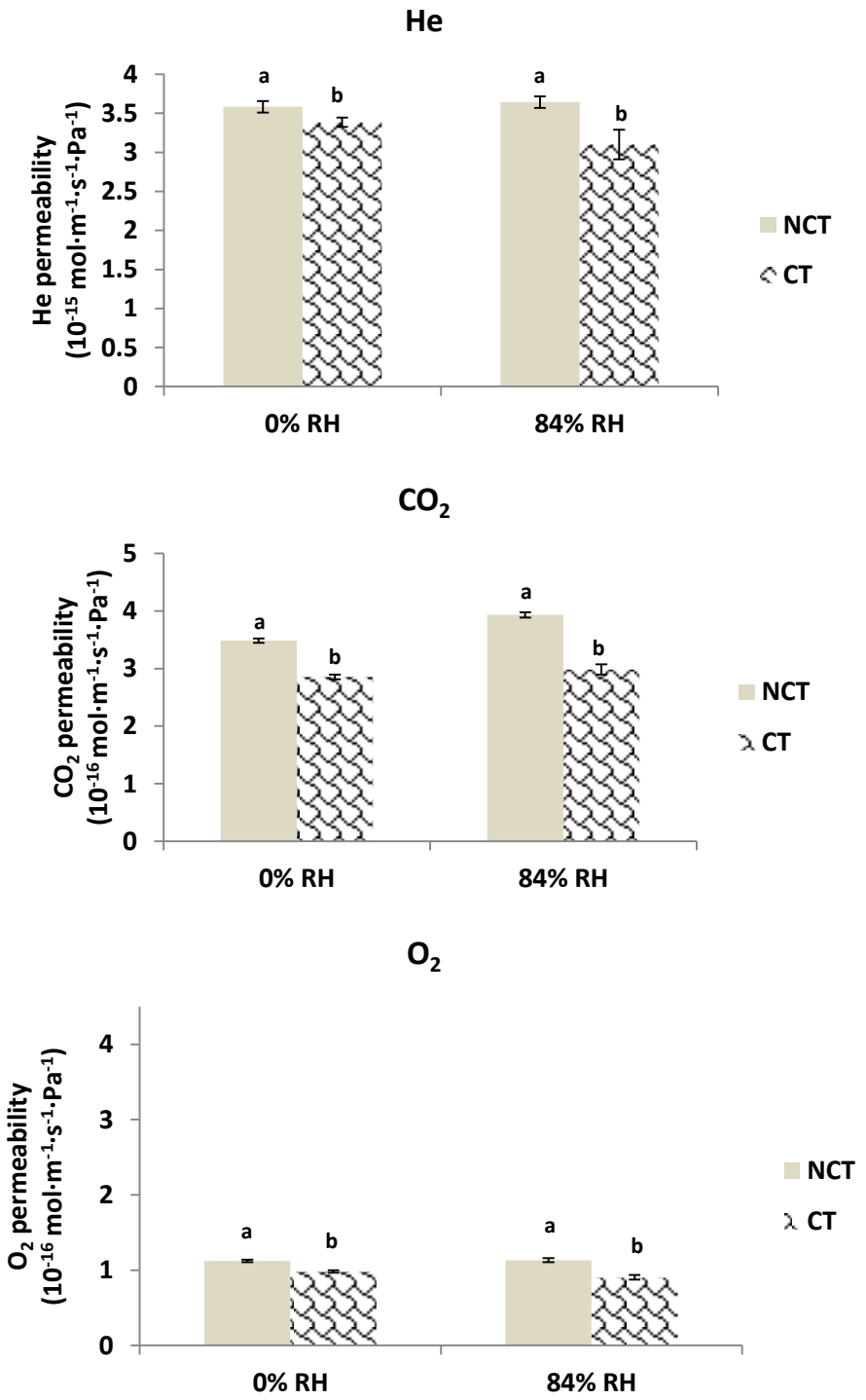

Figure 4. *Permeability of non-corona treated (NCT) and corona treated (CT) films to He, CO_2 and O_2 in dry (0 % RH) and wet conditions (84 % RH) at 25 °C. Significant differences (p. value < 0.05) at the same humidity conditions are indicated with different letters*

4 Conclusions

This study unambiguously showed, and in agreement with literature, that corona treatment was able to physically and chemically modify the surface of PLA films at nanometer scale. In particular, AFM revealed that the treatment modified the topography of PLA films by increasing the roughness at nanoscale. XPS analysis displayed a slight increase of O elemental composition on the surface submitted to corona treatment, indicating that oxygen-containing polar groups were formed during treatment. Surface tension and goniometry analyses were in line with XPS and evidenced an increase on the surface polarity of films as a consequence of the new polar functionalities induced by corona treatment.

On the other hand, it is frequently reported that corona and air plasma treatments do not modify the bulk of PLA films. However, this study clearly showed that modifications were not limited to the surface but also impacted the bulk of PLA films. Structural analyses revealed an increase of crystallinity degree, which was able to induce some small changes the mechanical behaviour of PLA films. The most reasonable cause behind this physical modification was found on temperature increase ($>T_g$) associated to corona treatment by promoting physical changes (*e.g.* relaxation, crystallization and crystal grow) of a pre-organized structure as biaxial orientated PLA chains. Bi-orientation step represent a crucial technology for packaging industries to enhance functional properties of PLA films (such as barrier and mechanical) by improving the PLA crystallization capability, and consequently it should be considered when studying modifications of PLA film properties for packaging purposes. Most of the PLA samples analysed in previous studies were produced at lab scale and did not include such step, and probably it is the most significant reason of no reported bulk modification of PLA films after been treated by corona or air plasma.

The barrier properties were slightly improved by the corona treatment as a result of both surface and bulk modification. Findings suggested that increased crystallinity and especially the increased polarity were the responsible of the improvement. It could be interesting to understand in further studies how much the increase of polarity could affect the barrier properties of PLA.

It is important to highlight that these modifications, even if gave evidence of structural and surface changes, were not strong enough to influence the barrier and mechanical performances of PLA films from a practical point of view. However, it could be important to understand if these modifications could have an impact on the PLA stability during time.

Corona treatment is a necessary strategy to coat PLA with more hydrophilic biobased polymers. Indeed, coating layers of wheat gluten, chitosan or gelatine may improve PLA gas barrier properties such as O_2 and CO_2. Improved PLA gas barrier properties could make this material suitable for new packaging applications, such as modified atmosphere packaging (MAP) of fresh foods, reduction of aroma absorption or loss from flavoured foods, etc. Lastly, the results of this study also suggested that a combination of both technologies bi-

orientation and corona treatment could have an additive or synergic impact on the functional properties of PLA films, which could be of industrial interest to deeply understand.

Acknowledgements

The authors acknowledge the European Social Found – Friuli Venezia Giulia Region – Operational Program 2007/2013 for supporting this project (Regional code: FP1340303009), the RMB plateau of UMR PAM for mechanical, goniometry and thermal analyses and Marie Laure Leonard for TGA analysis.

References

1. European Bioplastics Association. Global production capacities of bioplastics 2013 (by material type). http://en.european-bioplastics.org/market/market-development/production-capacity/. Retrieved on 06/30/2015.

2. Plastics Europe Association. Plastics: The Facts 2014/2015. http://www.plasticseurope.org/Document/plastics-the-facts-20142015.aspx?FolID=2. Retrieved on 07/22/2015.

3. Auras, R.; Harte, B.; Selke, S. An overview of polylactides as packaging materials. *Macromolecular Bioscience* **2004,** *4* (9), 835-864.

4. Rasal, R. M.; Janorkar, A. V.; Hirt, D. E. Poly(lactic acid) modifications. *Progress in Polymer Science* **2010,** *35* (3), 338-356.

5. Fabra, M. J.; Busolo, M. A.; Lopez-Rubio, A.; Lagaron, J. M. Nanostructured biolayers in food packaging. *Trends in Food Science & Technology* **2013,** *31* (1), 79-87.

6. Jamshidian, M.; Tehrany, E. A.; Imran, M.; Jacquot, M.; Desobry, S. Poly-lactic acid: production, applications, nanocomposites, and release studies. *Comprehensive Reviews in Food Science and Food Safety* **2010,** *9* (5), 552-571.

7. Wang, S. G.; Cui, W. J.; Bei, J. Z. Bulk and surface modifications of polylactide. *Analytical and Bioanalytical Chemistry* **2005,** *381* (3), 547-556.

8. Kurek, M.; Debeaufort, F., Surface modification of packaging films by coatings with bioactive compounds and biopolymers. In *Bioactive packaging of foods: quality and safety issues* Kontominas, M., Ed. Destech Publications: 2015.

9. Ozdemir, M.; Yurteri, C. U.; Sadikoglu, H. Physical polymer surface modification methods and applications in food packaging polymers. *Critical Reviews in Food Science and Nutrition* **1999,** *39* (5), 457-477.

10. Pankaj, S. K.; Bueno-Ferrer, C.; Misra, N. N.; Milosavljevic, V.; O'Donnell, C. P.; Bourke, P.; Keener, K. M.; Cullen, P. J. Applications of cold plasma technology in food packaging. *Trends in Food Science & Technology* **2014,** *35* (1), 5-17.

11. Owens, D. K.; Wendt, R. C. Estimation of the surface free energy of polymers. *Journal of Applied Polymer Science* **1969,** *13* (8), 1741-1747.

12. Ström, G.; Fredriksson, M.; Stenius, P. Contact angles, work of adhesion, and interfacial tensions at a dissolving hydrocarbon surface. *Journal of Colloid and Interface Science* **1987,** *119* (2), 352-361.

13. Fowkes, F. M. Attractive forces at interfaces. *Industrial and Engineering Chemistry* **1964,** *56* (12), 40-52.

14. Fischer, E. W.; Sterzel, H. J.; Wegner, G. Investigation of the structure of solution grown crystals of lactide copolymers by means of chemical reactions. *Kolloid-Zeitschrift and Zeitschrift fur polymere* **1973,** *251*, 980-990.

15. International Organization for Standardization (ISO). Plastiques 2012. Détermination des propriétés en traction. Partie 1: Principes généraux NF EN ISO 527-1.

16. Molinaro, S.; Romero, M. C.; Boaro, M.; Sensidoni, A.; Lagazio, C.; Morris, M.; Kerry, J. Effect of nanoclay-type and PLA optical purity on the characteristics of PLA-based nanocomposite films. *Journal of Food Engineering* **2013,** *117* (1), 113-123.

17 Chaiwong, C.; Rachtanapun, P.; Wongchaiya, P.; Auras, R.; Boonyawan, D. Effect of plasma treatment on hydrophobicity and barrier property of polylactic acid. *Surface & Coatings Technology* **2010,** *204* (18-19), 2933-2939.

18. Jorda-Vilaplana, A.; Fombuena, V.; Garcia-Garcia, D.; Samper, M. D.; Sanchez-Nacher, L. Surface modification of polylactic acid (PLA) by air atmospheric plasma treatment. *European Polymer Journal* **2014,** *58*, 23-33.

19. Bitinis, N.; Verdejo, R.; Bras, J.; Fortunati, E.; Kenny, J. M.; Torre, L.; Lopez-Manchado, M. A. Poly(lactic acid)/natural rubber/cellulose nanocrystal bionanocomposites Part I. Processing and morphology. *Carbohydrate Polymers* **2013,** *96* (2), 611-20.

20. Goncalves, C. M. B.; Coutinho, J. A. P.; Marrucho, I. M., Optical properties. In *Poly(lactic acid): synthesis, structures, properties, processing, and applications*; Auras, R.; Lim, L.-T.; Selke, S. E. M.; Tsuji, H., Eds.; Wiley: Hoboken, N.J., 2010.

21. Morent, R.; De Geyter, N.; Trentesaux, M.; Gengembre, L.; Dubruel, P.; Leys, C.; Payen, E. Influence of discharge atmosphere on the ageing behaviour of plasma-treated polylactic acid. *Plasma Chemistry and Plasma Processing* **2010,** *30* (4), 525-536.

22. De Geyter, N.; Morent, R.; Desmet, T.; Trentesaux, M.; Gengembre, L.; Dubruel, P.; Leys, C.; Payen, E. Plasma modification of polylactic acid in a medium pressure DBD. *Surface & Coatings Technology* **2010,** *204* (20), 3272-3279.

23. De Geyter, N. Influence of dielectric barrier discharge atmosphere on polylactic acid (PLA) surface modification. *Surface & Coatings Technology* **2013,** *214*, 69-76.

24. Reno, F.; D'Angelo, D.; Gottardi, G.; Rizzi, M.; Aragno, D.; Piacenza, G.; Cartasegna, F.; Biasizzo, M.; Trotta, F.; Cannas, M. Atmospheric pressure plasma surface modification of poly(D,L-lactic acid) increases fibroblast, osteoblast and keratinocyte adhesion and proliferation. *Plasma Processes and Polymers* **2012,** *9* (5), 491-502.

25. Liu, H. Z.; Cui, N. Y.; Brown, N. M. D.; Meenan, B. J. Effects of DBD plasma operating parameters on the polymer surface modification. *Surface & Coatings Technology* **2004,** *185* (2-3), 311-320.

26. Pankaj, S. K.; Bueno-Ferrer, C.; Misra, N. N.; O'Neill, L.; Jimenez, A.; Bourke, P.; Cullen, P. J. Characterization of polylactic acid films for food packaging as affected by dielectric barrier discharge atmospheric plasma. *Innovative Food Science & Emerging Technologies* **2014,** *21*, 107-113.

27. Teraoka, F.; Nakagawa, M.; Hara, M. Surface modification of poly(L-lactide) by atmospheric pressure plasma treatment and cell response. *Dental Materials Journal* **2006,** *25* (3), 560-565.

28. Armentano, I.; Ciapetti, G.; Pennacchi, M.; Dottori, M.; Devescovi, V.; Granchi, D.; Baldini, N.; Olalde, B.; Jurado, M. J.; Alava, J. I. M.; Kenny, J. M. Role of PLLA plasma surface modification in the interaction with human marrow stromal cells. *Journal of Applied Polymer Science* **2009,** *114* (6), 3602-3611.

29. Chichti, E.; Henrion, G.; Cleymand, F.; Jamshidian, M.; Linder, M.; Arab-Tehrany, E. Effects of Ar-N_2-O_2 microwave plasma on poly-L-lactic acid thin films designed for tissue engineering. *Plasma Processes and Polymers* **2013,** *10* (6), 535-543.

30. Mattioli, S.; Kenny, J. M.; Armentano, I. Plasma surface modification of porous PLLA films: analysis of surface properties and in vitro hydrolytic degradation. *Journal of Applied Polymer Science* **2012,** *125*, E239-E247.

31. Sarapirom, S.; Yu, L. D.; Boonyawan, D.; Chaiwong, C. Effect of surface modification of poly(lactic acid) by low-pressure ammonia plasma on adsorption of human serum albumin. *Applied Surface Science* **2014,** *310*, 42-50.

32. Karbowiak, T.; Debeaufort, F.; Voilley, A. Importance of surface tension characterization for food, pharmaceutical and packaging products: a review. *Critical Reviews in Food Science and Nutrition* **2006,** *46* (5), 391-407.

33. Armentano, I.; Dottori, M.; Fortunati, E.; Mattioli, S.; Kenny, J. M. Biodegradable polymer matrix nanocomposites for tissue engineering: a review. *Polymer Degradation and Stability* **2010,** *95* (11), 2126-2146.

34. Delpouve, N.; Stoclet, G.; Saiter, A.; Dargent, E.; Marais, S. Water barrier properties in biaxially drawn poly(lactic acid) films. *Journal of Physical Chemistry B* **2012,** *116* (15), 4615-4625.

35. Ou, X.; Cakmak, M. Comparative study on development of structural hierarchy in constrained annealed simultaneous and sequential biaxially stretched polylactic acid films. *Polymer* **2010,** *51* (3), 783-792.

36. Stoclet, G.; Seguela, R.; Lefebvre, J. M.; Elkoun, S.; Vanmansart, C. Strain-induced molecular ordering in polylactide upon uniaxial stretching. *Macromolecules* **2010,** *43* (3), 1488-1498.

37. Wang, Y.; Li, M.; Wang, K.; Shao, C.; Li, Q.; Shen, C. Unusual structural evolution of poly(lactic acid) upon annealing in the presence of an initially oriented mesophase. *Soft Matter* **2014,** *10* (10), 1512-1518.

38. Ou, X.; Cakmak, M. Influence of biaxial stretching mode on the crystalline texture in polylactic acid films. *Polymer* **2008,** *49* (24), 5344-5352.

39. Jorda-Vilaplana, A. Optimización de las propiedades de uniones adhesivas de polímeros biodegradables de ácido poliláctico (PLA) con adhesivos de carácter natural mediante el empleo de tecnologías de plasma atmosférico. Universitat Politècnica de València, 2013. PhD thesis.

40. Perego, G.; Cella, G. D., Mechanical properties. In *Poly(lactic acid): synthesis, structures, properties, processing, and applications*; Auras, R.; Lim, L.-T.; Selke, S. E. M.; Tsuji, H., Eds.; Wiley: Hoboken, N.J., 2010.

41. Jariyasakoolroj, P.; Tashiro, K.; Wang, H.; Yamamoto, H.; Chinsirikul, W.; Kerddonfag, N.; Chirachanchai, S. Isotropically small crystalline lamellae induced by high biaxial-stretching rate as a key microstructure for super-tough polylactide film. *Polymer* **2015,** *68*, 234-245.

42. Stoclet, G.; Seguela, R.; Lefebvre, J. M.; Rochas, C. New insights on the strain-induced mesophase of poly(D,L-lactide): in situ WAXS and DSC study of the thermo-mechanical stability. *Macromolecules* **2010,** *43* (17), 7228-7237.

Effect of lipid incorporation on functional properties of wheat gluten based edible films

Rocca-Smith, J. R.; Marcuzzo, E.; Karbowiak, T.; Centa, J.; Giacometti, M.; Scapin, F.; Venir, E.; Sensidoni, A.; Debeaufort, F. Effect of lipid incorporation on functional properties of wheat gluten based edible films. *Journal of Cereal Science* 2016, *69*, 275-282.

Abstract

Wheat gluten is an inexpensive protein derived from mill industries with good film forming properties, which allows producing semipermeable membranes able to slow down water migration in foods.

The first objective of this study was to evaluate the effects of the incorporation of a lipid phase (25 wt%, dry basis) in wheat gluten on the functional properties of the film, such water sorption, surface hydrophilicity, water barrier properties, mechanical properties and thermal properties. The second one was to asses if such incorporation was able to reduce the water sensitivity of film mechanical properties.

Findings clearly showed that the incorporation of a lipid phase was able to decrease the water sorption, water affinity (hydrophilicity) and water transfer (≈ 2 times) of wheat gluten films. Moreover, mechanical properties are also affected by the lipid addition with a decrease in rigidity and, at high a_w, an increase in extensibility. However, the sensitivity of the mechanical properties to water was not modified. Lastly, DSC (Differential Scanning Calorimetry) analysis proved that changes in mechanical properties of films as a function of hydration state were the consequence of glass transition depletion, which allowed them to turn from a glassy-like behaviour to a rubber-like behaviour.

Keywords

Wheat gluten-lipid edible films; water barrier properties; glass transition; water plasticization

1 Introduction

Wheat crop ranked the first agricultural commodity in Europe in 2013, and the fourth in the world, with a world production of ≈ 716 million tons, after sugar cane, maize and rice.[1] This large production covers the large amount of the wheat-based foods available and consumed by humans such as baked goods, pasta, snacks and breakfast products. One of the most significant reasons behind this success lies on the functional properties of the gluten-forming proteins (gliadins and glutenins) contained in wheat endosperm. Gliadins and glutenins are able to interact and to form a protein network (wheat gluten) as in dough making, which provides the essential viscoelastic properties for producing most of the wheat based foods consumed by humans.[2] Depending on the quantity of wheat gluten bought, purity and supplier, the wheat gluten price varies from 0.5 to 2 dollars per kilogram. Wheat gluten is no more a co-product of the mill industry but it is now produced at large scale from wheat starch. It takes advantage of its functional properties, which are of industrial importance for food and not-food applications. Wheat gluten is largely used to fortify flours for improving their dough baking properties. It is also added in meat products to bind fat and water for improving taste and texture of sliced products such as hamburgers and hams. It is used by vegetarian industries to mimic the texture of meatballs, steaks or cheese. And, it is an important ingredient in pet foods and in cosmetics.[2-3]

An interesting approach to valorise this cheap protein is to use it as raw material for developing bio-packaging. It has been shown that wheat gluten has good film forming properties,[4] which can create semipermeable membranes to water vapour, oxygen and carbon dioxide molecules.[5-7] It can also be used as encapsulating agent of aromas compounds as D-limonene.[8] Wheat gluten films could be thus applied as food coatings or edible films on naturally gluten containing foods (*e.g.* bakery products) in order to slow down mass transfer phenomena such as water and oxygen, which are known to decrease the food quality. Water migration from different food domains or water sorption from the surrounding atmosphere could induce changes in the physical state of foods, increase the rates of chemical reactions and alterative phenomena such as microbial growth, therefore reducing the shelf-life.[9] In a similar way, oxygen transfer could favour oxidation reactions of lipids or pigments contained in foods and generate off flavours and undesirable colour change in the products.

One of the main issues related to the utilization of wheat gluten films is their inherent water sensitivity. The mechanical and the barrier properties are highly modified in wet conditions due to water sorption and subsequent plasticization.[5,7,10] One strategy largely considered for reducing water sorption and water transfer through edible films is to incorporate a hydrophobic phase constituted by edible lipids into the protein or polysaccharide matrix. Lipid incorporation is expected to increase the hydrophobicity of these films, to reduce the interactions with water and in contrast to other more invasive techniques (*e.g.* chemical hydrophobization) not to compromise the edibility of films. Several variables need to be considered to obtain satisfactory results.

They include the nature and concentration of lipids, the crystal type, the size and distribution of lipids and the processing used.[11,12,13]

The first objective of this study was to evaluate the effects of the incorporation of an emulsified lipid phase in wheat gluten film properties. The second one was to determine if such incorporation was able to reduce the water sensitivity of film mechanical properties. To that end, a comparative study between wheat gluten films with and without a lipid phase was conducted. Water sorption, surface hydrophilicity, barrier properties to water, mechanical properties and the thermal events of both types of films were assessed.

2 Material and methods

2.1 Film preparation

Two edible films based on wheat gluten were prepared using a solvent casting method adapted from Marcuzzo *et al.* (2010).[14] Both films contained 25 wt% glycerol (wheat gluten basis) as plasticizer (99.5 %, Sigma-Aldrich, St Louis, MO, USA). The two films differed by lipid incorporation and were referred to as WG (wheat gluten film without lipid phase) and EWG (emulsified wheat gluten film with lipid phase). Wheat gluten (protein purity of 83 %) was purchased from Sigma-Aldrich. The lipid phase (25 wt%, total dry basis) was constituted by a commercial blend of acetic esters of mono and di-glycerides and beeswax (Grindsted barrier system 2000, Danisco, Copenhagen, Denmark, melting point ≈ 57 °C) with glycerol monostereate (10 wt%, lipid basis) as emulsifier (99 % purity, Prolabo, Fontenay-sous-Bois, France).

Briefly, 2.5 g of glycerol, 10 g of wheat gluten, 40 g of milli-Q deionized water, 50 g of absolute ethanol and hydrochloric acid were stirred for 30 minutes at room temperature to produce gluten acid film-forming dispersions at pH = 4 (adjusted with HCl). This low pH increases the solubility of wheat gluten and thus favours the formation of transparent films compared to high pH (>8) which induced brown and opaque films. The film-forming dispersions were submitted to ultrasound treatment (UPS200S ultrasonic processor Hielscher Gmbh, Teltow, Germany) for 12 min, and thermally treated for 15 min at 70 °C under magnetic stirring. The ultrasound device was equipped with sonotrode (2 mm of tip diameter), at an output power of 200 W, an ultrasonic intensity of 600 W/cm^2 and a frequency of 24 kHz. In the case of WG films, the gluten film-forming dispersions were directly cast on PVC (polyvinyl chloride)-coated plates using a thin-layer chromatography spreader (Desaga Heidelerg, Germany) and dried at ≈ 25 °C for 20 h. In the case of EWG films, the lipid phase and the emulsifier were melted at 70 °C and incorporated in the gluten film-forming dispersions using a homogenizer (Polytron PT3000, Kinematica AG., Littau, Switzerland). The obtained dispersions were cast at 65 °C on PVC-coated plates as for WG films. Because of the lower solvent evaporation rate, two consecutive drying steps of EWG films were conducted, first at 25 °C for ≈ 24 h and then at 40 °C for 1.5 h using an oven (mod. HME061X,

Lainox Ali S.P.A, Treviso, Italy). WG and EWG films were then equilibrated at 53 % Relative Humidity (RH) using microclimate chambers at 25 °C containing magnesium nitrate saturated salt solution ($Mg(NO_3)_2$, Carlo Erba, Rodano, Italia) previously to all experiments.[15]

2.2 Water vapour sorption isotherm

The water vapour sorption isotherm of WG and EWG films were determined at 25 °C using the microclimate method as described by Bell and Labuza (2000)[16] with some modifications. Films were firstly cut into small pieces and dehydrated in desiccators contained silica gel for 2-3 weeks. Samples (1 – 1.5 g) were then placed for 21 days into chambers with fixed water activity values (a_w) ranging from 0.11 to 0.84 using saturated salt solutions (LiCl = 0.11, CH_3COOK = 0.23, K_2CO_3 = 0.43, $Mg(NO_3)_2$ = 0.53, $NaNO_2$ = 0.65, NaCl = 0.75 and KCl = 0.84).[15,17] Once equilibrium was reached, samples were weighed and dried in a vacuum oven (Vuotomatic 50, Bicasa, Milan, Italy) at 70 °C and 9.7 kPa for 12 hours. The moisture content was calculated as the weight difference before and after drying, and it was expressed as mass percentage on dry basis. The moisture determination was carried out in triplicate. The water vapour sorption isotherm was modeled using the Guggenheim-Anderson-de Boer (GAB) equation (Equation 1).

$$m = \frac{m_0 k C a_w}{(1 - k a_w)(1 - k a_w + k C a_w)} \qquad (Eq. 1)$$

Where *m* is the moisture content (%, dry basis), m_0 is the monolayer moisture content (%, dry basis), *C* and *k* are constants related to the sorption enthalpies of the first and of subsequent layers, respectively.

2.3 Surface hydrophilicity

The surface hydrophilicity of WG and EWG films was assessed with water contact angle measurements. Initial water contact angle (Θ) was measured using the sessile drop method on a goniometer (EasyDrop, Krüss, Hamburg, Germany) equipped with image analysis software (Drop Shape Analysis, Krüss). At least 10 water drops (volume ≈ 1 µL) were deposited on film surfaces at room conditions. During experiments both surfaces of films were considered and referred to as “Air side” (side in contact with air during drying) and “Support side” (side in contact with the support during drying).

2.4 Water barrier properties

The water vapour transfer rate (WVTR) of WG and EWG films was measured gravimetrically at 25 °C using a modification of the ASTM (American Society for Testing and Materials) standard method E 96-80 (1990).[18] In particular, the film samples were placed and sealed into permeability cups (Payne 1003, Sheen Instruments, Cambridge, UK) containing 10 mL milli-Q deionized water (to fix 100 % RH). The permeability cups were then transferred into a climatic room maintained at 23 % RH with potassium acetate saturated salt solution. The weight of the permeability cup was recorded periodically using an analytical balance. During permeability

experiments, the surface of films was taken into account by exposing either the air side or the support side to the highest RH atmosphere. Analyses were carried out in triplicates. The WVTR of films was determined from the steady state according to Equation 2.

$$WVTR = \frac{\Delta m}{A\Delta t} \qquad (Eq. 2)$$

Where *Δm* is the weight loss of the permeation cell (g), *A* is the film exposure area (m^2) and *Δt* is the time (s).

The liquid water transfer rate (LWTR) was calculated from the volume kinetics of a water drop (≈ 1 µL) deposited onto the film surface. LWTR represents the absorbed volume of water per time unit and base area unit (Equation 3).[19] As films were previously equilibrated at 0.53 a_w, the gradient for determining LWTR can be considered as 53 – 100 % RH.

$$LWTR = \frac{dV}{A_b(t)dt} \qquad (Eq. 3)$$

Where *dV* is the volume variation of the water drop (µL), *dt* is the time (s) and $A_b(t)$ is the base area of the water drop at time t (mm^2). The LWTR is expressed as [$g \cdot m^{-2} \cdot s^{-1}$], considering the density of water = 1 g/mL. Analyses were carried out with a goniometer (EasyDrop), equipped with image analysis software (Drop Shape Analysis) at room conditions. The experiment was performed on both surfaces of films (air and support). At least 3 water drops were analysed for each condition.

2.5 Thermal events

Thermal transitions related to glass transition and melting of WG and EWG films were evaluated with differential scanning calorimetry (DSC). Film samples were weighed (around 40 mg) and sealed into aluminium pans before been subjected to a double heating-cooling cycle from -100 to 100 °C under N_2 atmosphere using a Mettler TA 400 calorimeter (Mettler Toledo, Greifensee, Switzerland). The heat rate during the first cycle was 10 °C/min and during the second one was 20 °C/min. The glass transition temperature was determined from the inflection point (T_g) of the heat capacity change of the first cycle. The first cycle was considered to avoid modifications induced by evaporation of water. Samples were equilibrated at different a_w (0.11, 0.43, 0.53 and 0.75) before analysis.

The dependence of T_g on water content was evaluated using the Gordon-Taylor equation (Equation 4). [20]

$$T_{gm} = \frac{w_1 T_{g1} + k_{GT} w_2 T_{g2}}{w_1 + k_{GT} w_2} \qquad (Eq. 4)$$

In that equation, w_1 is the weight fraction of the polymer film and w_2 is the weight fraction of water. T_{g1} is the T_g (K) of the film without water. T_{g2} is the T_g of water taken as 136 K.[21] T_{gm} is the T_g (K) of the mixture (water and film). k_{GT} is an adjustable parameter which indicates strength of interaction between the two components (water and film). A non-linear least square analysis based on Levenberg–Marquardt algorithm was used to carry out the data treatment with Matlab software (The Mathworks, Natick, MA, USA). The fit was optimized between the T_{gm} values obtained experimentally and those calculated using the Gordon-Taylor equation, considering T_{g1} and k_{GT} as adjustable parameters. T_{gm} was estimated for $0 < w_2 < 1$.

2.6 Mechanical properties

The mechanical behaviour of WG and EWG samples equilibrated at 7 a_w (0.11, 0.23, 0.43, 0.53, 0.65, 0.75 and 0.84) was evaluated by uniaxial tensile testing at 25 °C, using a texture analyser equipped with a 5 kg load cell (T.A.XT. Plus, Texture Technologies, Hamilton, MA, USA). The initial gauge length was 6 cm and the crosshead speed was 1 mm/s. The Young modulus (Y.M., MPa), tensile strength (T.S., MPa) and elongation at break (E.B., %) were determined from stress – strain curves. At least 6 rectangular specimens having dimensions of 8 x 2 cm were analysed per each condition.

2.7 Thickness

Thickness of samples was measured using a micrometer (Elcometer 345, Elcometer Instruments Ltd, Manchester, UK) in at least 6 different positions.

2.8 Statistical analysis

Data were analysed using a student comparison test or using one–way analysis of variance (ANOVA) and Tukey-Kramer multiple comparison tests with GraphPad Prism software (version 5.01, GraphPad Software Inc., La Jolla, CA, USA). The significance level of all tests was set to 0.05.

3 Results and Discussion

3.1 Relationship between moisture and wheat gluten films

Water sorption isotherms of films and the calculated GAB parameters are reported in Figure 1. GAB model is considered one of the most versatile and effective model to predict the water content in foods[22] and in cereal grain protein based films[23] for water activities up to 0.85.

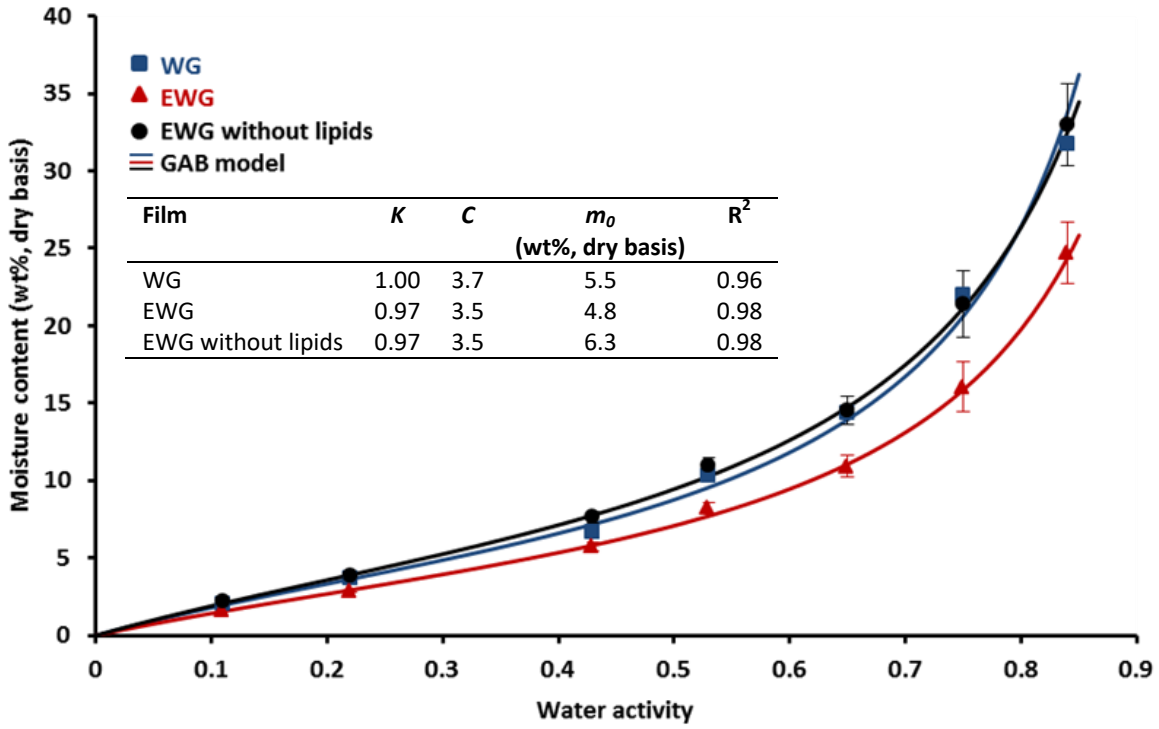

Film	*K*	*C*	m_0 (wt%, dry basis)	R^2
WG	1.00	3.7	5.5	0.96
EWG	0.97	3.5	4.8	0.98
EWG without lipids	0.97	3.5	6.3	0.98

Figure 1. *Water sorption isotherm at 25 °C of WG (wheat gluten films), EWG (emulsified wheat gluten films) and EWG films recalculated without considering its lipid content, and their corresponding parameters of the Guggenheim-Anderson-de Boer (GAB, Eq. 1) model.*

Moisture sorption isotherms revealed a lower capability of EWG films to sorb water compared to WG, particularly at intermediate and high a_w. This was also evidenced by the calculations of monolayer moisture content (m_0). Addition of a lipid phase in EWG not only reduced the quantity of water sorbed at high a_w, but also the water molecules associated to the first solvation layer, probably because of a minor availability of polar/hydrophilic groups able to act as water sorption sites. Moreover, when the water vapour sorption isotherm of EWG was re-calculated without considering the lipid content, the resulted values fully matched those of WG. This indicated that lipid addition did not take part in the water sorption and did not modify the sorption phenomena by hiding sorption sites of the protein continuous phase (wheat gluten and its plasticizer glycerol). The reduction observed in the quantity sorbed when lipid is added is therefore only due to a decrease in the quantity of the protein phase. The m_0 values obtained in this study were about 50 % lower than those observed by Gennadios and Weller (1994)[23] and Roy *et al.* (2000)[24] for wheat gluten films. A possible explanation of such difference can be attributed to the minor quantity of glycerol used in WG and EWG films (25 %, wheat gluten basis) compared to that one used in the previously cited works (40 %, wheat gluten basis). Glycerol is a well-known hydrophilic plasticizer and its utilization in a higher quantity most likely increased the water quantity sorbed. Moreover, as the multilayer factor (*k)* of WG and EWG films was very close to 1, sorption isotherms were very likely to follow the Brunauer-Emmet-Teller (BET) model, that is to say monolayer

water sorption essentially occurred. In the same way, no big differences were found in the surface heat constant (*C*), suggesting that water molecules were bound with the same energy in both films.

Water sorption isotherm of films provides information from the thermodynamic equilibrium between the film and the water vapour at interface. In a similar way, water contact angle (Θ) measurement involves equilibrium between a liquid water drop and the film surface, and provides information of the surface properties of films. Water contact angle can be used as an indicator of surface hydrophilicity of materials. According to Vogler (1998)[25] surfaces exhibiting values higher or lower than 65 °C can be considered hydrophobic or hydrophilic, respectively. If a surface has high affinity to water, the water drop would tend to maximize the contact area and to assume a spread disposition decreasing consequently its contact angle. On the contrary, if the surface tested has low water affinity, the water drop would tend to minimize the contact area and to assume a spherical shape increasing thus its contact angle.[19]

All surfaces analysed in this study (WG-air, WG-support, EWG-air and EWG-support) displayed a hydrophilic nature, as no water contact angle value exceeded 65 ° (Table 1). It is worthy to note that WG films displayed significantly lower contact angle values compared to EWG films. In addition, the air surface of WG films is more hydrophilic compared to their support surface. A higher quantity of polar groups were probably exposed to the air surface, possibly as a consequence of glycerol migration during film drying and/or of solvent evaporation conditions (evaporation rate, unidirectional mass flux, contact with hydrophobic support). Moreover, the addition of a lipid phase significantly decreased the surface hydrophilicity of EWG films without inducing any phase separation, since air and support sides displayed similar water contact angle. These findings therefore suggested that the lipid phase was rather homogenously distributed in the protein matrix, which is probably the reason why it induced a homogenous distribution of polar and non-polar groups in both surfaces of EWG films.

Table 1. *Water contact angle (Θ), water vapour transfer rate (WVTR) and liquid water transfer rate (LWTR) of WG and EWG films. Values are represented as mean ± standard deviation. Significant differences ($p < 0.05$) are indicated with different letters in the same column.*

Film	side	Thickness (µm)	Θ (°)	WVTR (10^{-3} g·m^{-2}·s^{-1})	LWTR (g·m^{-2}·s^{-1})
WG	air	47.8 ± 1.7^{a}	35.7 ± 6.5^{a}	15.8 ± 0.3^{a}	1.32 ± 0.12^{a}
	support	46.8 ± 1.5^{a}	53.6 ± 5.1^{b}	17.3 ± 0.1^{b}	1.38 ± 0.37^{a}
EWG	air	43.0 ± 2.0^{b}	64.3 ± 4.0^{c}	7.2 ± 0.3^{c}	0.52 ± 0.03^{b}
	support	43.0 ± 2.0^{b}	65.2 ± 3.9^{c}	7.2 ± 0.3^{c}	0.48 ± 0.02^{b}

3.2 Water transfer through films

The incorporation of a lipid phase is a strategy which aims at improving the liquid and vapour water barrier properties of edible films. It is well known that edible waxes, such as beeswax, are the most efficient

substances in decreasing water interaction of edible films, due to their low polarity, high melting point and crystallinity organization [12,13] However, their sole utilization as a lipid source it is not recommended because they could compromise the mechanical properties of edible films, which easily become brittle and fragile.[6,11-13,26]

To avoid a rigid behaviour in wheat gluten films, the lipid phase used in this study was constituted of beeswax blended with molecules having higher polarity, such as acetic acids of mono and di-glycerides. Such lipid phase, introduced at 25 wt% in the film formulation, was able to increase the barrier properties to water by ≈ 60 % either in liquid or in vapour state (Table 1). This improvement could be considered satisfactory, since it has been reported a similar decrease in water vapour permeability (≈ 75 %) when incorporating only beeswaxes.[6]

When air and support surfaces of films were compared (Table 1), no differences were clearly noticeable either in water vapour transfer rate (WVTR) or in liquid water transfer rate (LWTR), indicating that barrier properties were principally influenced by the bulk (molecular organization, physical state of polymer chains, hydrophilicity) rather than the surface properties (surface polarity, topography). This was particularly evident in the case of WG films, whose surfaces exhibited different hydrophilicity.

In addition, the water barrier properties of films were strongly affected by the physical state of water. The quantity of transferred water in the liquid state was ≈ 2 order of magnitude higher than the quantity of vapour water transmitted (Table 1), indicating that the barrier efficiency of wheat gluten was decreased in the presence of liquid water. This reduction becomes even more evident when comparing the moisture gradient, which was higher in WVTR determination (23 – 100%) than in LWTR (53 – 100%). Morillon *et al.* (2000)[27] showed that liquid water highly favoured water permeation in hydrophilic films, as a consequence of interactions between permeant and the hydrophilic matrix, including phenomena of sorption, swelling and changes in the macromolecular structure. The intrinsic hydrophilicity of WG and EWG films could therefore originate this behaviour. Furthermore, the reduction appeared to be lower in the wheat gluten films containing the lipid phase (EWG ≈ 70 times vs WG ≈ 80 times), probably as a consequence of the decreased hydrophilicity, which led to less interaction with water.

3.3 Thermal events

The thermal events of films equilibrated at different a_w were evaluated to better understand the physical state of films as a function of water content. WG and EWG films were analysed using Differential Scanning Calorimetry (DSC) from -100 to 100 °C (Figure 2).

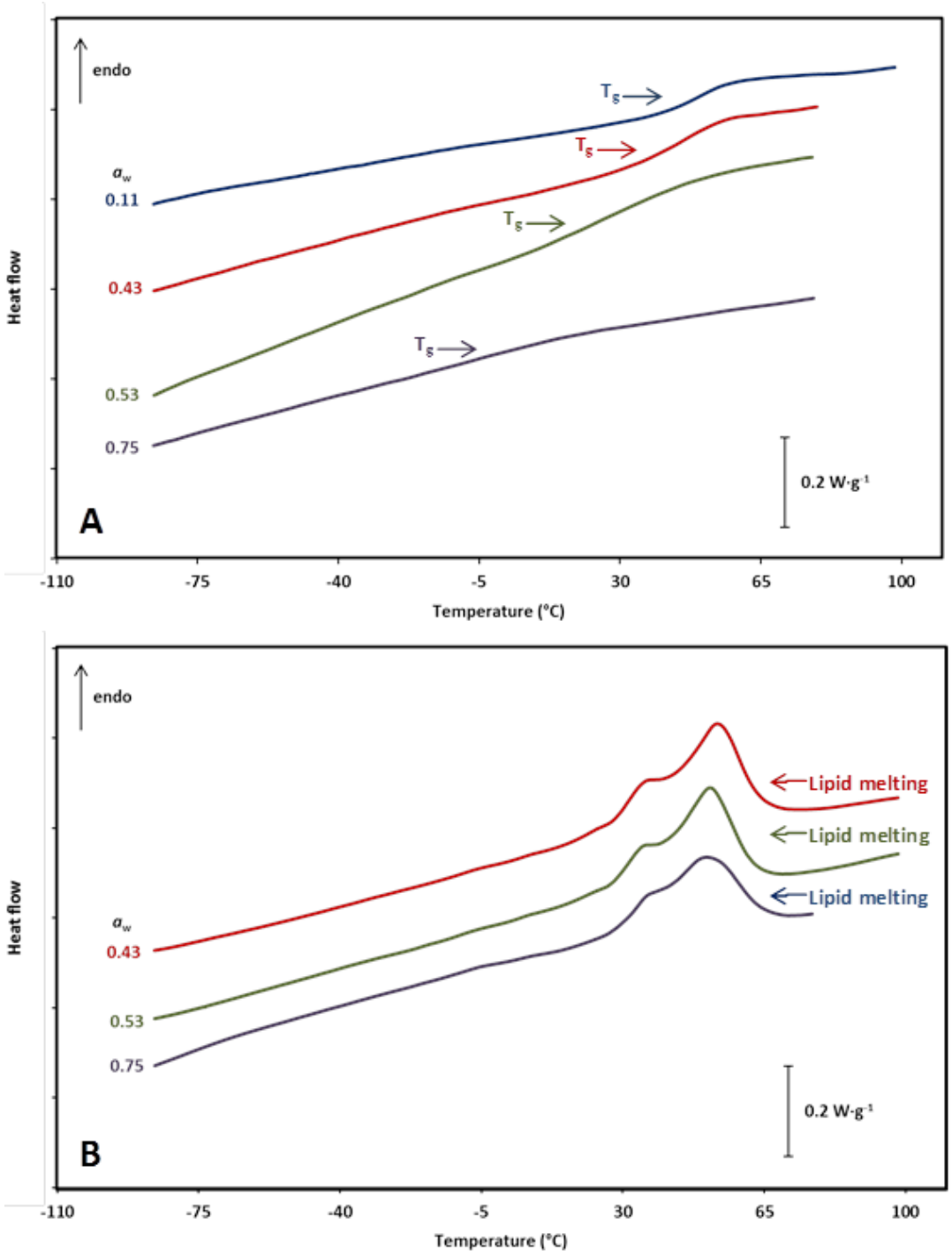

Figure 2. *Differential scanning calorimetry curves (first heating) of WG (wheat gluten films, A) and EWG (emulsified wheat gluten films, B) previously equilibrated at different water activities.*

DSC curves of WG films (Figure 2A) displayed a single reversible thermal event, which was characterized by a slow baseline shift to higher values. This indicated that wheat gluten films were fully amorphous materials, and exhibited a largely spread transition from a glassy state to a rubbery state during heating. The glass transition temperature (T_g) decreased when a_w increased. Water is known to act as plasticizer of hydrophilic biopolymers

such as wheat gluten. It can increase the free volume of the system by solvating hydrophilic groups, which results in a depletion of the glass transition. Glass transition temperatures lower than 25 °C were detected for WG films stored at a_w > 0.43 (Table 2). The resulted T_g depletion appeared to follow the Gordon-Taylor model as displayed in Figure 3 (R^2 = 0.94,). From such modeling k_{GT} is found to be around 2.1 which is lower than 5 as reported by Kalichevsky *et al*. (1992).[28] The higher is k_{GT} the greater is the interaction between water and the film. However it should noticed than in the present case the film is not pure wheat gluten but is already plasticized with glycerol, which obviously reduced the global strength of interactions. This is also evidenced by the value of T_{g1} (59 °C) which is much lower than the T_g value of pure wheat gluten (162 °C).[28]

DSC curves of EWG films (Figure 2B) showed an additional endothermic event ranging between 30 and 70 °C, attributed to the melting of lipids, which probably exhibited polymorphism as two maxima (≈ 40 and 50 °C) were observed during this transition. No thermal events related to glass transition were detected by DSC, because the strong signal of the lipid melting overlapped the slow baseline change related to the glass transition of wheat gluten. Similar T_g for WG and EWG can be hypothesized, since the no difference in the water sorption behaviour was previously noticed between WG and EWG without considering lipid content (Figure 1).

Table 2. *Glass transition temperature (T_g) of WG films equilibrated at different water activity levels (a_w).*

a_w	T_g (°C)	Amorphous state at 25°C
0.11	48.9 ± 2.1	Glassy
0.43	43.1 ± 3.4	Glassy
0.53	22.7 ± 1.1	Rubbery
0.75	-3.0 ± 3.9	Rubbery

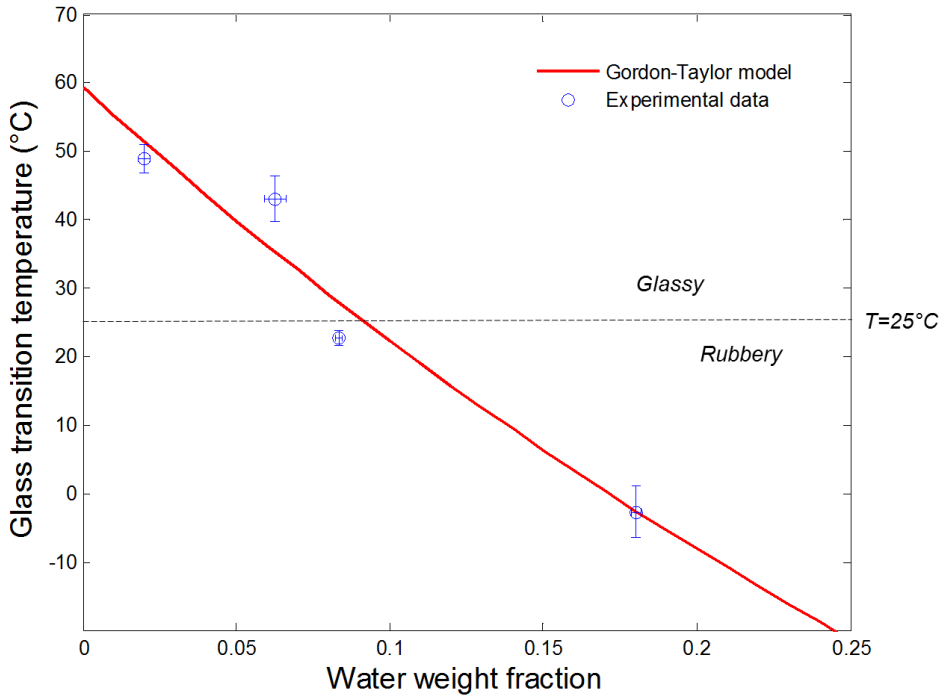

***Figure 3**. Experimental glass transition temperature of WG (wheat gluten films, blue circle) as a function of water weight fraction, and modeling according to the Gordon-Taylor equation (red line). The dot line at 25 °C represents the storage temperature of films and evidences the glassy or rubbery state.*

3.4 Mechanical properties affected by both lipid and water activity

The mechanical properties of films can provide information regarding the molecular structure of the matrix. For example, if the interaction energy between molecular chains is high, the obtained films are resistant, cohesive and relative less deformable. On the contrary, if the interaction energy is low, the obtained films are less cohesive and more extensible.[29] Studying these properties at different a_w levels can be also a useful tool to predict the mechanical behaviour of films when applied as food coatings or used as biodegradable packaging. As suggested by DSC analysis, the structure of the polymer matrix could be modified by the relative humidity induced by the coated food or by the environment. For these reasons, the mechanical properties of WG and EWG were studied under tensile stress at different a_w ranging from 0.11 to 0.84 in order to simulate various foods or environments. The Young modulus (Y.M.), the tensile strength (T.S.) and the elongation at break (E.B.) as a function of a_w are reported in Figure 4.

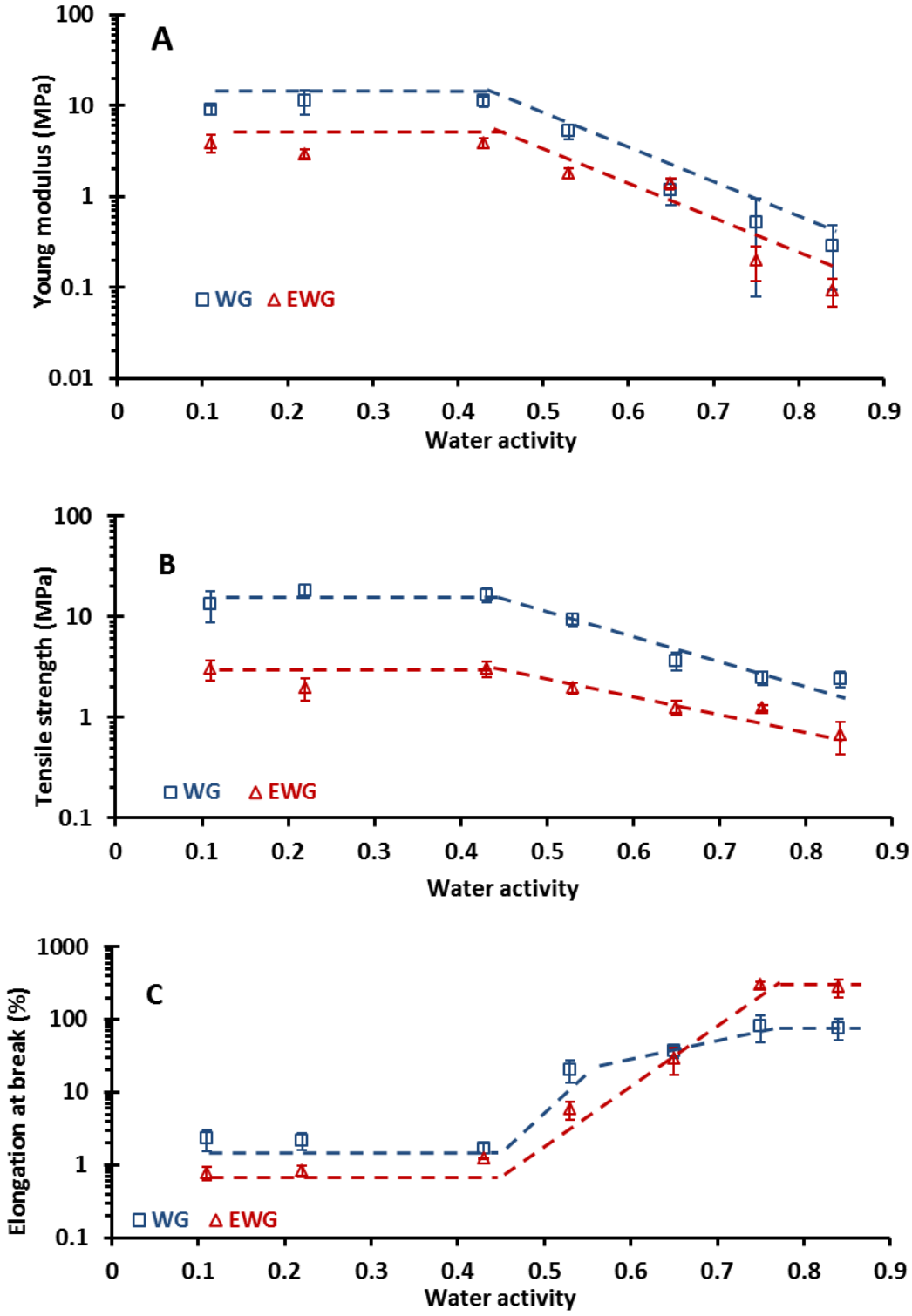

Figure 4. *Mechanical properties of WG (wheat gluten films) and EWG (emulsified wheat gluten films) as a function of water activity at 25 °C. (A) Young modulus, (B) Tensile strength, (C) Elongation at break.*

The mechanical properties of wheat gluten based films are highly modified by water sorption and changes were similar in both films, WG or EWG. The films exhibited a brittle behaviour for a_w values lower than approx. 0.4 as evidenced by the high Y.M., high T.S. and low E.B. When WG and EWG exceeded a_w of about 0.4, the films turned to display an extensible behaviour as clearly revealed by the increase in E.B and decrease in Y.M. and T.S. Additionally, no significant differences were noticed on mechanical parameters when $a_w \leq$ ~0.4 considering each film formulation. On the contrary when a_w was > ~0.4, they displayed a strong dependence on a_w. These findings highlighted the important role of water on mechanical properties of wheat gluten films. They were fully in line with DSC analysis. As previously evidenced, wheat gluten films displayed a transition from a glassy to a rubbery state, which is shifted to lower temperatures for increasing a_w, due to water plasticization. When amorphous materials are stored at temperatures lower than their T_g, they display low molecular mobility, high internal viscosity and glassy like behaviour (rigid, non-deformable, fragile). If the temperature is over their T_g, macromolecules are more mobile, translational motions are possible, the internal viscosity decreases and they exhibit a rubber–like behaviour (extensible, deformable).[30] Based on those considerations, the extensible behaviour of WG films at a_w > ~0.4 is unambiguously attributed to the T_g depletion induced by water sorption. Clearly, for those a_w the T_g of WG films became lower than 25 °C (Table 2). Similar considerations can be also done for EWG, considering the sensitivity of the protein network to water.

The dependence of mechanical properties on water activity was similar in WG and EWG, indicating that lipid incorporation at 25 wt% (dry basis) did not reduced the water sensitivity of wheat gluten films. Therefore, the continuous phase of the EWG not only sorbed the same quantity of water than WG (as revealed by the EWG water sorption isotherm without considering lipids), but also its mechanical behaviour to tensile stress resulted sensitive to water in analogous way to WG.

Nevertheless, the lipid addition clearly influenced the structure of films for the whole a_w range considered as shown by the decrease in Y.M. and T.S. Similar results were also observed by Gontard *et al.* (1994)[6] in wheat gluten films containing beeswax or sucroester of stearic acid, as analysed with puncture test at 58 % RH and 30 °C. The decrease in these parameters indicated a lower cohesion in the polymer network, probably because the lipid phase physically hindered the formation of intermolecular bonds between proteins and favoured the formation hydrophobic interactions during film drying. Findings also displayed a lower E.B of EWG compared to WG for a_w < 0.75, supporting the hypothesis of discontinuities induced by lipid particles in the continuous protein matrix. However, a higher extensible behaviour of EWG than WG (E.B > 250 vs. ≈ 80 %) at high a_w levels (0.75 and 0.84) was also evidenced. A possible cause of such behaviour lies in the amphiphilic compounds (*e.g.* acetic acids of mono and di-glycerides, and glycerol monostereate) included with the lipid phase, which could

act as lubricants favouring sliding of molecular chains, and therefore a gentle and highly extensible polymer network.

4 Conclusions

This study clearly showed that the incorporation of a lipid phase was able to reduce the water sorption, the water affinity and the water transfer in wheat gluten films. In particular, the water vapour sorption isotherm revealed a lower capacity for water sorption in emulsified films over the a_w range considered. Water contact angle measurements displayed a lower surface hydrophilicity for films containing lipids and did not evidenced any lipid phase separation, suggesting a rather homogenous distribution of lipids in the wheat gluten polymer matrix. The barrier properties to water molecules in liquid or vapour state were twice increased after lipid addition, and should be considered for application in food products. However, the incorporation of lipids induced a weaker network structuration, probably because the lipid phase physically hindered the formation of intra-chain bonds during film forming. It could be therefore interesting to better understand the parameters of the processing which could influence the polymorphism and size of lipid crystals, such as homogenization, orientation and drying.

However the sensitivity of mechanical properties to water remains similar in films emulsified with lipids, even if the matrix was less hydrophilic and interactions with water reduced. All films, including lipids or not, were characterized by a physical change from a glassy-like behaviour to a rubber like-behaviour when a_w of 0.43 was exceeded, as a consequence of T_g depletion induced by water sorption, as revealed by DSC analysis. An interesting strategy to reduce the water sensitivity could be found in reducing the quantity of plasticizers as glycerol, especially when amphiphilic lipid compounds with lubricating effect are used.

As a final remark, goniometry findings also showed an interesting capability of wheat gluten films without lipid phase to display different hydrophilicity on both surfaces (air and support), which could be considered for modulating adhesive properties of natural polymers on other surfaces.

Acknowledgements

The authors acknowledge the European Social Found – Friuli Venezia Giulia Region – Operational Program 2007/2013 for supporting this project (Regional code: FP1340303009).

References

1. FAOSTAT, 2013. Food and Agriculture Organization of the United Nations Statistics Division. http://faostat3.fao.org/browse/rankings/commodities_by_regions/E Retrieved on 03/10/2015.

2. Lagrain, B.; Goderis, B.; Brijs, K.; Delcour, J. A. Molecular basis of processing wheat gluten toward biobased materials. *Biomacromolecules* **2010,** *11* (3), 533-541.

3. Day, L.; Augustin, M. A.; Batey, I. L.; Wrigley, C. W. Wheat-gluten uses and industry needs. *Trends in Food Science & Technology* **2006,** *17* (2), 82-90.

4. Gontard, N.; Guilbert, S.; Cuq, J.-L. Edible wheat gluten films: influence of the main process variables on film properties using response surface methodology. *Journal of Food Science* **1992,** *57* (1), 190-195.

5. Gontard, N.; Guilbert, S.; Cuq, J.-L. Water and glycerol as plasticizers affect mechanical and water vapor barrier properties of an edible wheat gluten film. *Journal of Food Science* **1993,** *58* (1), 206-211.

6. Gontard, N.; Duchez, C.; Cuq, J.-L.; Guilbert, S. Edible composite films of wheat gluten and lipids: water vapour permeability and other physical properties. *International Journal of Food Science & Technology* **1994,** *29* (1), 39-50.

7. Gontard, N.; Thibault, R.; Cuq, B.; Guilbert, S. Influence of relative humidity and film composition on oxygen and carbon dioxide permeabilities of edible films. *Journal of Agricultural and Food Chemistry* **1996,** *44* (4), 1064-1069.

8. Marcuzzo, E.; Debeaufort, F.; Sensidoni, A.; Tat, L.; Beney, L.; Hambleton, A.; Peressini, D.; Voilley, A. Release behavior and stability of encapsulated D-limonene from emulsion-based edible films. *Journal of Agricultural and Food Chemistry* **2012,** *60* (49), 12177-12185.

9. Labuza, T. P.; Hyman, C. R. Moisture migration and control in multi-domain foods. *Trends in Food Science & Technology* **1998,** *9* (2), 47-55.

10. Lens, J. P.; de Graaf, L. A.; Stevels, W. M.; Dietz, C. H. J. T.; Verhelst, K. C. S.; Vereijken, J. M.; Kolster, P. Influence of processing and storage conditions on the mechanical and barrier properties of films cast from aqueous wheat gluten dispersions. *Industrial Crops and Products* **2003,** *17* (2), 119-130.

11. Callegarin, F.; Quezada-Gallo, J. A.; Debeaufort, F.; Voilley, A. Lipids and biopackaging. *Journal of the American Oil Chemists Society* **1997,** *74* (10), 1183-1192.

12. Debeaufort, F.; Voilley, A., Lipid-based edible films and coatings. In *Edible Films and Coatings for Food Applications*; Embuscado, M. E.; Huber, K. C., Eds.; Springer: Dordrecht ; London, 2009.

13. Morillon, V.; Debeaufort, F.; Blond, G.; Capelle, M.; Voilley, A. Factors affecting the moisture permeability of lipid-based edible films: A review. *Critical Reviews in Food Science and Nutrition* **2002,** *42* (1), 67-89.

14. Marcuzzo, E.; Peressini, D.; Debeaufort, F.; Sensidoni, A. Effect of ultrasound treatment on properties of gluten-based film. *Innovative Food Science & Emerging Technologies* **2010,** *11* (3), 451-457.

15. Greenspan, L. Humidity fixed points of binary saturated aqueous solutions. *Journal of Research of the National Bureau of Standards Section a-Physics and Chemistry* **1977,** *81* (1), 89-96.

16. Bell, L. N.; Labuza, T. P. *Moisture sorption: practical aspects of isotherm measurement and use*; American Association of Cereal Chemists: St. Paul, MN, 2000.

17. Labuza, T. P.; Kaanane, A.; Chen, J. Y. Effect of temperature on the moisture sorption isotherms and water activity shift of two dehydrated foods. *Journal of Food Science* **1985,** *50* (2), 385-392.

18. ASTM E96-80, 1990. Standard test method for water vapor transmission of materials. In: *Annual Book of ASTM Standards.* American Society for Testing and Materials, Philadelphia, PA.

19. Karbowiak, T.; Debeaufort, F.; Champion, D.; Voilley, A. Wetting properties at the surface of iota-carrageenan-based edible films. *Journal of Colloid and Interface Science* **2006,** *294* (2), 400-410.

20. Gordon, M.; Taylor, J. S. Ideal copolymers and the second-order transitions of synthetic rubbers. i. non-crystalline copolymers. *Journal of Applied Chemistry* **1952,** *2* (9), 493-500.

21. Hallbrucker, A.; Mayer, E.; Johari, G. P. The heat capacity and glass transition of hyperquenched glassy water. *Philosophical Magazine Part B* **1989,** *60* (2), 179-187.

22. Labuza, T. P.; Altunakar, B., Water activity prediction and moisture sorption isotherm. In *Water activity in foods: fundamentals and applications*; Barbosa-Cánovas, G. V.; Fontana, A. J.; Schmidt, S. J.; Labuza, T. P., Eds.; Blackwell Pub.: Ames, Iowa, 2007.

23. Gennadios, A.; Weller, C. L. Moisture adsorption by grain protein films. *Transactions of the Asae* **1994,** *37* (2), 535-539.

24. Roy, S., Gennadios, A., Weller, C.L., Testin, R.F., 2000. Water vapor transport parameters of a cast wheat gluten film. Industrial Crops and Products 11, 43–50.

25. Vogler, E. A. Structure and reactivity of water at biomaterial surfaces. *Advances in Colloid and Interface Science* **1998,** *74*, 69-117.

26. Kester, J.J. ; Fennema, O.R. Edible films and coatings: a review. *Food Technology* **1986,** *40* (12), 47-59.

27. Morillon, V.; Debeaufort, F.; Capelle, M.; Blond, G.; Voilley, A. Influence of the Physical State of Water on the Barrier Properties of Hydrophilic and Hydrophobic Films. *Journal of Agricultural and Food Chemistry* **2000,** *48* (1), 11-16.

28. Kalichevsky, M. T.; Jaroszkiewicz, E. M.; Blanshard, J. M. V. Glass transition of gluten. 1: Gluten and gluten—sugar mixtures. *International Journal of Biological Macromolecules* **1992,** *14* (5), 257-266.

29. Guilbert, S.; Gontard, N.; Morel, M. H.; Chalier, P.; Micard, V.; Redl, A., Formation and properties of wheat gluten films and coatings. In *Protein-based films and coatings*; Gennadios, A., Ed. CRC Press: Boca Raton, 2002.

30. Roos, Y. H., Water activity and glass transition. In *Water activity in foods: fundamentals and applications*; Barbosa-Cánovas, G. V.; Fontana, A. J.; Schmidt, S. J.; Labuza, T. P., Eds.; Blackwell Pub.: Ames, Iowa, 2007.

PART III

IMPACT OF ASSEMBLY PROCESS OF PLA-WHEAT GLUTEN-PLA MULTILAYER COMPLEXES ON THEIR STRUCTURE AND FUNCTIONAL PROPERTIES

Multilayer complexes from PLA and wheat gluten

Rocca-Smith J.R; Pasquarelli R.; Lagorce-Tachon A.; Rousseau J.; Fontaine S.; Karbowiak T. and Debeaufort F *PLA/protein complex gluten films: multilayer process and properties* (to be submitted to ACS Applied Materials and Interfaces).

1 Introduction

Even if Poly(lactic acid) or PLA is known to react with water molecules by hydrolysis,[1] it can be considered as a hydrophobic polyester with a contact angle ranging between 80 and 85 °.[2] It sorbs small quantities of water (< 1.1 wt% at T = 25 °C and close to saturation)[3] and benefits of similar barrier performances to water vapour to poly(ethyleneterephtalate) (PET)[4] and better than most of biobased and biodegradable materials. However, one of the drawbacks related to PLA is its low barrier performances to gases such as oxygen (O_2) and carbon dioxide (CO_2).[5] This is a key issue which limits its use for applications requiring low gas transfer, such as modified atmosphere packaging (MAP) or as packaging of products sensitive to oxidation.

An interesting strategy to overcome these drawbacks is to develop complexes between PLA and complementary materials, such as proteins and polysaccharides, which are also biodegradable materials. Proteins and polysaccharides are able to form films with hydrophilic characteristics, which in contrast to PLA are characterized by a reduced barrier proprieties to water vapour, but by much better barrier performances to gases.[6] The development of such complexes could thus open on new eco-friendly application scenarios for PLA, without compromising its intrinsic biodegradability.

Most of the studies available in literature related to biobased complexes of PLA deals with the development of blended or composite morphology.[5] It is probably due to the relative easiness to produce a composite structure in comparison to the creation of a laminate or multilayer structure. Since the development of a composite morphology can be achieved by mixing the components, it usually involves less steps of production than a laminate structure. For PLA complexes with a multilayer morphology, additional steps should be added such as the production and the adhesion of the complementary layers. Nevertheless, the former approach generally produces materials with intermediate barrier performances of the polymers considered, and generally closer to the lower barrier as the limiting step remains the continuous layer and is not drastically changed using this strategy. On the contrary, the latter takes maximum advantage of both polymers used, by forcing the permeant molecules to pass through the continuous phases with complementary barrier performances and really act as an additional limiting step to mass transfer.[5]

An interesting candidate for developing PLA complexes is wheat gluten protein. It benefits of a rather apolar character (it is not soluble in water) and it is able to form translucent films, with good mechanical properties and with low permeability to gases.[7] The O_2 and the CO_2 transfer of such films can reach in dry environments values comparable to high barrier plastics, such as PET, polyamide 6 (PA6), poly(vinyl chloride (PVC) and ethylene-vinyl alcohol (EVOH).[7] That means that the barrier efficiency of PLA to gases could be increased from 10 to 100 times. Although, it has been shown that its functional properties are sensitive to moisture,[8-10] a sandwiched structure PLA-WG-PLA could limit its exposition to water molecules. Furthermore, the use of wheat gluten as laminates could be considered as an innovative approach to valorise this protein, which is a co-product of wheat mill industry.

Based on this considerations, the main objective of this section is to develop multilayer complexes PLA-WG-PLA as a new system able to increase the performance of Poly(lactic acid) (PLA) film as barrier to oxygen (O_2) and carbon dioxide (CO_2). To reach this objective, different technologies of industrial interest were considered, such as high pressure homogenization of wheat gluten film forming dispersion, corona treatment of PLA films, and multilayer shaping processes such as wet casting and hot press.

In order to better discuss the influence of such processing technologies, the study was divided in three parts:

- The first one focuses on the influence of high pressure homogenization on the functional properties of the wheat gluten coating layer.
- The second one deals with the surface modifications induced by corona treatment on the PLA support layer.
- The third one reports on the influence of process variables largely used for multilayer production such as corona treatment, coating thickness, layer assembly (as single layers or bilayers) processes (wet coating and hot press) on the barrier properties of the so-produced complexes.

Most of the results obtained in this study were in continuity with the two previous studies reported in this thesis (Part II, Paper 4)[11] and (Part II, Paper 5)[10], which dealt with the characterization of the support and coating layers, respectively.

2 Materials and methods

2.1 Samples

2.1.1 Production of support layer (PLA film)

Corona Treated (CT) and Non-Corona Treated (NCT) PLA films available in the market for food packaging applications (thickness = 20 µm, Nativia NTSS, Taghleef Industries, San Giorgio di Nogaro, Udine, Italy) were used as support layer. Both films were subjected to bi-orientation and annealing processes during production.

The drawn ratio and the temperature of the orientation in the Machine Direction of processing line (MD) was 2-3 and 50-65 °C, while in Transversal Direction (TD) was 4-5 and 70-85 °C, respectively. Only one surface of films was treated by corona (30 $W \cdot m^{-2} \cdot min^{-1}$) and called CT-treated, the other surface was named CT-untreated. In the case of NCT films the surfaces were named NCT-A and NCT-B. To reduce the effect of time on PLA film properties, the samples were stored at -30 °C until their use and characterisations.

2.1.2 Production of coating layer (Wheat gluten film)

Wheat gluten film (WG) was used as coating layer. They were produced using the solvent casting method adapted from Rocca-Smith *et al.* (2016)[10]. Briefly, 2.5 g of glycerol (≥ 99.5 %, Sigma-Aldrich, St Louis, MO, USA), 10 g of gluten from wheat (protein purity 85 %, Sigma-Aldrich), 40 g of milli-Q deionized water, 50 g of ethanol (96 % v/v, Sigma-Aldrich) and 0.7 mL of hydrochloric acid (4 M, Sigma-Aldrich) were stirred at 25 °C for 30 min. The film-forming dispersions (pH=4) were thermally treated for 15 min at 70 °C under magnetic stirring. The dispersion was then submitted to high pressure homogenization for 7 cycles at 100 MPa (LM10 Microfluidizer™, Microfluidics, Westwood, MA, USA) in a multi-slotted Z-type chamber. The high pressure circuit was covered with ice to prevent an excessive temperature increase of the solution. After high pressure homogenization, 10, 15, 20 or 25 mL of the film-forming dispersion was poured in polystyrene Petri dishes (diameter = 14 cm) or casted on Poly(methyl methacrylate) (PMMA) supports using an automatic film applicator (Model: 1137, Sheen Instruments, Surrey, UK). The different volumes ensured to cover a thickness range from 60 to 150 µm. Films were peeled after been dried at 25 °C and 40 % Relative Humidity (RH) for ≈ 15 hours. The films were then equilibrated at 50 % RH, using microclimate chambers at 25 °C containing magnesium nitrate saturated salt solution (53 % RH, $Mg(NO_3)_2$, Sigma-Aldrich). WG films without high pressure homogenization step were also produced. Samples were referred to as WG-high pressure and WG-no high pressure. Both sides of films were taken into consideration for surface characterization. The surface in contact with air during drying was named “Air side”, and the surface in contact with the support during drying was named “Support side”.

2.1.3 Production of PLA-WG complexes

Bilayer films

The film-forming dispersion subjected to high pressure homogenization was deposited at around 60 °C on the surface of the PLA films by wet casting. The WG coating was always in contact with the CT-treated side or with the NCT-A side. The bilayer complexes were named “CT + WG” or “NCT + WG”.

For coating layers with thickness of approximatively 20 and 60 µm, 12 and 36 mL film-forming dispersion were casted on PLA films (surface area of about 20 x 30 cm^2) using the automatic film applicator (Model: 1137, Sheen instruments, Surrey, UK), respectively.

Trilayer films

The laminates were produced with a hot press (LabPro 600, Fontijne Presses, Vlaardingen, Netherlands) using preformed single films (CT, NCT and WG-high pressure) or from preformed bilayers obtained by wet casting (CT + WG, NCT + WG), as previously described and called bilayer. The layers were prepared as squares of 15 x 15 cm and were overlapped in the PLA-WG-PLA disposition. Both surfaces of the WG film were always in direct contact with the CT-treated side or NCT- A side. The layers were intercalated between two Teflon sheets, in order to prevent adhesion, and then placed between two metal plates. The system was heated to 130 °C at 10 °C·min^{-1} and then hot pressed at 10 MPa for 10 minutes. The trilayers were cooled down to 25 °C at 10 °C·min^{-1}. Pressure was released when the samples reached 30 °C. The trilayer complexes were then stored at 50 % RH at 25 °C. The samples made from preformed single films were named CT/WG/CT and NCT/WG/NCT, while the trilayers prepared from bilayers (previously made by coating) were coded CT+WG/CT and NCT+WG/NCT

Figure 1 summarizes the sampling design, with the processing conditions and samples considered in this study.

2.2 Characterization of film-forming dispersions

2.2.1 Particle size distribution

The particle size distribution in the WG film-forming dispersion was determined by laser light scattering (Mastersizer 3000, Malvern, Malvern, UK). The Mie theory[12] was applied considering particles as spheres, and using a refractive index of 1.35 and 1.45 for the dispersant and wheat gluten, respectively. A cylindrical vessel (HydroSM MAZ 3150, Malvern) was filled with the dispersant medium (water-ethanol, 4:5 in weigh). A stirring speed of 1200 rpm was used for the circulating medium. The particle size distribution was measured in triplicate (from three different film forming suspensions), and each sample was scanned three times. The mean volume diameter ($d_{4,3}$) was calculated according to Equation 1.

$$d_{4,3} = \frac{\sum_i n_i d_i^4}{\sum_i n_i d_i^3} \qquad (Eq. 1)$$

where n_i is the number of particles of diameter d_i.

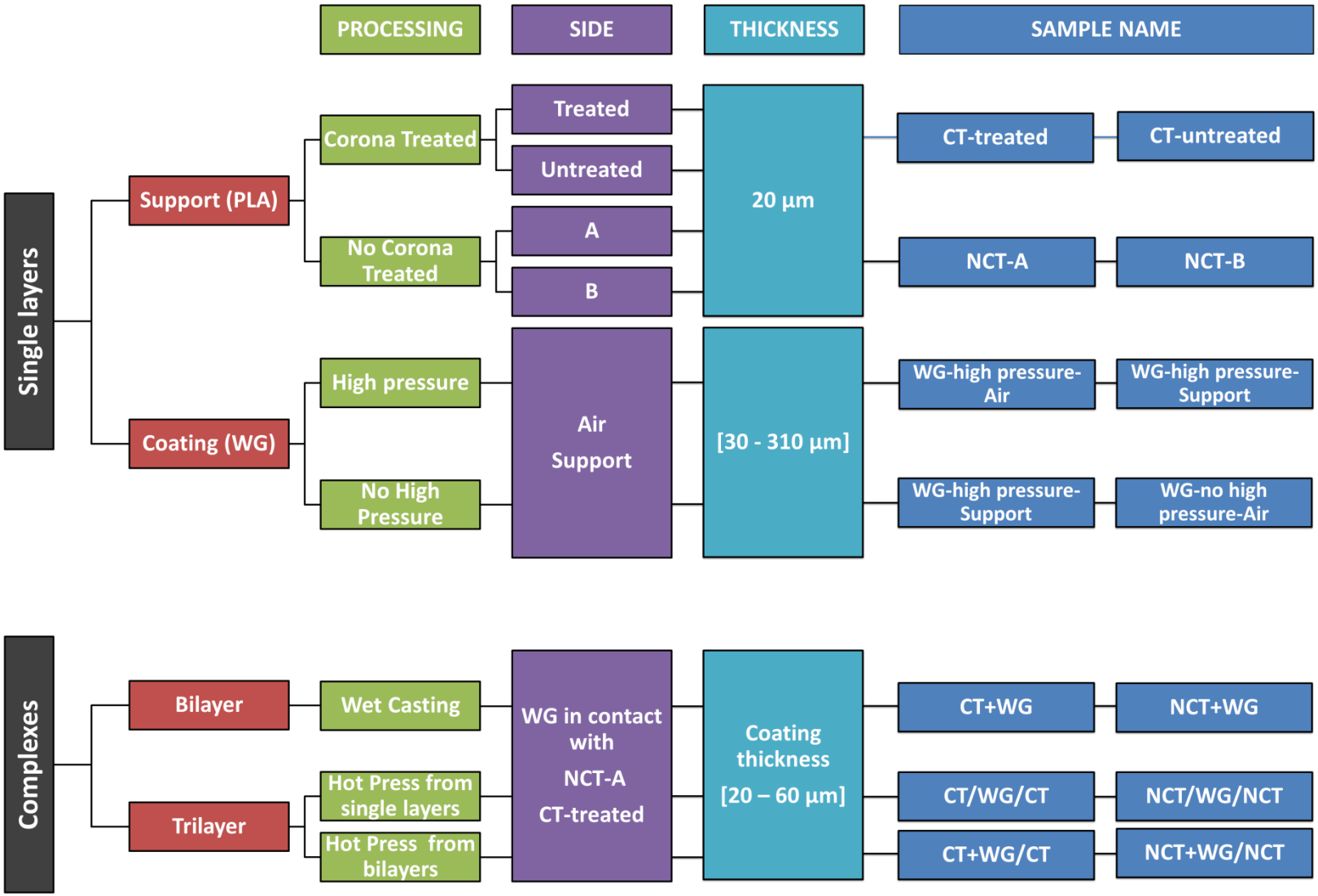

Figure 1. *Sampling design with the processing conditions and samples considered in this study.*

2.3 Characterizations of films

2.3.1 Surface properties

Surface tension

The surface tension of films (γ_s), and its polar (γ_s^p) and dispersive (γ_s^d) components, were determined by goniometry and using the Owens-Wendt method (Equations 2 and 3).[13]

$$\gamma_s = \gamma_s^d + \gamma_s^p \qquad (Eq. 2)$$

$$\gamma_l(1 + \cos\theta) = 2\left(\gamma_s^d \gamma_l^d\right)^{0.5} + 2(\gamma_s^p \gamma_l^p)^{0.5} \qquad (Eq. 3)$$

where, θ, $\gamma_l, \gamma_l^d, \gamma_l^p$ are the contact angle, the surface tension, the dispersive component and the polar component of the liquid used; γ_s^d and γ_s^p are the dispersive and the polar components of the film surface tested. The contact angle is expressed in degrees and all the surface tension parameters are expressed in mN·m^{-1}. Three liquids were used: water, ethylene glycol and diiodomethane. According to Ström *et al.* (1987)[14] and Fowkes (1964)[15], their liquid polar contributions (γ_l^p) are 51.0, 16.8 and 0 mN·m^{-1}, while their corresponding dispersive contributions (γ_l^d) are 21.8, 30.9 and 50.8 mN·m^{-1}, respectively. The contact angles (θ) were measured using the sessile drop method with a goniometer (Drop Shape Analyser 30, Krüss GmbH, Hamburg, Germany) equipped with image analysis software (ADVANCE - Drop Shape, version 1.4.2, Krüss GmbH). Five drops for each liquid (volume ≈ 1 µL) were deposited on film surfaces. The both surfaces of each film were analysed. Measurements were done at 50 % RH and 25 °C in a temperature and RH controlled room.

Work of adhesion

The work of adhesion (W_a) at the interface of PLA – WG complexes was calculated using the Dupré expression (Equation 4).[16]

$$W_a = 2\left(\gamma_1^d \gamma_2^d\right)^{0.5} + 2(\gamma_1^p \gamma_2^p)^{0.5} \qquad (Eq. 4)$$

Where γ_1^d, γ_1^p, γ_2^d and γ_2^p are the dispersive and the polar contributions of the surface tension of the layers 1 (PLA) and 2 (WG), respectively.

T-Peel Test

The T-peel strength of PLA-WG complexes was measured using a texture analyser (TA HD plus, Texture Technologies, Hamilton, MA, USA) according to the D 1876-01 ASTM standard method.[17] The load cell was 5 kg, the crosshead speed was 100 mm·min^{-1} and the trigger force was 0.1 g. At least seven rectangular specimens (15 x 2.5 cm) with unbounded ends (2.5 x 3 cm) were tested for each condition. The test was

performed in the transversal direction (TD) of films. Before analysis, the samples were stored at 50 % RH at 25 °C.

2.3.2 Structural properties

Two-photon microscopy

Two-photon microscopy was performed to investigate the internal structure of wheat gluten films, thanks to fluorescence associated to wheat gluten proteins. Images were collected using a Nikon A1-MP scanning microscope equipped with a Plan Apo IR x 60 objective (NA: 1.27, Water Immersion, Nikon, Tokyo, Japan) at a scanning speed of 1 frame per second. An InfraRed laser (Chameleon, Coherent, Santa Clara, CA, USA) was used to provide a 820 nm excitation. Fluorescence emission was collected on two detection channels: FF01-492/SP-25 (400-492 nm), FF03-525/50-25 (500-550 nm) (Semrock, Rochester, NY, USA). The samples were previously casted on a coverslip and stored at 100 % RH for four days before observation in order to achieve better resolution (Rayleigh resolution value was 360 nm).

Cross-section microstructure

The microstructure of the cross-section of PLA-WG complexes was assessed by SEM (Scanning Electron Microscopy) analysis. Images were collected using a JSM-7600F scanning electron microscope (JEOL USA Inc., Peabody, MA, USA) with 1 kV accelerated voltage, 9 x 10^{-6} Pa vacuum and lower detector (LEI) as secondary electron detector.

Molecular weight distribution

The molecular weight distribution of PLA films was analysed by Size-Exclusion Chromatography (SEC), using a 1260 Infinity liquid chromatography system (Agilent Technologies, Santa Clara, CA, USA). The device was composed of 2 Polypore Size Exclusion columns (Agilent Technologies) connected in series. PLA samples (approx. 50 mg) were completely dissolved in 1 mL of tetrahydrofuran (THF, Carlo Erba reagents, Val de Reuil, France) using a shaker (PL-SP 260VS, Agilent technologies) for 20 min at 25 °C. The dissolved samples were then filtrated using a syringe filter with a PTFE (polytetrafluoroethylene) membrane (pore diameter 0.2 µm, Dominique Dutscher SAS, Brumath, France) and transferred in 1.5 mL vials. 10 µL was automatically injected in the instrument. Filtered THF with a constant flow rate of 1 mL·min^{-1} was used as the mobile phase and a refractive index detector was used in this analysis. The separation was carried out at a controlled temperature of 45 °C. Polystyrene standards ranging from 1.28 to 1820 kDa (Advancing Polymer Solutions, Agilent Technologies) were used for calibration. The number average molecular weight ($\overline{M_n}$), the weight average molecular weight ($\overline{M_w}$) and the polydispersity index (*PDI*) were calculated from the experimental molecular weight distribution curve using Agilent GPC/SEC software (version 1.2, Agilent Technologies) and according to Equations 5, 6 and 7, respectively.

$$\overline{M_n} = \frac{\sum n_i M_i}{\sum n_i} \qquad (Eq. 5)$$

$$\overline{M_w} = \frac{\sum n_i {M_i}^2}{\sum n_i M_i} \qquad (Eq. 6)$$

$$PDI = \frac{\overline{M_w}}{\overline{M_n}} \qquad (Eq. 7)$$

Where M_i is the molecular weight (g·mol^{-1}) of a molecule and n_i is the number of molecules having that molecular weight.

Thermal transitions

The thermal transitions related to amorphous and to crystalline phases of the WG and PLA films were analysed by Differential Scanning Calorimetry (DSC) using a Q20 calorimeter (TA instruments, New Castle, DE, USA). Samples were weighed (WG ≈ 40 mg, PLA ≈ 5 mg) and sealed into T-zero aluminium pans (TA instruments) and submitted to different heating programs at 10 °C·min^{-1} under N_2 atmosphere (flow rate = 25 mL·min^{-1}). Analysis was done using TA Universal Analysis 2000 software (version 4.5 A, TA instruments). At least four samples were analysed for each tested condition.

WG films (amorphous materials) were subjected to a double heating-program from -50 to 100 °C. The first cycle removed the excess of enthalpy associated to the glass transition, the second one allowed better estimating the variation of specific heat (ΔC_p) and the glass transition temperature (T_g inflexion point). PLA films (semicrystalline materials) were subjected to two different heating programs. One down to low temperatures (double heating from -10 to 100 °C) to estimate the thermal transition of the amorphous phase of PLA (T_g and ΔC_p) in a similar way than WG films. The second one up to higher temperatures (double heating from -10 to 190 °C) in order to better study the transitions related to the crystalline phase of PLA, T_m and ΔH_m. In this last case, the thermal parameters were estimated from the first heating, while their reversibility was assessed from the second heating.

The crystallinity percentage (X_c) of PLA films was calculated according to Equation 8.

$$X_c = \frac{\Delta H_m - \Delta H_{cc}}{\Delta H_m^0} \times 100 \qquad (Eq. 8)$$

Where ΔH_m (J·g^{-1}) is the enthalpy corresponding to the area under the melting peak, ΔH_m^0 (= 93 J·g^{-1})[18] is the enthalpy of melting of pure crystalline PLA and ΔH_{cc} (J·g^{-1}) is the enthalpy corresponding to the peak area associated to cold crystallization. Since no cold crystallization was observed in the first heating of the program related to the crystalline phase study, its value is null (ΔH_{cc}= 0 J·g^{-1}).

The percentage of Mobile Amorphous Phase (X_{MAP}) and the percentage of the Rigid Amorphous Fraction (X_{RAF}) in the PLA films were also calculated, according to Arnoult *et al.* (2007)[19] (Equations 9 and 10, respectively).

$$X_{MAP} = \frac{\Delta C_p}{\Delta C_p^0} \times 100 \qquad (Eq. 9)$$

$$X_c + X_{MAP} + X_{RAF} = 1 \qquad (Eq. 10)$$

Where ΔC_p is the measured variation of specific heat for the glass transition associated to the mobile amorphous phase, and ΔC_p^0 is that corresponding to a 100 % amorphous PLA sample ($\Delta C_p^0 = 0.48$ J·g^{-1}·K^{-1}).[19-20] Since two glass transitions were observed in the mobile amorphous phase, the ΔC_p used in the formula was the sum of the both transitions ($\Delta C_p = \Delta C_{p1} + \Delta C_{p2}$).

2.3.3 Transfer properties of films to gases and water vapour

The permeance of films to oxygen (P_{O_2}) and carbon dioxide (P_{CO_2}) was determined using a manometric method on a permeability testing apparatus (GDP-C permeameter, Brugger Feinmechanik GmbH, Munich, Germany) under dry (0 % RH) and wet conditions (50 and 84 % RH) at 25 °C. In dry conditions, the permeation system was previously outgassed under primary vacuum. At time zero, one side of the film was flushed with the gas (at a flow rate of ≈ 100 cm^3·min^{-1}) and the pressure increase was recorded over time on the other side. In wet conditions, only one side of the permeation cell was outgassed, while the other side was flushed by the humidified gas at the desired RH. At time zero, the primary vacuum was stopped and the pressure increase was recorded. The Gas transfer rate (GTR) was measured at the steady state that allowed calculating the permeance according to Equation 11. Analyses were carried out in triplicates. Film samples were previously equilibrated at the same RH of the test before analysis. The permeance to gases was expressed in mol·m^{-2}·s^{-1}·Pa^{-1}.

$$P = \frac{GTR}{p_1 - p_2} = \frac{\Delta n}{A \Delta t (p_1 - p_2)} \qquad (Eq. 11)$$

Where P is the permeance and GTR is the gas transfer rate of oxygen or carbon dioxide (GTR_{O_2} or GTR_{CO_2}), Δn is the variation of moles associated to the pressure increase in the permeation cell (mol), A is the film exposure area (m^2), Δt is the time (s), p_1 and p_2 is the initial gas pressure difference at both sides of the permeation cell (Pa).

The permeance of films to water vapour (P_{H_2O}) was measured gravimetrically at 25 °C using a modified ASTM E96-80 (American Society for Testing and Materials) standard method.[21] Three different relative humidity differentials were tested (0 – 30 % RH, 30 – 75 % RH and 30 – 100 % RH). Film samples were placed and sealed into permeability cells. The permeability cells contained either silica gel (Sigma-Aldrich), NaCl (Sigma-Aldrich) saturated solution or deionized water for maintaining 0, 75 or 100 % RH, respectively.

The permeability cups were then transferred into a climatic chamber maintained 30 % RH and 25°C. The weight of the permeability cup was recorded twice a day using an analytical balance. Analyses were carried out in quadruplicates. The permeance to water was determined from measurement of the water vapour transfer rate (WVTR) at the steady state according to Equation 12.

$$P_{H_2O} = \frac{WVTR}{p_1 - p_2} = \frac{\Delta m}{A\Delta t(p_1 - p_2)} \qquad (Eq. 12)$$

Where WVTR is the water vapour transfer rate, Δm is the weight change of the permeation cell (g), A is the film exposure area (m^2), Δt is the time (s), p_1 and p_2 are respectively the higher and the lower vapour pressure (Pa) of the vapour gradient. The permeance to water vapour was expressed as $g \cdot m^{-2} \cdot s^{-1} \cdot Pa^{-1}$

2.3.4 Thickness

The thickness of films was measured in at least 5 different positions using a micrometer (Coolant Proof micrometer IP 65, Mitutoyo, Aurora, IL, USA).

2.4 Statistical analysis

Data were analysed with Student t-test and, when required (groups > 2), with one–way analysis of variance (ANOVA) and with Tukey-Kramer multiple comparison test, using GraphPad Prism software (version 5.01, GraphPad Software Inc., La Jolla, CA, USA). The significance level of all statistical tests was fixed at 0.05.

3 Results and discussion

3.1 Influence of high pressure homogenization on wheat gluten films

High pressure homogenization is an innovative technology, which seems it has not been previously applied for wheat gluten film production. This section reports on the effects of such technology on the particle size distribution of film forming dispersions, on the macroscopic appearance and on the structure of WG films as well as on its barrier functional properties.

3.1.1 Particle size distribution of film forming dispersion

The film forming dispersions were subjected to high pressure homogenization for 7 cycles at 100 MPa.

The particle size distribution in volume of the film forming dispersions prior to high pressure homogenization followed a unimodal distribution. It was centred on large diameter sizes (≈ 270 µm) (Figure 2). After being homogenised, the particle size distribution shifted to lower values of at least one order of magnitude, and it also turned to a multimodal distribution. The wheat gluten particles were thus sensitive to high pressure and two overlapping populations were clearly observed, one centred on diameters of approx. 15 µm and the other one centred on approx. 3 µm. The corresponding $d_{4,3}$ value, even if it is just a rough indicator when dealing with multimodal distributions, decreased from 314.0 to 8.3 µm after homogenization. Therefore, the high pressure treatment of the film forming solution was applied in order

to help in the dispersion of wheat gluten and to prevent the formation of aggregates in the film, which is a key issue when working with non-water soluble proteins.

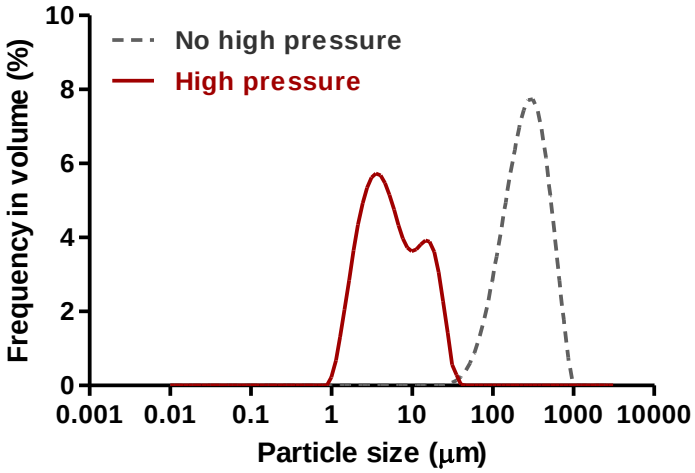

Figure 2. *Particle size distribution of film forming dispersions subjected or not to 7 cycles high pressure homogenization (100 MPa).*

3.1.2 Macroscopic appearance and internal structure by two photon microscopy

The high pressure treatment strongly influenced the appearance of WG films (Figure 3). When the WG films were produced without involving high pressure process, the films were whitish opaque and characterized by the presence of a large quantity of irregular aggregates, which generated a very rough and heterogeneous surface. On the contrary, when high pressure was applied to the film forming dispersion, translucent WG films were obtained, with smooth and homogenous surface, without aggregates.

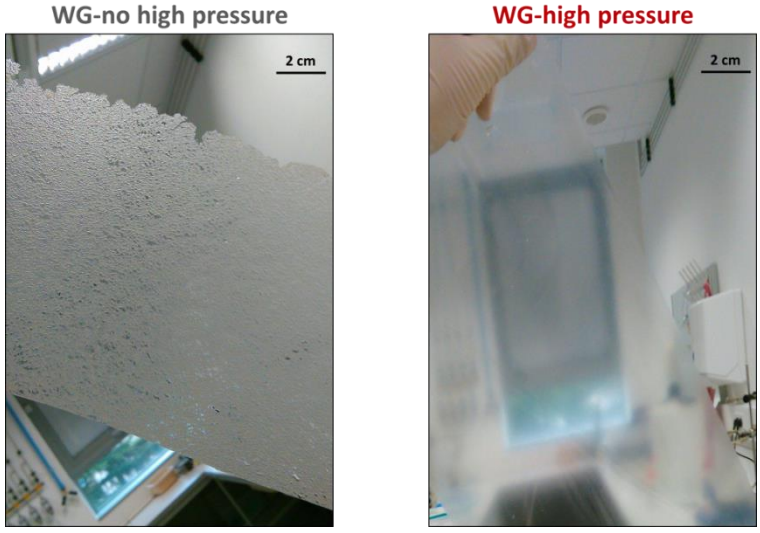

Figure 3. *Appearance of WG films produced from film forming dispersions subjected (WG-high pressure) or not (WG-no high pressure) to high pressure treatment (100 MPa, 7 cycles).*

In other to have more information at the microscopic level, WG films were analysed with two-photon microscopy. This analysis aimed at assessing the distribution of the wheat gluten protein aggregates within the films, based on their fluorescence properties to generate 3D images. Although this technique has mainly been used for imaging of living tissues, it has also successfully been applied for visualizing the distribution of lignin aggregates in chitosan composite films.[22]

Figure 4 clearly shows a different structure of the protein matrix of WG films. From the intensity and distribution of the light blue colour, which corresponds to wheat gluten proteins, it can be easily observed that the wheat gluten protein in WG-no high pressure films was not homogenously distributed. Several protein aggregates of irregular shape were randomly distributed in the film, indicating that a continuous polymer matrix was not properly achieved. It is interesting to notice the big aggregate of around 60 µm observed in the WG-no high pressure image. In contrast, when the high pressure treatment was applied, wheat gluten proteins were more homogenously distributed, as suggested by the continuous light blue colour in the image background, which can be attributed to a protein network. Although some small discontinuities were still observed in WG-high pressure films, the high pressure homogenization was a very suitable strategy for dispersing the wheat gluten and for creating a continuous and better structured polymer matrix.

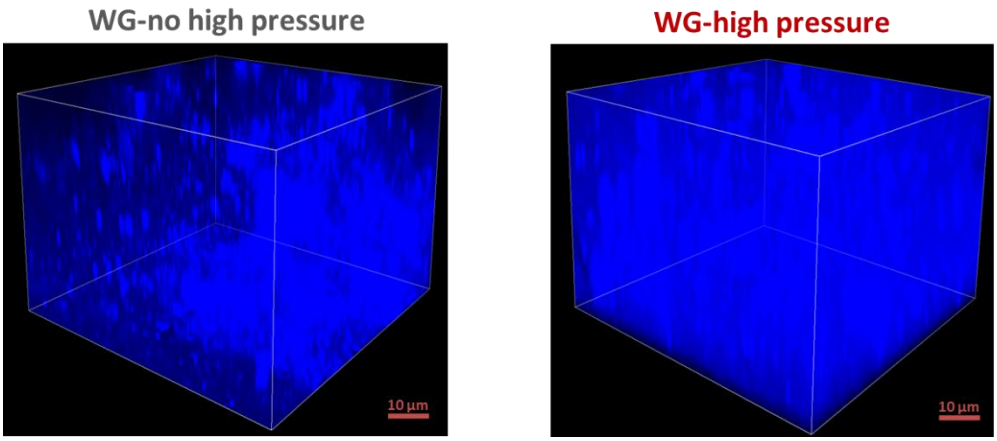

Figure 4. *3D reconstruction of the internal structure of WG films using two-photon fluorescence microscopy. WG films were produced from film forming dispersions subjected (WG-high pressure) or not (WG-no high pressure) to high pressure treatment (100 MPa, 7 cycles).*

The difference in the polymer structuration was also evidenced by a small thickness study of WG-high pressure and WG-no high pressure films (Figure 5). Different volumes of film forming dispersions were used for casting on a same surface area in order to produce films with different thicknesses. The thickness of WG-no high pressure and WG-high pressure films linearly increased when increasing the volume of the casted film forming dispersion. This is in accordance with the corresponding increased quantity of wheat gluten solid matter. Nevertheless, WG-high pressure film thickness was always lower than that of films not submitted to high pressure treatment. WG-high pressure films with thickness around 60 and 240 µm were

produced using around 10 and 40 mL of homogenized film forming dispersions, respectively. In contrast, when the same volumes of non-homogenized dispersion were used, the thicknesses of the corresponding films were 110 and 320 µm, respectively. Since the quantity of solids per volume was constant, the reduced thickness of the WG-high pressure films indicated a better structuration of the polymer network. It means that the interactions between wheat gluten proteins could be favoured by high pressure homogenization. This also induced an increase of the film density as the thickness was reduced for the same amount of dry matter per area unit.

The high pressure homogenization could in fact contribute to increase the structuration and densification of the wheat protein matrix at different levels. For example, the increased exposed surface of the smaller wheat gluten particles as well unfolding protein phenomena induced by the homogenization treatment can highly increase the interaction sites for forming and interconnect the polymer matrix.

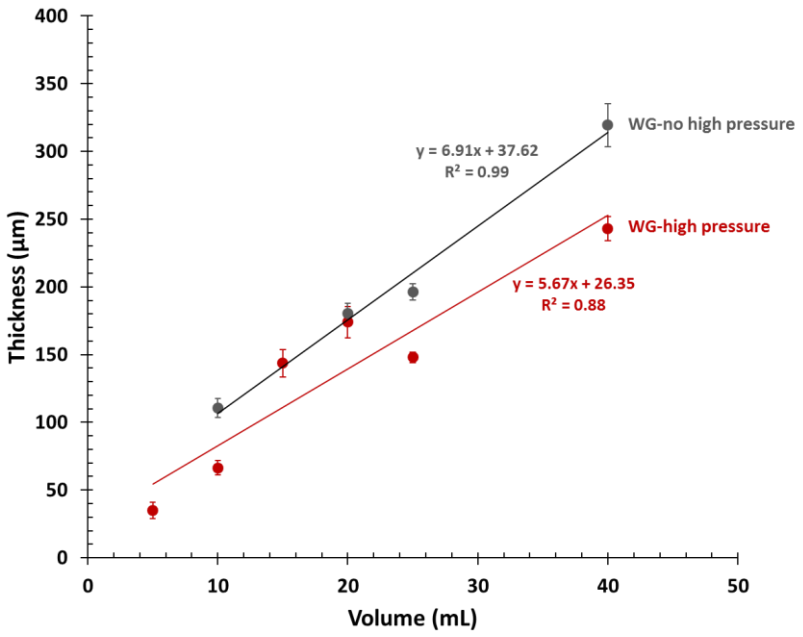

Figure 5. Thickness of WG films deriving from different volumes of the same film forming dispersion.
WG films were produced from film forming dispersions subjected (WG-high pressure) or not (WG-no high pressure) to high pressure treatment (100 MPa, 7 cycles). Lines and equations derived from linear regression. Error bars are standard deviation.

3.1.3 Effects on barrier properties to water vapour and oxygen

The high pressure homogenization also influenced the functional properties of WG films.

Table 1 reports the water vapour transfer rate (WVTR) of WG-high pressure and WG-no high pressure films at three water vapour pressure differentials.

Table 1. *Water vapour transfer rates (WVTR) of WG films at three relative humidity differentials at 25 °C.*

Film	Thickness (μm)	WVTR (10^{-4}·g·m^{-2}·s^{-1})		
		0-30 % RH	**30-75 % RH**	**30-100 % RH**
WG-no high pressure	108 ± 7	3.5 ± 0.5[a]	46.6 ± 1.7[a]	109.6 ± 17.2[a]
WG-high pressure	58 ± 8	2.7 ± 0.3[b]	40.5 ± 1.4[b]	100.5 ± 8.4[a]

Values are reported as mean *± S.D. Significant differences (p. value < 0.05) are indicated with different letters in the same column.*

The analyses for all the three RH differentials clearly confirmed that high pressure homogenization not only allowed producing thinner films, but also improved their water barrier properties. The most probable explanation of this different behaviour comes again from the different structuration and densification of the polymer matrix. A polymer matrix with discontinuities and not well interconnected would generate zones where the transfer of small molecules can easily occur. It is noteworthy that the WVTR of high pressure films, though the films are thinner, is always lower than that of no-high pressure treated films.

It is also interesting to notice that WVTR of both films highly increased with increasing vapour pressure gradients. From the lowest to the highest RH differential, the WVTR was increased by approximately 30 times. This is attributed to the well-known plasticization effect of water molecules.[9, 23] When WVTR were normalized by the effective gradient (*i.e.* water vapour permeance calculation), the permeance values were also increased by approximately 15 times. This deviation from an ideal behaviour indicated the presence of interactions between the permeant (water) and the film, and probably a swelling related to plasticization, which favours the permeation phenomenon.

This behaviour is a well-known phenomenon for hydrophilic materials such as wheat gluten films. They are characterized by a high density of polar groups (*e.g.* hydroxyl, amino, carboxyl, sulfhydryl) from hydrophilic amino acids or plasticizer (glycerol), which interact with water, inducing subsequent plasticization and swelling. This reduces the intermolecular interactions, increases the internal mobility and thus favours the mass transfer of molecules, such as water or gas. As previously shown (Part II, paper 5)[10] the conditions with the highest RH favoured a high sorption of water molecules, which completely modified the internal structure of WG films.

The impact of water plasticization on the barrier properties was further evidenced by the mass transfer of oxygen (Table 2). Table 2 shows the oxygen transfer rate (GTR_{O_2}) measured at three levels of relative humidity (0, 50, 84 % RH) and at 25 °C.

Similar to water vapour transfer, the transfer of O_2 increased of around 30 times from the lower to the higher RH. In this case, such increase was fully attributed to the water plasticization effect and not to the different vapour pressure, since its contribution (2780 Pa of water vapour pressure at 84% RH) to the total pressure gradient was reduced compared to the oxygen pressure (98545 Pa).

Table 2. *Oxygen transfer rate (GTR_{O_2}) of WG-high pressure films at three relative humidity (RH) at 25 °C.*

Film	Thickness (µm)	GTR_{O_2} (10^{-9}·mol·m^{-2}·s^{-1})		
		0 % RH	50 % RH	84 % RH
WG- high pressure	62 ± 4	1.5 ± 0.3^{a}	20.7 ± 1.9^{b}	49.0 ± 1.6^{c}

Values are reported as mean *± S.D. Significant differences (p. value < 0.05) are indicated with different letters in the same row.*

It is very interesting to notice the good barrier properties to O_2 of WG-high pressure in comparison to conventional plastics. Guilbert *et al.* (2002)[7] reported O_2 permeability (dry conditions, 23 °C) of 0.16, 11.9, 11.9 and 16.0 10^{-18}·m^{-1}·s^{-1}·Pa^{-1} for EVOH (ethylene-vinyl alcohol), PET (Poly(ethylenterephtalate)), PA 6 (Polyamide 6) and rigid PVC (poly(vinyl chloride), respectively. The calculated O_2 permeability of the WG-high pressure films in this PhD project was 0.9, 12.9 and 30.9 10^{-18}·mol·m^{-1}·s^{-1}·Pa^{-1} at 0, 50 and 84 % RH, respectively. Mujica-Paz and Gontard (1997)[24] obtained O_2 permeability values more than 10 times higher (156 10^{-18}·mol·m^{-1}·s^{-1}·Pa^{-1}) than ours at 50 % RH and 24 °C in gluten films plasticised with glycerol (33%, protein basis). Probably the high concentration of glycerol used and the lack of homogenization step in such study are the principal reason behind of such difference. Thus, it results evident that the WG films produced in this PhD project can be an interesting alternative to high oxygen barrier plastics, even at 50 % RH. It is noticeable at 84 % RH that the WG films remained in the same order of magnitude than at 50 % RH, indicating that WG keep its good performances also at level of hydration.

The influence of the thickness of WG-high pressure films on the oxygen barrier properties at 50 % RH is reported in Figure 6.

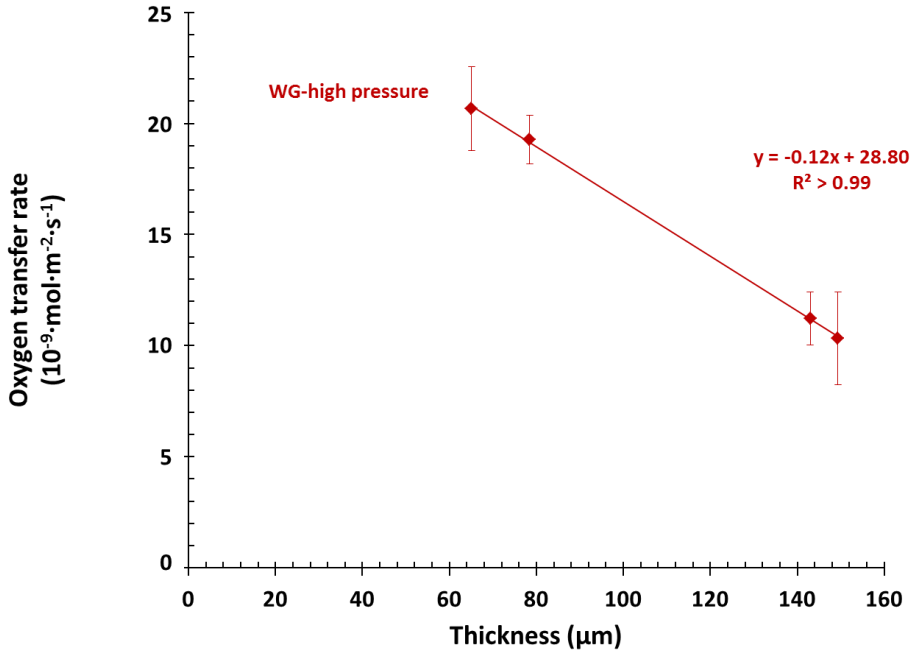

Figure 6. *Oxygen transfer rate (GTR_{O_2}) of WG-high pressure films at 50 % Relative Humidity at 25 °C.* Error bars are standard deviation.

According to the first Fick's law, Figure 6 shows a linear decrease of GTR_{O_2} as a function of the thickness in the range 50-150 µm. From this ideal behaviour, it can be inferred that O_2 did not induce structural changes in the polymer matrix of WG-high pressure during its permeation. It is important to report that it was not possible to carry out the same experiment with WG-no high pressure films. Breakable films and leaks were detected almost in all samples tested, most likely induced by the total pressure difference between both sides of the film (approximately 1000 hPa). The poor structuration of the polymer matrix without any additional treatment during processing could not give to films an appropriate resistance to such pressure difference, generating cracks or micro-cracks.

3.1.4 Surface properties of WG-high pressure films

The surface properties of WG films were assessed in order to better understand the further adhesion with other layers such as PLA. Some interesting differences between the air and the support sides were noticed, indicating that both surfaces might induce a different interfacial behaviour (Table 3).

Table 3. *Surface properties of both sides of WG-high pressure films.*
Contact angle (θ) with liquids with different polarities (water, ethylene glycol and diiodo methane) and surface tension (γ_s) with polar (γ_s^p) and dispersive contributions (γ_s^d).

Film surface	Contact angle(°)			Surface tension (mN·m^{-1})		
	θ_{water}	$\theta_{ethylene\ glycol}$	$\theta_{diiodo\ methane}$	γ_s^p	γ_s^d	γ_s
WG-high pressure-air	91.0 ± 5.2[a]	51.5 ± 3.0[a]	52.0 ± 0.5[a]	1.5	34.3	35.8
WG-high pressure-support	76.4 ± 1.6[b]	33.0 ± 1.4[b]	50.0 ± 2.3[a]	6.1	35.1	41.2

Values are reported as mean *± S.D. Significant differences (p. value < 0.05) are indicated with different letters in the same column.*

The water contact angles at the air surface were significantly higher than those of the support surface (approx. 91 vs 76 °), indicating a much lower water affinity of the surface exposed to drying air. Such difference can be considered surprising, considering that air sides of edible films usually give surfaces with higher water affinity than the surface in contact with the hydrophobic plastic support. In addition, these results were also in contrast with a previous study conducted in WG films produced with ultrasound treatment (Part II, paper 5).[10] Indeed, not only an opposite behaviour was noticed but also a much higher water affinity of both surfaces (θ_{water} ≈ 36 and 50 ° for air and support surfaces, respectively). As a consequence, when the surface tension of both surfaces was calculated in the present study, an important contribution of the polar component to the surface tension appeared for the support surface. Such peculiar behaviour of the WG produced in this present study can be a consequence of the high pressure homogenization treatment, which needs to be understood. Several speculations can be done, such as higher concentration of disulphide bonds (S-S) occurring at the air surface and favoured by the better dispersion of wheat gluten protein.

Corona treatment is a well-known strategy for improving the printability and adhesion properties of conventional plastics with coatings. Recently, this strategy has been also adopted in the industrial production of bioplastics such as PLA. Since one of the aims of this PhD thesis was to develop multilayer complexes PLA-WG-PLA, corona treated and non-corona treated PLA films were considered as support layer. It was thus important to check the impact of this technology and if it would favour a gluten layer deposition/coating

3.2 Influence of corona treatment on PLA film

For the production of PLA-WG complexes, a new industrial batch of PLA films was used in comparison with our previous study dealing with corona treatment (Part II, paper 4).[11] This choice allowed reducing the effects of storage time, especially considering the polarity lost by the materials after been corona treated.

In this section, the effects of corona treatment on the surface, structure and barrier properties of PLA films are reported. Almost all the results agreed with the main findings published in a previous study (Part II, paper 4).[11]

3.2.1 PLA surface properties

Table 4 reports the surface properties of the PLA films subjected or not to corona treatment.

Table 4. *Surface properties of both sides of NCT and CT films.*
Contact angle (θ) with liquids with different polarities (water, ethylene glycol and diiodo methane) and surface tension (γ_s) with polar (γ_s^p) and dispersive contributions (γ_s^d).

Film surface	Contact angle(°)			Surface tension (mN·m^{-1})		
	θ_{water}	$\theta_{ethylene\ glycol}$	$\theta_{diiodo\ methane}$	γ_s^p	γ_s^d	γ_s
NTC-A	77.7 ± 1.6^a	58.0 ± 0.8^a	43.7 ± 0.9^a	4.8	32.9	37.7
NTC-B	72.3 ± 0.7^b	54.4 ± 0.5^b	38.2 ± 1.2^b	6.3	34.5	40.8
CT-untreated	78.3 ± 3.1^a	57.8 ± 2.1^a	49.6 ± 0.6^c	5.3	30.6	35.9
CT-treated	65.8 ± 1.2^c	48.3 ± 1.2^c	46.0 ± 1.6^a	10.6	31.3	41.9

Values are reported as mean *± S.D. Significant differences (p. value < 0.05) are indicated with different letters in the same column.*

In agreement with the well-known effects of the corona treatment, the water contact angle of the CT-treated surface was significantly lower than the three untreated surfaces (NCT-A, NCT-B and CT-untreated). When the three surfaces were compared, no significant difference was noticeable between CT-untreated and NCT-A, but unexpectedly, they differed with NCT-B. The latter surface was more hydrophilic, but largely less than CT-treated. Such results were unexpected and were in contrast with the trend observed in the previous study (Part II, paper 4),[11] where the intermediate behaviour was detected by the CT-untreated surface, which was probably induced by the physical contact with the corona treated surface after production. However, such explanation is not appropriate for the present study. Different reasons could

explain this behaviour, such as contaminations from the line production or manipulations, or it could indicate a different concentration of additives at the surfaces.

From this analysis, the calculation of the surface tension unambiguously confirmed that the corona treatment increased the surface tension of films, by increasing the polar contribution. In our previous study (Part II, paper 4),[11] the XPS (X-ray Photoelectron Spectroscopy) analysis suggested that such increase was due to an increase of oxygen atoms in the very top layers (<10 nm) of CT films.

3.2.2 PLA bulk properties

The modifications in the bulk properties induced by corona treatment were also assessed in this study. Figure 7a shows the first heating (from -10 to 190 °C) DSC curves up to complete melting of PLA films. Figure 7b shows the second heating (from -10 to 100 °C) DSC curves up to lower temperatures, between glass transition and melting. And Table 5 shows the corresponding thermal events.

The calorimetry analysis clearly showed that the corona treatment did not influence the thermal events of PLA films. The parameters associated to the amorphous phase of PLA (T_{g1}, T_{g2}, C_{p1}, C_{p2}) and to the crystalline phase (T_m and ΔH_m) were the same in CT and NCT films. As a result, the X_C, X_{MAP}, X_{RAF} did not change. These results partially agreed with the analysis carried out in a previous batch of PLA film (Part II, paper 4).[11] We detected an increase in the crystallinity degree in the former PLA samples, which most likely was due to a local temperature increase (higher than T_g) that allowed relaxation and crystallization of the oriented chains. It seems thus that during the second batch production of the PLA films, there was a better control of the temperature increase associated to corona treatment.

The number average molecular weight ($\overline{M_n}$), the weight average molecular weight ($\overline{M_w}$) and the polydispersity index (*PDI*) were determined by SEC analysis (Table 5). No modifications were observed in the molecular weight distribution in the PLA films after corona treatment. This analysis thus suggested that no strong chemical reactions occurred during surface modification treatment, such as chain degradation or degradation, confirming the results obtained by ATR-FIR (Attenuated Total Reflectance Fourier InfraRed spectroscopy) and TGA (ThermoGravimetric Analysis) in the previous work (Part II, paper 4).[11]

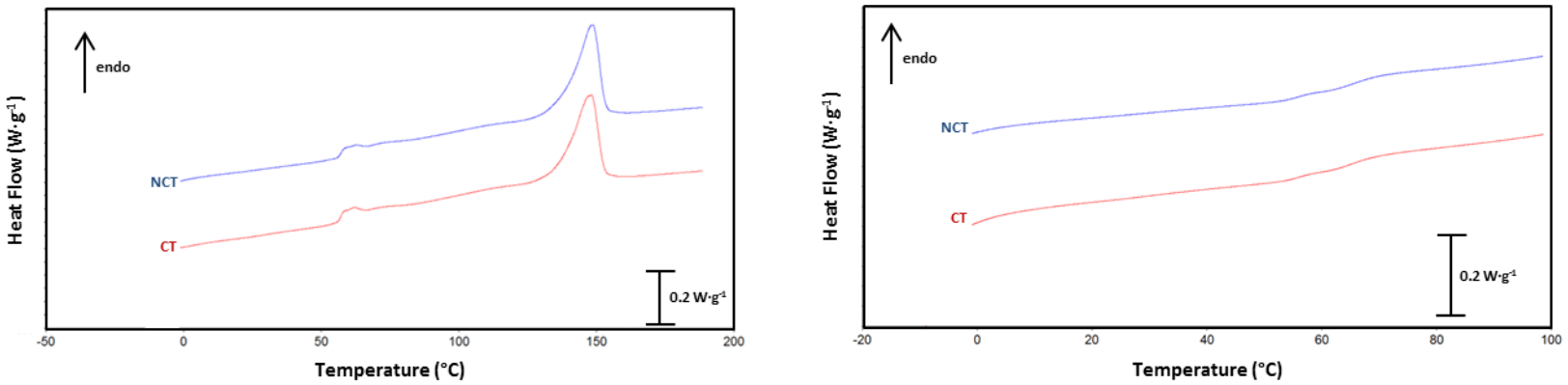

Figure 7. *DSC curves of NCT and CT films. a) First heating from -10 to 190 °C to achieve complete melting. b) Second heating DSC curves of PLA films from -10 to 100 °C (final temperature stopped before melting).*

Table 5. *Chemical and physical properties related to the amorphous and crystalline phases of NCT and CT films.*

	Physical properties[1]									**Chemical properties[2]**		
	Amorphous phase				**Crystalline phase**		**Three phase model**			**Molecular weight distribution**		
Film	T_{g1} (°C)	ΔC_{p1} ($J \cdot g^{-1} \cdot °C^{-1}$)	T_{g2} (°C)	ΔC_{p2} ($J \cdot g^{-1} \cdot °C^{-1}$)	T_m (°C)	ΔH_m ($J \cdot g^{-1}$)	X_c (%)	X_{MAP} (%)	X_{RAF} (%)	$\overline{M_n}$ ($10^3 \cdot g \cdot mol^{-1}$)	$\overline{M_w}$ ($10^3 \cdot g \cdot mol^{-1}$)	*PDI* (-)
NCT	56.4 ± 0.6[a]	0.10 ± 0.01[a]	62.6 ± 0.7[a]	0.19 ± 0.01[a]	148.7 ± 0.2[a]	25.2 ± 1.6[a]	27.1 ± 1.7[a]	61.2 ± 2.2[a]	11.7 ± 2.4[a]	83.0 ± 2.8[a]	172.9 ± 4.3[a]	2.08 ± 0.03[a]
CT	56.6 ± 0.8[a]	0.11 ± 0.01[a]	65.7 ± 1.5[a]	0.19 ± 0.03[a]	148.6 ± 0.4[a]	26.5 ± 1.4[a]	28.5 ± 1.5[a]	63.5 ± 2.9[a]	8.0 ± 2.9[a]	86.3 ± 4.2[a]	176.8 ± 9.1[a]	2.05 ± 0.04[a]

[1] *Determined by DSC analysis.*
[2] *Determined by SEC analysis.*
Values are reported as mean *± S.D. Significant differences (p. value < 0.05) are indicated with different letters in the same column.*
T_{g1} = first glass transition temperature, T_{g2} = second glass transition temperature, ΔC_{p1} = first change in specific heat, ΔC_{p2} = second change in specific heat, T_m = temperature of melting, ΔH_m = enthalpy of melting, X_c = crystallinity percentage, X_{MAP} = mobile amorphous phase percentage, X_{RAF} = rigid amorphous fraction percentage, $\overline{M_n}$ = number average molecular weight, $\overline{M_w}$ = weight average molecular weight and PDI = polydispersity index.

.

3.2.3 Barrier properties of PLA

The impact of corona treatment on the barrier properties was also studied. Table 6 reports the WVTR of both films at three different water pressure gradients.

Table 6. *Water vapour transfer rate (WVTR) and oxygen transfer rate (GTR_{O_2}) of NCT and CT films at different Relative Humidity (RH) conditions at 25 °C.*

Film	Thickness (µm)	WVTR (10^{-4}·g·m^{-2}·s^{-1})			GTR_{O_2} (10^{-7}·mol·m^{-2}·s^{-1})
		0-30 % RH	30-75 % RH	30-100 % RH	0 % RH
NCT	20.0 ± 0.1[a]	5.1 ± 0.2[a]	8.6 ± 0.3[a]	16.4 ± 0.5[a]	8.4 ± 1.3[a]
CT	20.0 ± 0.1[a]	5.3 ± 0.2[a]	8.2 ± 0.4[a]	16.1 ± 0.6[a]	5.3 ± 0.4[b]

Values are reported as mean *± S.D. Significant differences (p. value < 0.05) are indicated with different letters in the same column.*

Table 6 clearly shows that corona treatment did not influence the water barrier properties of PLA films, since no significant difference was observed for any condition tested. It is important to notice that even if PLA films displayed similar WVTR than WG at the driest testing conditions ≈ 5.2 vs 2.7 (10^{-4}·g·m^{-2}·s^{-1}) (Table 1), the water sensitivity of PLA films was largely reduced compared to WG. When the permeance was calculated a slight increase from ≈ 5.5 to 7.3 (10^{7} g·m^{-2}·s^{-1}·Pa^{-1}) was observed in PLA, while the increase in WG films was higher than one order of magnitude. Although the increase in permeance of PLA films (NCT and CT) was reduced, such increase was statistically significant, most likely indicating a small plasticization effect by water molecules.

Table 6 also shows that the oxygen barrier properties of PLA were influenced by corona treatment. A significant reduction of approx. 40 % in the oxygen transfer was observed. In a previous study (Part II, Paper 4),[11] a significant improvement of barrier properties to non-polar gases was also reported after corona treatment. In the case of oxygen, a reduction of around 10 % was observed in dry conditions. We could hypothesize that the increase in polarity associated to the surface treatment was the main reason of such improvement. The results of the present study tent to confirm such hypothesis. Indeed, the polarity of the CT films (θ_{water} = 66 ° and γ_s^p = 11) was higher than the former study (θ_{water} = 71 ° and γ_s^p = 7). In addition, the increase in the oxygen barrier properties cannot be associated to a slight increase of the crystalline phase, as it occurred in the previous study.

3.3 PLA – WG complexes

Hot press process at a lab scale is able to mimic industrial lamination process for making multilayer films. Limited studies reported the fabrication of 2-layers or 3-layers films based on PLA keeping their biodegradability. Only Cho *et al.* (2010) [25] reported the production of wheat gluten and PLA laminates. This complex aims to keep the gas barrier properties of wheat gluten by intercalation between two layers of

PLA, which may protect from moisture plasticization as well as maintaining the biodegradability and sustainability of this complex.

After several tests ranging from 10 to 20 MPa and 110 to 150 °C for 10 min, it was found that the most appropriated condition to produce the PLA-WG complexes was 10 MPa at 130 °C for 10 min. More precisely, the system was heated to 130 °C at 10 °C·min^{-1} and then hot pressed at 10 MPa for 10 minutes. The trilayers were cooled down to 25 °C at 10 °C·min^{-1} and the pressure was released when the samples reached 30 °C. Multilayer shaping processes with higher temperatures induced colour changes in WG films, probably indicating thermal degradation or other chemical reactions. On the other hand, higher pressures increased the frequency of deformed multilayers. The shaping conditions used in this study were similar to those described by Cho *et al*. (2010).[25] The complexes in the present study were produced with the PLA-WG-PLA disposition, either from preformed single layers or from wet casted bilayers (WG+PLA).

The following sections report on the influence of process variables largely used for multilayer production such as corona treatment, coating thickness, layer assembly (as single layers or bilayers) processes (wet coating and/or hot press). Particular attention was paid to their effects on the adhesion and on the barrier performances to water vapour and gases (O_2 and CO_2)

3.3.1 Influence of hot press process on the PLA films

Although the condition adopted during hot press allowed producing PLA-WG complexes, it might also induce modifications in the physical and chemical properties of layers. The temperature of WG and PLA largely exceeded their T_g during processing. As a consequence, the polymer chain mobility increased, which could induce structural changes. Therefore, physical or chemical changes cannot be discarded, especially considering that high pressure could favour new rearrangement of the polymer chains and high temperature may induce crystallization.

As a control, NCT and CT films were thus submitted to hot press with the same temperature, time and pressure conditions than those for multilayer shaping. The modifications of physical structure of NCT and CT films were studied by DSC analysis (Figure 8ab and Table 7). The modifications of the chemical properties driven by strong reactions such as polymerization or degradation were assessed by the SEC analysis (Table 7). The effect on the water and O_2 barrier properties was also determined (Table 8).

Modifications in the physical and chemical properties

Thermograms clearly showed that the crystalline phase of both PLA films (NCT and CT) was highly modified (Figure 8ab and Table 7) in comparison with the thermal events prior to hot press (Figure 7ab and Table 5). An additional melting peak (centred at 131 °C) and consequently a significant increase of the crystallinity (from ≈ 28 to 34 %) were observed in PLA films after being hot pressed. The main melting temperature (centred at 149 °C) appeared not to be influenced, indicating that such processing induced the formation of

less thermostable or imperfect crystals. It is interesting to notice that the melting temperature of the new crystallites can be considered almost the same as the operational temperature. Cold crystallization is a well-known phenomenon occurring when the amorphous chains of materials able to crystallize (such as semicrystalline PLA or PET) are in the rubber state.

No strong modification was observed in the thermal events associated to the amorphous phase before and after hot press. No difference was noticeable in T_{g1}, T_{g2}, and C_{p1}. The hot press only affected C_{p2}. Consequently, the calculated X_{MAP} value was slightly reduced after this treatment. Thus, these results suggested that only the PLA chains of the more constrained mobile amorphous phase were able to cold crystallize during hot press. No modification in the molecular weight distribution was observed after treatment, indicating that no strong chemical reaction such as polymer degradation or polymerization was induced. Lastly, it is also important to notice that no significant difference in the thermal events when the corona treatment was applied neither in the molecular weight distribution was observed in the NCT and CT films after being hot pressed, suggesting that no synergistic effect of both corona and hot press processes occurred.

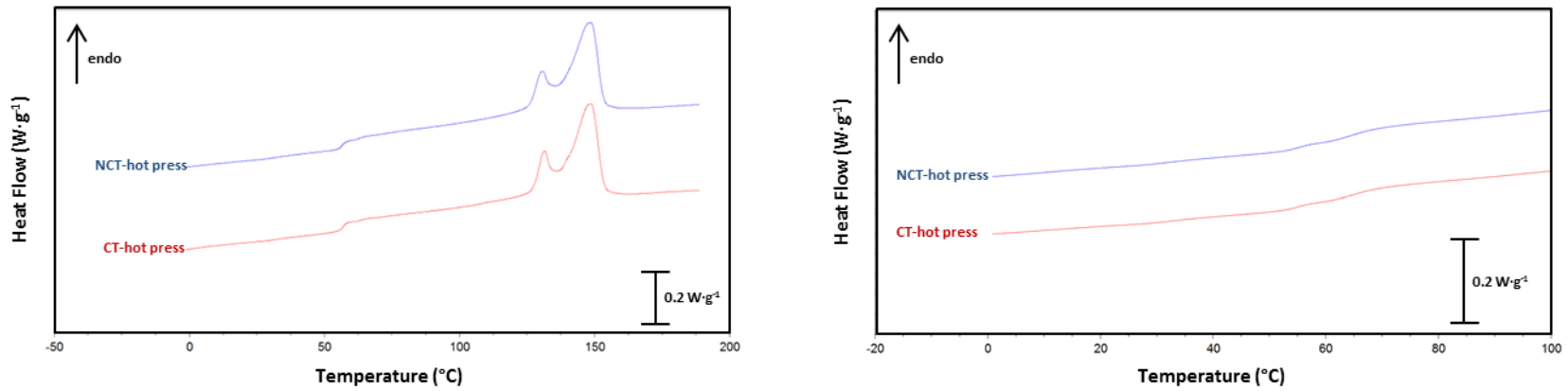

Figure 8. *DSC curves of NCT and CT after been submitted to hot press treatment (NCT-hot press and CT-hot press). a) First heating from -10 to 190 °C to achieve complete melting. b) Second heating DSC curves of PLA films from -10 to 100 °C (final temperature stopped before melting).*

Table 7. *Chemical and physical properties related to the amorphous and crystalline phases of NCT and CT after been submitted to hot press treatment (NCT-hot press and CT-hot press).*

Film	Physical properties[1]										Chemical properties[2]		
	Amorphous phase				Crystalline phase			Three phase model			Molecular weight distribution		
	T_{g1} (°C)	ΔC_{p1} ($J \cdot g^{-1} \cdot °C^{-1}$)	T_{g2} (°C)	ΔC_{p2} ($J \cdot g^{-1} \cdot °C^{-1}$)	T_{m1} (°C)	T_{m2} (°C)	ΔH_m ($J \cdot g^{-1}$)	X_c (%)	X_{MAP} (%)	X_{RAF} (%)	$\overline{M_n}$ ($10^3 \cdot g \cdot mol^{-1}$)	$\overline{M_w}$ ($10^3 \cdot g \cdot mol^{-1}$)	PDI (-)
NCT-hot press	55.2 ± 0.6[a]	0.08 ± 0.01[a]	64.3 ± 0.8[a]	0.15 ± 0.01[a]	131.1 ± 0.3[a]	149.0 ± 0.3[a]	31.2 ± 0.6[a]	33.5 ± 0.7[a]	48.4 ± 1.9[a]	18.1 ± 2.5[a]	87.6 ± 2.8[a]	177.3 ± 4.9[a]	2.02 ± 0.04[a]
CT-hot press	54.9 ± 0.2[a]	0.09 ± 0.01[a]	64.2 ± 0.3[a]	0.14 ± 0.01[a]	131.5 ± 0.1[a]	149.0 ± 0.3[a]	31.8 ± 0.7[a]	34.2 ± 0.7[a]	48.0 ± 2.1[a]	17.8 ± 1.5[a]	84.8 ± 4.1[a]	176.6 ± 9.0[a]	2.08 ± 0.03[a]

[1] *Determined by DSC analysis.*
[2] *Determined by SEC analysis.*
Values are reported as mean *± S.D. Significant differences (p. value < 0.05) are indicated with different letters in the same column.*
T_{g1} = first glass transition temperature, T_{g2} = second glass transition temperature, ΔC_{p1} = first change in specific heat, ΔC_{p2} = second change in specific heat, T_m = temperature of melting, ΔH_m = enthalpy of melting, X_c = crystallinity percentage, X_{MAP} = mobile amorphous phase percentage, X_{RAF} = rigid amorphous fraction percentage, $\overline{M_n}$ = number average molecular weight, $\overline{M_w}$ = weight average molecular weight and PDI = polydispersity index.

Modifications in the barrier properties to water vapour and oxygen

In order to better understand if the over mentioned modifications in the crystalline phase influenced or not the barrier properties of the hot-pressed films, the transfer rate of water vapour at different RH differentials and of oxygen in dry condition were determined (Table 8).

Table 8. *Water vapour transfer rate (WVTR) and oxygen transfer rate (GTR_{O_2}) of NCT-hot press and CT-hot press films at different Relative Humidity (RH) conditions at 25 °C.*

Film	Thickness (μm)	WVTR (10^{-4}·g·m^{-2}·s^{-1})			GTR_{O_2} (10^{-7}·mol·m^{-2}·s^{-1})
		0-30 % RH	30-75 % RH	30-100 % RH	0 % RH
NCT-hot press	20.0 ± 0.1[a]	4.4 ± 0.1[a]	6.9 ± 0.2[a]	12.5 ± 0.4[a]	3.8 ± 0. 1[a]
CT-hot press	20.0 ± 0.1[a]	4.1 ± 0.2[b]	7.5 ± 0.3[b]	10.1 ± 0.4[b]	3.5 ± 0.1 [b]

Values are reported as mean *± S.D. Significant differences (p. value < 0.05) are indicated with different letters in the same column.*

A comparison between the barrier properties of PLA films prior (Table 6) and after hot press (Table 8) revealed that hot press slightly but significantly improved the barrier performances of PLA films, whatever the molecule (H_2O or O_2) or the RH differential tested. Although contradictory results regarding the real influence of crystallinity percentage on the barrier properties of PLA films can be found in the literature, the results of this study indicated that the increase from ≈ 28 to 34 % in the crystalline percentage un ambiguously induced a decrease of transfer rates of water vapour and oxygen through PLA film. The most accepted explanation of such phenomenon is associated to the very limited diffusion of molecules through high order phases such crystals in comparison to the diffusion through amorphous phases.

Dealing with the transfer rate of oxygen, a slight but significant higher barrier properties of CT-hot press films was obtained in comparison to NCT-hot press. It was probably due to the higher polarity as reported in the PLA films prior to hot press (section 3.2.3, Table 6). However, it is important to notice the difference between both films was much smaller after hot press. Prior to hot press, the oxygen transfer was 37 % lower in CT films, while after hot press it was only 8 % lower than NCT-hot press. This behaviour clearly indicated a high influence of the hot press treatment, which was able to bring both films at the same level of barrier properties, probably due to the induced increase in crystallinity. When the barrier properties to water of the films submitted to hot press were compared, a non-clear behaviour was observed in the films submitted to corona treatment, but only a tendency to lower the WVTR values. The improvement of the barrier properties due to corona was masked by hot press, indicating a dominant effect of the crystallinity of films, over its polarity.

3.3.2 Barrier properties of PLA-WG-PLA complexes

The effects of the different variables (*i.e*. corona treatment, coating thickness, coating deposition and hot press) considered during the production of the multilayer complexes on the permeation of water vapour and gases (O_2, CO_2) are reported in the following sections.

Water vapour transfer rate (WVTR)

The WVTR were determined at three different RH differentials at 25 °C in order to simulate different environments, where PLA can be exposed during its use (Table 9). The WVTR values of NCT-hot press, CT-hot press and WG-high pressure are also reported in Table 9 for comparison.

The WVTR of the trilayers at the lowest vapour pressure differential (0 – 30 % RH) displayed similar values for all processing conditions. It thus indicated that the coating thickness, the coating deposition, and contrarily to what was previously observed, the corona treatment did not modify the permeation of water molecules. However, the WVTR of the control films (NCT-hot press, CT-hot press and WG-high pressure) were very similar, indicating that the water permeation at the driest conditions was not controlled by one of the single layers, but influenced by all of them. It means that each layer of the PLA-WG-PLA complex was able to significantly contribute to water barrier efficacy in this RH differential. As a result, the water transfer of the complex was approximately reduced by 60 % in comparison to PLA-hot press films with 40 µm of thickness. This result is of particular interest because it shows that WG films can effectively contribute to reduce the permeation of water molecules of PLA at low RH, even when containing a high quantity of plasticizer (25 wt % glycerol). Therefore, it denotes an intrinsic and an interesting potential of WG films to act also as an effective barrier to water.

For the 30 – 75 % RH differential, the WVTR of WG-high pressure films increased of one order of magnitude, while the WVTR of PLA-hot press films only very slightly increased, compared to the 0-30 % RH differential. The hydrophilic nature of WG films and the more hydrophobic nature of PLA films can be considered as the main factor responsible of such difference in water sensitivity. Nevertheless, this difference also indicated that PLA layers can act as a limiting step for moisture permeation through PLA-WG-PLA complex films. The measured WVTR of complexes clearly confirmed such hypothesis, being very close to the WVTR values of the PLA control film. At this testing condition, no influence of the coating thickness, coating shaping and corona treatment was evidenced. All WVTR values of complexes were around $4.0 \cdot 10^{-4} \cdot g \cdot m^{-2} \cdot s^{-1}$.

When the relative humidity differential increased to 30 – 100 % RH, the role of the PLA layer as a limiting step of the water vapour transfer was even greater. The difference in the WVTR values of the WG control films was of approximately 16 times greater than that of PLA control films, but the measured WVTR of complexes (approx. $6.5 \cdot 10^{-4} \cdot g \cdot m^{-2} \cdot s^{-1}$) was very close to the PLA control film. Also in this case, no effect of coating thickness, coating shaping neither of corona treatment was evidenced.

Table 9. *Water vapour transfer rate (WVTR) of PLA-WG-PLA complexes at three different Relative Humidity (RH) differentials at 25 °C.*

Film type	Film name	Total film thickness (µm)	WG coating thickness (µm)	WVTR (10^{-4}·g·m^{-2}·s^{-1})		
				0 – 30 % RH	30 – 75 % RH	30 – 100 % RH
Control films	NCT-hot press[1]	40 ± 1	-	2.2 ± 0.1	3.4 ± 0.1	6.3 ± 0.2
	CT-hot press[1]	40 ± 1	-	2.0 ± 0.1	3.7 ± 0.1	5.0 ± 0.2
	WG-high pressure[2]	58 ± 8	-	2.7 ± 0.3	40.5 ± 1.4	100.5 ± 8.4
Trilayers from bilayers	NCT+WG/NCT	71 ± 4	31 ± 4	1.3 ± 0.1	4.1 ± 0.1	6.9 ± 0.4
		81 ± 3	41 ± 3	1.4 ± 0.1	4.4 ± 0.3	6.1 ± 0.4
	CT+WG/CT	62 ± 2	22 ± 2	1.7 ± 0.4	3.7 ± 0.1	6.2 ± 0.1
		85 ± 5	45 ± 5	1.3 ± 0.2	3.8 ± 0.2	6.4 ± 0.2
Trilayers from single layers	NCT/WG/NCT	61 ± 2	21 ± 2	1.4 ± 0.2	4.2 ± 0.4	5.7 ± 0.5
		82 ± 5	42 ± 5	1.3 ± 0.4	4.1 ± 0.2	6.9 ± 0.3
	CT/WG/CT	60 ± 1	20 ± 1	1.4 ± 0.1	3.5 ± 0.2	6.4 ± 0.2
		103 ± 12	63 ± 12	1.0 ± 0.4	4.3 ± 0.4	7.9 ± 1.7

[1] *WVTR values calculated from table 8.*
[2] *WVTR values from Table 1.*
Values are reported as mean ± S.D.

Gas transfer rate (GTR_{O_2} and GTR_{CO_2})

The transfer rates of O_2 and CO_2 of the multilayer films were measured at 25 °C at 50 % RH in order to simulate applications for semi-moist food products (Table 10). Since the transfer rates through WG films were highly influenced by the RH, GTR of WG films tested in the same RH condition were used as reference. This choice however was not necessary in the case of PLA-control films, since the impact of the RH is limited. In a previous work, [11] we reported changes lower than 10 % in the GTR_{O_2} and GTR_{CO_2} of CT and NCT films, when the RH rose from 0 to 84 % RH. Similarly, Auras *et al.* (2003) reported a reduction of about 20 % in the O_2 permeability of semicrystalline PLA films having a crystallinity of 25 %, when the RH increased in a larger range, from 0 to 90 % RH at 23 °C.[26] In the same study, the O_2 permeability of semicrystalline PLA films with a crystallinity of 40 % appeared to be constant for these different RH conditions.

Table 9 clearly showed that WG coating improved the barrier properties of PLA to O_2 and CO_2 of approximately 10 to 20 times, indicating that WG coatings efficiently acted as the limiting step for the transfer of both gases. Hosseini *et al* (2015)[27] obtained an improvement of around 8 times of the oxygen barrier properties of PLA using coating layers of fish gelatine in a similar study. In addition, no effect of the corona treatment was evidenced neither for O_2 nor for CO_2, probably because this treatment modified the properties of PLA, but not the transfer limiting step layer (WG. On the contrary, the technologies which directly affect the limiting step (WG), such as coating thickness and layer assembly (preformed single layers or bilayers) are expected to affect to a greater extent the mass transfer.

From a more detailed analysis, it was noticed that the coating thickness and layer assembly used for shaping the multilayers (from preformed single layers or from bilayers) did not influenced the GTR_{O_2}, which varied around $14 \cdot 10^{-9}$ mol·m^{-2}·s^{-1}. The absence of coating thickness effect is surprising, since the dimensions of the limiting layer (WG) changed. They were in contrast with the linear decrease of GTR_{O_2} with the thickness increase of WG films prior hot press (section 3.1.3, Figure 6). Using the equation which describes that linear decrease (Figure 6), the GTR_{O_2} value of complexes corresponds to the GTR_{O_2} of WG films (prior hot press) having thickness around 120 µm, indicating a much efficient reduction of oxygen transfer when the multilayer is shaped.

Similarly, the GTR_{CO_2} values of the complexes did not display a clear effect of the WG thickness. However, they were characterized by an interesting effect of the layer assembly, which need to be understood. In comparison to PLA, the GTR_{CO_2} values decreased approximately 8 times when the WG coating of PLA was used, and approximately 16 times, when the WG film was sandwiched from preformed single layers. Since the major difference between the two layer assembly processes was: 1) in the case of bilayers only one surface adhered to PLA by hot press, because the other face was previously covered by wet casting, 2) in the case of single layers, the two surfaces of WG films adhered to PLA when the hot press was applied.

The double decrease in the CO_2 transfer could thus suggests a densification or reorganization phenomena of WG chains, occurring at the interface PLA/WG, when layer adhesion occurs by hot press. This proposed

Table 10. *Gas transfer rate (GTR) of O_2 and CO_2 of PLA-WG-PLA complexes at 50 % Relative Humidity (RH) at 25 °C.*

Film type	Film name	Total film thickness (μm)	WG coating thickness (μm)	GTR (10^{-9}·mol·m^{-2}·s^{-1})	
				O_2	CO_2
Control films	NCT	40 ± 1		192 ± 3[1]	878 ± 17 [4]
	CT	40 ± 1		175 ± 1[2]	721 ± 18[5]
	WG	65 ± 4		21 ± 2[3]	
Trilayers from bilayers	NCT+WG/NCT	74 ± 5	34 ± 5	12 ± 2	116 ± 31
		91 ± 7	51 ± 7	16 ± 5	110 ± 12
	CT+WG/CT	69 ± 5	29 ± 5	17 ± 2	111 ± 3
		87 ± 8	47 ± 8	14 ± 2	96 ± 17
Trilayers from single layers	NCT/WG/NCT	59 ± 2	19 ± 2	15 ± 3	62 ± 13
		83 ± 3	43 ± 3	11 ± 3	39 ± 17
	CT/WG/CT	66 ± 5	26 ± 5	14 ± 1	65 ± 4
		93 ± 5	53 ± 5	9 ± 1	35 ± 10

[1] NCT-hot press, calculated from Table 8, analysis done in dry conditions at 25 °C.
[2] CT-hot press, calculated from Table 8, analysis done in dry conditions at 25 °C.
[3] WG-high pressure, calculated from Table 1, analysis done at 50 % RH at 25 °C.
[4] NCT calculated from Rocca-Smith et al.(2016),[11] analysis done in dry conditions at 25 °C.
[5] CT calculated from Rocca-Smith et al.(2016),[11] analysis done in dry conditions at 25 °C.
Values are reported as mean ± S.D.

phenomenon could explain the absence of thickness effect in the gas transfer since thinnest limiting layer were probably formed. This phenomenon was probably not completely evidenced in the previous analysis (since no effect of layer assembly in GTR_{O_2} was observed), because of the low transfer O_2, which masked or hindered the effects of densification or restructuration when submitted to temperature and pressure.

3.3.3 Adhesion of layers

Corona treatment has been largely used by industries since several decades in order to enhance the surface hydrophilicity, printability and adhesion properties of conventional plastic films. And since a few years, this surface modification technology is also used in the industrial production of alternative materials such as PLA films and other bioplastics. Although, several typologies of PLA material treated by corona are now available in the market, limited information related to the real influence of such industrial technology is available in literature. Additionally, the scientific studies involving this topic are usually not done at industrial scale production. This is of critical importance considering that industries use standardized and optimized procedures to improve or tailor the PLA film surface properties, which are very difficult to reproduce at laboratory scale. This is the main reason behind the choice of PLA films and corona treatment applied at industrial scale. A preliminary study dealing with the induced modification in the surface, structure and barrier properties of PLA films has been first carried out.[11] However, more specific studies were further required in order to understand if the increase in the surface tension and in its polar contribution associated to the corona treatment influenced the adhesion between PLA and WG layers and the barrier properties of the resulting complexes. Although no conclusive answers were obtained regarding the real influence of corona treatment in the adhesion of WG layer when hot press technology was applied, some interesting phenomena at the interlayer (WG/PLA) were observed. This section reports on these investigations of the influence of corona treatment, in particular on the adhesion properties of PLA-WG-PLA complexes.

The work of adhesion of all the interfaces between CT (CT-treated, CT-untreated), NCT (NCT-A, NCT-B) and WG films (WG-ait, WG-support) in the WG sandwiched disposition were determined (Table 11) from the contact angle measurements previously reported in Table 3 and 4. We have to specify that contact angle measurements were not determined after delamination on the surfaces of films in contact between layers, but only on films surface prior layer assembly and hot press process.

Although the work of adhesion parameters were calculated values from the polar and dispersive contributions to the film surface tension, they are of high importance for practical industrial applications. They give an estimation of the potential adhesivity between the layers. If the polar contributions to the surface tension of both layers are similar, their adhesion would be easier, and the calculated work of adhesion would be higher. For industrial applications, work of adhesion values higher than 70 $mN \cdot m^{-1}$ are considered adequate for latex painting applications to surfaces, values around 65 $mN \cdot m^{-1}$ for organic applications to metals, and values of 60 $mN \cdot m^{-1}$ are appropriate for printing paper and polymer films.[28]

From these considerations, it is clear that the adhesion between WG and PLA layers should be good for all cases, even for interfaces not developed in this study. In this study the WG layer are always in contact with surface CT-treated or with the surface NCT-A. In addition, the surface tension of layers shows that the dispersive contribution clearly dominates the interactions at the interface PLA/WG.

Since the determination of W_a is generally subjected to 5 % of error, no strong effects were observed for any surface considered. However, mean W_a values tend to slightly increase when surfaces treated by corona are considered, suggesting a slight improvement of the adhesivity of PLA/WG.

Table 11: *Work of adhesion of film surfaces determined from contact angle measurement at 25°C and 50% RH.*

Layer interface	**Work of adhesion (mN·m^{-1})**	**Surface tension (mN·m^{-1})[1]**				
	W_a	γ_1^p	γ_1^d	/	γ_2^p	γ_2^d
<u>Interfaces developed in this study</u>						
CT-treated/WG-air	74	10.6	31.3	/	1.5	34.3
CT-treated/WG-support	82	10.6	31.3	/	6.1	35.1
NCT-A/WG-air	73	4.8	32.9	/	1.5	34.3
NCT-A/WG support	79	4.8	32.9	/	6.1	35.1
<u>Interfaces non developed in this study</u>						
CT-untreated/WG-air	70	5.3	30.6	/	1.5	34.3
CT-untreated/WG-support	77	5.3	30.6	/	6.1	35.1
NCT-B/WG-air	75	6.3	34.5	/	1.5	34.3
NCT-B/WG-support	82	6.3	34.5	/	6.1	35.1

[1] *Surface tension values for WG and PLA films were taken from Table 3 and 4, respectively.*
Values are reported as mean.
W_a = work of adhesion, γ_1^p = polar contribution to the surface tension of the PLA layer, γ_1^d = dispersive contribution to the surface tension of the PLA layer, γ_2^p = polar contribution to the surface tension of the WG layer and γ_2^d = dispersive contribution to the surface tension of the WG layer

To further understand the influence of corona treatment on the adhesion properties, the T-peel strength of CT and NCT layers adhering to WG by hot press was determined. The D 1876-01 ASTM standard method was used. The interfaces considered were CT-treated/WG-air and NCT-A/WG-Air from trilayer complexes deriving from pre formed bilayers (Table 12).

Table 12. *T-peel strength of CT and NCT layers adhering to WG by hot press*.

Layer interface	T-peel strength ($N \cdot m^{-1}$)
CT-treated/WG-air	0.8 ± 0.2^{a}
NCT-A/WG-air	1.1 ± 0.3^{a}

Values are reported as mean *± S.D. Significant differences (p. value < 0.05) are indicated with different letters in the same column.*

Surprisingly very low T-peel strength values were measured in this study, in contrast with the work adhesion values. They were approximately two order of magnitude lower than the values reported by Cho *et al.* (2010)[25] in a similar work, which involved the production and characterization of PLA/WG/PLA laminates. In addition, these findings also indicated that corona treatment did not influence the adhesion of PLA and WG layers in the interface studied. In order to better understand the possible reason of this unexpected behaviour, a comparison analysis in the production of the complexes was necessary. The particular conditions adopted by Cho *et al.* (2010)[25] for WG film making suggested a key role of the water content. They produced WG films with very low water content, by hot pressing dough mixtures of wheat gluten and glycerol, without adding water. In contrast, the WG films used in the present study were hydrated and equilibrated at 50 % RH (water content ≈ 10 % wt%, dry basis)[10] before being submitted to hot press. Therefore, when our complexes were formed, evaporation of water molecules also occurred at the WG/PLA interface, while in the study of Cho *et al.* (2010)[25] that phenomenon was limited. Evaporation could have induced shrinkage of polymer chains, reducing the effective contact area with the PLA layer and thus adhesion. It is very interesting to notice that evaporation and the presence of water vapour at the interface could also explain the hypothesis of densification or restructuration of WG occurring at the interface PLA-WG, previously advanced in the discussion of CO_2 transfer properties.

Figure 9 shows the cross section microstructure of a NCT+WG/NCT complex with a WG coating of approximately 25 µm, obtained by SEM analysis.

The microstructure analysis tends to confirm our hypothesis. Firstly, two clear phenomena occurred at each interface PLA-WG. One interface was clearly adhered, and no discontinuities or empty spaces were observed. At the other interface, the contact of layers was very limited, and presented discontinuities of ≈ 1 µm, indicating a poor adhesion. The former interface was the one formed by wet casting prior to hot press operation (WG+PLA). The latter corresponds to the interface formed by hot press (WG/PLA). Considering the WG layer, the microstructure suggested a different physical structure. Several irregularities nearby to the WG/PLA interface were observed, possibility indicating a more brittle behaviour of WG in that region than in the proximity of the other interphase (WG+PLA), favoured by water evaporation. These findings thus indicate that the different interphases created by the two coating deposition techniques (*i.e.* solvent casting vs hot press) have important role in the adhesion properties of layers.

From these results therefore results evident that the influence or not of corona treatment on adhesion of layers was masked by the effect of processing, when the interfaces WG/PLA are formed by wet WG films and hot press.

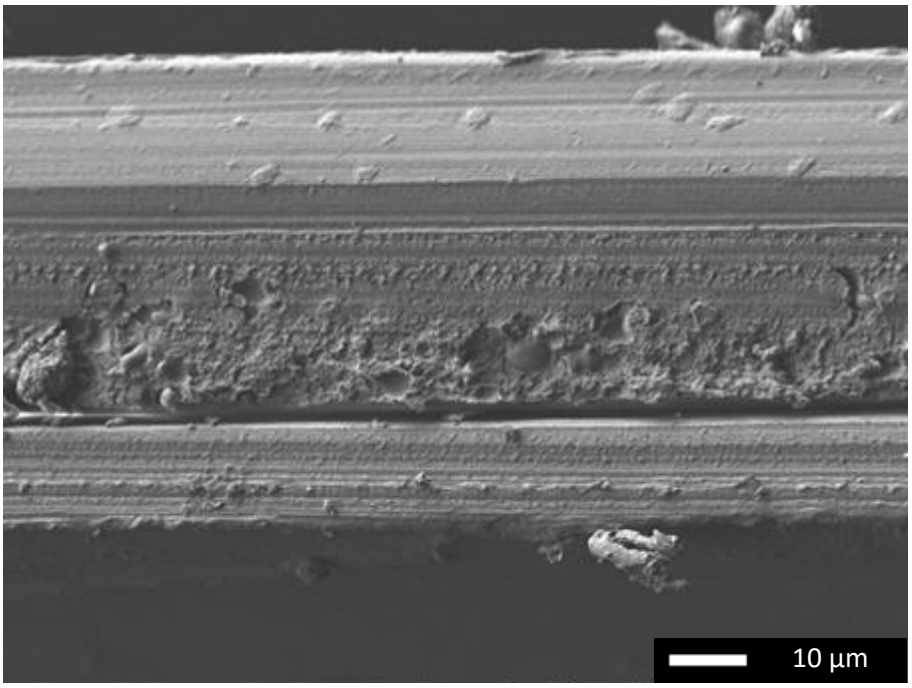

Figure 9. *Cross section microstructure of a NCT+WG/NCT complex with a WG coating of approximately 25 µm.*

4 Conclusions

This study unambiguously showed that the development of PLA-WG-PLA increased of approximately 10 times the overall barrier properties of WG and PLA. This improvement can be considered satisfactory considering that the transfer rates were determined in realistic conditions for food packaging application (50 % RH) and not in dry conditions, where the improvement should more efficient. The reduction of the transfer rates of O_2 and CO_2 was driven by WG layers, while the reduction of the water vapour rates was driven by the PLA layers. Both types of films (PLA and WG), thus acted as complementary limiting step to mas transfer.

Considering the effects of different technologies applied to the single layers, it has been shown that high pressure homogenization induced a more efficient structuration of the wheat gluten polymer matrix, improving the overall functional properties of WG films. Corona treatment increased the surface tension of PLA films by increasing the polar contribution. The barrier properties to O_2 were improved of approximately 40 % by corona treatment probably due to the higher polarity of films.

When the multilayers were shaped, a strong influence of hot press over the corona technology was observed. Hot press induced further crystallization in PLA, which increased its overall barrier properties of approximately 40 % and 60 %, for water and oxygen respectively. Since the improvement of barrier properties associated to hot press was higher than corona treatment, no strong effects of corona treatment

was observed when both technologies were applied. Hot press most likely also induced a particular wheat gluten restructuration driven by water evaporation phenomenon at the interface WG/PLA, which generated a limited adhesion of layers but unexpectedly improved the barrier properties to gases of complexes.

References

1. Tsuji, H., Hydrolytic degradation. In *Poly(lactic acid): synthesis, structures, properties, processing, and applications*; Auras, R.; Lim, L.-T.; Selke, S. E. M.; Tsuji, H., Eds.; Wiley: Hoboken, N.J., 2010.

2. Rasal, R. M. Surface and bulk modification of Poly(lactic acid). Clemson University, Clemson, SC, 2009. PhD thesis.

3. Witzke, D. R. Introduction to properties, engineering, and prospects of polylactide polymers. Michigan State University East Lansing, MI, 1997. PhD thesis.

4. Auras, R.; Harte, B.; Selke, S. An overview of polylactides as packaging materials. *Macromolecular Bioscience* **2004,** *4* (9), 835-864.

5. Fabra, M. J.; Busolo, M. A.; Lopez-Rubio, A.; Lagaron, J. M. Nanostructured biolayers in food packaging. *Trends in Food Science & Technology* **2013,** *31* (1), 79-87.

6. Baldwin, E. A.; Hagenmaier, R. D.; Bai, J. *Edible coatings and films to improve food quality*; CRC Press: Boca Raton, FL, 2012.

7. Guilbert, S.; Gontard, N.; Morel, M. H.; Chalier, P.; Micard, V.; Redl, A., Formation and properties of wheat gluten films and coatings. In *Protein-based films and coatings*; Gennadios, A., Ed. CRC Press: Boca Raton, 2002.

8. Gontard, N.; Thibault, R.; Cuq, B.; Guilbert, S. Influence of relative humidity and film composition on oxygen and carbon dioxide permeabilities of edible films. *Journal of Agricultural and Food Chemistry* **1996,** *44* (4), 1064-1069.

9. Gontard, N.; Ring, S. Edible wheat gluten film: influence of water content on glass transition temperature. *Journal of Agricultural and Food Chemistry* **1996,** *44* (11), 3474-3478.

10. Rocca-Smith, J. R.; Marcuzzo, E.; Karbowiak, T.; Centa, J.; Giacometti, M.; Scapin, F.; Venir, E.; Sensidoni, A.; Debeaufort, F. Effect of lipid incorporation on functional properties of wheat gluten based edible films. *Journal of Cereal Science* **2016,** *69*, 275-282.

11. Rocca-Smith, J. R.; Karbowiak, T.; Marcuzzo, E.; Sensidoni, A.; Piasente, F.; Champion, D.; Heinz, O.; Vitry, P.; Bourillot, E.; Lesniewska, E.; Debeaufort, F. Impact of corona treatment on PLA film properties. *Polymer Degradation and Stability* **2016,** *132*, 109-116.

12. Mie, G. Contributions to the optics of turbid media, particularly of colloidal metal solutions. *Annalen der Physik* **1908,** *25*, 377-445.

13. Owens, D. K.; Wendt, R. C. Estimation of the surface free energy of polymers. *Journal of Applied Polymer Science* **1969,** *13* (8), 1741-1747.

14. Ström, G.; Fredriksson, M.; Stenius, P. Contact angles, work of adhesion, and interfacial tensions at a dissolving hydrocarbon surface. *Journal of Colloid and Interface Science* **1987,** *119* (2), 352-361.

15. Fowkes, F. M. Attractive forces at interfaces. *Industrial & Engineering Chemistry* **1964,** *56* (12), 40-52.

16. Dupre, A. *Theorie mecanique de la chaleur*;Gauthier-Villan: Paris, 1869.

17. ASTM D 1876-01, 2001 Standard Test Method for Peel Resistance of Adhesives (T-Peel Test). In: *Annual Book of ASTM Standards.* American Society for Testing and Materials, Philadelphia, PA.

18. Fischer, E. W.; Sterzel, H. J.; Wegner, G. Investigation of the structure of solution grown crystals of lactide copolymers by means of chemical reactions. *Kolloid-Zeitschrift und Zeitschrift für Polymere* **1973,** *251* (11), 980-990.

19. Arnoult, M.; Dargent, E.; Mano, J. F. Mobile amorphous phase fragility in semi-crystalline polymers: Comparison of PET and PLLA. *Polymer* **2007,** *48* (4), 1012-1019.

20. Delpouve, N.; Arnoult, M.; Saiter, A.; Dargent, E.; Saiter, J. M. Evidence of two mobile amorphous phases in semicrystalline polylactide observed from calorimetric investigations. *Polymer Engineering and Science* **2014,** *54* (5), 1144-1150.

21. ASTM E96-80, 1990. Standard test method for water vapor transmission of materials. In: *Annual Book of ASTM Standards.* American Society for Testing and Materials, Philadelphia, PA.

22. Crouvisier-Urion, K.; Bodart, P. R.; Winckler, P.; Raya, J.; Gougeon, R. D.; Cayot, P.; Domenek, S.; Debeaufort, F.; Karbowiak, T. Biobased composite films from chitosan and lignin: antioxidant activity related to structure and moisture. *ACS Sustainable Chemistry & Engineering* **2016,** *4* (12), 6371-6381.

23. Gontard, N.; Guilbert, S.; Cuq, J. L. Water and glycerol as plasticizers affect mechanical and water-vapor barrier properties of an edible wheat gluten film. *Journal of Food Science* **1993,** *58* (1), 206-211.

24. Mujica-Paz, H.; Gontard, N. Oxygen and carbon dioxide permeability of wheat gluten film: effect of relative humidity and temperature. *Journal of Agricultural and Food Chemistry* **1997,** *45* (10), 4101-4105.

25. Cho, S.-W.; Gallstedt, M.; Hedenqvist, M. S. Properties of wheat gluten/poly(lactic acid) laminates. *Journal of Agricultural and Food Chemistry* **2010,** *58* (12), 7344-7350.

26. Auras, R.; Harte, B.; Selke, S. Effect of water on the oxygen barrier properties of poly(ethylene terephthalate) and polylactide films. *Journal of Applied Polymer Science* **2004,** *92* (3), 1790-1803.

27. Hosseini, S. F.; Javidi, Z.; Rezaei, M. Efficient gas barrier properties of multi-layer films based on poly(lactic acid) and fish gelatin. *International Journal of Biological Macromolecules* **2016,** *92*, 1205-1214.

28. GmbH, K. *Adhesion energy and interfacial tension (application report AR232e)*; 2003.

CONCLUSIONS AND PERSPECTIVES

Conclusions and perspectives

Poly(lactic acid) (PLA) is considered as the most promising substitute of conventional plastics. Even if it is mainly used for food packaging applications, some drawbacks limit its applications. On the one hand, its low barrier performance to gases (*e.g.* O_2 and CO_2) limits its use for applications requiring low gas transfer, such as modified atmosphere packaging (MAP) or for carbonate beverage packing. On the other hand, its natural water sensitivity which contributes to its biodegradation, limits its use for high moisture foods with long shelf life. Biodegradable/bio-sourced materials such as protein or polysaccharide can be considered as interesting materials because of their complementary properties to PLA. They are much more water sensitive, but they display better gas barrier properties in dry surroundings. Literature suggested that the barrier properties of wheat gluten films (WG) to oxygen are from 10 to 100 times better than that of PLA films. This complementarity in barrier performances drove us to study the development of multilayer complexes PLA-WG-PLA and to open un-explored application scenarios for these biopolymers.

This PhD project was thus intended to better understand how food components and use conditions could affect the performances of PLA films and how these performances could be optimized by surface modifications. To that aim two objectives were targeted:

- To study the stability of PLA films in contact with different molecules (carbon dioxide and water), in contact with vapour or liquid phases, with different pH.
- To assess the impact of surface treatments (such as corona treatment and coatings) and consequently their combination with wheat gluten as multilayers to increase the overall barrier properties.

Different processing technologies and methodologies were adopted to mimic industrial applications and storage/utilization conditions. The physical and chemical properties of PLA films were investigated at both the bulk and surface levels. Different techniques coming from material science and food science were used, such as Differential Scanning Calorimetry (DSC), ThermoGravimetric Analysis (TGA), uniaxial tensile analysis, permeability measurements, Size-Exclusion Chromatography (SEC), Atomic Force Microscopy (AFM), Scanning Electron Microscopy (SEM), Attenuated Total Reflectance Fourier Transform InfraRed spectroscopy (ATR-FTIR) and X-ray Photoelectron Spectroscopy (XPS).

Aiming at the use of PLA films for modified atmosphere packaging or for carbonated beverage, we studied the behaviour and changes of PLA structure and chemistry when exposed to high pressure of CO_2. The interactions between PLA and CO_2 only influenced the physical properties of PLA but not its chemical

properties. The CO_2 sorption isotherm at 25 °C gave strong evidence of a physisorption mechanism and of a hysteresis phenomenon particularly at the lowest pressures. The hysteresis is due to a plasticization and swelling phenomena induced by CO_2, which not only modified the PLA structure, but at the same time modified its functional properties. CO_2 plasticization reduced the glass transition temperature of PLA. Consequently, the permeability and solubility coefficients to CO_2 increased and the physical ageing of the polymer was accelerated (Figure 1).

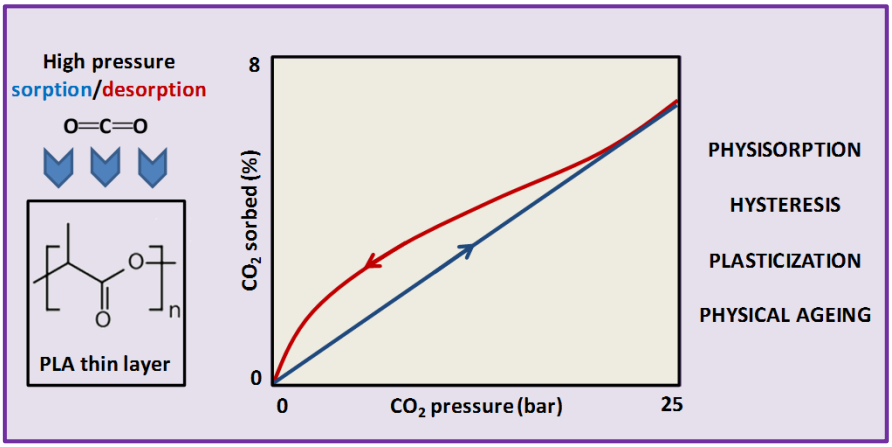

Figure 1. *"How high pressure CO_2 impacts PLA film properties".*

These results were of significant scientific importance, since it was the first time that physisorption, hysteresis and physical ageing phenomena driven by CO_2 have been reported in PLA to our knowledge. CO_2 plasticization effect should be taken in consideration in industrial applications if PLA is submitted to high pressure processing in the presence of CO_2, for example for decontamination of the packaging surface or of packed foods. It would induce modifications in the functional properties of films. However in applications where the CO_2 pressure is low, such as MAP (CO_2 pressure slightly higher than 1 atm) or carbonate beverage (CO_2 pressure around 3 – 4 bars) the sorption of CO_2 is limited enough (approximately 1 % wt) to induce significant modifications. This finding thus confirms that the main drawback related to PLA for food packing applications in contact with CO_2 is its high permeability. This could be faced through surface modification technologies such as coatings. Nevertheless, our study related to the impact of CO_2 on the PLA film behaviour was conducted in dry conditions. Therefore, a further investigation of influence of CO_2 in the presence of moisture (liquid or vapour) would be welcome.

Since the applications for MAP or for other food packing applications not only involve interactions with CO_2, but also with water molecules coming from the food or from the surrounding atmosphere, it was necessary to study the stability of PLA at different wet environments. PLA was thus exposed to various moist environments ranging from 50 to 100 % RH or immersed in liquid water for approximately two months. The effects of water molecules on the stability of PLA (kinetic aspects) were studied using accelerated storage tests at 50 °C (Figure 2). The modifications of its physical (appearance, amorphous phases, crystalline

phases) and chemical properties (molecular weight distribution, surface hydrophobicity) were assessed. The temperature of the storage tests was lower but close to glass transition temperature in order to accelerate phenomena, without inducing strong physical changes such as transition from glassy to rubbery state. In these conditions, the interaction with water vapour molecules surprisingly accelerated PLA changes. The investigations undoubtedly evidenced that the chemical potential of water and its physical state (liquid or vapour) influenced the stability PLA films and its hydrolysis mechanism. When the chemical potential of water (or water activity) increased, the hydrolysis rate increased, and the modifications were accelerated. An increase from 50 to 100 % RH accelerated of seven times the rate of decrease of the molecular weight and of 8 times the rate of increase of the crystallinity, both associated to hydrolysis. Indeed, the transparency was reduced, the glass transition decrease by 30 °C, the crystallinity increased from 24 to 37 %. In addition, hydrolysis also drove to the production of hydrophilic and acidic degradation products, which actually act as catalyst of the hydrolysis reaction. A different behaviour of degradation products was observed according to the physical state water. When PLA was exposed to water vapours in a range of 50 to 100 % RH, the degradation products were accumulated in the polymer matrix, increasing water sorption and reactivity. On the contrary, when PLA was immersed in liquid water, degradation products migrated toward the film surface and were solubilised into the aqueous medium in contact with. As a result, the hydrolysis rate of the PLA films exposed to environments at water activity close to one (100% RH in vapour phase) was 30 % higher than the hydrolysis rate of films immersed in liquid water, even if the chemical potential were comparable (≈1).

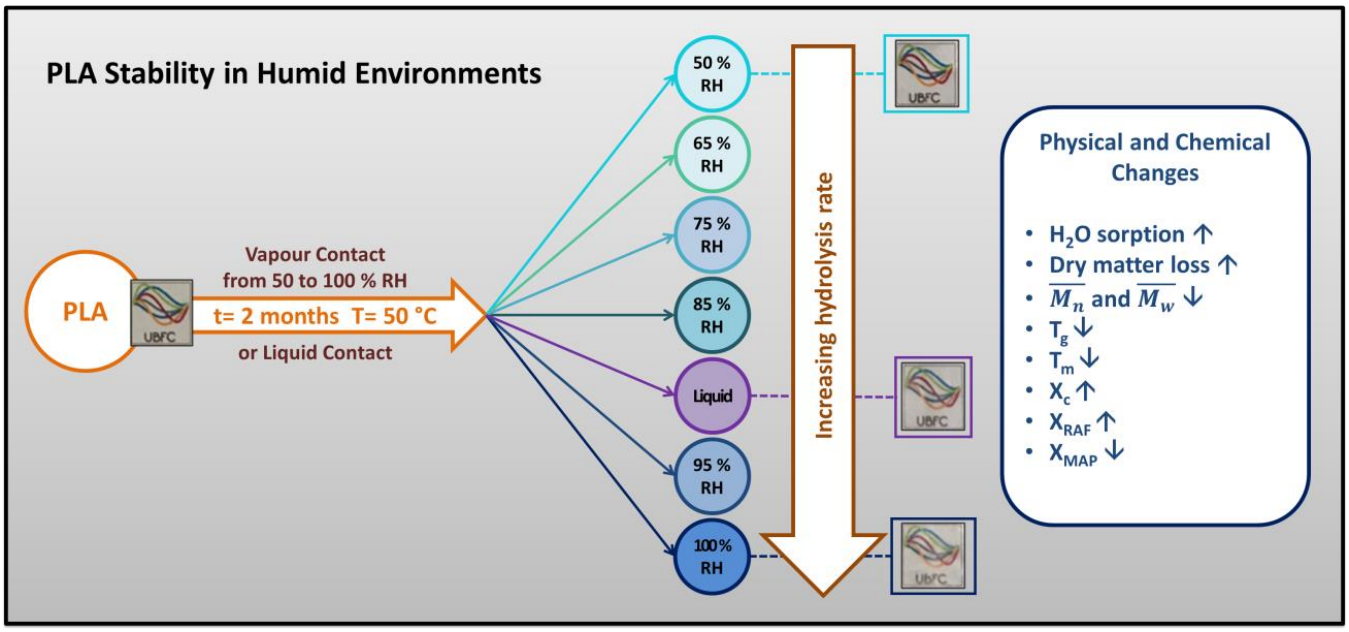

Figure 2. *"Beyond biodegradability of PLA: physical and chemical stability in humid environments".*

Further investigations on the influence of water at the liquid state on the hydrolysis mechanism were also carried out at pHs ranging from 3 to 7 (buffer solutions), and in pure water without a controlled pH. The

aim was to know if the pH of foods or beverages could influence or not the rate of hydrolysis. The analysis of the molecular weight distribution of PLA chains displayed that pH had no influence on the rate of hydrolysis (Figure 3). This is a key information for the application of PLA films in contact with moist foods whatever their acidity. Indeed, our work displayed that a very wide range of moist food products (cooked or fresh fruits and vegetables, cheeses, dairy products, meat and meat based products, delicatessen, tomato paste, *etc.*) can be packed in PLA films or trays without any influence on the shelf life of the PLA material that should be longer than that of the packed product.

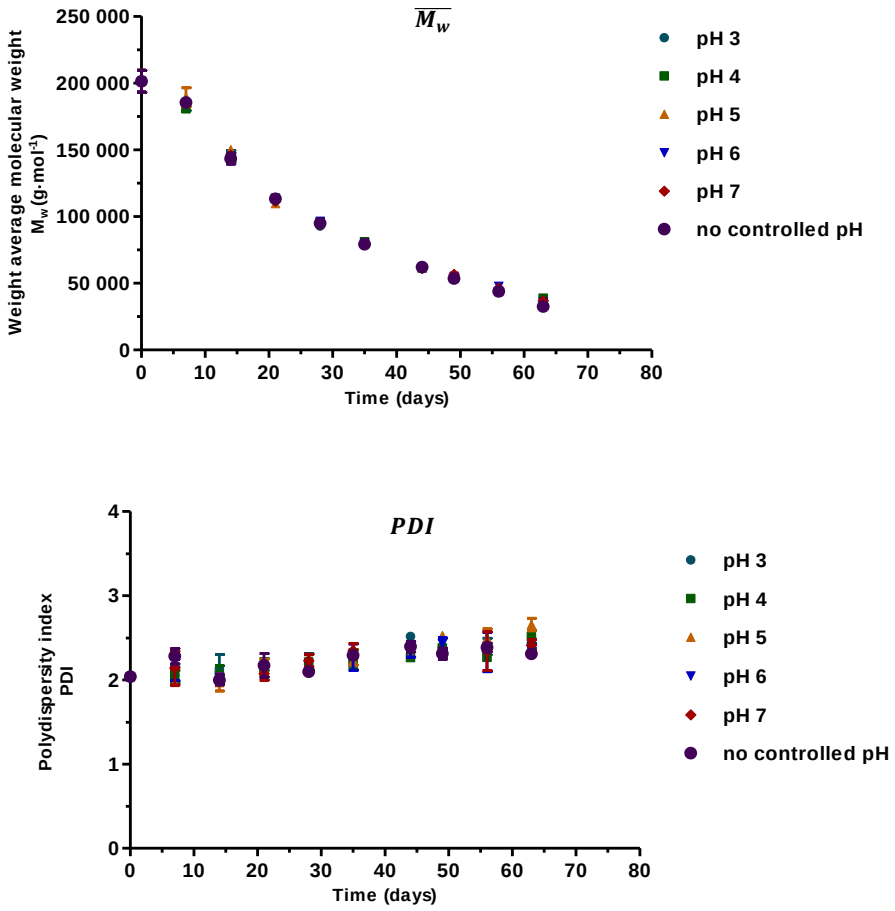

Figure 3. *Kinetics of weight average molecular weight ($\overline{M_w}$) and polydispersity index (PDI) of PLA films immersed in liquid water at different controlled pH and not at 50 °C*

Knowing much better the limitation of PLA films dedicated to food products, the challenge was to improve its functional properties by surface modifications and combination with high gas barrier bio-sourced and biodegradable polymers (proteins) in order to extend the food shelf-life. Gluten, the main protein fraction from wheat flour, is able to make films, when associated to a plasticizer such as glycerol, and exhibits a very low gas permeability (same order than poly-vinylidene chloride PVDC, or ethylene-vinyl alcohol EVOH) when isolated from high RH.

Therefore, multilayer complexes made by assemblies of two PLA layers and a wheat gluten layer were envisaged. Different processing technologies were considered such as incorporation of lipids in wheat gluten films, high pressure homogenization of protein film forming dispersions, surface modification of PLA films (corona treatment) and layer assembly (as single layers or as bilayers) having different thicknesses by hot press.

A previous study on the incorporation of a lipid phase in the gluten matrix displayed that the fat was able to reduce the water sorption of approximatively 10 % (at 84 % RH and 25 °C), and to decrease by 60 % the water affinity and the water transfer of the wheat gluten films. However, it induced a weaker structuration of the gluten network and therefore a loss of its mechanical and transparency properties, indicating that lipid incorporation was not a good strategy to reduce hydrophilicity. For these reasons, wheat gluten layers containing dispersed lipids were not included in experimental design dedicated to the development of the multilayer PLA/wheat gluten complexes. In contrast, an innovative way to process the film-forming dispersions based on gluten was adopted to optimize the film structure. Indeed, high pressure homogenization was applied to wheat gluten dispersions at liquid state. This technology highly reduced the particle size of wheat gluten from 314 to 8.3 µm ($d_{4,3}$ values). The wheat gluten particle size reduction and their better distribution within the film thickness favoured a more efficient structuration of the protein matrix, which improved its functional properties (appearance, mechanical properties and barrier properties to water and O_2).

For the assembly of the complexes, the compatibility between wheat gluten layer and PLA layers, such as adhesion, should be verified and facilitated. The impact on the PLA film properties of the corona treatment at industrial scale, which is the most common surface treatment to improve printing and layer assemblies, was assessed. Corona treatment of PLA films was conducted on the industrial lines of Taghleef Industries, using the conventional technology already set up for both polypropylene and PLA films. Our findings clearly showed that corona treatment was able to physically and chemically modify the surface of PLA films at the nanometer scale. The surface roughness increased from 3 to 7 nm and the oxygen elemental composition (O) at the very top nanolayers (<10 nm) increased approximately by 10 %. These modifications induced an enhancement of the surface tension and of it polar contribution. An interesting improvement of the barrier properties to non-polar gases such as He, O_2 and CO_2 was also noticed. The maximum improvement observed for oxygen was approximately of 40 % (from 17 to 10 10^{-17}·mol·m^{-1} ·s^{-1}·Pa^{-1}). For the helium, the improvement was of 6 % (from 358 to 339 10^{-17}·mol·m^{-1}·s^{-1}·Pa^{-1}) and for CO_2 was of 18 % (from 35 to 29 10^{-17}·mol·m^{-1} ·s^{-1}·Pa^{-1}). Findings strongly suggested that the increased hydrophilicity was the main reason of such improvement. In addition, some slight modifications in the bulk properties occurred (relaxation of PLA chains and increased crystallization), which slightly modified the mechanical properties of films. These modifications were probably the consequence of the local temperature increase induced by the corona

process. These findings thus suggested that corona treatment could positively influence the development of PLA-WG-PLA complexes by facilitating the adhesion between layers and by improving the barrier properties to gases (O_2 and CO_2). For these reasons corona treated PLA films were used for the PLA-WG-PLA complexes development.

Nevertheless, some preliminary results dealing with hydrolysis of PLA films treated by corona or not, conducted at 85 % RH and 50 °C, suggested that corona treatment also induced an acceleration of hydrolysis, probably due to an increased interaction with water driven by the higher polarity (Figure 4). It is thus important to consider the possible effects of such treatment on the PLA material shelf-life and consequently on its storage and utilization.

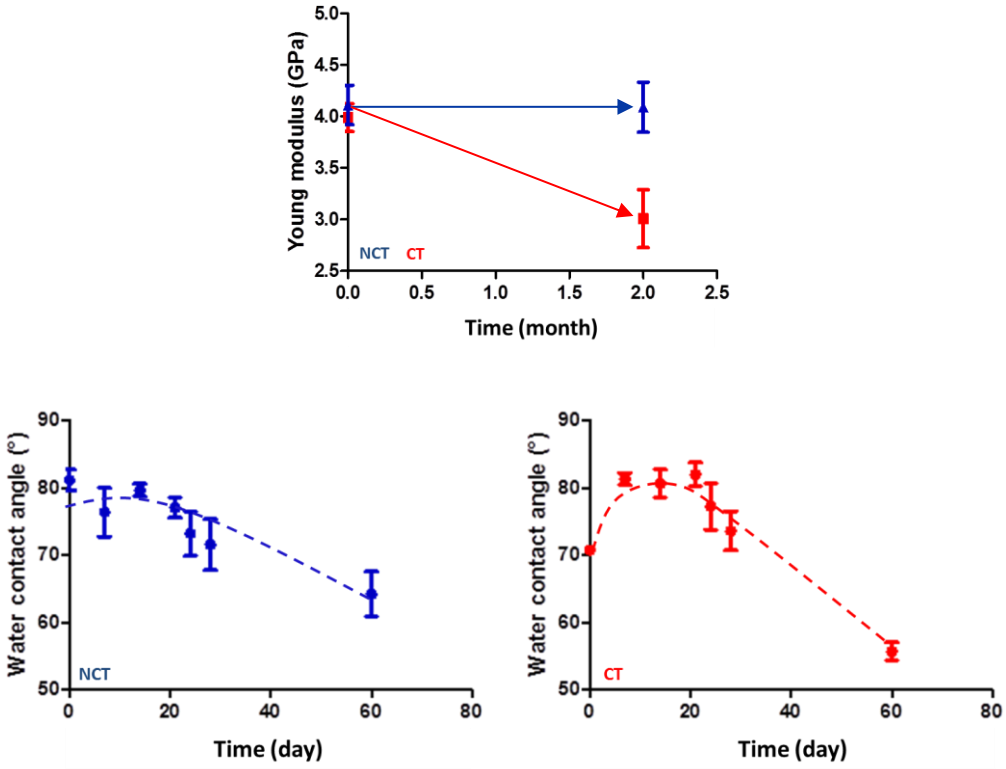

Figure 4. *Young modulus and water contact angles of PLA films treated (CT) or not by corona treatment (NCT) stored at 85 % RH at 50 °C for two months.*

Since the complexes were obtained by hot press treatments in a range of temperatures and pressures of 110-150 °C and 10 –20 MPa respectively, its impact on the PLA film properties was also assessed. The hot press treatment reduced the transfer through PLA films by 40 % for water vapour (from 16 to 10 10^{-4}·g·m^{-2}·s^{-1} considering the 30-100 % RH differential) and by 60% for oxygen (from 17 to 7 10^{-17}·mol·m^{-1}·s^{-1}·Pa^{-1} at 0% RH), most likely because it favoured an increase of the crystallinity of films (from 28 to 34 %). Such improvement was higher than the improvement associated to corona treatment. However, no synergetic effects were observed when PLA films subjected to corona treatment were submitted to hot press process.

Consequently, the improvement on the barrier properties related to corona was masked by hot press. This indicated a predominant effect of the crystallinity of films, over its polarity.

Based on these considerations, the PLA-WG-PLA complexes were finally and successfully developed using the hot press technology. After been hot pressed, the barrier properties of complexes to water were then improved from 10 to 20 times compared to WG, depending on the RH differential, while those to O_2 and CO_2 were also improved of same magnitude compared to PLA. This improvement can be considered satisfactory considering that the transfer rates were determined in realistic conditions for food packaging application (50 % RH). The reduction of the transfer of O_2 and CO_2 was driven by the WG layers, as expected, while the reduction of the water vapour rates was due to the PLA layers. Each layer of PLA and wheat gluten thus acted as complementary limiting steps to mass transfer.

Even if barrier properties were ameliorated, it is of great importance to consider other functional properties such as mechanical or optical, which depends partly on the adhesion between layers. The work of adhesion of the WG/PLA interfaces indicated that the adhesion of WG/PLA layers should be good, since the achieved values are similar to that of painting applications to surfaces. Nevertheless, the t-peel strength revealed a poor adhesion of the WG/PLA interfaces after hot press assembly. These contradictory results were better understood by the cross section microstructure analysis. Microscopy observations displayed a poor adhesion/contact at the interface WG/PLA after hot press assembly, but a much higher adhesion/contact of layers at interface WG+PLA when the latter was formed by wet casting. In addition the microstructure of the WG coating appeared brittle and with several irregularities in the areas near to the interface WG/PLA. On the contrary, a more homogeneous microstructure of the WG layer was observed near to the WG+PLA interface. This particular behaviour displayed an interesting phenomenon at the interface PLA/WG, probably not enough considered in our work. The temperature during hot press (130 °C) most likely favoured water evaporation at the interface, the water vapour thus limiting the surface contact between layers. This water evaporation from the WG layer combined with the high pressure conditions (10 MPa) induced a particular restructuration/densification of the wheat gluten chains. The evaporation at the interface WG+PLA might be limited during hot press using a more dried wheat gluten layer. Moreover, the hot press process effect certainly masked as well the influence (or not) of the corona treatment on adhesion. So, further experiments of hot press assembly of PLA and wheat gluten layer should be conducted at different water content levels in aim to better understand the impact of evaporation on the trilayer complexes performances.

Maybe this very interesting phenomenon could be linked to another particular behaviour of the PLA-WG-PLA complexes. Indeed, surprisingly no effect of the WG layer thickness (from 20 to 60 µm) was observed in the barrier properties to oxygen of the complexes, even if the WG layer is the limiting step to the gas

transfer. Same behaviour was also observed to a lesser extend for CO_2. This peculiar behaviour suggests that the restructuration of WG chains driven by hot press probably acted as thinner but denser limiting layer, which strongly improve the barrier properties of complexes. WG coatings from 20 to 60 micrometres were found to have similar barrier properties to O_2 than WG films of 120 micrometres prior to multilayer shaping by hot press. If this could be verified for much lower thickness of wheat gluten layer, this should make easier the application of the layer of wheat gluten, reducing the drying time and the amount of protein used for complexes production. Consequently, some preliminary trials have already been conducted to apply onto PLA very thin gluten layers by spin coating. Figures 5 shows the cross-section microstructure of some of samples obtained after spin coating deposition of the wheat gluten dispersion on PLA films. The images clearly indicate that the objective of reducing the thickness of WG coating was successfully reached. The new samples had a WG thickness ranging from approximately 0.7 to 5 µm, and it is planned to check if their barrier properties to gases follows the same trend as those observed for the previous trilayer complexes. From the images, it also seems that the adhesion between layers is also optimized compared to previous wet coating complexes (Part II, Paper 6). This could probably be related to the reduced amount of water, and thus a lower impact of water of evaporation phenomenon.

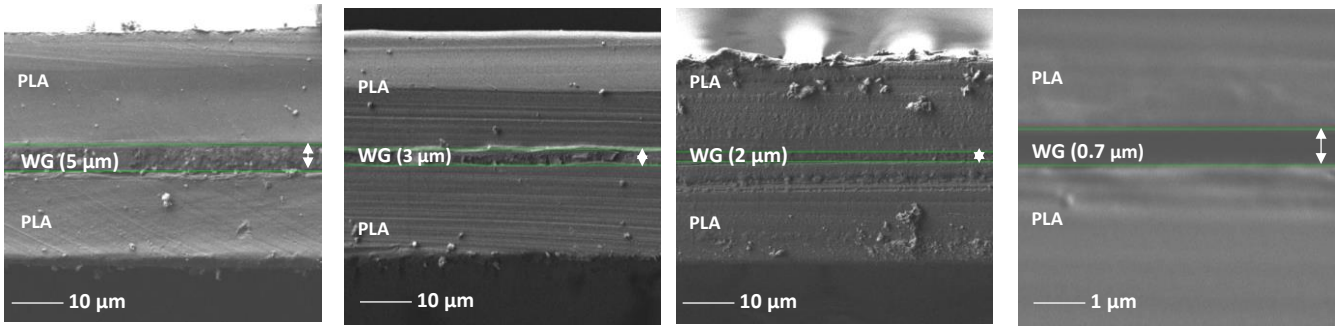

Figure 5. *Cross section microstructure of PLA+WG/PLA complexes obtained by spin coating and hot press, having WG coating layers of approximately 5, 3, 2 and 0.7 µm of thickness*

This PhD project thus showed the real potential of bio polymer complexes such as PLA-WG-PLA as an eco-friendly strategy for substituting conventional plastics for high barrier requirements such as MAP, opening un-explored industrial scenario for both biopolymers. The results of this PhD thesis give strong basis for going further on the processing aspects for this kind of materials in industrial applications. They need to be confirmed and optimized at pilot or semi industrial lines scales. It is also of scientific and practical interest to explore the potentialities of high pressure homogenization as a tool for improving the functional properties of wheat gluten or other hydrocolloid-based films. More studies dealing with the effect of high pressure homogenization coupled with technologies of thin layer application to reduce time of the drying duration, such as flexography or ink/varnish printing technologies, will probably generate new procedures, which can highly reduce the time for production of complexes. Additionally the results of this project could motivate the investigations on multilayer complexes with PLA using other biopolymers/hydrocolloids

coming from agro industrial waste or by products such chitosan, which could highly decrease the cost of production and at the same time being consumer-friendly. It is well known that chitosan, a waste from seafood industry, has similar barrier performances to gases than wheat gluten.